INFORMATION TO USERS

This manuscript has been reproduced from the microfilm master. UMI films the text directly from the original or copy submitted. Thus, some thesis and dissertation copies are in typewriter face, while others may be from any type of computer printer.

The quality of this reproduction is dependent upon the quality of the copy submitted. Broken or indistinct print, colored or poor quality illustrations and photographs, print bleedthrough, substandard margins, and improper alignment can adversely affect reproduction.

In the unlikely event that the author did not send UMI a complete manuscript and there are missing pages, these will be noted. Also, if unauthorized copyright material had to be removed, a note will indicate the deletion.

Oversize materials (e.g., maps, drawings, charts) are reproduced by sectioning the original, beginning at the upper left-hand corner and continuing from left to right in equal sections with small overlaps.

Photographs included in the original manuscript have been reproduced xerographically in this copy. Higher quality 6" x 9" black and white photographic prints are available for any photographs or illustrations appearing in this copy for an additional charge. Contact UMI directly to order.

ProQuest Information and Learning
300 North Zeeb Road, Ann Arbor, MI 48106-1346 USA
800-521-0600

DISSERTATION

MODELING THE SPATIAL VARIABILITY OF FOREST FUEL ARRAYS

Submitted by

JOSE GERMAN FLORES GARNICA

Department of Forest Sciences

In partial fulfillment of the requirements

for the Degree of Doctor of Philosophy

Colorado State University

Fort Collins, Colorado

Summer 2001

COLORADO STATE UNIVERSITY

June 1st, 2001

WE HEREBY RECOMMEND THAT THE DISSERTATION PREPARED UNDER OUR SUPERVISION BY **JOSE GERMAN FLORES GARNICA** ENTITLED "**MODELING THE SPATIAL VARIABILITY OF FOREST FUEL ARRAYS**" BE ACCEPTED AS FULFILLING IN PART REQUIREMENTS FOR THE DEGREE OF DOCTOR OF PHILOSOPHY.

Committee on Graduate Work

Advisor

Department Head

ABSTRACT OF DISSERTATION

MODELING THE SPATIAL VARIABILITY OF FOREST FUEL ARRAYS

This project focuses on the need for a comprehensive approach for forest fuels mapping based on spatial interpolation techniques. Instead of working only with the fuel-model concept, this investigation is focused on the generation of four different fuel maps. Three of them are based on fuel timelag (measure of the rate at which a specified size of dead fuel gains or loses moisture) [1-HR, 10-HR and 100-HR fuel classes]. The fourth one corresponds to the live-fuels category [Live Woody]. This allowed better definition of the spatial variations in fuels, even within an area classified into the same fuel-model class. A total of twelve interpolation options were compared, five statisticals (spline, polygonal mapping, inverse distance weighting [power 1 and 2]) and seven geostatisticals (ordinary kriging, universal kriging [1st and 2nd degree], cokriging, point kriging and block kriging), in order to get the continuous surfaces that more precisely represent the spatial distribution for each of the mentioned fuel classes. The ancillary data required in cokriging were gathered from a Digital Elevation Model, a Landsat 5 TM and a forest inventory. Field data were collected from the "ejido" El Largo y Anexos, Cd. Madera (Chihuahua, México). These variables were analyzed to define more significant auxiliary variables.

The four fuel classes showed significant autocorrelation and cross-correlation, thus it was possible to model the spatial continuity of each of the four fuel classes. The

average spatial dissimilarity between data points allowed defining a structural distribution (variogram), with the corresponding sill, range and nugget effect. Traditional "conditionally positive definite" models were good enough to characterize the pattern of spatial continuity, and to define weighting factors for both kriging and cokriging. Based on the mean square error values, in general, geostatistical techniques performed better than the traditional alternatives. As a result, three out of the four fuel classes (1-HR, 100-HR, LW) were better modeled through cokriging, with elevation as an ancillary variable. The ancillary variables that showed the best performance when cokriged with fuel classes were elevation and principal component 3. Inverse distance weighting (IDW, power 1) was the best alternative to define the spatial distribution of 10-HR fuel. Although, it was not possible to establish a unique "best" spatial interpolation method, IDW showed a more constant performance. The worst results were obtained using spline, and Thiessen interpolation techniques.

Since there was not a spatially explicit fire behavior model that could use the four fuel-type maps, a spatial simulation model (SSM) was developed under a raster approach. This model was compared with FARSITE, an existing spatially explicit fire behavior model that is based on the fuel-model concept. The required fuel-model map for FARSITE was developed under the "Conditional Fuels Loading Concept" (CFLC), which considers that each fuel-model has a characteristic fuels loading combination. There were some differences in fire behavior, such as rate of spread and reaction intensity, when comparing the simulation model of this study (SSM) versus FARSITE, which was the result of the variation of fuel loading.

Forest fire phenomena are complex, thus a more accurate prediction of fire behavior should consider not only the evaluation of more variables, but also determine their spatial inter-dependencies. It is recommended that future fuels evaluation should be based on the integration of a multi-resource approach and geostatistical techniques. Furthermore, nonlinear kriging techniques should be tested in the interpolation of forest fuels. On the other hand, geostatistical techniques can be used to monitor and predict changes in the spatial distribution of forest fuels. Also the CFLC should be further tested not only regarding the "Timber litter" fuel complex, but also with the other fuel groups. Further research is needed to define the more adequate sample design when interpolating fuels' spatial distribution.

José Germán Flores Garnica
Department of Forest Sciences
Colorado State University
Fort Collins, CO 80523
Summer, 2001

ACKNOWLEDGEMENTS

Deep appreciation is expressed to Dr. Philip N. Omi, my advisor for his guidance, support, patience, and friendship throughout my doctoral program. I also want to thanks to my committee members, Dr. Robin M. Reich for sharing his knowledge of the fascinating world of geostatistics, Dr. Celedonio Aguirre Bravo for his support and encouragement, and Dr. Wayne L. Leininger for his advice. Thanks to all of them for their review and suggested improvements on this dissertation.

I would like to extend my appreciation to the following persons: to Ing. Alfonso Domínguez Pereida, Ing Armando Bojorquez Chávez, and to all the crew members of the UCODEFO 2, for their valuable support in the fuels inventory; to all the researchers of the INIFAP in Cd. Madera, for their support; to Dr. Cesar Guerra, for sharing his knowledge in computer programming; to Dr. Mohammed Kalkhan, for his support in the remote sensing analysis; to Dr. Robert E. Keane, for sharing his experience in forest fuel mapping; and to Dr. Susan Stafford for helping me to participate in some conferences.

Appreciation is extended to Stanley Best, Jose R. Valdez and Juan de Dios Benavides. We walk together an important part of this journey. Thanks for their friendship, support, and encouragement.

Thanks to the Instituto Nacional de Investigaciones Forestales, Agrícolas y Pecuarias (INIFAP-México) and to the Consejo Nacional de Ciencia y Tecnología (CONACYT-México) for their financial support in my graduate studies. Thanks to the USDA Forest Service for its financial support in the inventory phase.

I am eternally grateful for all the love, support, encouragement, and patience that my wife Chuy provided all these years. A very special thanks to Aldo and Karla, our children, who sometimes understood why I had to spend more time working instead to be playing with them. Thanks to them for all the few moments that we spent together during my doctoral program.

Finally, Mom and Dad, by your love and life you gave me a start. Thanks. Thanks also to Beto, Martin, Sandra y Gloria, my brothers and sisters, for keeping the warm of our family.

DEDICATION

To my father,

for give me the opportunity of my education.

I miss you.

TABLE OF CONTENTS

LIST OF TABLES

LIST OF FIGURES

CHAPTER I

1 INTRODUCTION

The development of computer models to spatially simulate fire behavior has represented a valuable tool in support of fire management. Fuels characterization and spatial distribution are critical factors to use such models. However, fuel maps have been both costly and difficult to build (Keane *et al.* 1998). In an attempt to simplify fuels characterization, the "fuel model" concept was created (Keane *et al.* 1998; Burgan and Rothermel, 1984). This concept allows the generation of fuel maps, where a given region is classified into areas according to corresponding fuel-models. However, fuels' mapping, based on the fuel models concept, has resulted in two major problems. First, the definition of the spatial distribution of fuel models has represented one of the more complicated challenges facing forest fire scientists. Forest managers who do not have experience in fire or fuels' modeling find it difficult to create new fuel models accurately and consistently (Hardwick *et al.* 1996; Burgan and Rothermel, 1984). However, few studies exist with the unique purpose of mapping fuels to predict fire behavior (Keane *et al.* 1999a; Keane *et al.* 1999b). Although, the existing alternatives require mastering many disciplines, such as geographical information systems, remote sensing, fire ecology and fire behavior modeling, the accuracy achieved has been rather low (Krauter, 1999; Burgan *et al.* 1998; Keane *et al.* 1999a). The reason for this is the high spatial variability of fuels, vegetation and environmental conditions (Keane *et al.* 1999b). Second, when a given area is classified as a certain fuel-model, the expected fire predictions during a given projection period (i.e., wind, fuel moisture, and slope constant) will be the same in

the whole area, regardless of variations in the spatial distribution of fuels. However, the spatial distribution of forest fuels tends to be rather discontinuous and highly variable (Brown and Bevins, 1986). An assumption of fuel homogeneity could preclude changes in fire behavior due to changes in fuel distribution. For instance, temperatures reached during an experimental fire could vary spatially because of variation in fuel distribution (Hobbs and Atkins, 1988). These changes of temperature can be associated with changes in flame length, fireline intensity, reaction intensity, and heat per unit area. Thus, changes in fuel distribution could occur even within a given fuel model. Considering that such variations could mean the difference between a fire easily controllable and a dangerous fire, it is important to generate fuel maps as accurately as possible.

Fuel models represent a set of fuel properties that are required for mathematical fire behavior models (Rothermel, 1972). These models are organized into four groups: grass, shrub, timber, and slash (International Fire Service Training Association, 1998). "*The differences in fire behavior among these groups are basically related to the fuel load and its distribution among the fuel particle size classes*" (Anderson, 1982, page 1). The rate at which a specified size class of dead fuel gains or loses moisture (timelag) allows one to definition of four fuel classes: (a) 1-hour fuels map (0-$^1/_4$ inch diameter); (b) 10-hours fuels maps ($^1/_4$-1 inch diameter); (c) 100-hours fuels map (1-3 inches diameter); and (d) 1000-hours (>3 inches). On the other hand, there are two classes of live fuels: (a) woody (e.g. saplings and shrubs); and (b) herbs.

Accordingly, fuels mapping alternatives are needed that not only complement the fuels-model concept, but more importantly accurately capture the spatial variation of

forest fuels. One option is the use of spatial interpolation approaches that have been successfully used in many fields, such as mining, petrology, soils and meteorology (Hunner, 2000; Laslett *et al.* 1987; Webster and Oliver 1989; Lee *et al.* 1997; Phillips *et al.* 1992). Nevertheless, the uses of interpolation techniques in forestry have been rare (Hunner, 2000), and most of the studies are focused on the prediction of pest dispersion (Liebhold *et al.* 1993; Reich and Geils, 1992; Regniere and Sharov, 1997; Hohn *et al.* 1993). Interpolation techniques are based in the First Law of Geography: "*everything is related to everything else, but near things are more related than distant things*" (Chou, 1992, page 170). This means that values at points close together in space are more likely to be similar than points further apart (Burrough and McDonnell, 1998). Interpolation is used to provide estimates of a given phenomena at unsampled sites from measurements made at point locations within the same area or region, and generate a continuous surface (Hunner, 2000; Burrough and McDonnell, 1998). In general, there are two major groups of interpolation techniques: a) those based on traditional statistics; and b) those based on geostatistics. The former require only an understanding of simple [deterministic] statistical methods, while the latter are based on a probabilistic approach that requires an understanding of the principles of statistical spatial autocorrelation (Burrough and McDonnell, 1998; Goovaerts, 1997). Geostatistical methods of interpolation are commonly known as *kriging*, and are considered as the "best linear unbiased estimator" (or optimal interpolator) (Hunner, 2000; Isaaks and Srivastava, 1989; Burrough 1986).

1.1 Objectives of the Study

Although Burrough and McDonnell (1998) suggested use of geostatistical techniques when data are sparse, there is not a rule for selecting the "best" interpolation

technique for a specific situation. Therefore, it is important to evaluate different interpolation alternatives. Nevertheless, very few studies exist that compare different interpolation techniques (Atkinson and Lloyd, 1997; Laslett *et al.* 1987; Asli and Marcotte, 1995). Moreover, there is only one study in forestry that compared seven different interpolation techniques (Hunner, 2000). Before the present study, no work examined the use and comparison of interpolation techniques for fuels mapping purposes. In this study, 5 traditional and 7 geostatistical interpolation techniques were evaluated and compared. These techniques were carried out for two reasons: (a) to compare the goodness of geostatistical alternatives in relation to traditional interpolation techniques; and (b) to evaluate the more commonly used interpolation techniques. Software availability was also considered. The objectives of this dissertation are summarized as follows:

I General Objective

To develop a comprehensive approach for forest fuels' mapping based on spatial interpolation techniques.

II Specific Objectives

A) Spatial Correlation and Spatial Continuity

1) To explore spatial autocorrelation of each fuel class (1-HR, 10 HR, 100-HR, and Live Woody fuels).

2) To explore spatial cross-correlation of each fuel class (1-HR, 10 HR, 100-HR, and Live Woody fuels).

3) To analyze and model the spatial continuity that characterizes each fuel class.

4) To analyze and model the joint spatial continuity of each fuel class and ancillary data.

B) Spatial Interpolation and Continuous Surfaces

5) To define continuous surfaces of each fuel class using the following geostatistical interpolation techniques: ordinary kriging, universal kriging [1st and 2nd degree], cokriging, point kriging and block kriging.

6) In the case of cokriging, to define the more significant secondary variables. Also to analyze and model the spatial cross-correlation between each fuel class and such variables (alone and combined).

7) To define continuous surfaces of each fuel class using the following statistical interpolation techniques: spline, polygonal mapping, inverse distance weighting (power 1 and 2).

8) To compare the different interpolation techniques, and select the best one for each fuel class.

C) Fire Behavior Simulation

9) To develop a system that allows punctual estimations of surface fire behavior based on fuel class loadings.

10) To define the characteristic combination of fuels' loading of each fuel-model that allows qualifying a given site into its corresponding fuel-model.

11) To develop a spatially explicit model (Spatial Simulation Model), under the raster approach, which simulates surface fire behavior based on the spatial distribution of fuel classes.

12) To compare the Spatial Simulation Model with an existing spatially explicit fire behavior model (FARSITE).

1.2 Hypotheses

To achieve the above objectives five null hypothesis were tested:

H_{o1}: There is no spatial autocorrelation among the sample values of each of the four fuel classes (1-hour fuels, 10-hours fuels, 100-hours fuels, and live woody fuels)

H_{o2}: There is no spatial cross-correlation between the sample values of each fuel class and ancillary data (i.e., observable trends in 1-hour fuels will be explained by other variables, such as elevation, aspect, tree density, etc.).

H_{o3}: Modeling the spatial continuity of each fuel class (regionalized variables) does not increase precision of geostatistical interpolation techniques (kriging) over traditional alternatives (i.e., Thiessen, spline, and inverse distance weighting).

H_{o4}: Modeling the joint spatial continuity of each fuel class (regionalized variables) and ancillary data (i.e., elevation, aspect, tree basal area, etc.) does not increase precision of geostatistical interpolation techniques (cokriging) over traditional alternatives (i.e., Thiessen, spline, and inverse distance weighting).

H_{o5}: The spatial behavior of a surface fire based on the distribution of fuel classes is not different than the spatial fire behavior defined by a system based on fuel models.

1.3 Structure Guide

This dissertation is divided into six general chapters and 14 sections. This chapter contains the introduction of this project (***Section 1***), which summarizes the rationale of this project and establishes both the objectives and the supporting null hypotheses. **Chapter II,** ***Section 2*** (Study Area) gives a description of the study area, and its

contextual geographic importance. **Chapter III** describes the context under which this project was carried out. ***Section 3*** (Forest Fuels Mapping) gives a background of the different methodologies that have been used to map forest fuels. ***Section 4*** (Spatial Interpolation Techniques) explains both deterministic and geostatistical interpolation techniques. Emphasis is given to the "regionalized variable" theory, on which kriging approach is based. ***Section 5*** (Spatial Fire Behavior Models) conceptualizes the simulation of spatial fire behavior, and to the two approaches used in Geographical Information Systems (vector and raster). **Chapter IV,** ***Section 6:*** (Methodology), describes data gathering for fuel maps generation and fire behavior simulation. **Chapter V** shows relevant results, as well as brief discussion. ***Section 7*** (Forest Inventory) refers to both fuels and stand information, resulting from the forest inventory. ***Section 8*** (Fuel-Models Map) analyzes fuel information to support the generation of a fuel-models map. ***Section 9*** (Thematic Information Extraction) shows the information gathered from satellite imagery. ***Section 10*** (Spatial Distribution of Fuels) compares all the interpolation techniques, and the selection of the best technique for each fuel class is described in this section. Both the resultant fuel-maps, and their corresponding error-of-estimation maps are shown. ***Section 11*** (Spatial Fire Behavior Simulation) describes the spatial model used to simulate surface fire behavior, based on fuels loading. An analytical comparison between this model and a model based only on the fuel-model concept is shown. In ***Section 12,*** **Chapter VI,** a general discussion of the results is shown, focused on the generation of fuel maps. ***Section 13*** presents final conclusions and thoughts about potential alternative approaches and future recommendations. In ***Section 14*** the literature consulted is shown.

CHAPTER II

2 STUDY AREA

2.1 Madrean-Apachian Forest Ecosystem Complex

The Madrean-Apachian Forest Ecosystem Complex (MAFEC) is a biogeographic province of North America (Brown *et al.* 1994), which is one of the most important transboundary ecoregions of the North American Ecosystem (México/United States) (Aguirre, 1997). Beyond its social and economic importance, this complex is recognized as one of the three mega-diversity centers of plant and animal species in the world. Nevertheless, currently there is not a comprehensive and integrated monitoring program aimed at providing interoperable data and information to properly manage this ecosystem (Aguirre and Reich, 1997). Therefore, the USDA Forest Service and the Ejido El Largo y Anexos (Cd. Madera, Chihuahua. México) have taken the initiative to carry out a major inventory and monitoring project for assessing the current and future condition of the MAFEC. This undertaking is proposed as a Pilot Study on Inventory and Monitoring of Forest Ecosystems so that other communities and landowners can learn and benefit from the results. This study is part of the Pilot.

2.2 Location

The study area is located within the region proposed for the Pilot Study on Inventory and Monitoring of Forest Ecosystems of the MAFEC. The total region covers approximately 250,000 hectares of primarily coniferous-oak forest, which is an important

component of the Sierra Madre Occidental of México (Aguirre and Reich, unpublished). Jurisdictionally, it is within the counties of Madera and Casas Grandes. This study was carried out using information from a commercial forest of the ejido El Largo y Anexos. This ejido is located within the region called Mesa del Huracan, at the northwest of Chihuahua state, México (approximately 320 kilometers SW from El Paso, Texas) (Figure 2.1).

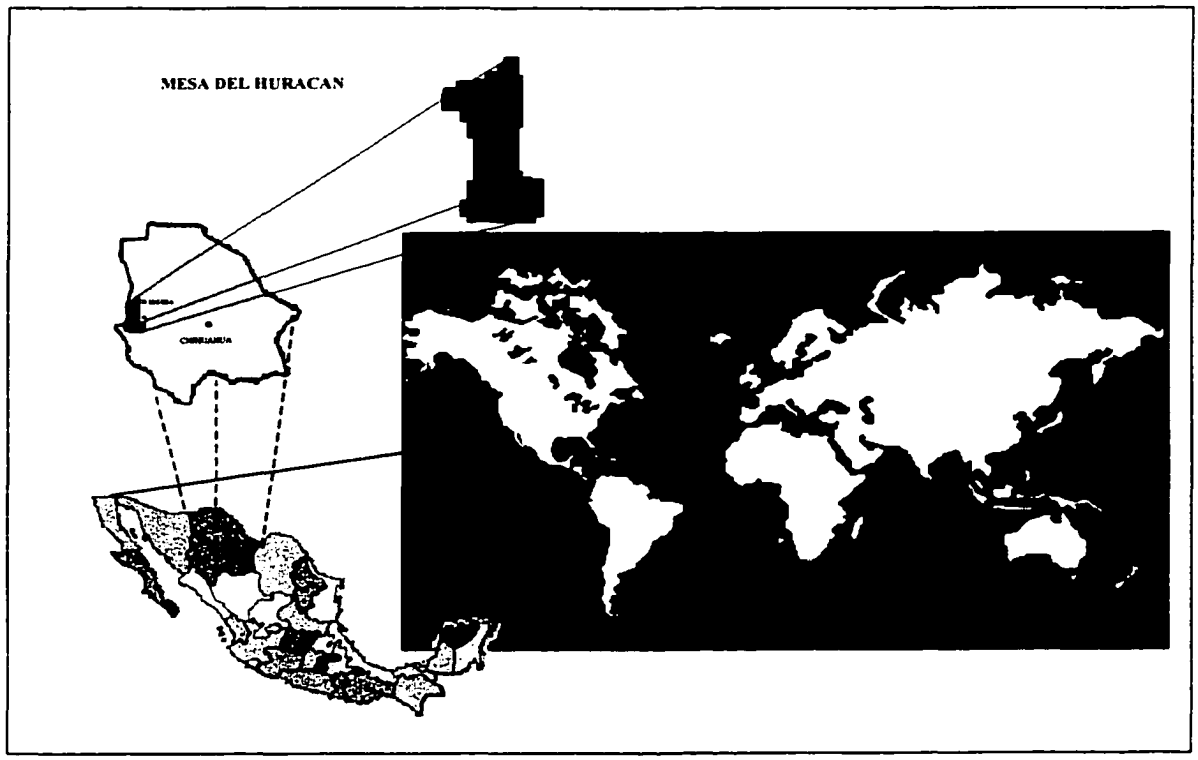

Figure 2.1. Approximate study area location within the region Mesa del Huracan, close to Cd. Madera (Chihuahua, México).

2.3 Environmental Characteristics

The predominant tree species are *Pinus durangensis, P. arizonica, P. engelmannii and Quercus sideroxyla.* This mix of species produces a unique load of fuels (basically 1

hour fuels). Most of the topography is mountainous, with some valleys. The annual mean temperature ranges from 8.5 to 12 degrees centigrade. The extreme minimum temperature registered is –26°C. The extreme maximum temperature is 38° C. The range of precipitation is between 690 and 1130 mm/year (most of the rainy season occurs from July to September). Elevations range from 1400 up to 2400 m. Fire season is in summer, during the dry season (from May to June) (UCODEFO No 2, 1997).

2.4 Digital Elevation Model

Within the region of the study area three general topographic conditions are defined (valleys, mountains, canyons [rivers]). The study area was located mostly within mountainous topography, which is representative of the forested area of the region. The resolution of the Digital Elevation Model (DEM) (90 x 90 m) limited the accuracy of estimation of the terrain parameters. Nevertheless, such estimations were similar to the field data. The information generated through the DEM was used as ancillary data to test both spatial cross-correlation and joint spatial continuity hypotheses for each of the four fuel classes.

2.4.1 Elevation

The variation of elevation within the study area is considerable, with a difference between the highest and the lowest point of 335 meters (Table 2.1). Nevertheless, most of the sample plots were located between 2300 and 2400 meters above sea level (m.a.s.l.) (Figure 2.2). The distribution of elevation is definitely normal, which resulted in very similar values between the mean and the median (2341.36 and 2337.13 m.a.s.l.). The minimum and maximum altitudes were 2189 and 2524 m.a.s.l., respectively.

The altitude variation defines a specific environment for certain tree species. Different species could have different rates of fuel production (Burrows and Burrows, 1992; Horbs and Atkins, 1988), thus elevation could define (indirectly) fuel spatial distribution. For example, as shown later in Table 7.2, *Pinus engelmannii* has a distribution limit below 2450 m.a.s.l., while *P. durangensis* has a distribution between 2300 and 2500 m.a.s.l. Although *P. arizonica* is reported within an elevation range from 2700 to 2800 m, this species was found mostly around the 2380 m level.

Table 2.1. Descriptive statistics of the parameters generated with the Digital Elevation Model within the study area (Cd. Madera, Chihuahua).

STATISTICS	ELEVATION (m)	ASPECT (degrees)	SLOPE (%)
Mean	2341.36	149.47	5.16
Median	2337.13	130.60	4.29
Maximum	2524.19	358.42	26.38
Minimum	2189.25	14.04	0.09
Standard deviation	72.73	76.03	4.09
Range	334.94	344.38	26.28
Skewness	0.02	0.65	1.59

2.4.2 Aspect

Most of the study area has a southern aspect (62.4%), followed by a southeast aspect (28.4%) (Figure 2.2). Due to the mountainous topography, in general, there were not zenithal areas. Although there were some northern facing areas, their proportion in the study area was very low (10.6%). The proportion of the study area with an east aspect was approximately 11%, while the west aspect represented 16 % of the study area.

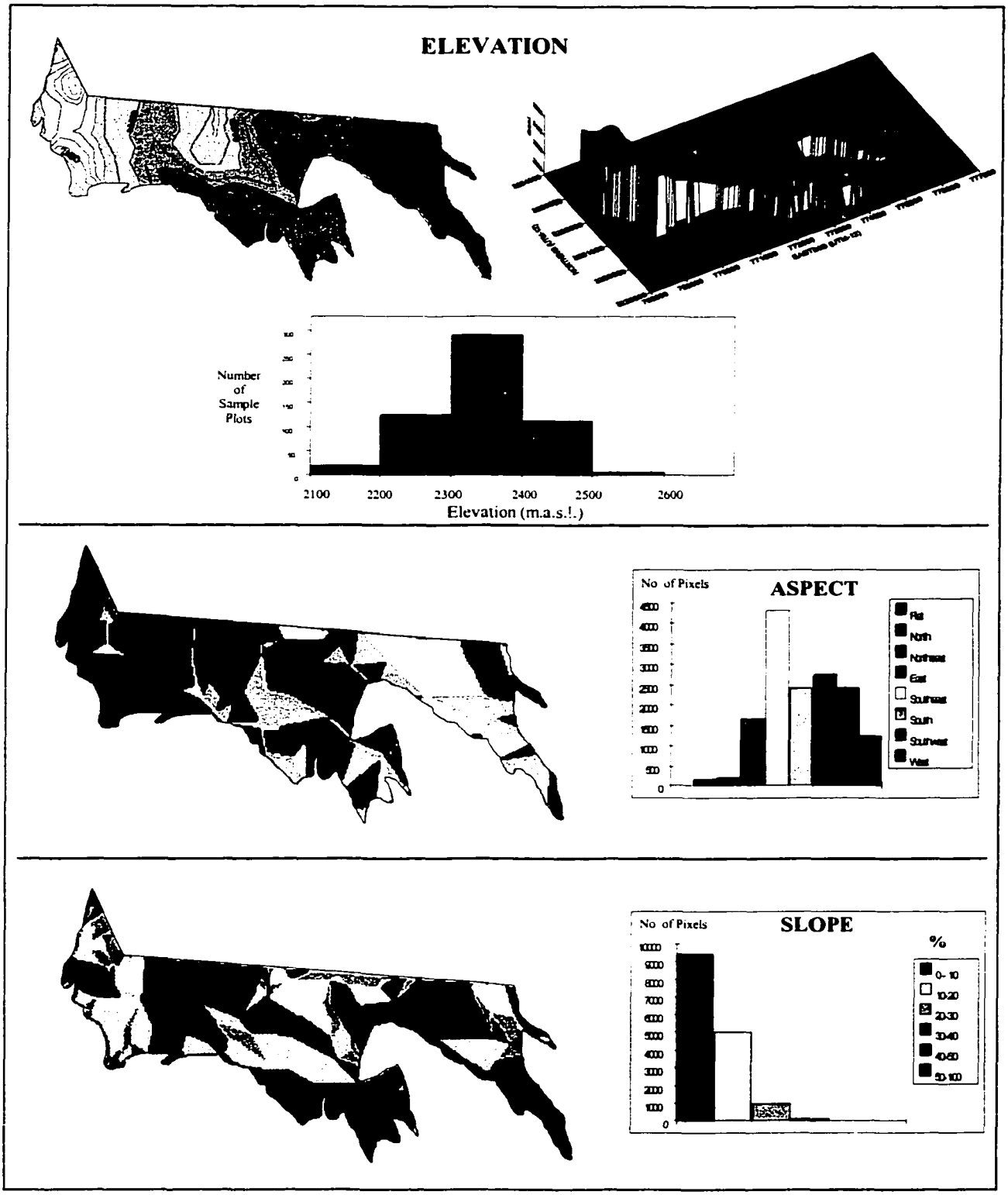

Figure 2.2. Variation of altitude (m.a.s.l.), aspect and slope (degrees) within the study area (Cd. Madera, Chihuahua), and the corresponding frequency distributions. The resolution of the Digital Elevation Model was 90 x 90 meters.

The predominant southern aspect in the study area suggests a warm environment. Although this condition could result in lower production of biomass (compared with northern facing areas), it also could define lower percentage fuel moisture. This should be considered not only in relation to fuel production (Stow *et al.* 1993), but also when fire behavior is simulated.

2.4.3. Slope

Although the topography of the study area is rather mountainous, 92% of the area has slopes lower than 20%. Very few sample plots were located on slopes of more than 50%. The maximum slope registered in a sample plot was of 58.6%. The proportion of the area with more than 30% slope was less than 2%. The slopes ranging between 20 and 30% represented 7% of the study area. Although there are a high proportion of slight slopes, this factor has a considerable influence on fire rate of spread. In general, a fire burning upslope shows a higher rate of spread than a fire in a flat terrain (Weise and Biging, 1997). For instance, compared with a flat terrain, a slope of 24% could double the fire rate of spread in areas classified as "timber litter" (National Wildfire Coordinating Group, 1994).

CHAPTER III

3 FOREST FUELS MAPPING

3.1 The Fuel Model Concept

Because it is difficult to describe all physical characteristics for all fuels in a forest, a generalized description (set of numerical values) of fuels' properties is used, which is called a "fuel model" (Omi, 1997; Keane *et al.* 1999b). Fuel models are organized into four groups: grass, shrub, timber, and slash (Anderson, 1982). Since fuel models also represent a measure of expected fire behavior, they are used to support fire behavior predictions (Omi, 1997; Keane *et al.* 1999b). Therefore, the current tendency of fuel mapping is to classify a given forest into its corresponding fuel models. The 13 fuel models developed by Rothermel (1972) are the most used for fire behavior prediction. Nevertheless, Deeming *et al.* (1977) constructed 20 fuel models for the National Fire Danger Rating System. Using the FUEL Subsystem of BEHAVE (Andrews, 1986; Burgan and Rothermel, 1984), it is possible to develop a fuel model that fulfills the specific conditions of a given forest. Fuel models do not quantify the fuels' characteristics needed for other applications such as fire effects estimations (Keane *et al.* 1999b).

3.1.1 Forest Fuel Classes and Categories

Fuel models represent different fire behaviors, which are basically related to the fuel load and its distribution among the fuel particle size classes (Anderson, 1982). The classification of dead fuels into size classes is a standard convention derived from the "time lag" concept. Time lag refers to the amount of time it takes the moisture content of a dead fuel to equalize with that of the surrounding air (International Fire Service

Training Association, 1998). Specifically a time-lag period describes the moisture exchange to the amount of 63% (1-1/e, where e= base of natural logarithms [2.7182]) of the departure from equilibrium (Pyne, 1984). Fuels of short time-lag fuels reach such moisture equilibrium quickly, but fuels of long time-lag reach it more slowly (Countryman, in Omi, 1997). This variation allows classifying fuels as 1-hour, 10-hour, 100-hour, and 1000-hour fuel classes. The actual duration depends on the properties of the fuel, such as size and diffusivity (Anderson, 1989; Pyne, 1984). Size is related to the ratio of fuel surface to fuel volume. Particles with large surface-to-volume-ratios [e.g., needles and small twigs] respond rapidly (Pyne, 1984). Table 3.1 shows fuel sizes that correspond to each fuel class.

Table 3.1. Description of the fuel classes based on the time-lag principles (based on International Fire Service Training Association, 1998; and Countryman [in Omi, 1997]).

FUEL CLASSES	FUEL SIZE	FUEL EXAMPLES
1-hour	<6.35 mm	Dead grass and foliage, and twigs
10-hour	6.35 to 25 mm	Twigs
100-hour	25 to 76 mm	Branches, limbs
1000-hour	76 to 203 mm	Limbs and logs

Fire behavior predictions based on the fuel-model concept only consider the loads of 1-hour, 10-hour, and 100-hour fuels (as dead fuels). The loads of woody and herbaceous live plants are also considered in the fuel-model concept (as live fuels). There is not a clear description of the role of the litter in the definition of fuel classes.

3.2 Direct Fuels Inventory

The principal advantage of the direct fuels inventory is that fuels are mapped from actual conditions directly inventoried or recognized on the ground (e.g., using fuel-models photo series [Chandler *et al.* 1983; Fischer, 1981]). Keane *et al.* (1999b) reported that one of the first antecedents of direct fuel inventory was carried out in 1936, where, instead of descriptions of actual fuels loading, resistance to control and rate of fire spread were mapped. Since then, alternative inventory strategies have been developed to provide estimates of fuel loading (weight per unit area) in support of fire behavior predictions, such as the planar intersect technique that is used to estimate downed woody material (Brown *et al.* 1994). On the other hand, sample collection and linear regression techniques (relationship between fuel-weight/fuel-bed-depth) have been used to estimate forest floor weights (Flores, 1994; Brown *et al.* 1982).

Although the mapping error of direct fuels' surveys is limited to erroneous fuel type evaluation and sampling errors, the cost and the amount of labor needed for this type of fuels' mapping could make its use impractical (Keane *et al.* 1999b). Nevertheless, the combination of direct inventory techniques (with an adequate sample strategy), and remote sensing techniques can reduce considerably the cost and human effort in fuels' inventory. Fuel loads can be estimated at a desired precision with reduced investment of time and funds using double sample techniques (Fulé and Covington, 1994)

3.3 Remote Sensing of Mapping Forest Fuels

Remote sensing has had many applications in the forest fire arena, such as classification of fire risk areas, detection of burning areas, evaluation of fire scars, fire

management support, damage assessment, prescribed fire evaluation, and defining the relation between fire and vegetation ecology (Bosiak, 1986; Matson and Holben, 1987; Chuvieco and Congalton, 1989; Cappellini *et al.* 1990; Bovio *et al.* 1990; Pereira and Setzer, 1993). Aerial photography has been used to estimate fuel loading, based on regression equations that relate fuel loading with unit crown area (Meeuwig *et al.* 1979). On the other hand, one of the first attempts to apply satellite imagery to fuel mapping was to identify critical fire locations, based on the application of Landsat digital technology (Kourtz, 1978). Salazar (1982) recorded fuel classes using Landsat Multispectral Scanner (MSS) imagery and color IR aerial photographs, in order to produce a fuel map. However, incompatibilities between fuel model descriptions and remote sensing discrimination ability were found. Therefore, a supervised classification to use with MSS data in the creation of a fire fuel type map was proposed by Wilson *et al.* (1994) and Burgan and Shasby (1984).

Although the assessment of log debris has been accomplished using Landsat MSS (Singh, 1987; Lee and Kvarv, 1983), the evaluation of forest fuel loading cannot be made directly (especially fine fuels). An alternative is to relate some features of forest, which are easier to measure through remote sensing (such as density, crown density, and percent cover), with fuels characteristics. For example, litter loading could be estimated from measurements of stand density, such as basal area and stand density index. However, woody fuel loading does not correlate well with such stand variables (Fulé and Covington, 1994; Beyerhelm and Sando, 1982; Johansen *et al.* 1981; McCaw *et al.* 1997).

3.3.1 Normalized Difference Vegetation Index

Since the direct evaluation of fuels loads is not possible through the use of satellite imagery, most of the efforts have been focused on relating fuels with vegetation characteristics, such as canopy, biomass, leaf area index (LAI), and percent of vegetation cover (Friedl *et al.* 1994). Greenness was one of the first parameters used to quantify such characteristics (Burgan and Hartford, 1993). Though vegetation reflectance varies according to the band or band combinations used, greenness is a vegetation characteristic easy to define. Several algorithms have been developed to reduce the multiple bands of data to a single number per pixel that predicts greenness (Jensen, 1996). These algorithms are known as Vegetation Indexes, where the Normalized Difference Vegetation Index (NDVI) is one of the most used. This index indicates the quantity of actively photosynthesizing biomass (Eidenshink, 1992). NDVI has been related to the fuel availability to burn. A high value indicates vegetation with considerable moisture content, while low values indicate dry vegetation. Burgan and Hartford (1993) reported the monitoring of vegetation greenness at 1-km resolution, using data from AVHRR (NOAA-11), to calculate biweekly composites of NDVI. This information can be used to monitor the condition of vegetation for fire (Burgan *et al.* 1996).

The fuel model concept has been used as a generalized measure of the potential fire behavior (Keane *et al.* 1999b). Thus, one of the most important goals when using remote sensing techniques has been to generate maps that classify a given area into fuel model classes (Burgan *et al.* 1998). Although these maps have been used in the National Fire Danger Rating System (Deeming *et al.* 1977), their low resolution (1-km) makes them difficult to use in operational activities (e.g., prescribed burns).

3.4 Gradient Modeling

Remote sensing and GIS techniques have been used to correlate some landscape parameters with forest fuels loads. However, one of the main problems has been to understand the interactions among the various components of a dominant ecosystem (Keane *et al.* 1996; Kessell, 1976). Gradient modeling is a technique that can help to integrate such information. Nevertheless, its use has been very limited because it requires integration of systems of relational databases and simulation models (Keane *et al.* 1999a). Gradient modeling applies techniques of gradient analysis and ordination to describe and quantify continuous variation in the landscape and its vegetation (Keane *et al.* 1999a; Keane *et al.* 1999b; Kessell, 1976). In this sense, continuous variables, such as elevation and aspect, can determine the species composition of a forest stand (Kessell, 1976). Gradient modeling and remote sensing techniques can allow a comprehensive estimation of potential fuel loads (Keane *et al.* 1999b; Kessell, 1979; Kessell, 1976).

In 1976, Kessell introduced one of the first applications of fuel mapping based on gradient modeling. He developed gradient models of fuel, based on ten major environmental influences, such as elevation, topographic-moisture, primary succession, and intensity of the last burn. These models could be used to calculate fire spread rate and intensity, hectare by hectare. Considering that fuels' distribution and characteristics are not uniform, a multistrata fuel model could be used (Kessell, 1976), where each stratum would represent certain fuel characteristics (i.e., fuel loading, packing ratio, moisture content, and potential fire behavior). In this way, gradient modeling can be used to predict fuel-model maps, based on three vegetation layers of potential vegetation type, cover type, and structural stage (Keane *et al.* 1998b). Moreover, gradients provide an

ecological context to understand and estimate fuel dynamics (Keane *et al.* 1998b). For example, a site with low precipitation, and high evapotranspiration could explain low fuel loadings. However, the fuel maps generated through gradient modeling have not had consistent results (Keane *et al.* 1998).

3.5 Biophysical Modeling

The development of fuel maps is difficult and complex, requiring expertise in several disciplines, such as fire behavior, remote sensing, and GIS (Keane *et al.* 1999b). Since none of the described approaches combine such disciplines, Keane *et al.* (1998), and Keane *et al.* (1999a) proposed the integrated use of remote sensing, GIS and biophysical modeling to map fuels for fire management. Through this approach fuel-model maps can be created based on three maps: (a) Biophysical setting, which describes the long-term environmental conditions across the landscape (e.g. soil, topography and climate); (b) Cover type, which describes the plant composition based on the plurality of canopy or basal area; and (c) Structural stage, which describes surface and aerial fuel characteristics (Keane *et al.* 1998). The biophysical modeling approach has been tested in some regions, however there has been high variability in the accuracy assessment of the fuel-model maps generated (from 30 to 70 %) (Keane *et al.* 1999a; Keane *et al.* 1998).

3.6 Quantitative Spatial Analysis

3.6.1 Geostatistic Techniques Applied in Forestry

Geographical information systems and geostatistics have been powerful tools to support the evaluation of spatial variations of some components of forest ecosystems, such as pests, soil, and trees (Wackernagel *et al.* 1988; Samra *et al.* 1989; Höck *et al.*

1993; Liebhold *et al.* 1993). These evaluations are based on spatial correlations that support kriging techniques (Mandallaz, 1993). Most of the use of geostatistics in forestry has been referred to large scales, in which interpolations are defined in large grid cells (e.g., 2 by 2 km) and for very large regions (Gribko *et al.* 1995; Liebhold *et al.* 1993; Phillips *et al.* 1992). On the other hand, kriging techniques at small scale levels have been used in forestry to estimate the spatial distribution of soil parameters (e.g., pH, exchangeable potassium and available phosphorous) (Webster and Oliver, 1989). Metzger (1997) used geostatistics techniques to predict forest stand structure, using a trend surface model to describe the large-scale spatial variability, and cokriging to model the small scale spatial variability. A similar process was used by Kallas (1997) to model the spatial variability in the density of armillaria root disease. Hunner (2000) reported the first study in forestry that compared various interpolation techniques [five geostatistical methods were compared against three traditional estimation methods], to spatially model the number of stems, total basal area, and number of seedlings.

3.6.2 Quantitative Spatial Analysis of Forest Fuels

Kalabokidis and Omi (1994) used a large scale to develop an isarithmic analysis of forest fire fuelbed arrays based on kriging interpolation. Although interpolation techniques have been used to make some estimations related to forest fires (Flannigan and Wotton, 1989), it seems that the work of Kalabokidis and Omi is unique in specifically analyzing forest fuel distribution using quantitative spatial analysis. Interpolation techniques allow managing information in different scale levels, which make possible the development of a system where the information on forest fuels can be systematically integrated.

3.7 Expert Judgment

Although many sophisticated methodologies have been developed for fuel mapping, the advice of experts is still an important element for fuel model classification. Experience with local conditions is the major value of such experts. Fire behavior specialists are valuable to refine a fuel-model classification, based on their experience with local conditions (Buckley, 2001). An ideal combination would be a person with experience in fire fighting, fuel-model mapping and fire behavior. Fire danger and fuel classifications are very often refined based on the opinion of fire managers familiar with a given area (Burgan *et al.* 1998; Hawkes *et al.* 1996). However, some problems could arise when using experts' advice: (a) it is not always possible to find an expert for a specific area of interest; (b) an expert's advice is subjectively based on experience; (c) the lack of experience in certain conditions could make useless the opinion of a expert; (d) there is no guarantee that two, or more experts arrive to the same conclusion when classifying the same forest; (e) many years of experience are required to become an expert. Nevertheless, whenever possible opinion of an expert may be necessary.

4 SPATIAL INTERPOLATION TECHNIQUES

4.1 Principles of Interpolation

Interpolation techniques are based in the First Law of Geography: "*everything is related to everything else, but near things are more related than distant things*" (Chou, 1992, page 170). This means that values at points close together in space are more likely to be similar than points farther apart (Burrough and McDonnell, 1998). This principle is used to predict values of given phenomena in non-sampled areas, based on weighted linear combinations of nearby sampled values (Hunner, 2000):

$$\hat{Z}^*(x_0) = \sum_{i=1}^{n} \hat{\lambda}_i * Z(x_i) \qquad [4.1]$$

where:

$\hat{Z}^*(x_0)$ = the predicted value of variable Z at an unsampled location x_o;

$\mathbf{Z(x_i)}$ = the observed value of variable Z at the sampled location x_i;

λ_i = the weight assigned to the observed value $Z(x_i)$; and

n = the number nearby observed values.

The diversity of interpolation techniques is based on the way in which the λ_i weights are defined (Hunner, 2000). Some of the most used interpolation techniques are summarized below.

4.2 Deterministic Techniques

The methods of interpolation based on traditional statistics are relatively

straightforward, because they require only an understanding of deterministic statistical methods (Burrough and McDonnell, 1998). These include spline, inverse distance weighting, polygonal mapping, and Thiessen polygons (Hunner, 2000; Burrough, 1986).

4.2.1 Spline

Splines are drafting aids used to draw smooth curves through a set of points. Weights are attached at the points to be connected and a flexible strip is shaped around the weights (Levine and McKinley, 1999). Based on such principles, spline interpolation functions are mathematical equivalents of a flexible sheet of rubber that is fitted to a small number of data points exactly (piece-wise functions), ensuring that the joints between one part of the sheet and another are continuous (Burrough and McDonnell, 1998; Burrough, 1996). This generates a smooth and continuous surface, which is an advantage compared with the erratic behavior resulting from a polynomial (Levine and McKinley, 1999). However, spline techniques could result in maximum or minimum values that do not occur at the data points (Burrough, 1996), even possible negative values. A detailed description of this technique is given in Burrough and McDonnell (1998).

Spline techniques has been applied in many different fields, such as climate (Lennon and Turner, 1995; Wotling *et al.* 2000; Custer *et al.* 1996), soil science (Bishop *et al.* 1999; Nemes *et al.* 1999; Ladewig and Marlander, 1997), hydrology (Arnold *et al.* 2000; Durrans *et al.* 1999), pollution (Montas *et al.* 1998; Ladewing and Marlander, 1981), and agriculture (Zanetti *et al.* 1999; Hill *et al.* 1989). Although spline interpolation

techniques have been used also in forestry (Degenhardt and Hempel, 1996; Mackey *et al.* 1996), only one paper was found regarding forest fire (Flannigan and Wotton, 1989). In this work, the smoothed cubic spline is applied to estimate fire danger between weather stations.

4.2.2 Inverse Distance Weighting

Inverse distance methods assume that the value of an unsampled point is a distance-weighted average of the values of observed points occurring nearby (Burrough and McDonnell, 1998). This interpolation technique gives more weight to closer observations than those that are farther away (Hunner, 2000). Such weights are inversely proportional to the distance between the point to be predicted and the data of nearby points computed, and are computed from a linear function (Potter and Eenigenburg, 1999; Burrough and McDonnell, 1998; Isaak and Srivastava, 1989):

$$\hat{\beta}^*(x_0) = \frac{\sum_{i=1}^{n} \frac{1}{d_i^p} * \beta(x_i)}{\sum_{i=1}^{n} \frac{1}{d_i^p}} \qquad [4.2]$$

where:

$\hat{\beta}^*(x_0)$ = estimated value at unsampled location x_0;

$\beta(x_i)$ = observed value at location x_i;

d_i = are the distances from each observed locations to the unsampled point;

p = distance exponent;

n = number of sampled points

The choice of power parameter (p) can significantly affect the interpolation results. As p increases, the individual weights become more similar, with most weight given to the nearest sample (Hunner, 2000). When p is decreased, the weights become more similar (Isaaks and Srivastava, 1989). Optimal inverse distance weighting is achieved when the p parameter is chosen on the basis of minimum mean absolute error (Collins and Bolstad, 1995). Estimates can often be improved by incorporating more nearby samples, however they can also be adversely affected if the nearby samples are strongly clustered (Isaaks and Srivastava, 1989).

Inverse distance weighting has been used in several fields, such as soil science (Dowdall and O'Dea, 1999; Kravchenko *et al.* 1999), hydrology (Dirks *et al.* 1998); atmospheric science (Price *et al.* 2000; Xia *et al.* 1999; Punyawardena and Kulasiri, 1998). In forestry inverse distance techniques have been applied in forest-climatic relationships (Nalder and Wein, 1998; Phillips *et al.* 1997; Xia *et al.* 1999), wood estimation (Fazakas *et al.* 1999) and surveying (Guardado and Sommers, 1977). No application of this technique was found with respect to forest fires. The reason for this could be that current studies of fuels mapping are mostly based on indirect methodologies, such as spectral classification (remote sensing), and relationships between fuels and biophysical parameters.

4.2.3. Polygonal Mapping

Polygonal mapping interpolation techniques assume that all important variation of a given variable occurs at boundaries (polygons), and that within boundaries the variation

is homogeneous and isotropic (Burrough, 1986). This approach results in the simplest method of interpolation, which incorporates the information of all the samples of a given polygon, weighting them all equally. Any value at unsampled locations, within the same polygon, is estimated using the polygon's mean (Hunner, 2000). This methodology generates a model of the landscape of discontinuous ("stepped") surface plateaus (Hunner, 2000; Burrough, 1986). Polygons are delineated using different criteria, such as forest density, species, soil and vegetation. Polygonal mapping may not be appropriate when the spatial variation of the variable of interest is gradual (Burrough, 1986).

The principal problem with polygonal mapping is inexact boundaries (Lowell, 1996). Thus, few works use this interpolation technique. Some of its applications have been in environmental surveys (Dowdall and O'Dea, 1999), representation of forest volume (Lowell, 1996), forest stand mapping (Magnussen, 1996), agroclimatological assessment (Soderstrom and Magnusson, 1995), and soil science (Burrough *et al.* 1991). Although not explicitly, this technique has been used in the forest fire arena to map fire history (Everett *et al.* 2000), and fire regimes (Roberts and Li, 1996). Nothing was found regarding fuels mapping.

4.2.4 Thiessen

This interpolation method is also known as Voronoi polygons (diagrams) or Dirichlet polygons (diagrams or cells) (DeMers, 1997). It is based on idea that the "best" value of an unsampled point is that that corresponds to the nearest sampled point. The sample layout determines the way in which a given region will be divided up into polygons. At the same time, the shape and size of such polygons depends on the configuration of the

sample points (Burrough, 1986). A polygon has the unique property that any location within the polygon is closer to that polygon's point than to the point of any other polygon (Gold, 1989). Since the value of an unsampled point is estimated by a sample of one, error margins of such estimation cannot be determined. The Thiessen approach contradicts the first law of geography, and therefore is best suggested for nominal data (e.g. vegetation or land use). Nevertheless, it is considered an exact predictor, because all estimations equal the values at the sample points (Burrough and McDonnell, 1998).

A common use of the Thiessen approach is with climatic data where, in absence of local data, one uses the observations from the nearest available weather station (Burrough, 1986). Thiessen interpolation is applied when data are discrete rather than continuous in space, as in the case of elevation or temperatures. This technique has been applied in diverse disciplines, such as atmospheric sciences (Lopes, 1996; Borga *et al.* 1994), soil science (Oberthurt *et al.* 1999; Goovaerts and Journel, 1995), hydrology (Mimikou and Baltas, 1996; Panagoulia, 1992). Some uses of Thiessen interpolation in forestry are: inventory (Raspe *et al.* 1989); landscape (Parresol *et al.* 1997); tree competition (Kenkel *et al.* 1989); and correlation patterns (Huhn and Langner, 1999). Impara (1997) used Thiessen polygons to define the spatial patterns and size of fire episodes.

4.3 Geostatistical Techniques

4.3.1 Regionalized Variable Theory

Deterministic estimation of unsampled points requires a model that describes in detail the spatial variation of a given phenomenon (e.g., soil, elevation, species, and

fuels). However, the uncertainty about how the phenomenon behaves between sample locations limits the application of deterministic models (Isaaks and Srivastava, 1989). Geostatistical techniques of interpolation (also known as kriging) attempt to deal with such uncertainty, describing the spatial variation (of a continuous phenomena) as a spatial structure [based on the first law of geography] that can be described by a stochastic approach (Hunner, 2000). With this idea, the data values are viewed as the outcomes of a random (probabilistic) mechanism (Goovaerts, 1997). Under this condition of randomness, a phenomenon is known as a "regionalized variable" (Burrough and McDonnell, 1998). Hunner (2000), Amstrong (1998), and Ramírez (1980) give a detailed description of the regionalized variable theory.

A regionalized variable has two characteristics (Hunner, 2000): (a) *a random, **erratic component** that is related to the local behavior of the phenomenon*; and (b) *a general, **structured component** that is related to the overall distribution of the phenomenon*. The stochastic approach provided by random functions takes these two characteristics into account (Hunner, 2000). A random function is a set of random variables that have a corresponding spatial location (Isaaks and Srivastava, 1989, Ramírez, 1980). Although many realizations of a random function are required in order to define its probability law, in practice one is limited to a single realization (Hunner, 2000). To deal with this problem the concept of stationarity is used, which refers to the degree of invariance in the characteristics of random functions (e.g., mean and variance), when shifting a given set of points from one place to another [within the area of interest]. Such homogeneity (invariance) implies that the observed values of two locations, separated by a distance h, can be considered as two different realizations of the same random variable

(Hunner, 2000). Thus, a condition of stationarity provides the potential of many realizations of the same random function, which permits a certain amount of statistical inference (Hunner, 2000). However, demonstration that a natural phenomenon shows a complete stationarity is very difficult. The alternative is to assume our random function under a second-order stationarity, where it is enough that two moments exist: (a) stationarity of the mean [$E[Z(x)\} = m, \quad \forall x$]; and (b) stationarity of the covariance [$C(h) = E\{Z(x) \cdot Z(x+h)\} - m^2, \quad \forall x$] (Hunner, 2000). The condition of an existing covariance implies the assumption of a finite *a priori* variance (Ramírez, 1980). Since many physical phenomena have an infinite capacity of variation, no *a priori* variance exists (Hunner, 2000). Thus, a "weak" second-order stationarity (intrinsic hypothesis) is assumed, in which the stationarity is limited to the increments [$Z(x)-Z(x + h)$] of the random function. In this way, the intrinsic hypothesis assumes only the existence and stationarity of the variogram (a second-order moment), which represents the variance of the increments of the random function ($Z(x)$) (Hunner, 2000).

4.3.2 Structural Analysis

Geostatistic interpolation consists of two processes: (1) a structural analysis; and (2) the kriging techniques. Structural analysis is the investigation and modeling of the patterns of spatial correlation that characterize a regionalized variable. The resulting features of this structural analysis are applied, through the kriging techniques, to define the weighting factors (Hunner, 2000). Structural analysis is based on spatial correlation (autocorrelation and cross-correlation). Spatial autocorrelation is a measure of the spatial similarity between two values in relation to their proximity. Measurements made in close proximity tend to be more alike than those taken farther apart (Bonham *et al.* 1995).

Direction and extent of this spatial effect ("first law of geography") is also indicated by spatial autocorrelation (Chou, 1992). On the other hand, spatial cross-correlation characterizes the spatial relationship between two regionalized variables (Bonham *et al.* 1995).

4.3.2.1 Spatial Correlation. Before starting any interpolation study, it is important to know if observed values are spatially correlated. Spatial autocorrelation testing determines if a variable is randomly distributed, or if its distribution follows a given pattern (Metzger, 1997). If the known values are spatially correlated, they can be used to predict values of interest in unsampled areas (Bonham *et al.* 1995). Although it is suggested to analyze both spatial autocorrelation and cross-correlation before working with geostatistic techniques, few works report such testing (Metzger, 1997; Kallas, 1997).

Moran's I. There are many available statistics to do an exploratory analysis of spatial autocorrelation, such as Moran's *I* coefficient, Geary's coefficient, spectral analysis, Mantel's test, wavelet analysis and joint count statistics (Czaplewski *et al.* 1994; Reich and Geils, 1992; Cliff and Ord, 1973). Moran's *I* provides a powerful test of hypothesis and it is more sensitive to extreme values than other methods (Czaplewski *et al.* 1994). The use of this coefficient has been reported in some forestry works focused on geostatistical analysis (Metzger, 1997; Kallas, 1997; Czaplewski *et al.* 1994; Reich *et al.* 1994). The following formula shows the Moran's *I* coefficient with generalized weights (Reich and Davis, 1998; Chou, 1991):

$$I = \frac{n\sum_{i=1}^{n}\sum_{j=1}^{n} W_{ij}(x_i - \bar{x})(x_j - \bar{x})}{S_0\sum_{i=1}^{n}(x_i - \bar{x})^2} \qquad [4.3]$$

where:

n = number of locations (or points);

W_{ij} = generalized weight denoting the spatial relationship between the i-th and the j-th locations;

x_i = observed value at the i-th location;

x_j = observed value at the j-th location;

S_o = $\Sigma_i\Sigma_j W_{ij}$ sum of the weights; and

$\bar{x}$ = Mean of observed values

This coefficient is analogous to a Pearson product-moment correlation coefficient, but the terms within the summation in the numerator are each weighted by an interlocality [W_{ij}] (Wartenberg, 1985). A large value (near to 1) of I indicates a positive correlation, while a small value (near to −1) indicates a negative correlation. A I value close to zero suggests no correlation (Reich and Davis, 1998). The expected value and the variance of this coefficient can be derived under the assumption of either randomness or normality (Chou *et al.* 1990). The former assumes a random permutation of data values, while the latter assumes the study variable is independent and identically distributed. The expected value is the same under either assumption (Chou *et al.* 1990). Under the assumption of normality, the expected value of Moran's I will be (Chou, 1989):

$$E(I) = 1/1\text{-}n \qquad [4.4]$$

The expected value is always negative (Chou, 1989). Detailed derivation of the statistical testing of Moran's *I* is given in Czaplewski *et al.* (1994) and (Chou, 1992).

Bivariate Moran's I. The exploratory analysis of the cross-correlation between two response variables (y_i and z_j) is estimated by the Bivariate Moran's *I*. The expected value of this statistic is (Metzger, 1997; Wartenberg, 1985):

$$I_{yz} = \frac{\sum_{i=1}^{n} \sum_{j=1}^{n} w_{ij} y_i z_j}{W \sqrt{m_y^2 m_z^2}} \qquad [4.5]$$

where;

w_{ij} = a scalar that quantified the degree of spatial association or proximity between location i and j;

y_i = the observed value of the variable y transformed to have a mean of zero (i=1,2,..,n);

z_j = the observed value of the variable z transformed to have mean of zero (j=1,2,..,n);

W = the sum of all n^2 values of w_{ij};

m_y^2 = the sample variance of y_i; and

m_z^2 = the sample variance of z_i.

The expected value of the cross-correlation statistic (I_{yz}), under the null hypothesis of no spatial correlation between two response variables (y_i and z_j) is given by (Metzger, 1997; Kallas, 1997):

$$E[I_{yz}] = \frac{-Cov(yz)}{(n-1)\sqrt{Var(y)Var(z)}} \quad [4.6]$$

Detailed derivation of the statistical testing of Bivariate Moran's I is given by Bonham *et al.* (1995), and Metzger (1997).

4.3.2.2 Spatial Continuity. *Variogram*. There are other indices to evaluate the spatial correlation between variables, such as the coefficient of correlation, the covariance and the moment of inertia about the line $x=y$ (Isaaks and Srivastava, 1989). These indices are used to model spatial continuity through the definition of correlograms, covariograms, and variograms, respectively. Correlograms are a special case of Moran's I that use 0-1 weights for a range of mutually exclusive lag spacings (Czaplewski *et al.* 1994). Geostatisticans prefer to work with variograms, because their definition requires only intrinsic stationarity (Hunner, 2000). The variogram is the basic tool of kriging, it is used to model the spatial correlation between observations. Once a mathematical model has been fitted to the experimental variogram, this model can be used (through kriging techniques) to estimate values at unsampled points.

If the conditions specified by the intrinsic hypothesis are fulfilled, the random (but spatially correlated) component of the regionalized variable can be estimated from the sample data through the calculation of the semivariance [$\gamma(h)$](Burrough and McDonnell, 1998). The semivariance is half of the squared difference for two data points separated by distance h (known as the lag), and can be estimated using the following equation (Hunner, 2000):

$$\gamma(h) = \frac{1}{2N(h)} \sum_{i=1}^{N(h)} [Z(x_i) - Z(x_i + h)]^2 \qquad [4.7]$$

where:

$Z(x_i)$ = the sample value of variable Z at location x_i;

$Z(x_i+h)$ = the sample value of variable Z at location x_i+h; and

$N(h)$ = the number of pairs of observations separated by distance h.

When we plot $\gamma(\mathbf{h})$ against $\mathbf{h}$ we get an experimental variogram, which is the first step toward a quantitative description of the regionalized variation. If the variogram increases faster than the squared value of h, which implies that the mean is not constant, the regionalized variable is not stationary (Armstrong, 1998). A variogram is used to describe how the average difference between observations of a regionalized variable changes as a function of distance (lag= h) and direction (Goovaerts, 1997; Isaaks and Srivastava, 1989). In general, such difference tends to increase with increasing lag distance (Hunner, 2000). A detailed description of a variogram structure is given by Hunner (2000), Goovaerts (1997), and Isaaks and Srivastava (1989).

There are three important features to characterize a variogram: the range, the sill, and the nugget effect. As the lag distance increases, the semivariance value increases. Eventually, the lag distance no longer affects the semivariance and then the variogram reaches a plateau (maximum value), which is called the ***sill***. The lag distance at which the variogram reaches this maximum value (sill) is called the ***range***. Sampling error, and short scale variability may cause values separated by extremely small distances to be quite different, producing a discontinuity at the origin of the variogram called the ***nugget***

effect. To select the lag distance, both lag increment and lag tolerance must be considered, tending to look for the "smoothest" variogram structure (Hunner, 2000). This process is iterative, depending on the amount and type of data, thus there are not specific rules. Beside lag distance, direction of the variogram is another important feature of the analysis of spatial continuity. When spatial correlation is independent of direction the variogram is isotropic, and is referred to as omnidirectional. On the other hand, an anisotropic variogram shows that spatial correlation changes with direction. In this case several directional variograms should be defined.

Once the experimental variogram has been defined, a mathematical model must be fitted to it. The reason for this is that may there are some distances, or directions, from which we do not have an observed variogram value (Isaaks and Srivastava, 1989). Although one could be tempted to use least squares or other automatic methods to fit variogram models, there are certain conditions for such modeling. Armstrong (1998) summarizes them as follow: (1) The model must be a positive definite function. This is *a guarantee that the variance of any random variable formed by a weighted linear combination of other random variables will be positive* (Isaaks and Srivastava, 1989). It is rare that polynomials resulting from least squares regression satisfy this condition; (2) Least squares regression assumes that sample points are independent observations. A variogram consists of square differences of spatially correlated values; and (3) It is vital to know the behavior of the variogram very close to the origin. Least squares regression does not take account of this.

Since it is not easy to verify the positive definiteness condition of new functions, one way to satisfy such condition is to use functions that are known to be positive definite. The following are some of the more applied variogram models that are conditionally positive definite (Hunner, 2000; Armstrong, 1998; Goovaerts, 1997):

(1) ***Spherical Model***:

If $h \leq a$: $\gamma(h) = C_0 + C_1 \cdot 1.5 \cdot h/a - 0.5 \cdot (h/a)^3$ **[4.8]**

Otherwise: $\gamma(h) = C_0 + C_1$ **[4.8b]**

where:

h = the lag distance;

a = the range;

C_0 = the nugget effect;

$C_0 + C_1$ = the sill; and

$\gamma(h)$ = the variogram value at lag distance (h)

This model has a linear behavior at small separation distances near the origin, however flattens out at larger distances, reaching the sill at a (Isaaks and Srivastava, 1989).

(2) Exponential Model:

$$\gamma(h) = C_0 + C_1 \cdot \left[1 - \exp\left(\frac{-3h}{a}\right)\right] \quad \textbf{[4.9]}$$

Since this model reaches its sill asymptotically, range a is defined as that distance at which the variogram value is 95% of the sill. Like the spherical model, this model is

linear at very short distances near the origin, but it rises more steeply and then flattens out more gradually than the former (Isaaks and Srivastava, 1989).

(3) Gaussian Model

$$\gamma(h) = C_0 + C_1 \cdot \left[1 - \exp\left(\frac{-3h^2}{a^2}\right)\right] \qquad \textbf{[4.10]}$$

This model is a transition model that is often used to model extremely continuous phenomena. Like the exponential model, the Gaussian model reaches its sill asymptotically (95% of range), but with a parabolic behavior near to the origin (Isaaks and Srivastava, 1989).

Cross-variogram. Let $Z_j(x_i)$ and $Z_k(x_i)$ be two regionalized variables having a joint probability distribution that satisfies the intrinsic hypothesis (see section 4.3.1), then the cross-variogram $\gamma_{jk}(h)$ is a measure of their joint spatial variability (Olea, 1991). As the Bivariate Moran's *I* analysis, the cross-variogram is applied to describe the cross-continuity between two regionalized variables. It is defined as half the non-centered covariance between h-increments (Goovaerts, 1997), and it pairs values of different variables at different locations (Hunner, 2000):

$$\gamma_{ZW}(h) = \frac{1}{2N(h)} \sum_{i,j=1}^{N(h)} [Z(x_i) - Z(x_i + h)] \cdot [W(x_j) - W(x_j + h)] \qquad \textbf{[4.11]}$$

where:

$\gamma_{ZW}(h)$ = the cross-variogram value for primary variable Z and secondary variable W separated by distance h;

$Z(x_i)$ = the value of the primary variable Z at location x_i;

$Z(x_i+h)$ = the value of the primary variable at location (x_i+h);

$W(x_j)$ = the value of the secondary variable at location x_j;

$W(x_j+h)$ = the value of the primary variable at location (x_j+h); and

$N(h)$ = the number of pairs of observations separated by distance h

Before calculating a cross-variogram, the experimental variograms for the two spatially correlated variables are modeled. Then the cross-variogram for the combination of both variables is modeled. All three models serve as input for the cokriging techniques. To ensure that the variance is non-negative, both the variogram and cross-variogram models must be conditionally positive semi-definite (Goovaerts, 1997). Hunner (2000) and Goovaerts (1997) gave a detailed description of cross-variogram theory.

4.3.3 Ordinary Kriging

Ordinary kriging (OK) is applied when the mean of the data values is stationary (constant), but unknown. OK is considered as the "best linear unbiased estimator" (Hunner, 2000; Isaaks and Srivastava, 1989): (a) Linear, because its estimates are weighted linear combinations of the available data; (b) Unbiased, because it tends to generate a mean square error equal to zero (E[Estimated(x_0)-True(x_0)] = 0, and $\Sigma\lambda_i = 0$); and (c) Best, because it aims at minimizing the variance of the errors (E{[Estimated(x_0) – True(x_0)]^2 = minimum). Isaaks and Srivastava (1989) described in detail the mathematical derivation of these constraints, and of the systems of equations to determine interpolation weights (λ_i). The following formulas are used to calculate the OK estimates and variance, respectively (Hunner, 2000; Isaaks and Srivastava, 1989):

$$\hat{\rho}_{OK}(x_0) = \sum_{i=1}^{n} \lambda_i \cdot \rho(x_i) \qquad \textbf{[4.12]}$$

$$\sigma^2_{OK}(x_0) = C(x_0, x_0) - \sum_{i=1}^{n} \lambda_i \cdot C(x_i, x_0) + \mu \qquad \textbf{[4.12b]}$$

where:

$\hat{\rho}_{OK}(x_0)$ = ordinary kriging estimate at location x_0;

λ_i = the weight for sample point i at location x_i;

$\rho(x_i)$ = the value of the observed variable ρ at location xi;

$\sigma^2_{OK}(x_0)$ = ordinary kriging variance at location x_0;

$C(x_0, x_0)$ = the covariance of the point to estimate at location x_0 with itself;

$C(x_i, x_0)$ = the covariance of the sample point at location x_i and the point to estimate at location x_0; and

μ = Lagrange parameter

The general process for ordinary kriging starts with the sample data, which are used to calculate an experimental variogram. Then, a variogram model is fitted to the experimental variogram. After that, the sample data and the variogram model are used as inputs of the ordinary kriging procedure. Finally both the ordinary kriging estimates and the ordinary kriging variances are generated (Hunner, 2000).

Ordinary kriging has been applied in many disciplines, such as ecology (Nash *et al.* 1992; Boyer *et al.* 1991), soil science (Lark, 2000; Jahangard, 1999; Kravchenko, 1999), and hydrology (Goovaerts, 2000; Prudhomme and Reed, 1999; Rizzo and Dougherty, 1994). Specifically in forestry, ordinary kriging has been used to compare sampling strategies (Dessard, 1999), to estimate ozone exposures (Phillips *et al.* 1997), to predict gypsy moth dynamics (Regniere and Sharov, 1997; Hohn *et al.* 1993; Liebhold *et al.* 1991), and to estimate site index (Höck *et al.* 1993). Kalabokidis and Omi (1995) and Robichaud (1996) reported the only applications of this technique in forest fire sciences.

The former study used ordinary kriging to support an isarithmic analysis of forest fire fuelbed arrays. The latter reports an evaluation of the spatial variability of fire severity factors using ordinary kriging.

4.3.3.1 Point Kriging. Ordinary kriging can be performed in point (same support as data) or block mode. In many cases, both ordinary kriging and point kriging are considered as synonymous. However, point kriging (or punctual kriging) is a specific mode of OK, in which both the observations and the estimates have the same support, as in the case when the supports are points (Olea, 1991). The counterpart is "block kriging" (OK performed in block mode. See 4.3.3.2). In geostatistics the term "support" refers to the size and volume of a sample (Armstrong, 1998). The variogram used in point kriging must be defined for the same support. The choice of point kriging should be made on the basis of sampling design and characteristics of the regionalized variables. If samples were taken to represent point values in a field, then point kriging may be appropriate (Robertson, 2000). Most of the applications of punctual kriging are related to soil science, where ordinary kriging is applied in the point mode (Burgess and Webster, 1980; Trangmar *et al.* 1986). No application of this technique in forestry was found.

4.3.3.2 Block Kriging. In many cases a regionalized variable is measured as the average within a predefined local area than at a point (Armstrong, 1998). This is referred as "block kriging", where the local area is discretized into many points and individual points estimates are averaged together over the area (Isaaks and Srivastava, 1989). By making this single alteration, we can convert the ordinary-point-kriging system to an ordinary-block-kriging system (Isaaks and Srivastava, 1989). In other words, block

kriging refers to the fact that the estimation is performed over larger support than the data (Goovaerts, 2001 personal communication). The estimation variances obtained for block kriging are substantially less than for ordinary-point-kriging, thus the resulting smoothed interpolated surface is free from the pits and spikes resulting from point kriging (Burrough, 1986). Goovaerts (1997), and Isaaks and Srivastava (1989) give a detailed description of the block kriging methodology.

Block kriging has been applied in many disciplines, however most of such applications have been in soil science (Andronikov *et al.* 2000; Coquet, 1998; Burgess and Webster, 1980). Other uses are related to atmospheric science (vanLeeuwen *et al.* 1996; Byers, 1987), pollution (Meuli *et al.* 1998), and hydrology (Grimes *et al.* 1999; Grewal, 1996). The application of this technique in forestry is also mostly focused on soil science: spatial and temporal patterns of soil biological activity (Gorres *et al.* 1998); improved soil monitoring (Bringmark and Bringmark, 1998); and geostatistical analysis of soil properties (Gonzalez and Zah, 1994). No applications of this technique in forest fire sciences were found.

4.3.4 Universal Kriging

In some data sets the stationarity condition is not clear, because there is a gradual trend (drift) in the data values. In these cases, OK should not be applied as it yields erroneous and biased results (Hunner, 2000). Alternatively, an adaptation of ordinary kriging that allows dealing with such trend (minimizing the error associated) is applied which is called universal kriging (UK). A synonym of UK is "kriging with a trend" (Goovaerts, 1997). One of the advantages of UK is that it can be used to estimate the

underlying trend itself (Isaaks and Srivastava, 1989). Once the trend has been estimated, it is subtracted from the observed sample values to obtain the corresponding residuals. Then the estimation is done on such residuals, and finally the trend is added back. The understanding of the genesis of the phenomenon allows choosing the more adequate trend model (Isaaks and Srivastava, 1989). The trend is assumed to be a linear combination, and it depends on the coordinates of the location being estimated and of the data location (Hunner, 2000; Goovaerts, 1997). The estimated trend, at any location, is obtained by combining the estimated coefficients with the values of the functions (typically 1^{st} and 2^{nd} degree polynomials) at that location (Hunner, 2000). For example, a linear trend has three functions and coefficients ($m(x) = a_0 + a_1x + a_2y\ldots$,[$x$ and y are coordinates]). Hunner (2000) gives a detailed description of the universal kriging process.

Universal kriging can produce good estimates, especially where the estimate is extrapolated rather than interpolated (Isaaks and Srivastava, 1989). UK has been applied in diverse disciplines, such as soil science (Berke, 1999; Crawford and Hergert, 1997; Bourennande *et al.* 1996), hydrology (Markus *et al.* 1999; Lopez *et al.* 1996), and climatology (Hudson and Wackernagel, 1994). Some of the applications of UK in forestry are related to pest management planning (Regniere and Sharov, 1999), forest inventory (Mandallaz, 1993), forest soils (Meshalkina *et al.* 1995), climatic data for forest growth models (Nalder and Wein, 1998), and modeling forest stand structure (Hunner *et al.* 2000). No applications of this technique in forest fire sciences were found.

4.3.5 Cokriging

In some cases, we can improve our estimations if we relate our variable of interest with ancillary data. In such cases we are using the potential cross-correlation between the

variable of interest and a secondary variable(s). The information contained in the ancillary variable(s) should help to reduce the variance of the estimation error (Isaaks and Srivastava, 1989). Cokriging is the method that allows dealing with such cross-correlation. It utilizes multivariate information to determine estimates at unsampled points (Hunner, 2000). One advantage of cokriging is that it is not necessary that secondary data be available at all locations being estimated (Goovaerts, 1997). Thus the usefulness of the ancillary variable(s) is often enhanced by the fact that the variable of interest is undersampled (Isaaks and Srivastava, 1989). The estimates are derived using a weighted linear combination of primary and ancillary data values, assuming stationarity of both primary and ancillary variables (Hunner, 200). The estimation of weights requires the variograms for both primary and ancillary variable(s), and the corresponding cross-variograms for the possible combination of such variables. Cokriging applies two unbiasedness conditions (Isaaks and Srivastava, cited by Hunner, 2000):

$$\sum_{i=1}^{n} \lambda_i^Z = 1 \qquad \text{and} \qquad \sum_{j=1}^{m} \lambda_j^W = 0 \qquad \textbf{[4.13]}$$

where:

λ_i^Z = the weights for the n data values of the primary variable Z. At least one sample value is required; and

λ_j^W = the weights for the m data values of the secondary variable W

The following equations are used to calculate the cokriging estimates and variance respectively (Hunner, 2000):

$$\hat{\alpha}_{CK}(x_0) = \sum_{i=1}^{n} \lambda_i^{\alpha} \cdot \alpha(x_i) + \sum_{j=1}^{m} \lambda_j^W \cdot W(x_j) \qquad \textbf{[4.14]}$$

$$\sigma^2_{CK}(x_0) = C^{\alpha}(x_0^{\alpha}, x_0^{\alpha}) + \mu_1 - \sum_{i=1}^{n} \lambda_i^{\alpha} \cdot C^{\alpha}(x_i^{\alpha}, x_0^{\alpha}) - \sum_{j=1}^{m} \lambda_j^{W} \cdot C^{W\alpha}(x_j^{W}, x_0^{\alpha}) \quad [4.15]$$

where:

$\hat{\alpha}_{CK}(x_0)$ = cokriging estimate at location x_0;

$\sigma^2_{CK}(x_0)$ = cokriging variance at location x_0;

$C^{\alpha}(x_o^{\alpha}, x_o^{\alpha})$ = the covariance of primary variable α at a unsampled location x_o with itself;

$C^{\alpha}(x_i^{\alpha}, x_o^{\alpha})$ = the covariance of primary variable α at a location x_i and a primary variable α at a an unsampled location x_o;

$C^{\alpha W}(x_j^{W}, x_o^{\alpha})$ = the cross-covariance of secondary variable W at location x_j and primary variable α at location x_o; and

μ_1 = the Lagrange parameter for the primary variable

Hunner (2000), Goovaerts (1997), and Isaaks and Srivastava (1989) give a detailed description of the cokriging methodology. Cokriging have been used in soil science (Juang *et al.* 2000; Pozdnyakova *et al.* 1999), hydrology (Li *et al.* 1999; Bracq and Delay, 1999; Martinez, 1996), atmospheric science (Goovaerts, 2000; Estrada, 2000), and ecology (Nash *et al.* 1992). Some forestry examples are the modeling of a forest stand structure (Hunner, 2000; Metzger, 1997), estimation of ozone exposure in forests (Phillips *et al.* (1997), analysis of precipitation in mountainous terrain (Phillips *et al.* 1992), and disease hazard rating mapping (Kallas, 1997). No applications of this technique in forest fires studies were found.

4.4 Cross-validation

Dealing with different interpolation methodologies requires a way to compare them, in order to be able to select the "best" one. Cross-validation can be used to evaluate

the performance of different interpolation techniques (Goovaerts, 1997). This methodology consists of removing the sample value at a particular location (at a time), then such value (at the same location) is re-estimated from the remaining data (Burroughs and McNonnell, 1998; Goovaerts, 1997; Isaaks and Srivastava, 1989). When each sample value has been left out and predicted, we can compare interpolated and actual values. The differences between interpolated and true values are called residuals [errors] (Hunner, 2000). The calculation of the residuals allows us to evaluate the performance of the different interpolation techniques. Diverse measures are used for such evaluation, some of them are described as follow:

A) Mean Square Error

If the interpolation suits perfectly the data, the mean of the error (bias) distribution should be zero, with a small variance (spread) (Armstrong, 1998). However, in practice this is very difficult, therefore our goals should be to get an error distribution with minimum spread and a mean close to zero (unbiased estimates). Mean square error (MSE) is a summary statistics that incorporates both the bias and the spread of the error distribution ($MSE=variance+bias^2$), which is calculated as (Isaaks and Srivastava, 1989):

$$MSE = \frac{1}{n}\sum_{i=1}^{n} r^2 \qquad \textbf{[4.16]}$$

where:

n = the number of sample points; and

r = the residuals

Using MSE as selection criterion, we are looking for the smaller MSE.

B) Histogram of the Residuals

A histogram displays the frequency distribution of errors, allowing the visual checking of their unbiasedness, small spread and normality (Hunner, 2000).

C) q-q Plot of the Residuals

A q-q plot is another way to evaluate the normality of residuals. This plot displays the quantiles of a data set versus the quantiles of a reference theoretical distribution. If the plot is a straight line, the data are normally distributed (Hunner, 2000).

D) Conditional Unbiasedness

A scattergram plotting the estimated values versus the residuals can be used to check on the properties of any range of errors (the errors should evenly spread around the zero line), which is called conditional unbiasedness (Hunner, 2000).

E) Scatterplot of Predicted Values versus True Values

This scatterplot allows checks on the bivariate distribution of estimated and actual values, where the closer the cloud of points to the 45-degree line, the better the estimation (Hunner, 2000).

F) Correlation Coefficient

The correlation coefficient detects the linear correlation between the estimated and actual values (the closer to 1 or -1 the better). This parameter can be applied to summarize how closely the points in the scatterplot of predicted values versus true values come to falling on a straight line (Hunner, 2000).

5 FIRE BEHAVIOR SPATIAL MODELS

Forest fires are very complex natural phenomena. The lofting and subsequent ignition of secondary fires by burning debris constitutes an important form of wildland fire propagation The availability of faster computing hardware and more efficient numerical algorithms permits the consideration of more accurate modeling procedures than in the past (Garzon, 1997).

5.1 Major Conceptual Models

Forest fires require an information system that can support spatial and temporal query, analysis, and modeling. A fundamental problem is to store spatio-temporal data in an efficient form in terms of data storage and operation (Yuan, 1994a). Accordingly, there are four major conceptual models in order to design a GIS data model that is able to support spatio-temporal reasoning about forest fires (Figure 5.1): locational snapshots, fire entities, entity snapshots, and fire mosaics.

The **locational snapshot** model emphasizes that spatial units and locations are pre-determined. Individual spatial units describe reality, which is the basis of the cell based approach. Studies of fire forecasting use this approach, because most of data used are pre-determined from remote sensing and pixels. The model of **fire entities** is used to describe fire spread and motion according to individual fire spatial positions through time. Fire spread and or motion is described by its changes in burn positions through time. The model of **entity snapshots** differs from the model of locational snapshots in that descriptions are done according to a focussed entity, such as fire, instead of

locations. The model of **fire mosaics** describes reality by a set of spatially exhaustive polygons, each of which is different from its neighbors in terms of a certain attribute (e.g. the corresponding fuel model). The algorithms that support this approach are based on vector based models.

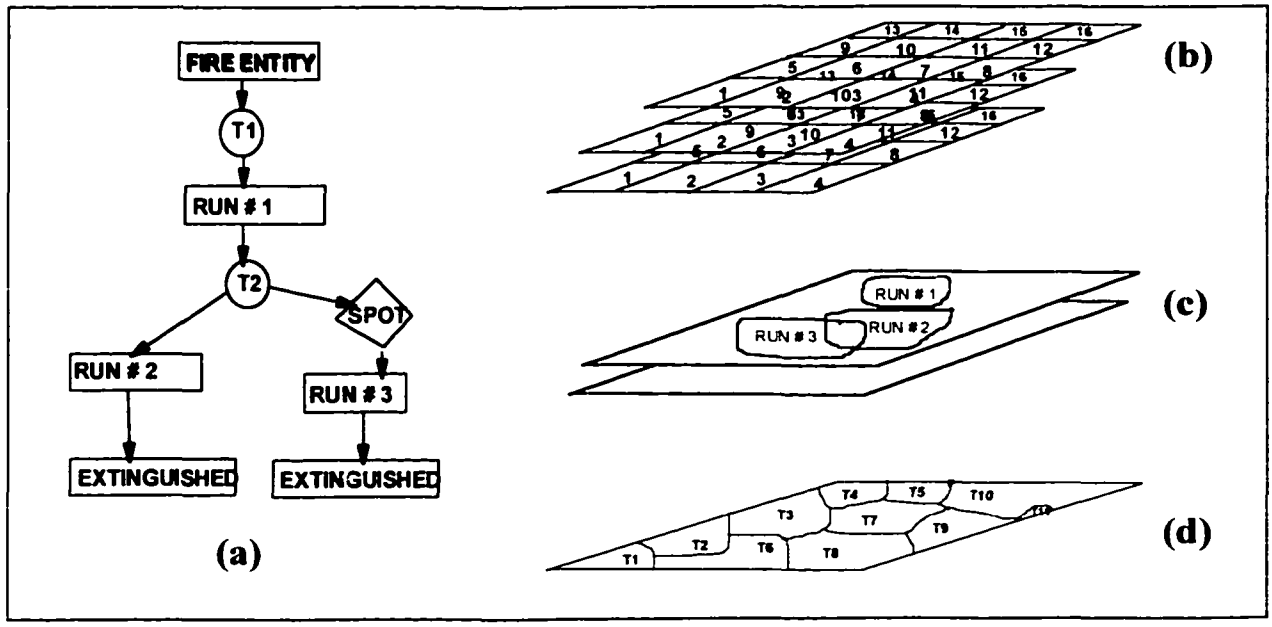

Figure 5.1. The four major wildfire conceptual models, after Yuan (1994b): (a) a fire entity; (b) locational snapshots; (c) entity snapshots; and (d) fire mosaics.

5.2 Cell based models

Cell based (grid) models have been the most common approach to estimate fire spread (Rothermel *et al.* 1994). They are based on the locational snapshot conceptualization (Yuan, 1994b), because growth simulations consider the cell where the fire is located and the 8 neighbor cells that surround it. After a fire is ignited, at a certain location on the grid cell, each neighboring cell is evaluated to determine which

neighboring cells will be affected by the current cell in the next cycle (Liu and Chou, 2000). A raster approach has three major advantages: (a) each raster cell is independent; (b) it is possible to know the value of a specific point; and (c) it is possible to handle continuous data. Nevertheless, raster models could result in a geometric distortion to the fire shape, which is produced by the fixed number of regular pathways where fire can travel (Finney, 1998). Trying to define more pathways, Frandsen and Andrews (1979) developed a method for predicting fire behavior based on the partitioning of the fuel into a honeycomb of "cells", each described independently according to its fuel quality. Another alternative is to increasing the number of neighboring cells influenced by each cell in the fire spread calculations (Feunekes, 1991, cited by Finney, 1998). Other techniques to reduce such geometric distortion of fire spread are the stochastic percolation techniques, and fractal algorithms (Finney, 1998). Other problems with the cell based approach is the difficulty in responding appropriately to temporal changes (e.g. direction and intensity of wind) (Finney, 1998). Nevertheless, some cell based models produce very responsive simulation of fire growth, such as IGNITE (Green, 1983), FIRESTORM (Daigle, 1999), and FireGIS (Pereira and Diogo, 1994). Moreover, cell based model programming code is much less complicated than in the vector approach.

5.3 Vector Based Models

The problems with cellular based models are avoided by the vector approach to fire growth modeling (Finney, 1998). Moreover, considering memory space and processing speed, in general, vector data structures are more efficient than raster structures (Yue, 1990). The vector approach models fire reality by a set of spatially

exhaustive polygons (fuel-models), which corresponds to the "fire mosaics" conceptual model (Yuan, 1994b). FARSITE is the most used fire behavior spatial model based on the vector approach (Keane *et al.* 1999b; Keane *et al.* 1998). FARSITE simulates fire growth through the Huygen's principle (Finney, 1998). This principle suggests the use of spaced points on the fire perimeter as new sources from which elliptical fires grow during each time step. Then a bounding polygon is drawn around the new ellipses forming the new perimeter for the next time step (Finney, 1998). Huygen's principle has been also used to develop a "radial propagation model", and analytically derive a differential equation that simulates fire propagation from any point using an elliptical fire shape (Finney, 1998).

FARSITE model is based on Rothermel's equation (Finney, 1996), and requires three topographic and five fuels data layers for surface and crown fire spatial and temporal simulation. Though FARSITE is a very versatile and friendly to use system, the difficulty of generating the required fuel-model maps has limited its use in many cases (Keane *et al.* 1999b).

CHAPTER IV

6 METHODOLOGY

6.1 Forest Inventory Data

The data for this study were collected based on the temporary forest inventory design of Ejido El Largo y Anexos, Chihuahua, México. Emphasis in this Ejido forest survey is on the timber resource for management planning purposes, with little consideration for the assessment of other ecosystem resources (Aguirre and Reich, unpublished). Based on this survey, the purpose of data collected for this dissertation was to evaluate forest fuels in a way that could be integrated into traditional forest inventory methodologies. Thus, data collection for the purpose of this dissertation was constrained by the sampling strategy of this temporary forest inventory.

6.1.1 Sampling Strategy

The forest of the ejido "El Largo" is divided into sections for management purposes, based on productivity potential. Every section is further subdivided into stands (based on density, slope and aspect) and sub-stand units (based on species and density) (Figure 6.1). Thus, the data for this study were taken from 554 sample-plots within the Section 3 of ejido "El Largo" (approximately 1,400 ha). According to the forest managers of this region, the number of sample plots per sub-stand is defined according to its size (UCODEFO No. 2, 1997) (Table 6.1). Sample plots were randomly distributed within sub-stands, with a minimum distance among them defined with the following formula:

$$\text{Distance} = (\text{Area } m^2/\text{Number of plots})^{1/2} \quad \text{[7.1]}$$

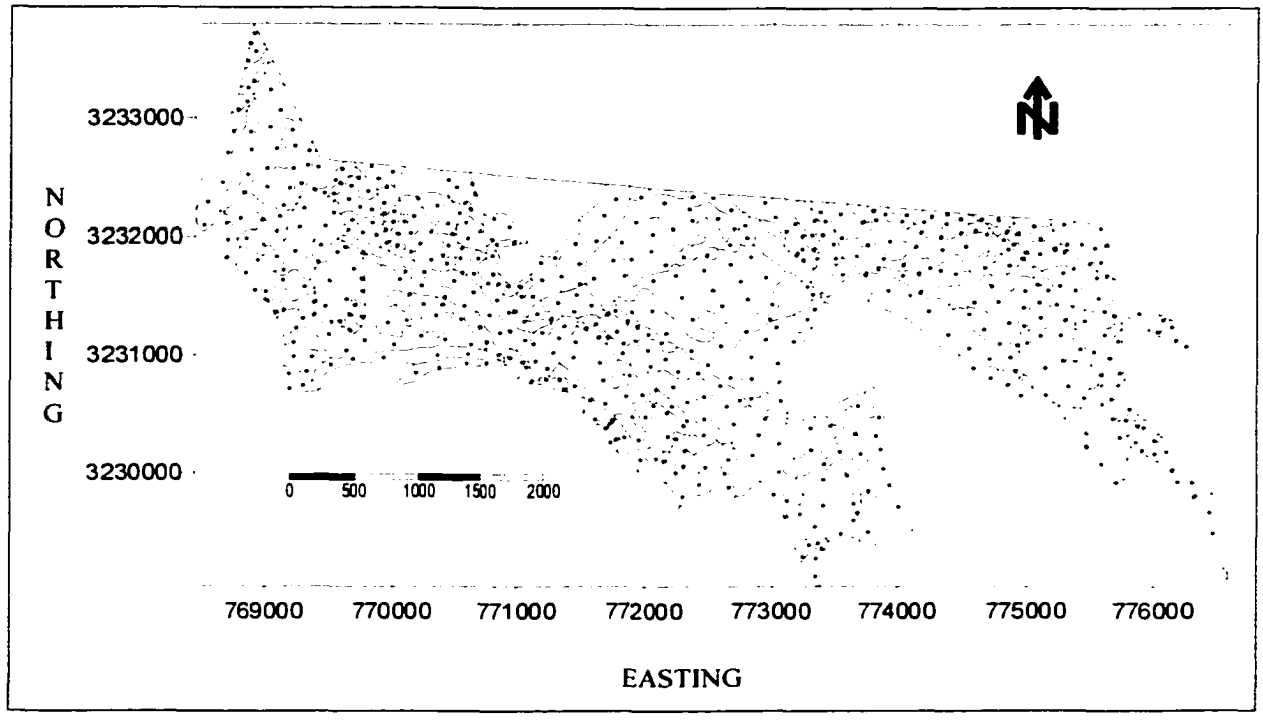

Figure 6.1. Location of the 554 sample plots within the study area. The divisions correspond to the 142 sub-stands in which the UCODEFO 2 (1997) classified the area (based on density, aspect and density). Coordinates correspond to the UTM zone 12.

Table 6.1. Number of sample plots per substand according to its size used for forest inventories in Cd. Madera, Chihuahua (UCODEFO 2, 1997).

Hectares per sub-stand	Number of sample plots
5-10 ha	4
11-15 ha	5
16-20 ha	6
21-25 ha	7

6.1.2 Sample Plots

Circular sample plots of 1000 m^2 were used. In addition, each of these plots had two concentric circular subplots of 400 and 80 m^2, respectively (Figure 6.2). The following site and forest stand data were collected within the 1000 m^2 plots: a) tree

species; b) diameter; c) height; d) crown height; and e) basal area. Saplings were measured within the 400-m^2 plots, while the information on natural regeneration was collected within the 80-m^2 sample plots. Fuels were inventoried within one of the three satellite 5m^2 sample plots located around the 1000 m^2 plots (at N, SE, and SW directions respectively). Plot center locations were determined using global positioning system (GPS) receivers.

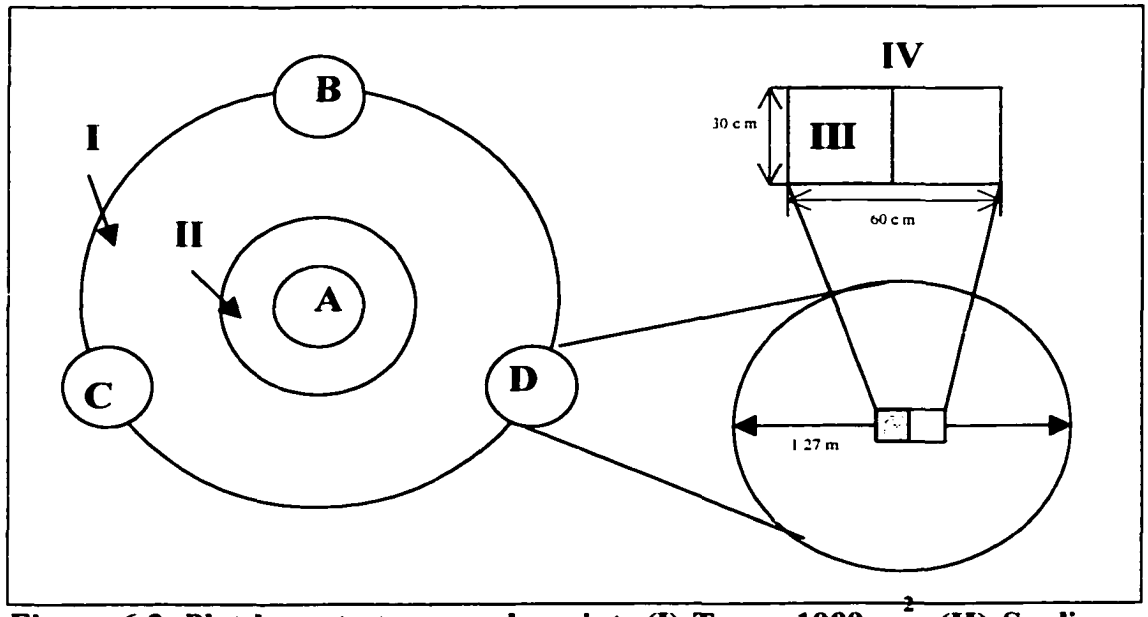

Figure 6.2. Plot layout at a sample point: (I) Trees, 1000 m^2; (II) Saplings, 400 m^2; (A) Regeneration, 80 m^2; (B-C-D) Fuels, 5 m^2; (III) Litter, 30 x 30 cm; (IV) Herbs and Forbes, 30 x 60 cm.

The following forest fuels data were inventoried:

a) - Litter depth (cm).

b) – Sampling of litter within 0.09 m^2 (g/m^2).

c) - Herbaceous vegetation within 0.18 m^2 (% dead, % cover, g/m^2).

d) - Shrub (stem diameter, height, % dead, %cover).

e) - Saplings (number/ha, height-cm).

f) - Downed woody material (diameter-cm).

The estimation of loadings for each fuel classes was based on the methodologies of the handbook for inventorying surface fuel biomass of Brown *et al.* (1982). The litter samples were dried until constant weight, and then the bulk density was calculated directly. This information was used to estimate litter weights based on the corresponding bed depth layer. The inventoried fuels were classified according to Table 6.2, which correspond to the inputs of the spatial model that was developed for this work.

Table 6.2. Criteria of classification of fuel classes according to the corresponding fuel classes used in the study area (Cd. Madera, Chihuahua).

FUEL CLASS	FUEL CHARACTERISTICS
1 hour	Litter (thin surface layer) and downed woody (0-0.63 cm).
10 hours	Downed woody (0.63-2.5 cm)
100 hours	Downed woody (2.5-7.6 cm)
Live Woody	Shrubs and saplings

6.1.3. Limitations of Current Inventory Design

Fuels survey was constrained by the sampling strategy of the forest inventory used. Thus, it is important to point out some of its limitations (Aguirre and Reich, unpublished): (A) Methods for determining sample size and sampling intensities are not explicitly defined. Sampling intensities are not well defined at stand level; (B) The sampling strategy is not designed under a multiresource approach (e.g. timber and fuels), but data collection process targeted only the timber resource; (C) The lack of an exact

definition of a forest ecosystem makes difficult the process to distinguish forest from other ecosystem resource groups; and (D) Data is collected without a clear understanding of how measurements taken in the field will be translated into meaningful indicators for assessing change or trends conditions.

6.1.4. Quality Assurance / Quality Control

This study represents the first attempt to evaluate forest fuels based on a traditional forest inventory of México. In part, and because of the limitations imposed by the sampling design, a small percentage of the data collected had extreme values that needed to be discarded from the data set. Though the crews that participated in the fuels survey had previous experience in forest inventory, as a measure of data quality assurance, they received an intensive training on fuels inventory. Moreover, the inventory process was continuously supervised not only on the way that fuels were measured but also on the accuracy of measures. Nevertheless, due to the lack of experience of the crews in fuels inventory, a certain proportion of erratic (or extreme) values was expected. These extreme values significantly impact the evaluation of spatial continuity (Armstrong, 1998; Isaaks and Srivastava, 1989). The variogram often does not clearly describe the spatial continuity because of a few erratic values (Isaaks and Srivastava, 1989). Therefore, before beginning the spatial analysis of the sample data it was important not only to identify such extreme values, but also to compare them with their closest neighbors in order to define a breakdown in the spatial continuity. The spatial location of extreme values along trends of similar data is helpful in detecting erroneous

data (Goovaerts, 1997; Isaaks and Srivastava, 1989). Such extreme values can be declared as values erroneous and removed (Goovaerts, 1997).

As a measure of data quality control some extreme values were removed. One way to spatially locate extreme values of fuel loads among sample plots is to graph such values, ordering the sample plots in such a way that every sample plot is located next to its closest neighbor. In this way extreme values that represent more than 2 times the average value of their neighbors can be easily identified. This approach was called "relative spatial continuity", and was used to identify and eliminate erratic fuel load values for each fuel type. A polynomial equation was adjusted to this relative spatial continuity, in order to evaluate any improvement when extreme values are removed.

6.1.5 Fuel Models Map

A fuel model map was required as support for a spatial fire behavior model (See 6.5). There were no experts available around the study area, nor enough data to carry out any of the classification methodologies. Therefore, in this project a practical alternative approach was proposed, based on a "fuel proportional concept". Based on the information gathered in the fuel inventory, and the experience acquired during this process, the study area was characterized as belonging to the "Timber litter" group of fuel complexes (i.e., fuel-models 8, 9, and 10 of the Intermountain Fire Sciences Laboratory (Anderson, 1982)). The next step was to classify each sample plot into its corresponding fuel-model class. To do this a set of conditions was evaluated, based on the proportion of the characteristic fuel loading of 1-hour, 10-hour, and 100-hour fuel classes that correspond to each fuel-model. A fuel-model value was defined for each sample. Then, the inverse

distance weighted (IDW) technique of *ArcView GIS* 3.1 (ESRI, 1998) was used to interpolate the fuel-model values for the 554 sample plots. As a result the corresponding fuel-model map was generated. IDW is a well-known interpolation technique and most of the GIS software packages have this technique.

6.2 Terrain Modeling Data

A Digital Elevation Model (DEM) with 90-x-90 m resolution was available for the study area. Elevation, aspect and slope maps were derived from this DEM, through the use of Geographical Information Systems (GIS). Then another database was defined containing elevation (m.a.s.l.), aspect (radians) and slope (degrees) for each sample plot. GIS packages *ARCInfo 3.5* (ESRI, 1996) and *ArcView GIS* 3.1 (ESRI, 1998) were used, not only to generate such maps, but also to store the corresponding information. This information was used as ancillary data in the subsequent spatial cross-correlation analysis.

6.3 Remote Sensing Data

The remotely sensed data used in this study were derived from a Thematic Mapper Landsat 5 satellite scene. Although most of the field survey was carried out during July (1998), the available Landsat TM images (July 6, and July 22) were highly covered by clouds (90%). The better, alternative was a scene from August 23rd, with 10% cloud cover. This Landsat TM image corresponds to the Path 34, and Row 40 (Scene identification number: LT5034040009821910) (Appendix 6.1). Its data format was band sequential, while the "nearest neighbor" was the resampling technique used. The

horizontal datum of such image was WGS84. The UTM was its map projection, and the image falls in the UTM zone 12. The pixel size was of 28.5 m. The image was geometrically corrected using a topographic map (code: San Pedro Madera H12D49, Chihuahua) from the "Instituto Nacional de Estadistica Geografia e Informática" of México (scale 1:50,000). *ERDAS IMAGINE 8.2* (ERDAS Inc., 1997) and *ArcView GIS* Version 3.1 (ESRI, 1998) were used to perform the digital image processing of this satellite scene.

For each sample plot, the seven spectral reflectance values were defined from the original image. Image contrast enhancement algorithms were applied to the data, such as "histogram equalization", "lut strech", and "level slice", in order to analyze alternative variations in spectral reflectance. Two special data transformation techniques were tested: (1) Principal components analysis (PCA) was applied to both original and enhanced images, then the corresponding PC value was extracted for each sample plot; and (2) The normalized difference vegetation index (NDVI) was calculated for both the original and the enhanced images. The corresponding NDVI was defined for each sample plot. All the new information generated in the analysis of the remote sensed data were considered as ancillary data for estimation of forest fuels, through subsequent spatial cross-correlation analyses.

6.4 Spatial Interpolation Techniques

Two indexes were calculated to support an exploratory spatial analysis. Moran's *I* was used to test the hypothesis of no spatial correlation of the four fuel classes (1-hour [1-HR], 10-hours [10-HR], 100-hours [100-HR], and live woody [LW]). The hypothesis

of no spatial cross-correlation between each of the fuel classes and auxiliary data was tested through the bivariate Moran's *I*. Spatial continuity hypotheses, for both autocorrelation and cross-correlation, were tested through the definition and selection of variograms and cross-variograms, respectively. The selected variograms and cross-variograms were used to support the estimation processes in the kriging techniques.

A total of 12 different spatial interpolation analyses were tested to get four fuel maps: (a) 1-HR; (b) 10-HR); (c) 100-HR); and (d) LW fuels. In general, such techniques were classified into two groups: (A) Traditional techniques: spline, inverse distance weighting (power 1 and 2), polygonal mapping, and Thiessen techniques: (B) Kriging: ordinary kriging, universal (1^{st} and 2^{nd} degree), point kriging, block kriging, and cokriging (using 2 different software packages). All the kriging techniques were applied under the assumption of an isotropic behavior of the data (omnidirectional approach). Both ordinary kriging and point kriging represent the same methodology. Nevertheless, due to the fact that they were estimated in different computer software (S-Plus [Reich and Davis, 1998] and GS+ [Robertson, 2000]), they were assumed as different analyses. Cokriging interpolations were supported by the ancillary data generated from the forest inventory, DEM, and satellite image digital analyses. A stepwise evaluation (linear correlation) was conducted in *SAS* (SAS Institute Inc., 1998) to select the statistically significant auxiliary variables. Based on the 554 plots, the interpolations produced a total of approximately 40,000 estimates, generated on a 30 x 30 m grid matrix. To evaluate and select the interpolation techniques, cross-validation was applied. Cross-validation was also applied to find the optimal number of nearest neighbors to include in the kriging processes. The residuals generated from the cross-validation were used to compute the

following measures of validation: (A) Mean square error (MSE); (B) Histogram of the residuals; (C) q-q plots of the residuals; (D) Conditional unbiasedness; (E) Scatterplot of predicted values versus actual values; and (F) Correlation coefficient (estimated-actual values). MSE was the principal criterion to select the best interpolation techniques.

The following software packages were used to compute the different interpolation techniques: **(I)** *ArcView GIS* Version 3.1 (ESRI, 1998): spline, polygonal mapping, and Thiessen; **(II)** *SPLUS* (Reich and Davis, 1998): ordinary kriging, universal kriging (1^{st} and 2^{nd} degree), and cokriging; and **(III)** *GS+* (Robertson, 2000): inverse distance weighting (power 1 and 2), point kriging; block kriging, and cokriging. The required variograms and cross-variograms were developed through *SPLUS* and *GS+*. The *SPLUS* functions used in this study are custom programs developed by Reich and Davis (1998), and are not included in the commercial version. *SPLUS* was used to conduct the cross-evaluation of ordinary kriging, universal kriging, and cokriging. *GS+* was used to cross-evaluate inverse distance weighting, point kriging, block kriging, and cokriging. A system developed in *Excel* (Microsoft, 1997) was used to calculate both MSE's and correlation coefficients. SPLUS was used to display the graphical evaluation measures. The SURFER graphic program, version 7.02 (Golden Software Inc., 1999), was used to display contour and surface maps of interpolations and standard deviations.

6.5 Spatial Fire Behavior Model

The goal of this phase was to develop a model to predict spatial fire behavior variations, based on fuels spatial distribution. The developed model was built based on the locational snapshot approach (see 5.1).

6.5.1 Surface Fire Behavior System

A fuel model characterizes certain fuel properties, such as fuel depth, surface-area-to-volume ratio, and fuels loading. An accurate definition of the spatial variations of these properties would allow a more accurate prediction of spatial fire behavior. However, in practice it is difficult not only to measure such fuel properties, but also to define their spatial distribution. Thus, current spatial explicit fire behavior simulation systems consider such fuel properties constant within a given fuel model. In an attempt to improve the spatial fire behavior predictions, the spatial model developed in this study considers changes of fuels loading as a source of spatial variation of fire behavior. This model also considers the other fuel properties constant, thus the knowledge of the corresponding fuel models (within the area of interest) is still required. In this way, it was necessary to count with a system that allowed one to predict surface fire behavior punctually (i.e., for a given cell [pixel]) based not only on fuel models, but also on the variation of fuels loading. Since there does not exist a software package with such capability, a specific surface fire behavior system (SFBS) was developed in *Excel* (Microsoft, 1997). Such a system is based on Rothermel's model, and was calibrated with Nexus (Scott and Reinhardt, 1999). It only predicts surface fire behavior, based on variation of fuels loading within the same fuel model. Analysis was performed on the effect of fuels variation within fuel models 8, 9, and 10.

6.5.2 Fire Behavior Spatial Model

Before this project, no model existed that allowed simulation of the spatial behavior of fire, based on changes in fuels loading. Even FARSITE (Finney, 1998) has the

limitation that it is not possible to consider variations of spatial distribution of fuels within the same fuel model. Therefore, a specific GIS model that allows simulation of the potential spatial fire behavior was developed. Based on the SFBS the algorithm of this model calculates fire behavior in each pixel deterministically (under a raster approach). This allows working with point specified changes of fuels loading, slope, and wind. It simulates fire behavior, based on the spatial variation of all fuel classes. Finally, a simulation was run with this model and with FARSITE, under the same conditions, to support an analytical comparison.

CHAPTER V

7 FOREST INVENTORY

7.1 1-HR Fuels

7.1.1 Litter

Since it was not possible to sample each plot, the estimation of litter weight was made indirectly using depth. This was possible because there was a good relationship between litter depth and weight (Figure 7.1) based on oven-dried trials. A total of 28 samples were used to define the regression equation. The percentage of the area covered by litter, within an area of 30 x 30 cm (0.0929 m^2), was considered as a correction factor for the weight estimations. The resulting average bulk density was of 41.33 kg/m^3, with a standard deviation of 7.85. Overall, the average litter load was 2.07 tons per hectare, within a range between 0 and 5.05 ton/ha. Most of the samples resulted in less than 2 ton/ha, tending toward a normal distribution (Figure 7.2).

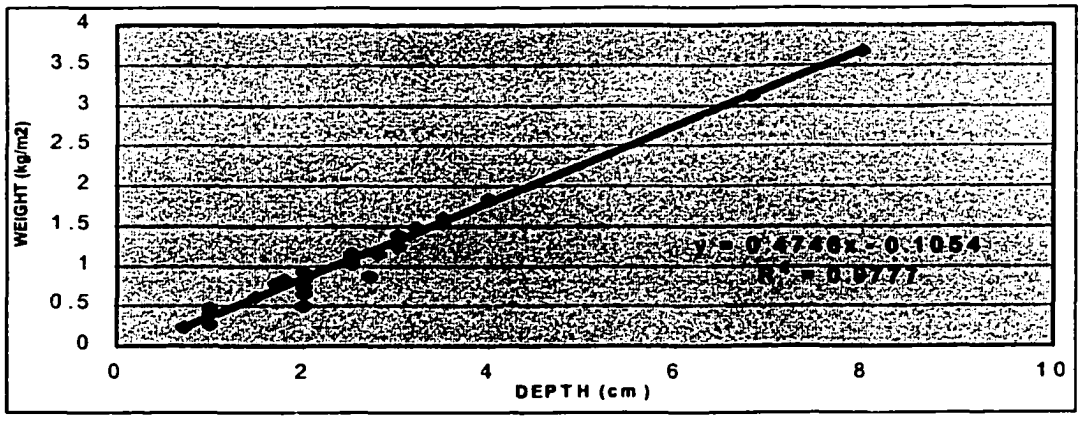

Figure 7.1. Correlation between depth of litter layer and the corresponding weight within 0.0929 m^2, based on oven-dried trials of 28 samples of Cd. Madera, Chihuahua.

7.1.2 Downed Woody Material

All the woody material less than 0.75 cm in diameter was also considered within the 1-hour fuel class. The range of these fuels has a maximum of 5.17 tons per hectare, and a minimum of 0, while the average was 0.41 ton/ha. Most of the samples resulted in less than 1 ton/ha, defining a non-normal distribution.

7.1.3 Total Loading of 1-HR Fuels

There is not a clear description of the role of litter in the definition of 1-HR. Countryman (in Omi, 1997) suggested that the thin surface layer of the litter can be classified as 1-HR, however the depth of such layer is not specified. Therefore, based on my own experience, and some specifications given by Countryman (in Omi, 1997) a surface layer of 0.64 cm ($^1/_4$ inch) was considered as a part of the 1-HR loading. To calculate the proportional fuel loading that corresponds to such a layer, it was assumed that the bulk density of the litter layer is the same regardless of the depth. Then the resultant litter loading, per each sample plot, was added to the total amount of downed 1-HR woody material. General statistics for all fuels are shown in Table 7.1. As expected, there is a notable variation of the 1-hour fuel loads, which can be appreciated in the Figure 7.2. Appendix 7.1 shows the sampling error of the 1-HR fuels per each stand sampled. 1-HR fuels have a slight tendency to a normal distribution, however most of the sample plots showed low load values. Linear estimators, such as ordinary kriging and universal kriging, may only be optimal when the variable under study has a normal distribution (Hunner, 2000).

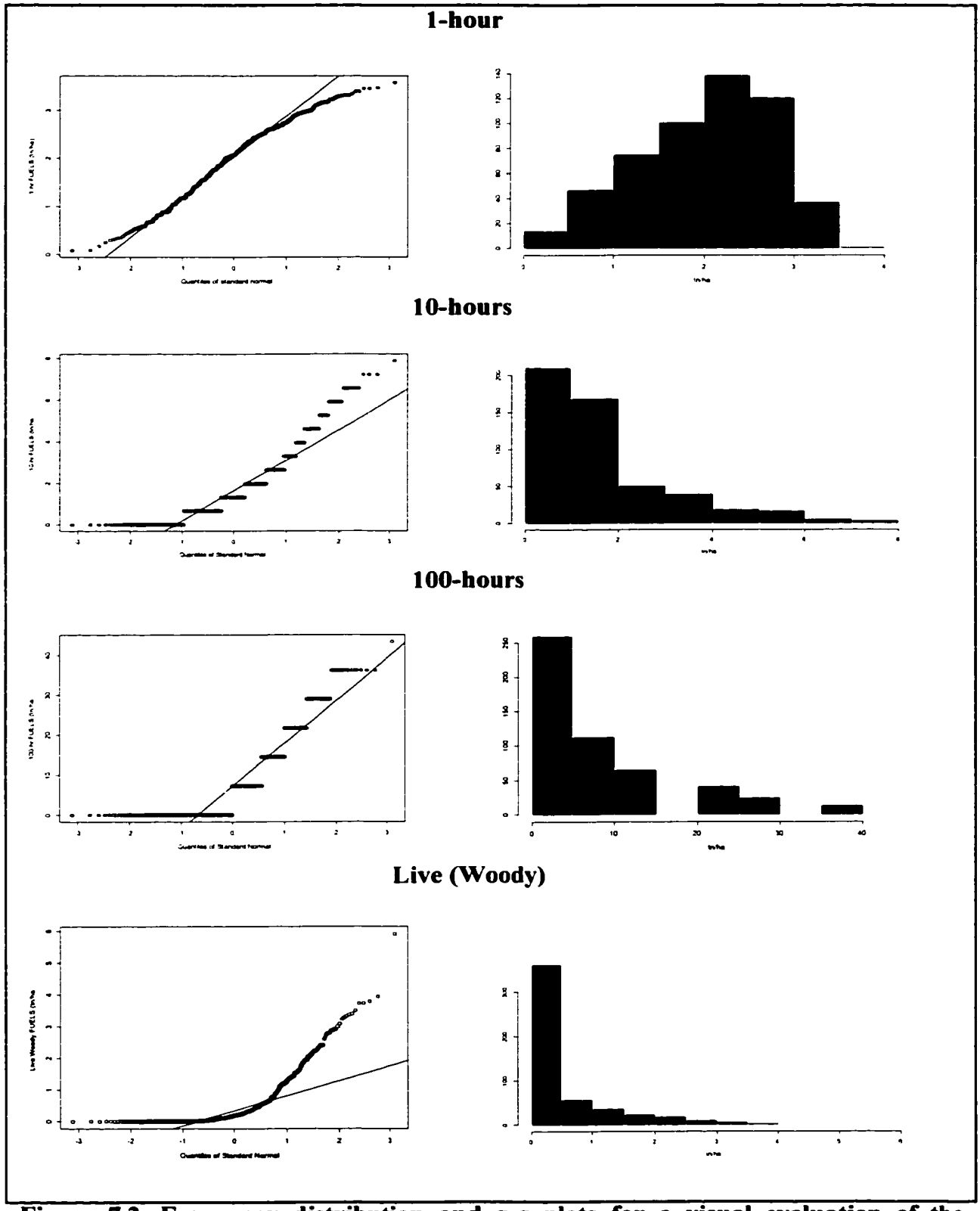

Figure 7.2. Frequency distribution and q-q plots for a visual evaluation of the normality of each of the four fuel classes of the study area (Cd. Madera Chihuahua.

Table 7.1. Overall statistics of the loadings (ton/ha) in four fuel classes surveyed within the study area, in Cd. Madera Chihuahua.

Statistic	1-hour	10-hours	100-hours	Live (woody)
Sample size	535	519	519	523
Sampling Error (%)	3.22	8.40	11.36	13.08
Minimum	0.03	0.00	0.00	0.00
Mean	2.01	1.74	7.45	0.54
Median	2.07	1.31	0.00	0.19
Maximum	3.58	11.16	36.12	3.94
Std. Deviation	0.75	1.67	9.63	0.814
Coef. of Variation	0.37	0.96	1.29	1.49

7.1.4 Relative Spatial Continuity

The graphic of relative spatial continuity corresponding to 1-hour fuels is depicted in Figure 7.3. A total of 19 extreme values were removed (3.43%). The white line represents a polynomial equation of 6^{th} order that better fit the spatial variation of plot loadings. An improvement in the fit of this polynomial was achieved when extreme values were removed. The 1-HR graphics depicts that higher fuel loads were located in the west portion of the study area.

7.2 10-HR Fuels

The statistics of downed woody material between 0.7 and 2.5 cm in diameter are shown in Table 7.1. The frequency distribution of this class also shows a non-normal tendency (Figure 7.2). The dispersion of the data is much higher than in the 1-HR fuels. Most of the sample plots had 10-HR fuel loads lower than two tons per hectare. There were very few sites with around 10 ton/ha. Appendix 7.1 shows the sampling error of the 10-HR fuels per each stand sampled.

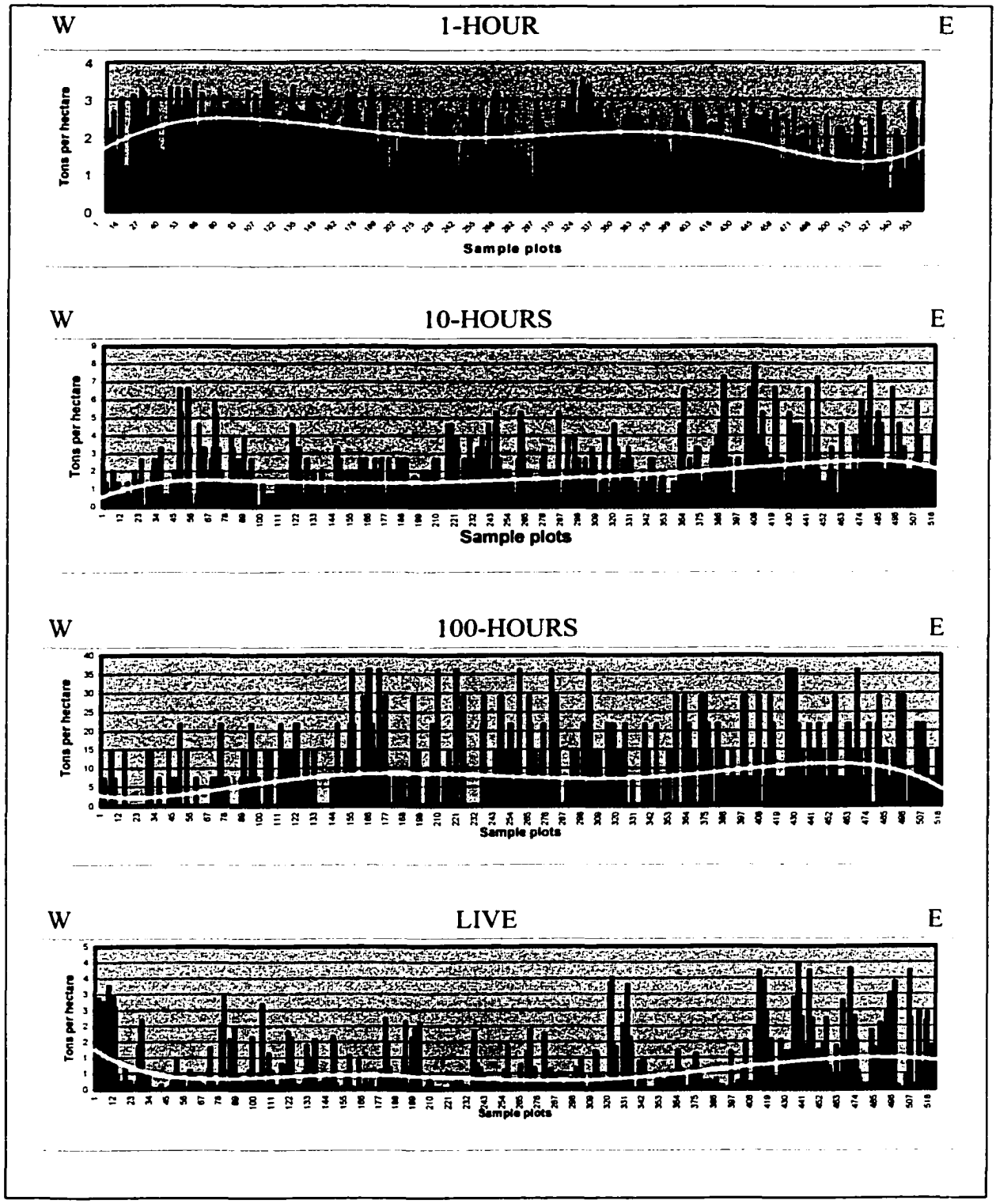

Figure 7.3. Relative Spatial Continuity (RSC), of loadings (ton/ha) for the four fuel classes within the study area (Cd. Madera, Chihuahua), where the closest sample plot was considered as the proximate neighbor. A 6^{th} polynomial equation, of 6 order is shown (white line) as a comparison criterion.

7.2.1 Relative Spatial Continuity

According to the Figure 7.3, the difference of fuel loading among closer neighbors is more marked in the spatial continuity of the 10-HR than in 1-HR fuels. A total of 35 extreme values were removed (6.3%) in order to define a better continuity. The order of the sample plots is the same as for the 1-HR, resulting in a certain similarity in shape. This indicates the similarity in the spatial continuity between 1-HR and 10-HR. The higher fuel loads are located at the east portion of the study, while the lower values occurred mostly in the central part of the study area.

7.3 100-HR Fuels

The range of downed woody material, between 2.5 and 7.5 cm in diameter included extreme values (0 and 36.12 ton/ha). However most of the sample plots resulted in less than 15 ton/ha. This frequency defined a non-normal distribution (Figure 7.2). The resultant standard deviation reflects such data variability. Appendix 7.1 shows the sampling error of the 100-HR fuels per each stand sampled.

7.3.1 Relative spatial continuity

The spatial continuity 100-HR was less defined than in 1-HR and 10-HR. The continuity of fuel loads is not constant because there are high loads close to low loads. Though, the polynomial line looks more stable than in 1-HR and 10-HR, this is the result of the averaging between high and low loads. In this case a total of 35 sample plots were removed (6.3%) in order to avoid extreme values. In general 100-HF were more evenly distributed in the study area, with decreases in the extreme west.

7.4 Live Woody Fuels

7.4.1 Shrubs

The three shrubs species that occurred in the study are: *Senecio salicnus* (jarilla), *Ceanothus buxifolius* (junco), and *Rubus pringlei* (encinillo). In average Junco was the more abundant than the other shrubs with 3,828.52 plants per hectare, with a maximum of 38,000 plants/ha. However encinillo shows the highest density within a sample plot, with 74,000 individuals per hectare. Nevertheless, encinillo was only present in 1.62% of the sample plots. Junco and jarilla occurred in 35.7 and 7.4 % of the sample plots, respectively. In general all the shrubs have very similar height, however on average, jarilla is the taller shrub (29.48 cm). Junco and encinillo have an average height of 18.8 and 17.9 cm, respectively. Estimated fuel loads were very similar among shrubs species. Considering the plots with shrubs, the average loads were 0.13, 0.09, and 0.1 ton/ha for jarilla, junco, and encinillo respectively.

7.4.2 Saplings

In general there were 2-3 sapling species per sample plot, however some plots contained up to 5 species. The more dominant species were *Pinus durangensis* and *Pinus arizonica; Quercus, Juniperus*, and *Abies* were less abundant. On average there was a total of 2156 saplings per hectare. The site with the most saplings represented 598,000 individuals per hectare. The average sapling height was of 1.29 m, with a minimum of 0.48 m, and a maximum of 2.8 m. The maximum fuel load resulted from saplings in a sample plot represents 39.96 tons per hectare, while the minimum fuel load was 0.02 ton/ha. Considering only the plots with saplings, the average was of 1.82 ton/ha.

7.4.3 Total Live Woody Fuels

In this study the average of "medium shrubs" weights (Brown *et al.* 1982) were used to calculate shrubs fuel loadings. The average live fuel load was 0.544 ton/ha. The maximum load in saplings influences the maximum live fuels load. Other statistics are shown in Table 7.1. According to the Figure 7.2 most of the sample plots contained less than 2 ton/ha of live woody fuels. This defines, as in all the other fuels, a non normal distribution. The relative spatial continuity graph (Figure 7.3) shows a tendency of the fuel loads among neighbors quite different than for the other fuel loads. The higher fuel loads were located at both east and west extremes of the study area, while the lower values were found in the central portion. A total of 31 sample plots that showed extreme values were removed (5.6%). Appendix 7.1 shows the sampling error of the LW fuels per each stand sampled.

7.5 Tree Species

Using the database gathered in the field inventory, a total of 96 maps were generated through the inverse distance technique. Most of these mapped parameters did not demonstrate a defined spatial distribution pattern, thus they were eliminated from subsequent analyses. This section describes the more relevant tree parameters that were used as ancillary data to test both spatial cross-correlation and joint spatial continuity hypotheses for each of the four fuel classes.

7.5.1 Number of Tree Species

The number of species per sample plot varied from 1 up to 7. However 80.3% of the sampled plots contained 1 or 2 species (Figure 7.4). Table 7.2 shows the 11 tree species that were found in the study area. The more frequent dominant species were *P. durangensis*, *P. arizonica* and *P. engelmannii* found on 45.49, 30.14 and 12.64 % of the sample plots, respectively. These 3 species also were the more common co-dominant species. The spatial distribution of 1 and 2 species per plot is evenly distributed along the study area (Figure 7.5). The areas with more than 3 species were rather scattered.

Table 7.2. Relation of species found in the study area (Cd. Madera Chihuahua) and temperature/rainfall (based on UCODEFO 2, 1997).

SPECIES	Altitude (m.a.s.l.)	Mean Annual Temperature (C°)	Mean Annual Rain (mm)
Pinus engelmannii	1800-2450	10.8	
Pinus durangensis	2300-2500	10.1	1132
Pinus arizonica	2700-2800		965
Pinus leiophylla			
Pinus ayacahuite	2100-2600		
Pinus herrerai	2100-2600		
Abies spp *			
Pseudotsuga spp *	2100-2600		
Quercus sideroxila	2300-2500	10.1	1132
Juniperus deppeana	2240		693
Pinus spp *			

* Species not identified.

7.5.2 Average Diameter

The average diameter (at breast height) of all tree species was 36.67 cm. The minimum and maximum diameters were 14.05 and 72.95 cm, respectively. Most of the sample plots defined average diameter within a range of 30 and 50 cm. Though this

parameter shows a strong tendency to a normal distribution (Figure 7.4), there was a high dispersion of the data that defines a high standard deviation (Table 7.3). In general, the forest of the study area can be considered mature, with both young and old stands.

The spatial distribution of average diameter is depicted in Figure 7.5, where the average diameters between 30 and 40 cm are distributed along most of the study area. Average diameters lower than 40 cm show a well defined spatial pattern. Although higher diameters also show areas with a well defined pattern, there are some scattered small areas that do not follow a specific spatial pattern.

Table 7.3. Descriptive statistics of tree characteristics resulting from the forest inventory carried out beside a fuels inventory in the 554 sample plots of the study area (Cd. Madera, Chihuahua).

STATISTICS	No. OF SPECIES	AVE. DIAM. (cm)	NUMBER OF TREES/HA	BASAL AREA (m^2/ha)	AVE. HEIGHT (m)
Mean	1.85	36.67	312.11	10.62	16.10
Median	2	34.80	204.99	9	15.69
Maximum	6	72.95	72.95	48	27.89
Minimum	1	14.05	14.05	1	4.85
Stand. Dev.	0.86	10.58	10.59	7.16	0.16
Range	5	58.90	58.90	47	23.04
Skewness	0.96	0.65	0.65	2.01	0.25

7.5.3 Average Height

Tree height values were less dispersed (Table 7.3), and also they tended to define a normal distribution (Figure 7.4). The average height was of 16.1 m, with a range between 4.85 and 27.89 m. Tree height values also show a tendency toward a normal distribution, with a low dispersion (S.D.= 7.16). The spatial distribution of this parameter was rather heterogeneous.

7.5.4 Basal area

Although basal area tends to define a normal distribution, there are some high values that skew such distribution to the right (Figure 7.4). There was a notable difference between the minimum and the maximum basal area values (Table 7.3). Nevertheless, the similarity between the corresponding mean and median suggests a tendency to a normal distribution. The spatial distribution of basal area shows a well defined spatial pattern for basal area classes between 5 and 20 m^2 (Figure 7.5).

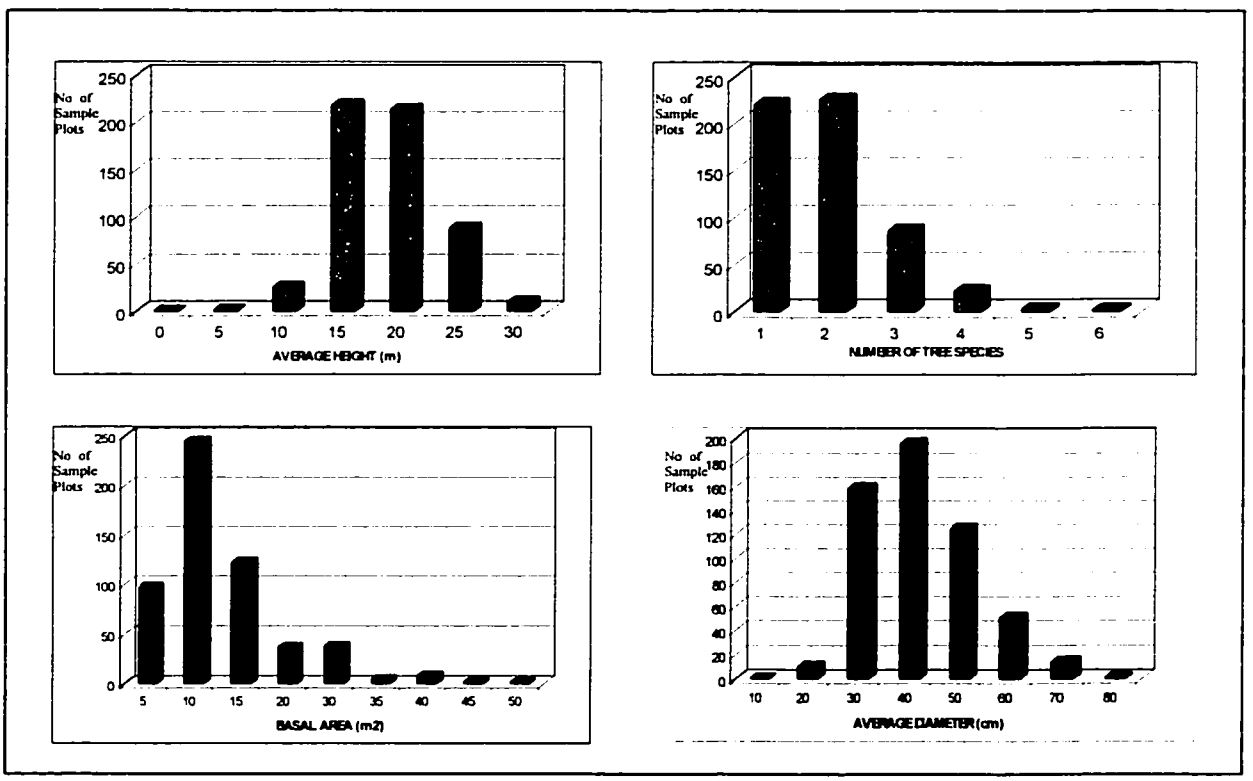

Figure 7.4. Frequency (F) distribution of tree characteristics resulting in the forest inventory of 554 sample plots within the study area (Cd. Madera, Chihuahua).

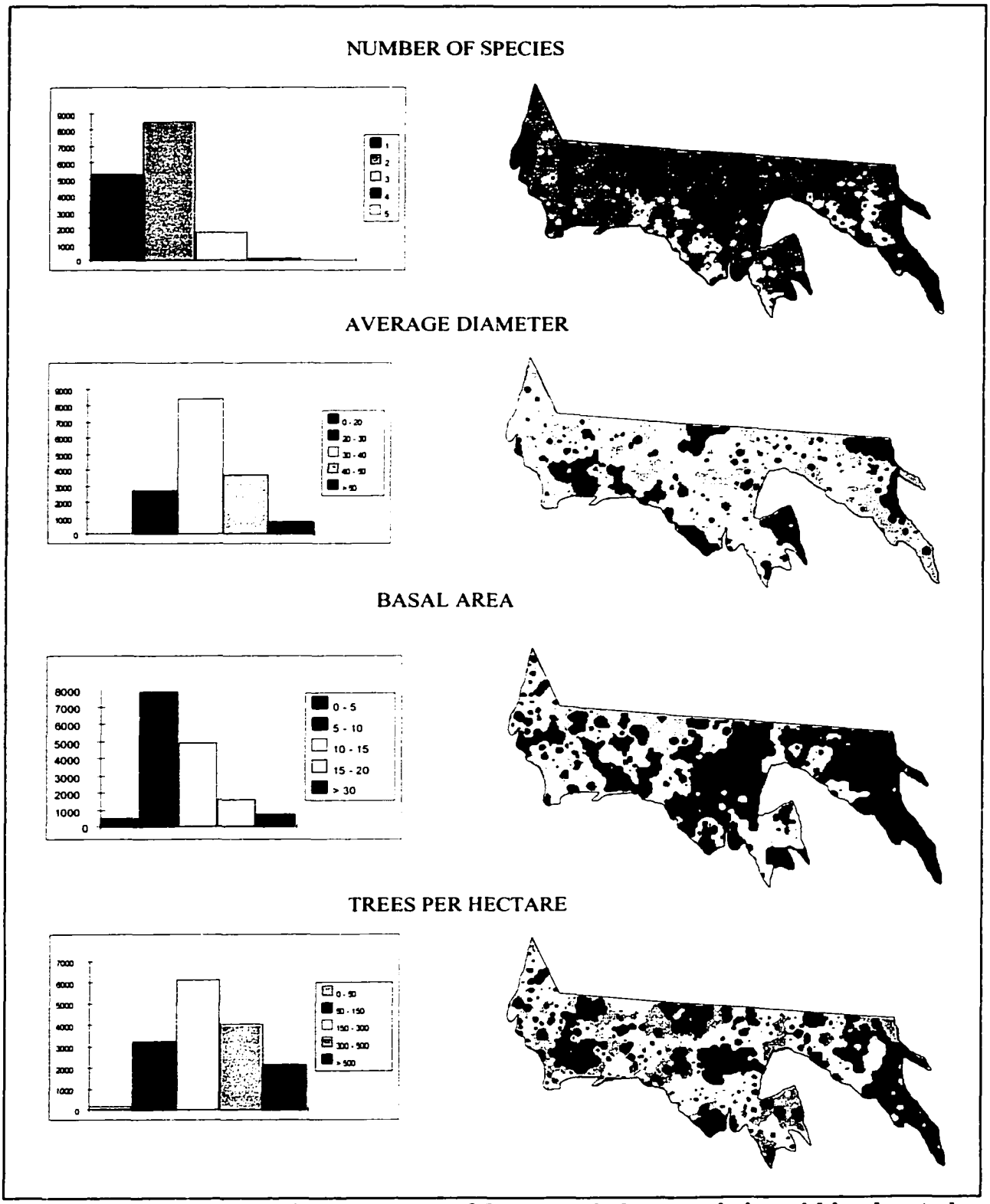

Figure 7.5. Spatial distribution maps of four stand characteristics within the study area (Cd. Madera, Chihuahua), derived through inverse distance weighted interpolation technique. Graphs illustrate the proportion of pixels per each map-class.

7.5.5 Number of Trees per Hectare

Tree density varied from 7 to 3,580 trees/ha, with a standard deviation of 376. The great difference between the mean (312) and the median (205) resulted in a tendency to a non-normal distribution for this parameter. Most of the sample plots contained less than 500 trees/ha. The spatial distribution of the number of tree per hectare is depicted in Figure 7.5. The density classes between 150 and 500 trees/ha showed a well defined spatial distribution pattern. In contrast, the >500 tree/ha class density was a rather scattered distribution.

8 FUEL-MODELS MAP

A fuel model characterizes certain fuels' properties, such as fuels' depth, surface-area-to-volume ratio, and fuels' loading. An accurate definition of the spatial variations of these properties would allow a more accurate prediction of spatial fire behavior. Thus, the spatial model developed in this study considers changes of fuels' loading as a source of spatial variation of fire behavior. This model considers other fuel properties constant, thus the knowledge of the corresponding fuel models (within the area of interest) is still required. To define the "fuel model" spatial distribution, it was necessary to classify each sample plot into a given fuel model. Based on the information gathered in the fuel inventory, and the experience acquired during this process, the study area was characterized by the "Timber litter" group of fuel complex (Table 8.1). The next step was to assign one of these fuel models to each sample plot. To do this the fuel loads suggested by Anderson (1982) were used to define a specific profile per each fuel model.

Table 8.1. Fuel loads (ton/ha) corresponding to the "Timber litter" fuel complex of the NFFL* classification (International Fire Service Training Association, 1998).

FUEL MODEL	TYPICAL FUEL COMPLEX	1-hr FUEL LOAD	10-hr FUEL LOAD	100-hr FUEL LOAD
FM-8	Closed timber litter	3.36	2.24	5.60
FM-9	Hardwood litter	6.55	0.92	0.34
FM-10	Timber (litter and understory)	6.75	4.88	11.23

* Northern Forest Fire Laboratory (Andrews, 1986).

8.1 Conditional Fuels Loading Concept

To classify each sample plot into its corresponding fuel-model, the "conditional fuels loading concept" (CFLC) was used, which considers that each fuel-model contains a characteristic amount of 1-HR, 10-HR, and 100-HR fuel classes. This concept is supported in the fact that the differences in fire behavior among fuel models are basically related to the fuel load and its distribution among the fuel particle size classes (Anderson, 1982). Thus, based on the characteristic fuels loading that corresponds to fuel-models 8, 9, 10 (Table 8.1), the following "conditional fuels loading" were evaluated for each sample plot:

(a) The sum of the characteristic10-HR and 100-HR fuels loading for FM-8 is 7.84 ton/ha. For practical purposes this value was considered as integer (=8). Thus:

$$\text{if } (10\text{-HR} + 100\text{-HR}) < 8 \quad \Rightarrow \text{FM-9} \quad \text{.....[1]}$$

(b) Based on a manual qualification of several sample plots, a factor of 18.8 (approx. 19) (that corresponds to the multiplication of 1-HR fuel loading times the 100-HR fuel loading) has been defined to separate sample plots between FM-8 and FM-10. Thus:

$$\text{if } (1\text{-HR} \times 100\text{-HR}) > 19 \quad \Rightarrow \text{FM-10} \quad \text{.....[2]}$$

(c) The remaining unclassified sites corresponded to FM-8.

(d) Oak species are typical in FM-9 (Anderson, 1982). Therefore, once the sites are classified, a final filter is used. Thus, all the sites where *Quercus* spp occurred will be reclassified as FM-9.

Some of the advantages of this classification methodology are: (1) it is based on actual fuel loads, and not only on vegetation structure and composition; (2) it is objective and avoids the bias of different classifiers (experts); and (3) it avoids the need of the advice of experts. This methodology was tested with information reported by Fischer (1981), resulting in the similar fuel models classification as those defined by Fischer through photo-guides. Nevertheless, further work is needed to validate the CFLC. Since there was no other alternative, this methodology was good enough for the purposes of this study.

Figure 8.1 shows the spatial pattern of the three fuel models, which resulted from an inverse distance weighting interpolation. Most of the study area falls in the fuel models 8 and 9 (38.1 and 34.8% respectively). FM 10 has a coverage of 15.1%.

8.2 Non-Forested Areas

89.3% of the study area was covered in different densities by forest vegetation (Figure 8.2). Croplands, orchards, wetlands, and areas with erosion were classified as non-forested areas, where it is assumed that fire could not run. Although these areas covered 8.5% of the total area, they were located as "small-islands" over the study area. None of these areas were sampled, thus this lack of information could affect the estimations of the spatial continuity of the forest fuels. On the other hand, these areas could be used as barriers when planning a prescribed fire.

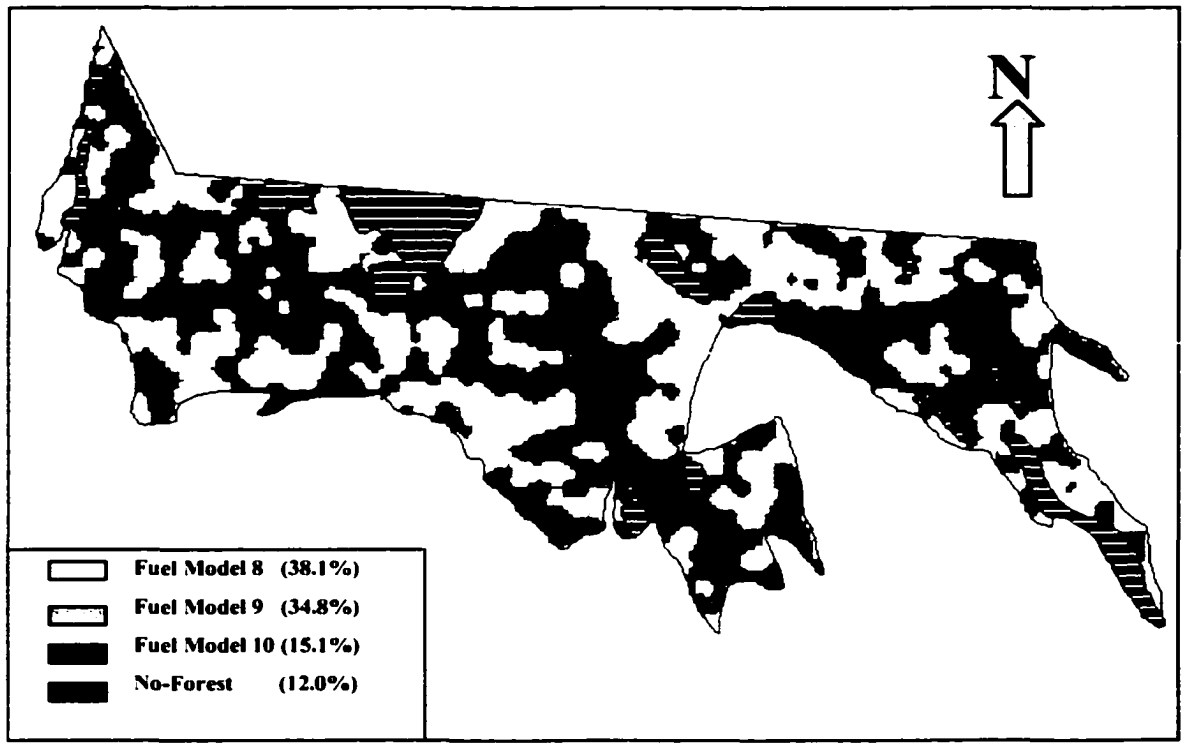

Figure 8.1. Spatial pattern of fuel models in the study area (Cd. Madera, Chihuahua), of the "Timber litter" complex, resulting from an ordinary kriging interpolation technique.

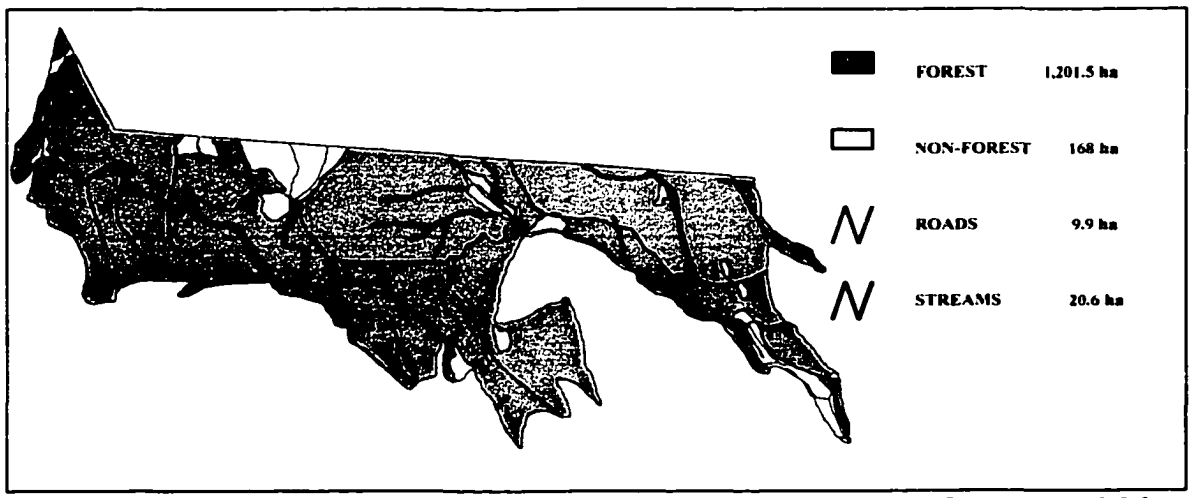

Figure 8.2. Location of areas with non-forest vegetation and forested within the study area (Cd. Madera, Chihuahua), which can influence the estimations of spatial distribution of forest fuels.

9 THEMATIC INFORMATION EXTRACTION

This section describes the alternative variations of spectral reflectance, defined for each sample plot, that were used as ancillary data to test both spatial cross-correlation and joint spatial continuity hypotheses for each of the four fuel classes. The spectral reflectance of each sample plot was measured under both original and enhanced conditions (Figure 9.1). Though several image enhancement techniques were used, only "histogram equalization" produced an improvement in the image contrast.

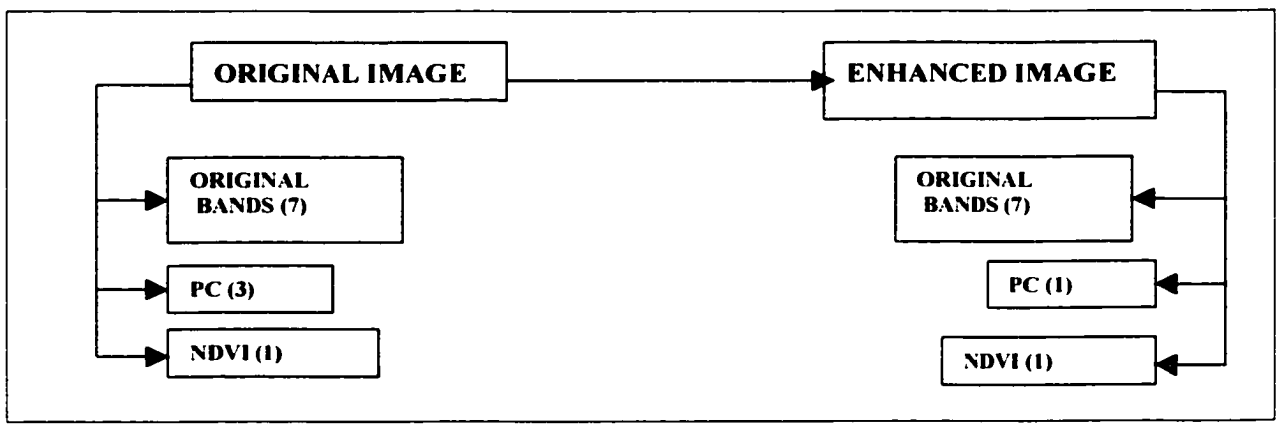

Figure 9.1. General process to define the reflectance sources for both original and enhanced images, based on Principal Components (PC) and the Normalized Difference Vegetation Index (NDVI). Numbers indicate amount of useful images generated.

9.1 Spectral Reflectance of Original Image

First of all, the reflectance values of each sample plot were obtained directly from the original image. This resulted in seven reflectance values, one per each band.

According to their corresponding histograms (Figure 9.2.), the reflectance of all the 7 bands is compressed in a small portion of the reflectance range, suggesting that the image is rather low in contrast (Jensen, 1996). Moreover, the histograms do not show peaks that denote different dominant types of land cover in the image. According to Table 9.1 and Figure 9.2 the highest variation occurs in band 5, while the lowest variation is shown in band 6.

Table 9.1. Univariate statistics of the reflectance data, from the original Landsat TM 5 image of the study area (Cd. Madera, Chihuahua).

STATISTICS	BAND 1	BAND 2	BAND 3	BAND 4	BAND 5	BAND 6	BAND7
Mean	59.5	24.3	25.9	58.9	69.4	133.8	29.7
Minimum	50	17	15	13	5	122	3
Maximum	89	56	102	128	173	146	88
Range	39	39	87	115	168	24	85

9.1.1 Principal Components

To avoid inherent data redundancy, a principal component analysis was carried out. Then an image file was created whose bands are the principal components of the input image file. This reduced the redundant data within the original image. Almost 95% of the variance within the entire 7 Landsat TM5 layers was contained in the three first PC bands (Table 9.2). Therefore, only the brightness (reflectance) values that corresponded to these three PC bands (Figure 9.3) were considered data to test both spatial cross-correlation and joint spatial continuity hypotheses.

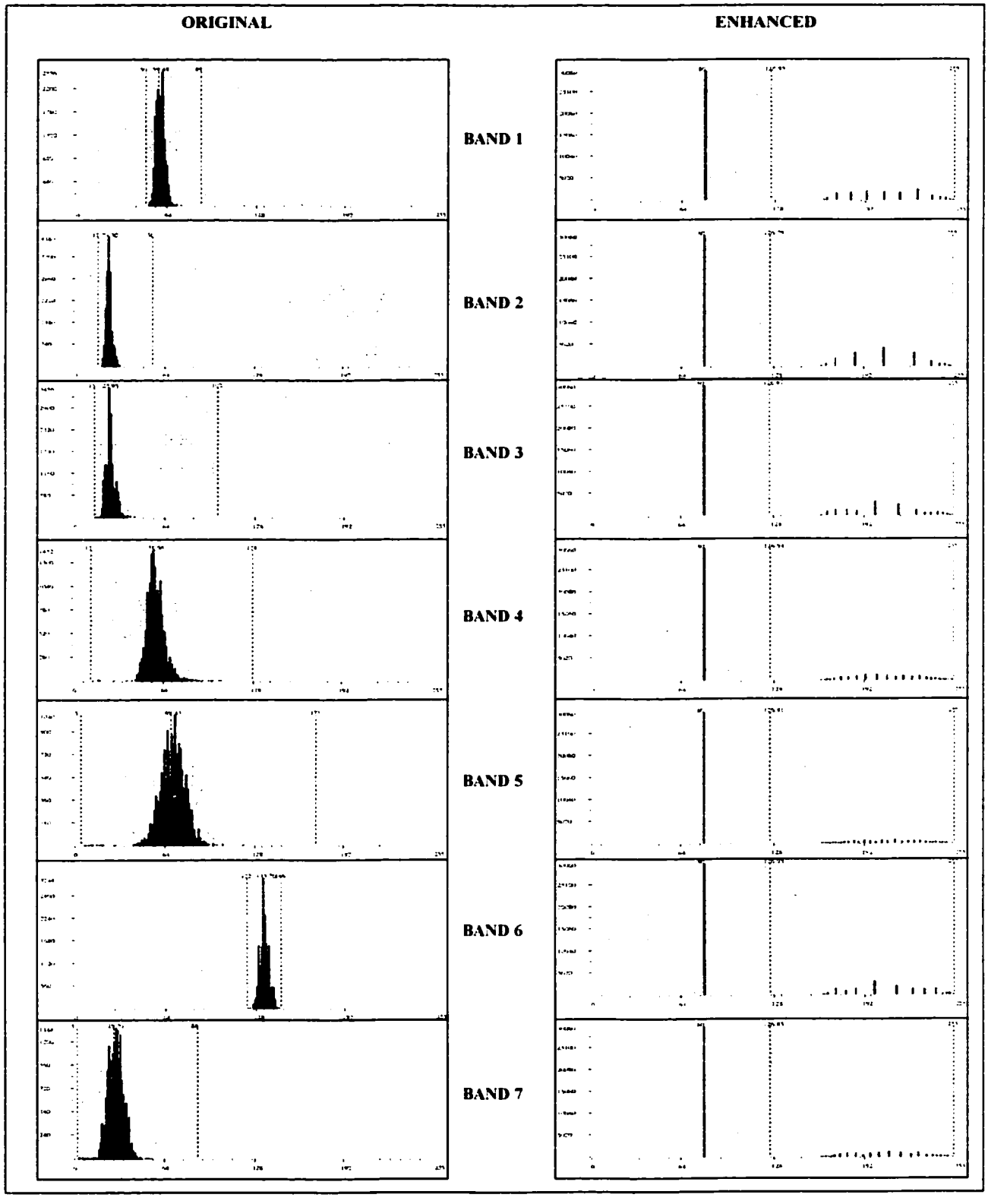

Figure 9.2. Comparison between the reflectance distribution before and after enhancement (Histogram equalization), within the study area (Cd. Madera Chihuahua). Horizontal axis = Brightness values (0-255); Vertical axis = Counts (Frequency).

Table 9.2. Percentage of the variance within the entire original seven bands of the Landsat TM 5 image (Cd. Madera, Chihuahua) resulting from a Principal Component Analysis.

PC	ORIGINAL IMAGE		ENHANCED IMAGE	
	PERCENTAGE	CUMULATIVE	PERCENTAGE	CUMULATIVE
1	65.8	65.8	97.12	97.12
2	23.3	89.1	1.34	98.46
3	5.6	94.7	0.53	98.99
4	2.2	96.9	0.44	99.43
5	1.7	98.6	0.30	99.73
6	1.06	99.66	0.15	99.88
7	0.34	100.0	0.12	100.00

9.1.2 Normalized Difference Vegetation Index (NDVI)

The NDVI was calculated as another auxiliary data source to test spatial cross-correlation and joint spatial continuity hypotheses. An NDVI image of the study area was computed using bands 3 and 4 (Figure 9.4). The reflectance (brightness) variations correspond to differences in phytomass occurrence. The brighter the pixel, the greater the amount of photosynthesizing vegetation present (Jensen, 1996). The corresponding frequency graphic shows a very strong tendency to a normal distribution, where most of the data are between 0.35 and 0.5 NDVI. Comparing with the original image (Figure 9.3), it is clear that the NDVI not only represent the forest vegetation, but also reflects other types of vegetation, such as croplands, and grasslands. Furthermore, since the reflectance of forest fuels cannot be measured directly, the NDVI represents an associated condition that can be used to define fuels potential.

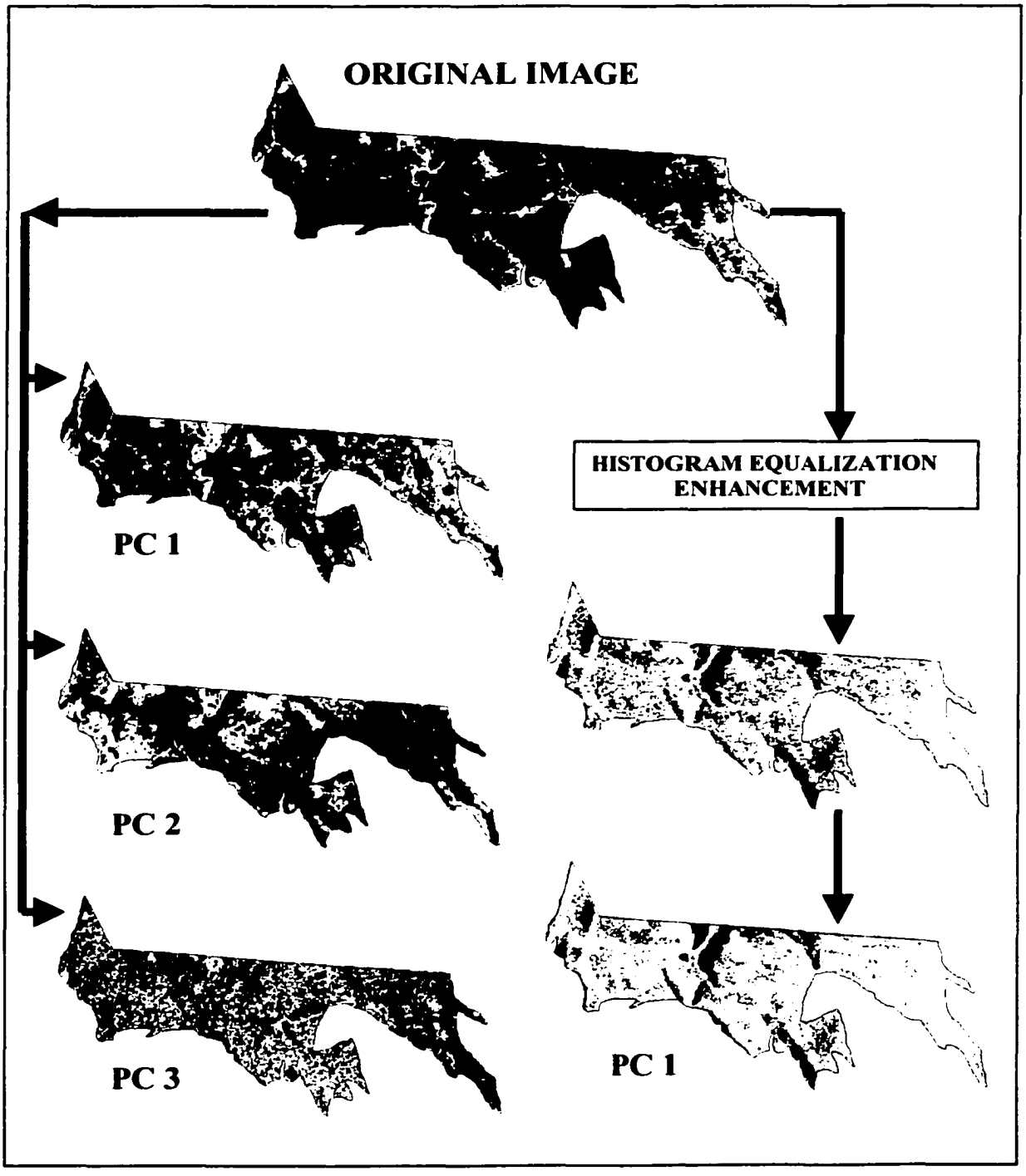

Figure 9.3. Images of the study area (Cd. Madera, Chihuahua) resulting from the original Landsat TM5 and two enhancement processes: (1) Principal Components Analysis (PC); (2) Histogram Equalization.

9.2 Spectral Reflectance of the Enhanced Image

Histogram equalization is a nonlinear contrast enhancement technique, which is helpful to interpret different cover types. It applies the greatest contrast enhancement to the most populated range of brightness values in the image, and reduces the contrast in the very light or dark parts of the images (Jensen, 1996). Figure 9.2 shows a dramatic difference in the range of distribution of the reflectance values of all the 7 bands, which suggests a relative increment of the image contrast (Jensen, 1996). "Lut Stretch", and "Level Slice" were also tested but they resulted in poor good contrast. The resultant image is depicted in Figure 9.3.

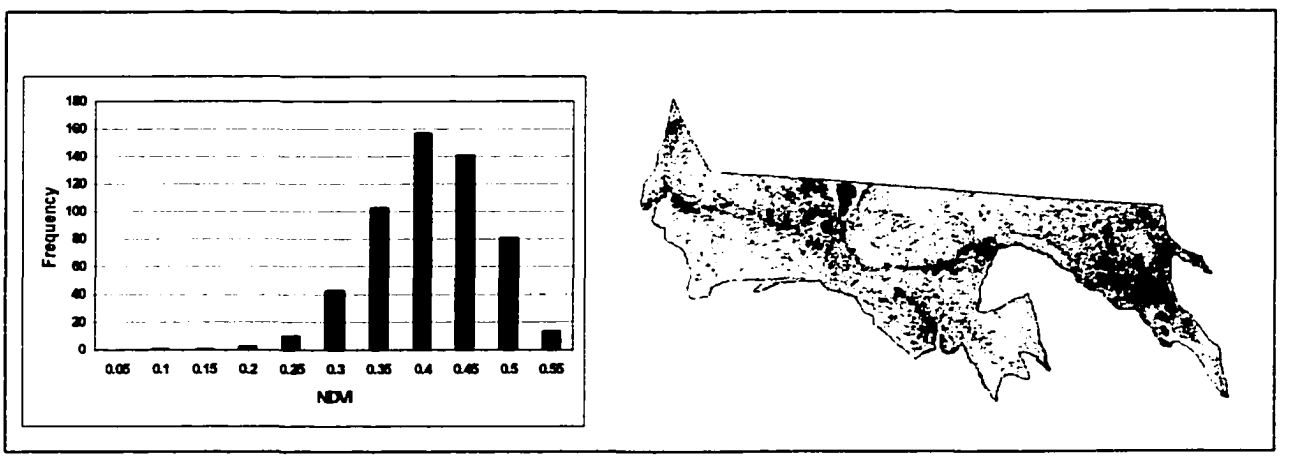

Figure 9.4. Normalized Difference Vegetation Index image of the study area (Cd. Madera, Chihuahua), derived from the original Landsat TM5 image, used as ancillary data in the fuel classes estimations.

9.2.1 Principal components

In the enhanced image the reduction of inherent data redundancy, through a principal component analysis, was more effective than in the original image. Thus, the

created image file of the PC1 represented up to 97.12% of the variance, within the entire 7 Landsat TM (Table 9.2). Therefore, only the brightness values that corresponded to the PC1 were recorded (Figure 9.3).

9.2.2 Normalized Difference Vegetation Index

The NDVI image resulting from the enhanced Landsat TM image is shown in Figure 9.5. In this case, the NDVI values varied from negative to positive values, within a range from –0.195 to 0.196. The brighter areas correspond to denser forest vegetation. The corresponding frequency graphic shows a very strong tendency to a normal distribution.

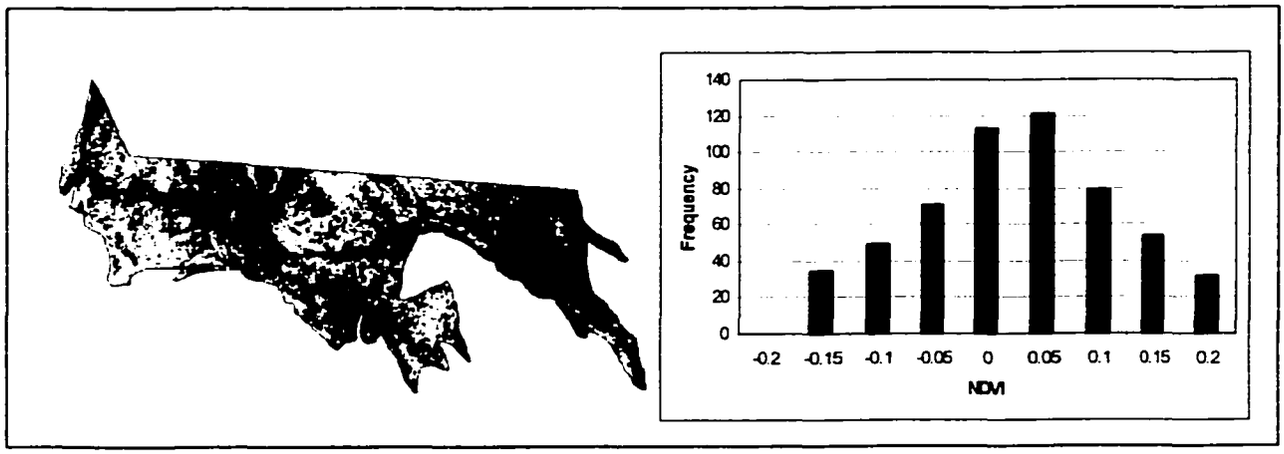

Figure 9.5. Normalized Difference Vegetation Index image of the study area (Cd. Madera, Chihuahua), derived from the enhanced (Histogram Equalization) Landsat TM5 image, used as ancillary data in the fuel classes estimations.

10 SPATIAL DISTRIBUTION OF FUELS

10.1 1-Hour Fuels

This section shows the process for selecting the best interpolation technique for mapping 1-hr fuels' loading (1-HR). Under the geostatistical approach, the hypotheses of no spatial correlation and no spatial cross-correlation are tested regarding the 1-hour fuels (1-HR). The rejection of any of these hypotheses suggest that the known 1-HR values can be used to predict 1-HR loading values in areas not sampled, through geostatistic techniques (kriging). To support this, both spatial continuity and joint spatial continuity hypotheses were tested in order to select the best kriging technique. Then, both deterministic and geostatistic interpolation techniques were compared.

10.1.1 Proximity Matrix

The results of a general proximity matrix are shown in Table 10.1. Although the maximum distance between points was more than 8.5 km, 75% of the sample plots have a distance lower than 3.8 km. The knowledge of the minimum distance between points (in this case 40 m) was useful to define the lag distance used to define the experimental variogram.

10.1.2 Spatial Correlation

According to Table 10.3, the result of the Moran's *I* analysis suggests that there is not enough evidence (P-value < 0.00) to support the null hypothesis H_{o1} (NO SPATIAL AUTOCORRELATION). This suggests that the known 1-HR values can be used to predict 1-HR loading in areas not sampled through geostatistical techniques.

Table 10.1. Characteristics of the distance matrix corresponding to the 1-hour fuels within the study area (Cd. Madera).

Number of sample plots	535	
Average distance between points	2791.10	m
Distance range	8599.28	m
Minimum distance between points	40	m
Quartiles		
First	1435.86	m
Median	2522.76	m
Third	3896.03	m
Maximum distance between points	8639.28	m

A stepwise process, considering 32 independent variables (gathered from inventory, GIS and remote sensing data) and 1-HR fuels as the dependent variable, resulted in the selection of 6 variables (Table 10.2). These variables were used as auxiliary variables in the prediction of 1-HR fuels. Table 10.3 shows the results of bivariate Moran's *I* that corresponds to the spatial cross-correlation between 1-HR fuels and elevation (this variable helps to define the lower MSE, see 10.1.3). These results (P-value < 0.00) suggest that the null hypothesis H_{o2} (NO SPATIAL CROSS-CORRELATION) should be rejected. Therefore, elevation (ELE) can be used to predict 1-HR loading in areas not sampled through geostatistical techniques (cokriging).

10.1.3 Spatial Continuity

Table 10.4 summarizes both the MSE's and the correlation coefficients of all the twelve interpolation techniques used to estimate the 1-hour fuel loading. The variation range of MSE goes from 0.929 to 0.162, which represents a considerable difference between the used interpolation techniques. The lower MSE was obtained through a cokriging (CK) procedure based on elevation (ELE), which showed a

significant results (P-value < 0.00) spatial cross-correlation with 1-HR fuels. (Table 10.3). This suggests rejecting H_{o4} (NO INCREASE IN PRECISION MODELING JOINT SPATIAL CONTINUITY). Thus the MSE could be minimized through cokriging techniques. It is important to point out that this procedure was run using two different software, S-Plus (Reich and Davis, 1998) and GS+ (Robertson, 2000), from which the former resulted in the best result.

Table 10.2. Secondary variables selected after a stepwise process for the estimation of 1-HR fuels in Cd. Madera (Chihuahua). No other variable met the 0.05 significance level for entry into the model.

Step	Variable Entered	Variable Removed	Number Vars In	Partial R-Square	Model R-Square	C(p)	F Value	Pr > F
1	ELE		1	0.1092	0.1092	95.5201	65.35	<.0001
2	PC3		2	0.0333	0.1425	74.1342	20.63	<.0001
3	TBA		3	0.0290	0.1715	55.7337	18.59	<.0001
4	TNS		4	0.0288	0.2003	37.4528	19.11	<.0001
5	AVEH		5	0.0255	0.2258	21.5208	17.42	<.0001
6	AVED		6	0.0072	0.2330	18.4617	4.95	0.0265

ELE: Elevation PC3: Principal Component 3 TBA: Total Basal Area
AVEH: Average Height AVED: Average Diameter TNS: Total Number of Species
C(p)=[sums of Square of error (model- p variables)MSE (pmax)] – N-2(p+1] (Gray, 2001)

Despite the fact that the distribution of the 1-HR fuels data was not perfectly normal, in general the geostatistical techniques showed better results than the traditional interpolation techniques. This response to a low normality is reported in other works (Hohn, 1998; cited by Hunner, 2000). Nevertheless, polygonal mapping was better than the 6 no-cokriging alternatives. This suggests that there is not enough evidence to reject H_{o3} (NO INCREASE IN PRECISION MODELING SPATIAL CONTINUITY). The worst techniques for the estimation of 1-HR fuels were Spline, Thiessen, and Universal Kriging (1^{rst} degree), with MSE's of 0.929, 0.773 and 0.565, respectively.

Table 10.3. Statistics resulting from the autocorrelation (+) and cross-correlation (*) analyses corresponding to 1-HR fuels and elevation (ELE), in Cd. Madera (Chihuahua).

VARIABLE	MORAN'S *I*			Z-VALUE	P-VALUE 2 Sided
	VALUE	MEAN	STAND. DEV		
1HR (+)	0.096829	-0.001873	0.003503	28.17618	0
ELE (+)	0.48083	-0.001873	0.003502	137.827687	0
1HR-ELE (*)	0.178989	-0.000606	0.002607	68.899628	0

(+) Simple Moran's *I*
(*) Bivariate Moran's *I*

Table 10.4. Ranking of the interpolation techniques used to estimate 1-HR fuels based on their corresponding mean square errors (MSE), for the study area (Cd. Madera, Chihuahua). Geostatistical and traditional interpolation techniques are shown according to the three software programs used (S-Plus, ArcView and GS+).

	TRADITIONAL					KRIGING						
	ARCVIEW			GS+		S-PLUS				GS+		
CRITERIA	SPLINE	POLYG. MAPPING	THIESSEN	IDW Power 1	IDW Power 2	ORDINARY KRIGING	UK 1st Degree	UK 2nd Degree	COKRIGING (ELE)	POINT KRIGING	BLOCK KRIGING	COKRIGING (ELE)
MSE	0.929	0.375	0.773	0.417	0.431	0.416	0.565	0.441	0.162	0.410	0.410	0.473
C. C.	0.308	0.577	0.313	0.429	0.457	0.487	0.240	0.467	0.845	0.494	0.494	0.423
RANKING	12	2	11	6	7	5	10	8	1	4	3	9

C. C.= Correlation Coefficient

Although the higher correlation coefficient (CC) corresponds to the lower MSE (CK-ELE), the general ranking, based on CC, was not the same as derived from MSE. For instance, according to the MSE criterion, UK (1st degree) technique was better than Spline, but using the CC criterion Spline was better than UK (1st degree). Thus the method that one can consider the best will depend on the yardstick that one choose (Isaaks and Srivastava, 1989). A graphical comparison of the twelve techniques used to estimate the spatial distribution of 1-HR fuel is displayed in Appendix 10.1. The smoothest surfaces were generated through Point kriging, Block kriging, and Ordinary kriging, which define very similar MSE's (0.410, 0.410 and 0.416 respectively). Although the MSE difference between the two Cokriging estimations was considerable higher, both estimations showed a very similar spatial distribution of the 1-HR fuels loading

10.1.4 Characteristics of the Best Interpolation Technique

Cokriging estimations (using the S-plus software) resulted in the lowest MSE (0.162). The use of elevation (ELE) as an auxiliary variable improved the estimation of the 1-HR fuels variable. This could be the result of a large correlation between 1-HR fuels and ELE (Hunner, 2000; Goovaerts, 1997). To get the maximum benefit in a cokriging process, a correlation coefficient of 0.4 (or above) is needed (Asli and Marcotte, 1995). However, the correlation coefficient between 1-HR fuels and ELE was only 0.1048. Nevertheless, the corresponding bivariate Moran's *I* value (Table 10.3) suggests a significant spatial cross-correlation between these two variables. The MSE resulting from the GS+ software was 191.97% higher than the MSE obtained with S-Plus.

Such difference could be the result of differences in procedures defined by the iterative capabilities of each software program. The finding of such differences is beyond the goals of this study. Nevertheless, it is clear that regarding the estimation of 1-HR fuels, much better results were achieved using S-Plus software (Reich, 1998).

Comparison of Secondary Variables Combinations

The 1-HR fuels variable was combined with the secondary variables resulting from the stepwise process. Table 10.5 shows that the lowest MSE's resulted from all possible combinations between 1-HR fuels (primary variable) and the secondary variables. Using elevation (ELE) as secondary variable, and modeling such relation with an exponential cross-variogram, resulted in the lower MSE (0.162). The combination between 1-HR fuels and principal component (PC3) produced a quite similar result (MSE= 0.163). However, using both ELE and PC3 as secondary variables [1-HR= f(PC3,ELE)] did not decrease the MSE (0.162).

Table 10.5. Mean square errors (MSE) resulting when cokriging 1-HR fuels using different combinations of secondary variables, with data of Cd. Madera (Chihuahua). Cross-variograms model the joint spatial continuity with 1-HR fuels.

SECONDARY VARIABLES		CROSS-VARIOGRAM	MSE
Total Number of Species	**(TNS)**	Spherical	0.164
Average Diameter	**(AVED)**	Exponential	0.164
Average Height	**(AVEH)**	Spherical	0.166
Total Basal Area	**(TAB)**	Exponential	0.164
Elevation	**(ELE)**	Exponential	0.162
Principal Component 3	**(PC3)**	Exponential	0.163
ELE and PC3		Exponential	0.162
ELE and AVED		Exponential	0.163
PC3 and AVED		Exponential	0.219

Spatial Continuity

The experimental variogram for 1-HR fuels and ELE, and the corresponding cross-variogram, are shown in Figure 10.1. The variogram ($\gamma|h|$) values, shown in these variograms, are scaled (Reich, 1998). The lag distance of 40 m showed best results in the definition of both experimental variograms and cross-variogram. The lag tolerance applied was one half of the lag distance. The models for these functions are also shown in Table 10.6. The 1-HR fuels variogram shows a marked nugget effect, which can be the result of a sampling error, or short scale variability. The sill (maximum variogram value) is reached at a range distance of 1000 m. After this distance, there is no longer correlation between samples. In the case of elevation, the variogram does not reach a sill, which represents a strong trend in data. However, it was possible to fit an exponential model (Table 10.20) in the experimental variogram distribution. The behavior of the elevation variogram near the origin, defining a quadratic shape, indicates a high degree of continuity in the variable (Armstrong, 1998).

According to the experimental cross-variogram, 1-HR fuels and ELE were positively spatially cross-correlated. This cross-correlation was significant [$P<0.05$] (Table 10.3). The definition of the cross-variogram model was strongly influenced by the 1-HR fuels' spatial continuity, resulting in an exponential model. Although this model did not fit well with the experimental variogram, its parameters (sill, range and nugget) allowed improving the precision of the 1-HR fuels' estimation (rejecting null hypothesis H_{o4}). Using 2 nearest neighbors in the cokriging prediction resulted in the smallest MSE (0.162).

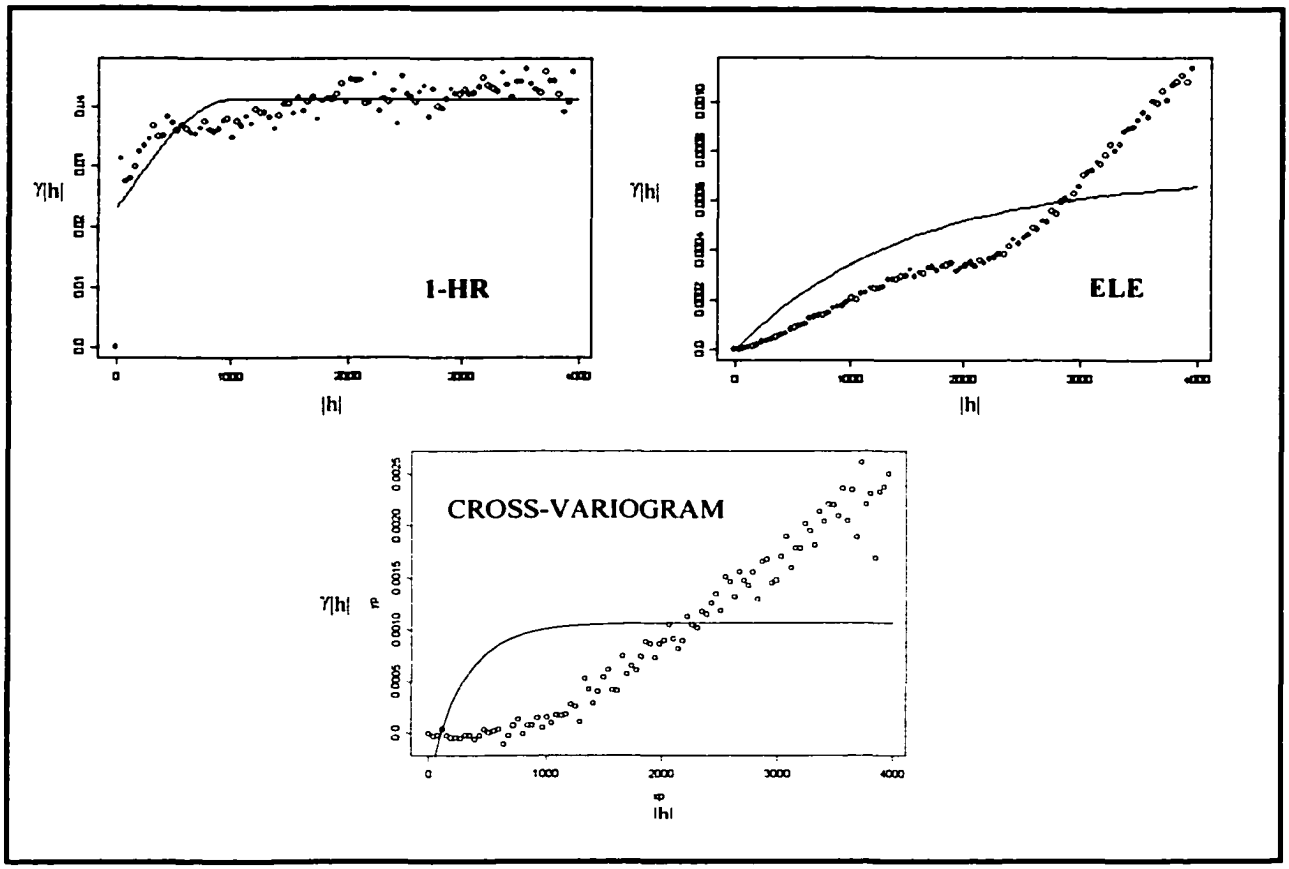

Figure 10.1. Experimental variograms (scaled values) and the corresponding models for 1-HR fuels [spherical] and elevation (ELE) [exponential] as the secondary variable, and the corresponding cross-variogram [exponential]. The variogram values ($\gamma|h|$) are half the average squared difference between the paired data values. Cd. Madera, Chihuahua.

Table 10.6. Characteristics (scaled values) of the models that correspond to the variograms and cross-variogram functions, in the relation between 1-HR fuels (primary variable) and elevation (ELE) as secondary variable. Cd. Madera Chihuahua.

VARIABLE	FUNCTION	MODEL	NUGGET	SILL	RANGE
1HR	Variogram	Spherical	0.2972	0.530146	1000
ELE	Variogram	Exponential	0.00	0.000704	1500
1HR-ELE	Cross-variogram	Exponential	0.0005	0.00107	300

Residuals

The histogram and the q-q plot depict in Figures 10.2a and 10.2b show that the distribution of residuals was almost normal, with a mean close to zero. The scatter plot of the residuals verses the estimated values (Figure 10.2d) indicates no deviations from the underlying assumptions of the linear model, which define a constant variance. There were not significant outliers. The plot of the true values verses the estimated values shows a strong positive linear relationship (r = 0.845). The ratio of variability (R^2) (Reich and Davis, 1998) between estimated values and observed values was 0.63.

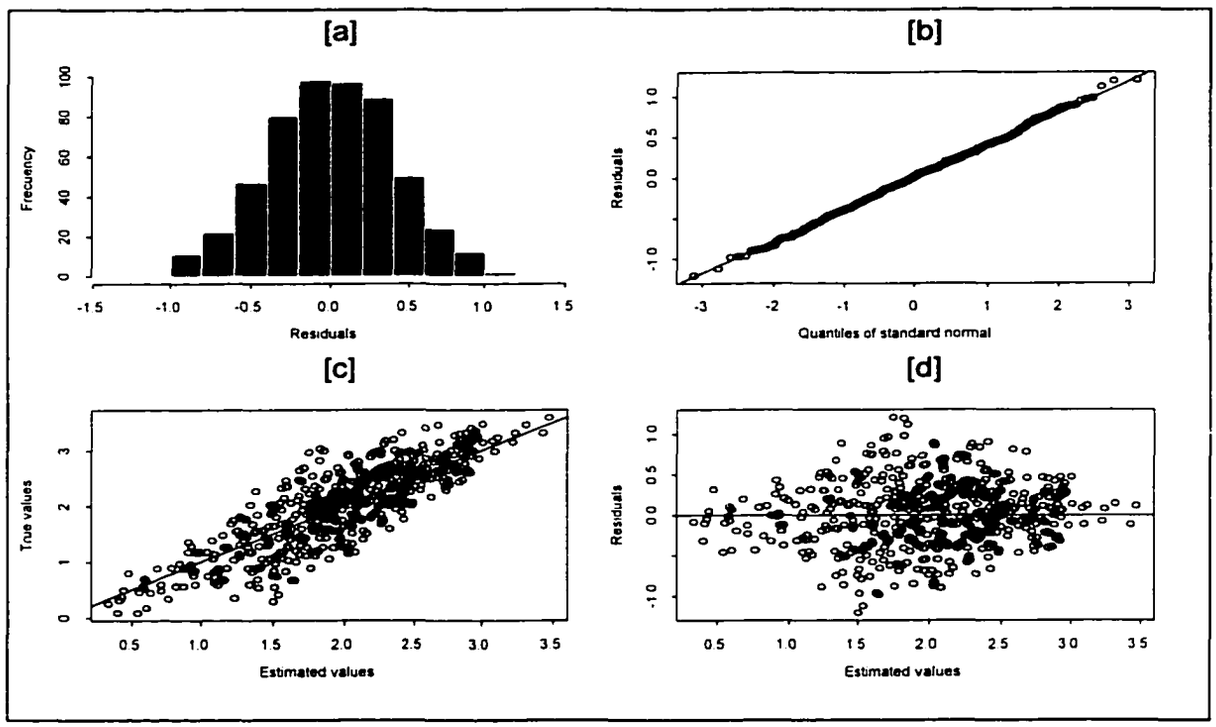

Figure 10.2. Graphical evaluation of cokriging estimations of 1-HR fuels based on elevation: (a) histogram of residuals; (b) quantiles of residuals vs. quantiles of a normal distribution; (c) scatterplot of estimated values vs. true values; (d) scatterplot of estimated values vs. residuals. Cd. Madera, Chihuahua.

10.1.5 1-HR Fuel Map

The resulting contour map of the cokriging estimations of 1-HR fuels, based on ELE, is displayed Figure 10.3. Most of the study area has more than 2 ton/ha of 1-HR fuels. The east portion of the study area shows the lowest values. The surface map indicates that the spatial distribution of the 1-HR fuels is very heterogeneous. The minimum value of the estimates was zero, while the maximum value was 3.47 ton/ha. Figure 10.3 also shows a contour map and a surface map of the standard deviations resulting from the estimation of 1-HR fuels. In the surface map, it is possible to appreciate that the standard deviation was quite homogeneous, corresponding mostly to values lower than 0.20. Such homogeneity could be explained because of the high concentration of sample plots. The minimum value was 0.19 and the maximum standard deviation was 0.245.

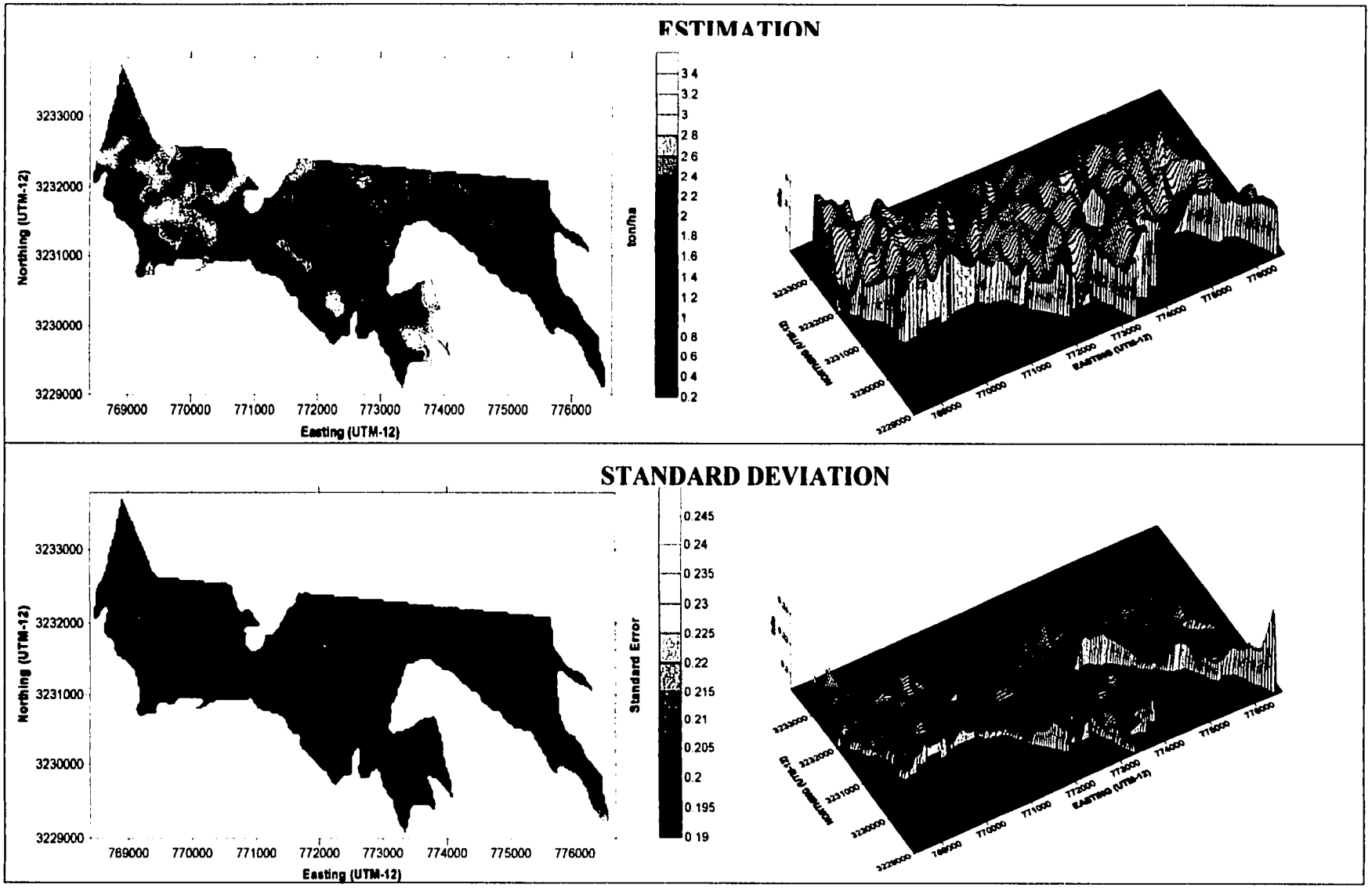

Figure 10.3. Spatial distribution of 1-HR fuels estimations based on Cokriging (with elevation as auxiliary data) for the study area (Cd. Madera, Chihuahua): contour map (top-left) and surface map (top-right). Spatial distribution of the corresponding standard deviations: contour map (bottom-left) and surface map (bottom-right).

10.2 10-Hour Fuels

The process followed to select the best interpolation technique to mapping 10-hr fuels' loading (10-HR) is shown in this section. Although under the geostatistical approach the hypotheses of no spatial correlation (H_{o1}) and no spatial cross-correlation (H_{o2}) were rejected, in this case the best interpolation technique was the inverse distance weighing (IDW). Therefore, there was not enough evidence to reject both H_{o3} and H_{o4} null hypotheses regarding precision increase, so this section is focused only on the relevant aspects regarding IDW technique. The IDW methodology does not require the definition of spatial continuity, thus variograms are not shown in this section.

10.2.1 Proximity Matrix

The results of the general proximity matrix are shown in Table 10.7. Although the maximum distance between points was more than 8.5 km, 75% of the sample plots have a distance lower than 3.92 km. The proximity matrix of 10-HR fuels is very similar to the 1-HR fuels.

Table 10.7. Characteristics of the distance matrix corresponding to the 10-hour fuels in the study area (Cd. Madera, Chihuahua).

Number of sample plots	519	
Average distance between points	2804.84	m
Distance range	8599.28	m
Minimum distance between points	40	m
Quartiles		
First	1431.72	m
Median	2534.31	m
Third	3921.97	m
Maximum distance between points	8639.28	m

10.2.2 Ranking of Spatial Statistical Techniques

Table 10.8 summarizes both the MSE's and the correlation coefficients of all the twelve interpolation techniques used to estimate the 10-hour fuel loading. The variation range of MSE goes from 4.385 to 2.157. The best result (lowest MSE) was obtained through the Inverse Distance Weighting (Power 1). Contrary to the estimation of 1-HR fuels, in this case the worst technique for the estimation of 10-HR fuels was Cokriging, based on PC3 (S-Plus [Reich, 1998]). This suggests there is not enough evidence to reject H_{o3} (NO INCREASE IN PRECISION MODELING SPATIAL CONTINUITY) and H_{o4} (NO INCREASE IN PRECISION MODELING JOINT SPATIAL CONTINUITY).

The highest correlation coefficient (CC) corresponds to the lowest MSE (IDW-P1). However, the general ranking based on CC's, was not the same as that based on MSE's. For instance, according to the CC criterion, the Cokriging-PC3 (GS+) technique was better than IDW-P2; but using MSE as criterion, IDW-P2 was better than Cokriging-PC3 (GS+). A similar situation happened for 1-HR fuels, thus again the method that we consider the best will depend on the yardstick we choose (Isaaks and Srivastava, 1989).

A graphical comparison of the twelve techniques used to estimate the spatial distribution of 10-HR fuels is displayed in Appendix 10.2. The smoothest surfaces resulted from both point kriging and block kriging. However, their ranking was 9 and 8 (MSE 3.224 and 3.215), respectively. The surface map of IDW (Power 1) was quite similar to both universal kriging (Degree 1 and 2) estimations. Their MSE's were 2.259, 2.353 and 2.36, respectively.

Table 10.8. Ranking of the interpolation techniques used to estimate 10-HR fuels based on their corresponding mean square errors (MSE), for the study area (Cd. Madera, Chihuahua). Geostatistical and traditional interpolation techniques are shown according to the three software programs used (S-Plus, ArcView and GS+).

	TRADITIONAL					KRIGING						
	ARCVIEW			GS+		S-PLUS				GS+		
CRITERIA	SPLINE	POLYG. MAPPING	THIESSEN	IDW Power 1	IDW Power 2	ORDINARY KRIGING	UK 1st Degree	UK 2nd Degree	COKRIGING (PC3)	POINT KRIGING	BLOCK KRIGING	COKRIGING (PC3)
MSE	4.022	3.048	3.780	2.157	2.259	2.353	2.353	2.360	4.385	3.224	3.215	2.571
C. C.	0.210	0.404	0.229	0.355	0.308	0.297	0.297	0.293	0.032	0.101	0.108	0.318
RANKING	11	7	10	1	2	4	3	5	12	9	8	6

C. C.= Correlation Coefficient

10.2.3 Best Interpolation Technique

The inverse distance weighting, both power 1 and power 2, was the best method to estimate 10-HR fuels (MSE 2.157 and 2.259, respectively) (Table 10.8). Power 1 resulted in the lowest MSE (2.157). Although kriging methods take the clustering of the sample points into account, it seems that the lack of normality in the distribution of 10-HR fuels affects the kriging estimations. Since the kriging methods used in this study corresponds to the linear geostatistics, a normal distribution of the 10-HR fuel data is required for optimal estimations (Hunner, 2000).

Residuals

Although the residuals tend toward a normal distribution (Figure 10.4a), data are skewed to the right. The q-q plot depicted in Figure 10.4b shows that the plot of residuals separate from the line of theoretical normal reference line, mainly in the right side. In this case, there was a slight indication of a deviation from the underlying assumptions of the linear model (Figure 10.4c), which could define a non-constant variance. Nevertheless, there were not significant outliers. The plot of the true values verses the estimated values (Figure 10.4d) shows a low positive linear relationship [r = 0.355] (Table 10.8). The lines formed in the scatter of Figures 10.4c and 10.4d are defined because 10-HR fuels were estimated through the number of interceptions of woody material < 0.64 cm [fuel dimensions are not considered] (Brown *et al.* 1982). The ratio of variability (R^2) (Reich and Davis, 1998) between estimated values and observed values was 0.874.

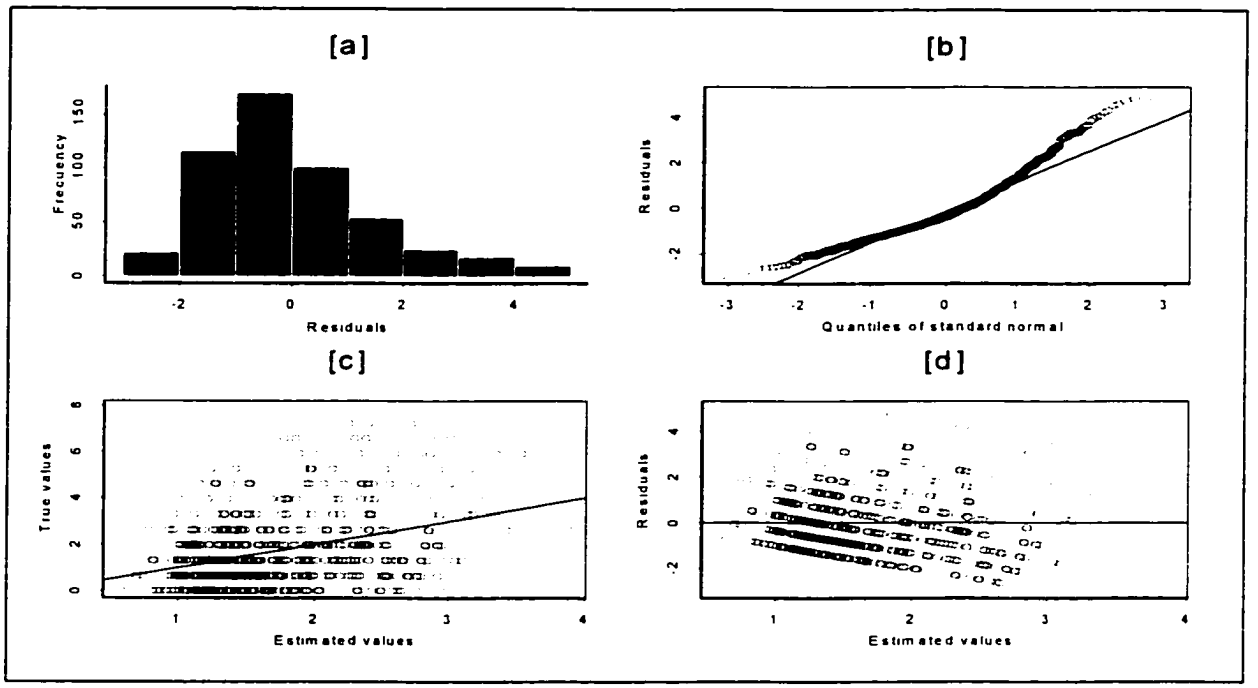

Figure 10.4. Graphical evaluation of IDW (Power 1) estimations of 10-HR fuels: (a) histogram of residuals; (b) quantiles of residuals vs. quantiles of a normal distribution; (c) scatterplot of estimated values vs. true values; (d) scatterplot of estimated values vs. residuals. Cd. Madera, Chihuahua.

10.2.4 10-HR Fuel Map

Figure 10.5 displays a continuous surface map of the IDW (power 1) of 10-HR fuels estimations. Although most of the study area shows less than 2.5 ton/ha, there were some picks of around 4 ton/ha. The minimum value of the estimations was zero, while the maximum value was 5 ton/ha.

The spatial distribution of the standard deviations resulting in the estimation of 10-HR fuels is shown in Figure 10.5. Contrary to the 1-HR estimations, the spatial distribution of the standard error for 10-HR fuels was quite heterogeneous. However, most of the area corresponds to less than 0.60 as the standard error value. The minimum value was 0.1, and the maximum value was 1.15.

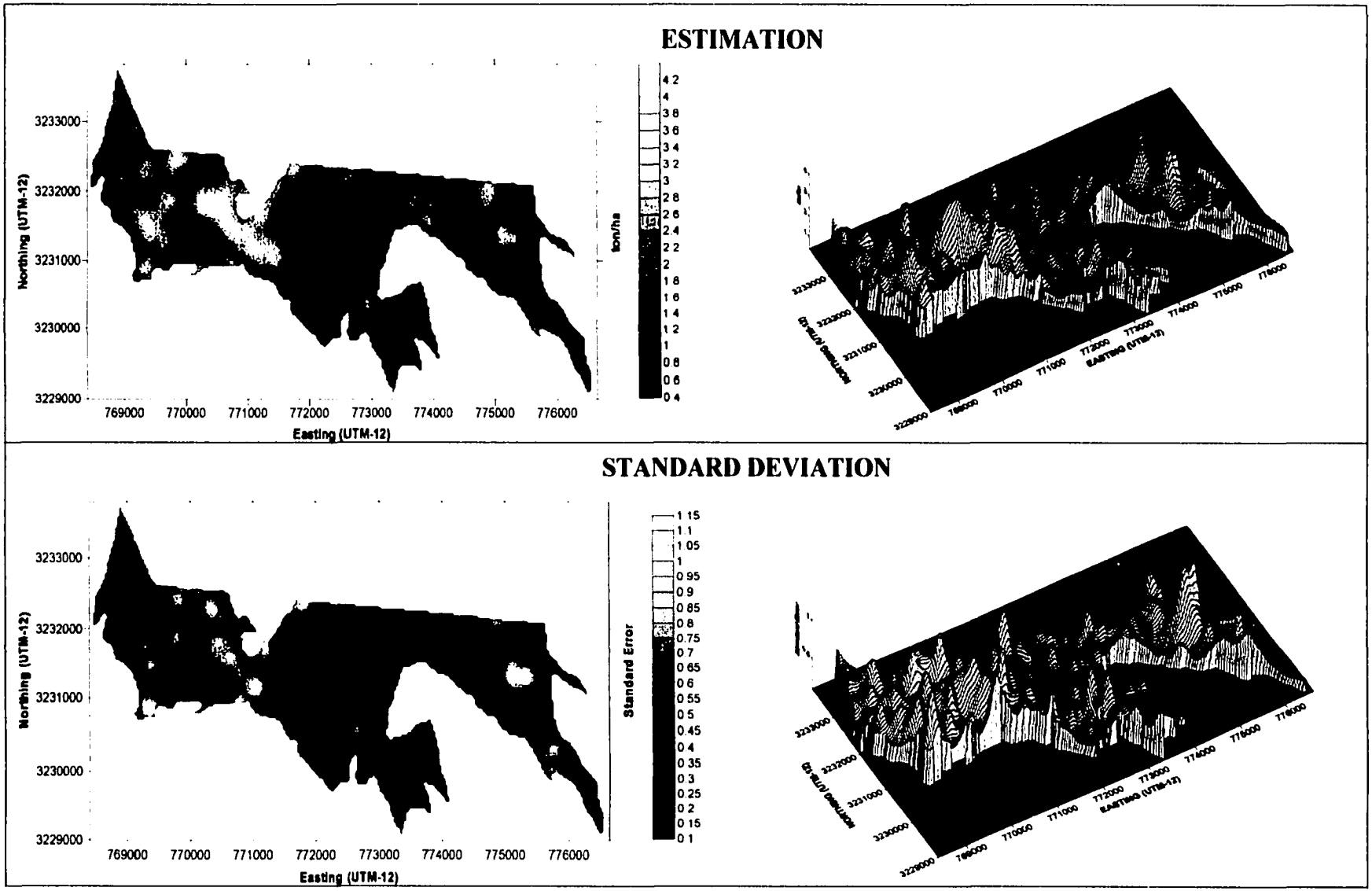

Figure 10.5. Spatial distribution of 10-HR fuels estimations based on Inverse Distance Weighting (Power 1) for the study area (Cd. Madera, Chihuahua): contour map (top-left) and surface map (top-right). Spatial distribution of the corresponding standard deviations: contour map (bottom-left) and surface map (bottom-right).

10.3 100-Hour Fuels

This section shows the process for selecting the best interpolation technique for mapping 100-hr fuels' loading (1-HR). Under the geostatistical approach, the hypotheses of no spatial correlation and no spatial cross-correlation are tested regarding the 1-hour fuels (1-HR). The rejection of any of these hypotheses suggest that the known 100-HR values can be used to predict 100-HR loading values in areas not sampled, through geostatistic techniques (kriging). To support this, both spatial continuity and joint spatial continuity hypotheses were tested in order to select the best kriging technique. Then, both deterministic and geostatistic interpolation techniques were compared.

10.3.1 Proximity Matrix

The results of a general proximity matrix (run in S-Plus) are shown in Table 10.9. Although the maximum distance between points was approximately 8.6 km, 75% of the sample plots have a distance lower than 3.9 km. The knowledge of the minimum distance between points (in this case 40 m) was useful to define the lag distance used to define the experimental variogram.

10.3.2 Spatial Correlation

According to Table 10.11, the result of the Moran's *I* analysis suggests that there is not enough evidence (P-value < 0.05) to support the null hypothesis H_{o1} (NO SPATIAL AUTOCORRELATION). In other words, the 100-hour fuels loading values are significantly spatially autocorrelated. Therefore, it is suggested that the known 100-HR values can be used to predict 100-HR loading in areas not sampled through geostatistical techniques.

Table 10.9. Characteristics of the distance matrix corresponding to the 100-hour fuels within the study area (Cd. Madera).

Number of sample plots	519	
Average distance between points	2800.14	m
Distance range	8599.28	m
Minimum distance between points	40	m
Quartiles		
First	1448.04	m
Median	2532.13	m
Third	3905.14	m
Maximum distance between points	8639.28	m

After a "stepwise" process (Table 10.10), the following variables were selected as auxiliary data, to be tested to improve 100-HR estimations: elevation (ELE), principal component 2 (PC2) and slope (SLP). In this analysis, 32 variables were considered. All variables left in the model were significant at the 0.05 level.

Table 10.10. Secondary variables selected after a stepwise process for the estimation of 100-HR fuels in Cd. Madera (Chihuahua). No other variable met the 0.05 significance level for entry into the model.

Step	Variable Entered	Variable Removed	Number Vars In	Partial R-Square	Model R-Square	C(p)	F Value	Pr > F
1	ELE		1	0.0258	0.0258	3.4240	13.70	0.0002
2	PC2		2	0.0173	0.0431	-3.7796	9.33	0.0024
3	SLP		3	0.0072	0.0503	-5.5999	3.89	0.0490

ELE: Elevation SLP: Slope PC2: Principal component 2
C(p)=[sums of Square of error (model- p variables)MSE (pmax)] – N-2(p+1] (Gray, 2001)

Table 10.11 shows the resulting bivariate Moran's *I* that corresponds to the spatial cross-correlation between 100-HR fuels and elevation (this variable helps to define the lower MSE, see 10.3.4). These results suggest that there is not enough evidence (P-value < 0.00) to support the null hypothesis H_{o2} (NO SPATIAL CROSS-CORRELATION). Therefore, elevation (ELE) can be used to predict 100-HR loading in areas not sampled, through cokriging techniques.

Table 10.11. Statistics resulting from the autocorrelation (+) and cross-correlation (*) analyses corresponding to 100-HR fuels and elevation (ELE), in Cd. Madera (Chihuahua).

VARIABLE	MORAN'S *I*			Z-VALUE	P-VALUE 2 Sided
	VALUE	MEAN	STAND. DEV		
100HR (+)	0.024659	0.001923	0.003602	7.379578	0
ELE (+)	0.48382	0.001923	0.003606	134.6908	0
100HR-ELE (*)	0.085307	-0.000315	0.002589	33.06708	0

(+) Simple Moran's *I* (*) Bivariate Moran's *I*

Table 10.12. Ranking of the interpolation techniques used to estimate 100-HR fuels based on their corresponding mean square errors (MSE) for the study area (Cd. Madera, Chihuahua). Geostatistical and traditional interpolation techniques are shown according to the three software programs used (S-Plus, ArcView and GS+).

	TRADITIONAL					KRIGING						
	ARCVIEW			GS+		S-PLUS				GS+		
CRITERIA	SPLINE	POLYG. MAPPING	THIESSEN	IDW Power 1	IDW Power 2	ORDINARY KRIGING	UK 1st Degree	UK 2nd Degree	COKRIGING (ELE)	POINT KRIGING	BLOCK KRIGING	COKRIGING (ELE)
MSE	183.370	109.930	168.278	93.536	96.538	93.494	94.398	94.933	39.844	95.231	95.016	114.370
C. C.	0.115	0.376	0.150	0.218	0.191	0.212	0.204	0.180	0.768	0.206	0.211	0.173
RANKING	12	9	11	3	8	2	4	5	1	7	6	10

C. C.= Correlation Coefficient

10.3.3 Spatial Continuity

Table 10.12 summarizes both the MSE's and the correlation coefficients of all the twelve interpolation techniques used to estimate the 100-hour fuel loading. The variation range of MSE goes from 183.37 to 39.844, which represents a considerable difference between the interpolation techniques used. The lower MSE (best result) was obtained through a cokriging procedure based on elevation (ELE), which showed a significant spatial cross-correlation with 100-HR fuels (Table 10.11). This suggests rejecting H_{o4} (NO INCREASE IN PRECISION MODELING JOINT SPATIAL CONTINUITY). Therefore, in this case the MSE could be minimized through cokriging techniques. As in the case of 1-HR fuels, the cokriging procedure was run using two different software programs, S-Plus (Reich and Davis, 1998) and GS+ (Robertson, 2000), where the former resulted in the best result.

Although the distribution of the 100-HR data did not tend to normality, in general, the geostatistical techniques showed better results than the traditional interpolation techniques. This response to a low normality is also reported in other works (Hohn, 1998; cited by Hunner, 2000). Ordinary kriging, which is based on simple spatial continuity, was better than any traditional interpolation technique tested. This suggests that there is not enough evidence to reject H_{o3} (NO INCREASE IN PRECISION MODELING SPATIAL CONTINUITY). Nevertheless, inverse distance weighting (IDW-Power1), a traditional technique, was better than 5 of the 7 kriging alternatives. The worst techniques for the estimation of 100-HR fuels were Spline, Thiessen, and Cokriging (GS+), with MSE's of 183.37, 168.278 and 114.37, respectively.

The higher correlation coefficient (CC) corresponded to the lower MSE (CK-ELE). Nevertheless, once again the general ranking, based on CC, was not the same as based on MSE. For instance, according to the MSE criterion, the IDW (Power 1) technique was better than Polygon Mapping, but using CC as criterion Polygon Mapping was better than IDW (Power 1). Therefore, the method that we consider the best will depend on the yardstick, or purposes, we choose (Isaaks and Srivastava, 1989). A graphical comparison of the twelve techniques used to estimate the spatial distribution of 100-HR fuel is displayed in Appendix 10.2. The smoothest surface resulted from point kriging, block kriging and universal kriging (Degree 1 and 2). These techniques defined very similar MSE's: 95.231, 95.016, 94.398 and 94.933, respectively. Despite the considerable difference between the MSE of the two Cokriging estimations, both showed very similar spatial distributions of 100-HR loading (similar to the resulted from Inverse Distance Weighting estimations).

10.3.4 Characteristics of the Best Interpolation Technique

Cokriging estimations (using the S-plus software) resulted in the lowest MSE's (39.844) of the various techniques tested. The use of elevation (ELE), as auxiliary variable, improved the estimation of the 100-HR variable. This could be the result of a large correlation between 100-HR and ELE (Hunner, 2000; Goovaerts, 1997). Although a correlation coefficient of 0.4 (or above) is needed to get the maximum benefit in a cokriging process (Asli and Marcotte, 1995), the correlation coefficient between 100-HR and ELE was only 0.0276. Nevertheless, the corresponding bivariate Moran's I value (Table 10.11) suggests a significant cross-correlation between these two variables. The

MSE resulting from the GS+ software was 187.04% higher than the MSE resulting with S-Plus. Such a large difference could be the result of differences in procedures defined by the iterative capabilities of each software program. Nevertheless, it is clear that a much better result was achieved using S-Plus software (Reich, 1998).

Comparison of Secondary Variables Combinations

The 100-HR variable was cokriged with the secondary variables resulting from the stepwise process. Table 10.13 shows the combinations resulting in the lowest MSE's. Using elevation (ELE) as a secondary variable, and modeling such relations with an exponential cross-variogram, resulted in the lowest MSE (39.844). The combination 100-HR and slope (SLP), with a Gaussian cross-variogram, resulted in almost the same MSE (39.845). The combination of 100-HR with more than two auxiliary variables did not improve the estimations.

Table 10.13. Mean square errors (MSE) resulting when cokriging 100-HR fuels using different combinations of secondary variables, with data of Cd. Madera (Chihuahua). Cross-variograms model the joint spatial continuity with 100-HR fuels.

SECONDARY VARIABLES		CROSS-VARIOGRAM	MSE
Elevation	**(ELE)**	Exponential	39.844
Principal Component 2	**(PC2)**	Exponential	39.964
Slope	**(SLP)**	Gaussian	39.845
PC2 and SLP		Exponential	49.527
ELE and SLP		Exponential	49.244
ELE and PC2		Exponential	49.239

Spatial Continuity

The experimental variogram for 100-HR fuels and ELE, and the corresponding cross-variogram, are shown in Figure 10.6. The $\gamma|h|$ values, shown in these variograms,

are scaled (Reich, 1998). The lag distance of 40 m showed best results in the definition of both experimental variograms and cross-variogram. The lag tolerance applied was one half of the lag distance. The models for these functions are shown in Table 10.14. The 100-HR variogram shows a marked nugget effect, which corresponds with the resulting low Moran's *I* value (0.024659). In other words, the discontinuity at the origin is to high that the data was close to define no spatial autocorrelation [total nugget effect] (Isaaks and Srivastava, 1989). The sill (maximum variogram value) is reached at a range distance of 1000 m. After this distance there is no longer correlation between samples. In the case of elevation, the variogram does not reach a sill, which represents a strong trend in data. However, it was possible to fit an exponential model (Table 10.20) in the experimental variogram distribution. The behavior of the variogram near the origin, defining a quadratic shape, indicates a high degree of continuity in the variable (Armstrong, 1998).

Table 10.14. Characteristics (scaled values) of the models that correspond to the variograms and cross-variogram functions, in the relation between 100-HR fuels and elevation (ELE) as auxiliary variable. Cd. Madera, Chihuahua.

VARIABLE	FUNCTION	MODEL	NUGGET	SILL	RANGE
100-HR	Variogram	Spherical	0.0419	0.053819	999.99
ELE	Variogram	Exponential	0	0.000606	1000
100HR-ELE	Cross-variogram	Exponential	0.0003	0.000859	1000

According to the cross-variogram, 100-HR fuels and ELE were positively spatially cross-correlated. This cross-correlation was significant [$P < 0.05$] (Table 10.11). Both the 100-HR fuels and elevation spatial continuity influenced the definition of the cross-variogram model, resulting in an exponential model. Although this model does not

fit well with the experimental variogram its parameters (sill, range and nugget) allowed improving the precision of the 100-HR fuels estimation (rejecting null hypothesis H_{o4}). Using 2 nearest neighbors in the cokriging prediction resulted in the smallest MSE (39.844).

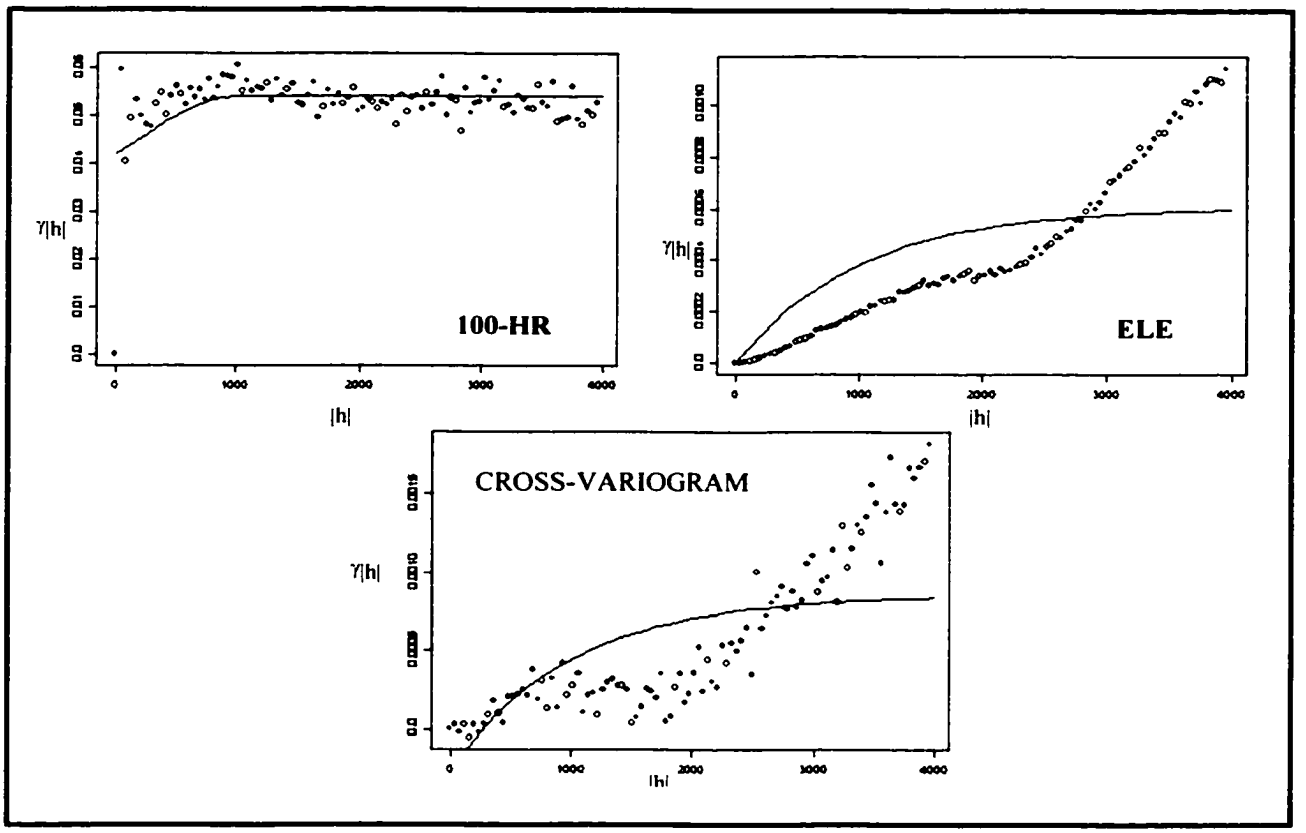

Figure 10.6. Experimental variograms (scaled values) and the corresponding models for 100-HR fuels [spherical] and elevation (ELE) [exponential] as the secondary variable, and the corresponding cross-variogram [exponential]. The variogram values ($\gamma|h|$) are half the average squared difference between the paired data values. Cd. Madera, Chihuahua.

Residuals

The histogram and the q-q plot depicted in Figure 10.7a and 107b show that the distribution of residuals tends to be normal, with a mean close to zero. However, data

tend to concentrate close to the mean, defining a certain skew toward both sides. The scatter plot of the residuals verses the estimated values (Figure 10.7d) shows unequal variances, which indicates certain deviations from the underlying assumptions of the linear model, which affects the constancy of variance. Nevertheless, there were not significant outliers. The plot of the true values verses the estimated values (10.7c) shows a positive linear relationship (r = 0.768). The lines formed in the scatter of Figures 10.7c and 10.7d are defined because 100-HR fuels were estimated through the number of interceptions of woody material with diameter between 0.64 and 2.54 cm [fuel dimensions are not considered] (Brown *et al.* 1982). The ratio of variability (R^2) (Reich and Davis, 1998) between estimated values and observed values was 0.411.

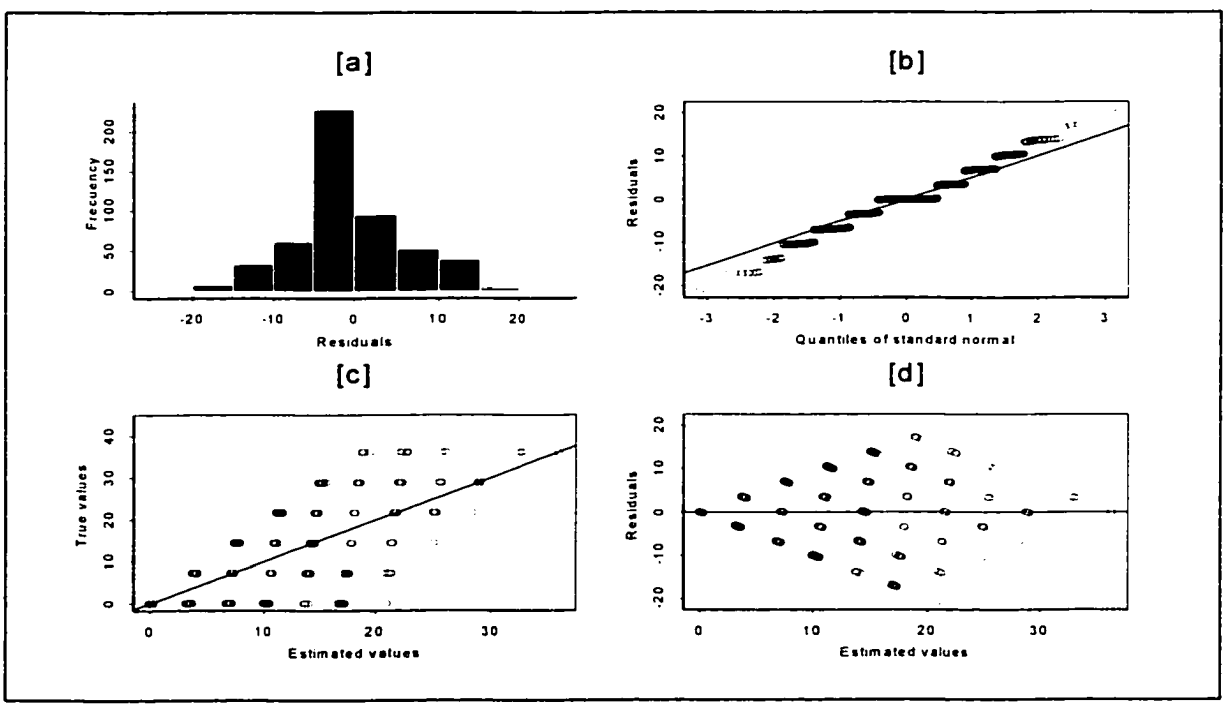

Figure 10.7. Graphical evaluation of cokriging estimations of 100-HR fuels based on elevation: (a) histogram of residuals; (b) quantiles of residuals vs. quantiles of a normal distribution; (c) scatterplot of estimated values vs. true values; (d) scatterplot of estimated values vs. residuals. Cd. Madera, Chihuahua.

10.3.5 100-HR Fuel Map

The resulting contour map of the cokriging estimations of 100-HR fuels, based on ELE, is displayed in Figure 10.8. Most of the area tends to have more than 10 ton/ha. The lower 100-HR fuels loading occurred in the north portion of the study area. The surface map indicates that the spatial distribution of the 100-HR fuels is very heterogeneous. The minimum value of the estimates was zero, while the maximum value was 32 ton/ha.

Figure 10.8 also shows a contour map and a surface map of the standard errors resulting from the estimation of 100-HR fuels. The standard deviation was spatially distributed quite homogeneously. Most of the standard error values were lower than 11.5. Such homogeneity could be explained because of the high concentration of sample plots. The minimum value was 10.9, and the maximum standard error was 12.2.

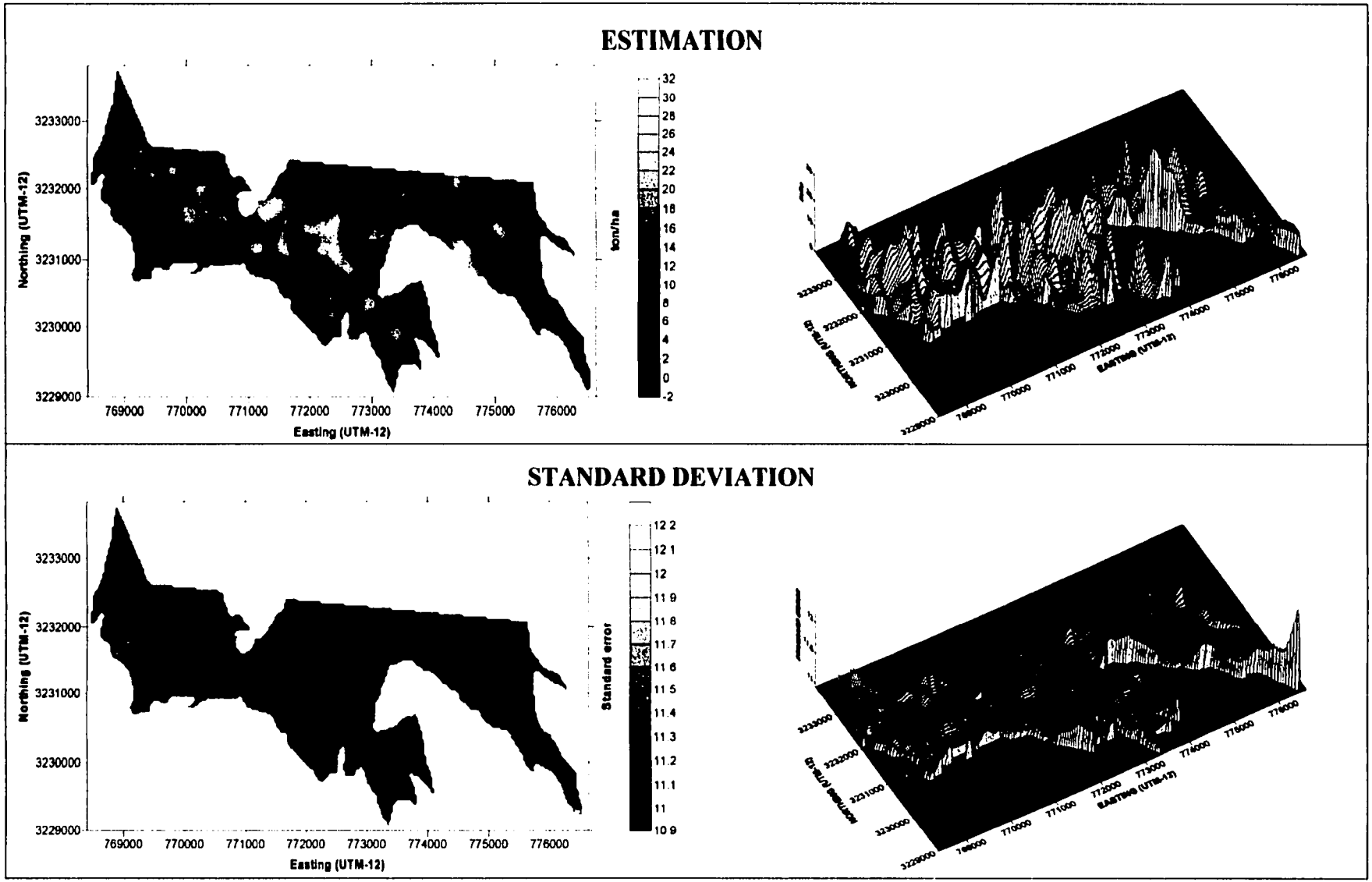

Figure 10.8. Spatial distribution of 100-HR fuels estimations based on Cokriging (with ELE as auxiliary data) for the study area (Cd. Madera, Chihuahua): contour map (top-left) and surface map (top-right). Spatial distribution of the corresponding standard deviations: contour map (bottom-left) and surface map (bottom-right).

10.4 Live Woody Fuels

The process for selecting the best interpolation technique for mapping Live Woody (LW) fuels loading is shown in this section. Under the geostatistical approach the hypotheses of no spatial correlation and no spatial cross-correlation were tested regarding the LW fuels. The rejection of any of these hypotheses suggest that the known LW values can be used to predict LW loading values in areas not sampled, through geostatistical techniques (kriging). To support this, both spatial continuity and joint spatial continuity hypotheses were tested in order to select the best kriging technique. Then, both deterministic and geostatistic interpolation techniques were compared.

10.4.1 Proximity Matrix

The results of the general proximity matrix are shown in Table 10.15. Although the maximum distance between points was approximately 8.6 km, 75% of the sample plots have a distance lower than 3.86 km. The knowledge of the minimum distance between points (in this case 40 m) helped to define the lag distance used to define the experimental variogram.

10.4.2 Spatial Correlation

According to Table 10.16, the result of the Moran's *I* analysis suggests that there is not enough evidence (P-value < 0.00) to support the null hypothesis H_{o1} (NO SPATIAL AUTOCORRELATION). This suggests that the known LW values can be used to predict LW loading in areas not sampled through geostatistical techniques.

Table 10.15. Characteristics of the distance matrix corresponding to the Live Woody fuels within the study area (Cd. Madera).

Number of sample plots	523	
Average distance between points	2778.26	m
Distance range	8599.28	m
Minimum distance between points	40	m
Quartiles		
First	1443.73	m
Median	2515.02	m
Third	3863.52	m
Maximum distance between points	8639.28	m

A stepwise process, considering 32 independent variables (gathered from inventory, GIS and remote sensing data) and LW as the dependent variable, resulted in the selection of 6 variables (Table 10.17). These were tested as auxiliary variables in the prediction of LW. All variables left in the model are significant at the P= 0.05 level. Table 10.16 shows the resulting bivariate Moran's *I* corresponding to the spatial cross-correlation between LW fuels and elevation (this variable helped to define the lower MSE [0.252]). These results suggest that there is not enough evidence (P-value < 0.00) to support the null hypothesis H_{o2} (NO SPATIAL CROSS-CORRELATION). Therefore, elevation (ELE) can be used to predict LW loading in areas not sampled, through cokriging techniques.

10.4.3 Spatial Continuity

Table 10.18 summarizes both the MSE's and the correlation coefficients of all the twelve interpolation techniques used to estimate the LW fuel loading. The variation range of MSE goes from 0.252 to 4.528, which represent a considerable difference between the interpolation techniques used. The lowest MSE (best result) was obtained through a cokriging procedure based on elevation (ELE), which showed a significant

spatial cross-correlation with LW fuels (Table 10.17). This suggests rejecting H_{o4} (NO INCREASE IN PRECISION MODELING JOINT SPATIAL CONTINUITY). Therefore, in this case the MSE could be minimized through cokriging techniques. It is important to point out that this procedure was run using two different software programs, S-Plus (Reich and Davis, 1998) and GS+ (Robertson, 2000), where the former resulted in the best result.

Table 10.16. Variables selected after a stepwise process for estimation of LW fuels in the study area (Cd. Madera, Chihuahua). No other variable met the 0.05 significance level for entry into the model.

Step	Variable Entered	Variable Removed	Number Vars In	Partial R-Square	Model R-Square	C(p)	F Value	Pr > F
1	ELE		1	0.0399	0.0399	40.0018	21.67	<.0001
2	ASP		2	0.0279	0.0679	25.7300	15.59	<.0001
3	TBA.		3	0.0169	0.0848	17.8946	9.58	0.0021
4	AVEC		4	0.0111	0.0959	13.4380	6.35	0.0120
5	TNS		5	0.0081	0.1040	10.7201	4.68	0.0311
6	N		6	0.0119	0.1159	5.7805	6.96	0.0086

ELE: Elevation N: Northing TAB: Total Basal Area
AVEC: Average Crown ASP: Aspect TNS: Total Number of Species
C(p)=[sums of Square of error (model- p variables)MSE (pmax)] – N-2(p+1] (Gray, 2001)

Although the distribution of the LW data did not tend to be normal, in general the geostatistical techniques showed better results than the traditional interpolation techniques. This response to a low normality is reported in other works (Hohn, 1998; cited by Hunner, 2000). Nevertheless, IDW (P1), a traditional technique, was the second best estimator (MSE 0.617) (better that the 6 no-cokriging alternatives). This suggests that there is not enough evidence to reject H_{o3} (NO INCREASE IN PRECISION MODELING SPATIAL CONTINUITY). The worst techniques for the estimation of LW fuels were Polygon Mapping, Spline and Thiessen, with MSE's of 4.528, 1.085 and 1.068, respectively.

Table 10.17. Statistics resulting from the autocorrelation (+) and cross-correlation (*) analyses corresponding to live woody fuels (LW) and Elevation (ELE) data, in Cd Madera Chihuahua.

VARIABLE	MORAN'S *I*			Z-VALUE	P-VALUE * 2 Sided
	VALUE	MEAN	STAND. DEV		
LW (+)	0.048534	0.001916	0.003544	14.195811	0
ELE (+)	0.475256	0.001916	0.003574	133.497898	0
LW-ELE (*)	0.095704	-0.000383	0.002581	37.235076	0

(+) Simple Moran's *I*
(*) Bivariate Moran's

Table 10.18. Ranking of the interpolation techniques used to estimate LW fuels based on their corresponding mean square errors (MSE), for the study area (Cd. Madera, Chihuahua). Geostatistical and traditional interpolation techniques are shown according to the three software programs used (S-Plus, ArcView and GS+).

	TRADITIONAL					KRIGING						
	ARCVIEW			GS+		S-PLUS				GS+		
CRITERIA	SPLINE	POLYG. MAPPING	THIESSEN	IDW Power 1	IDW Power 2	ORDINARY KRIGING	UK 1st Degree	UK 2nd Degree	COKRIGING (ELE)	POINT KRIGING	BLOCK KRIGING	COKRIGING (ELE)
MSE	1.085	4.528	1.068	0.617	0.630	0.800	0.625	0.633	0.252	0.632	0.627	0.716
C. C.	0.204	0.324	0.175	0.347	0.334	0.249	0.332	0.309	0.804	0.320	0.330	0.303
RANKING	11	12	10	2	5	9	3	7	1	6	4	8

C. C.= Correlation Coefficient

The higher correlation coefficient (0.804) corresponded to the lower MSE (CK-ELE). Nevertheless, as before, the general ranking based on the correlation coefficient was not the same as based on MSE. For instance, according to the MSE criterion, block kriging technique was better than IDW (Power 2). But the opposite happened when the criterion selected is the correlation coefficient. Therefore, the method that we consider the best will depend on the yardstick, or purpose we choose (Isaaks and Srivastava, 1989). A graphical comparison of the twelve techniques used to estimate the spatial distribution of LW fuel is displayed in Appendix 10.4. The smoothest surfaces resulted from point kriging and block kriging. Such techniques defined very similar MSE: 0.632 and 0.627, respectively. Despite the considerable difference between the MSE of the 2 cokriging estimations, both showed very similar spatial distributions of LW loading. This spatial distribution pattern was similar to the results from inverse distance weighting (power 1) estimations.

10.4.4 Characteristics of the Best Interpolation Technique

Cokriging estimations (using the S-plus software) resulted in the lowest MSE's (0.252) of the methods tested. The use of elevation (ELE), as auxiliary variable, improved the estimation of the LW variable. This could be the result of a large correlation between LW and ELE (Hunner, 2000; Goovaerts, 1997). However, the correlation coefficient between LW and ELE was 0.0516. Nevertheless, the bivariate Moran's *I* value (0.0957, p-value=0) (Table 10.16) suggests rejecting the null hypothesis of no spatial cross-correlation). The MSE resulting from the GS+ software was 184.13% higher than the MSE resulting from S-Plus. Such difference could be the result of a difference in procedures. Nevertheless, it is clear that a much better result was achieved

using S-Plus software (Reich, 1998). Such difference could be the result of differences in procedures defined by the iterative capabilities of each software program.

Comparison of Secondary Variables Combinations

The LW variable was cokriged with the secondary variables resulting from the stepwise process. Table 10.19 shows the combinations that resulted in the lowest MSE's. Using elevation (ELE) as a secondary variable to predict LW, based on a exponential cross-variogram, resulted in the lowest MSE (0.252). The combinations of LW with total number of species (TNS) [exponential cross-variogram], and LW with average crown height (AVEC) [Gaussian cross-variogram] resulted in the same MSE (0.254). The combination of LW with more than two auxiliary variables did not improve the estimations.

Table 10.19. Mean square errors (MSE) resulting when cokriging Live Woody fuels using different combinations of secondary variables, with data of Cd. Madera (Chihuahua). Cross-variograms model the joint spatial continuity with LW.

SECONDARY VARIABLES		CROSS-VARIOGRAM	MSE
Total Number of Species	**(TNS)**	Exponential	0.254
Average crown Height	**(AVEC)**	Gaussian	0.254
Total Basal Area	**(TAB)**	Exponential	0.256
Aspect	**(ASP)**	Exponential	0.303
Elevation	**(ELE)**	Exponential	0.252
TNS and AVEC		Spherical	11.804
TNS and ELE		Exponential	11.633
AVEC and ELE		Gaussian	11.781

Spatial Continuity

The experimental variogram for LW and ELE, and the corresponding cross-variogram, are shown in Figure 10.9. The $\gamma|h|$ values shown in these variograms, are

scaled (Reich, 1998). The lag distance of 40 m showed best results in the definition of both experimental variograms and cross-variogram. The lag tolerance applied was one half of the lag distance. The models for these functions are also shown in Table 12.20. As in the case of 100-HR fuels, the LW variogram shows a marked nugget effect, which corresponds with the resulting low Moran's *I* value (0.048534). Thus, the discontinuity at the origin is too high that the experimental variogram was close to represent a total nugget effect [no spatial autocorrelation] (Isaaks and Srivastava, 1989). The sill (maximum variogram value) is reached at a range distance of 1000 m. After this distance, there is no longer correlation between samples. In the case of elevation, the variogram does not reach a sill, which represents a strong trend in data. However, it was possible to fit an exponential model (Table 10.20) in the experimental variogram distribution. The behavior of the elevation variogram near the origin, defining a quadratic shape, indicates a high degree of continuity in the variable (Armstrong, 1998). According to the experimental cross-variogram, LW and ELE were positively spatially cross-correlated. Using 2 nearest neighbors in the cokriging prediction resulted in the smallest MSE (39.844).

According to the cross-variogram, LW and ELE were positively spatially cross-correlated. This cross-correlation was significant [$P < 0.05$] (Table 10.17). The definition of the cross-variogram model was strongly influenced by the LW fuels' spatial continuity, resulting in an exponential model. Although this model does not fit well with the experimental variogram, its parameters (sill, range and nugget) allowed improving the precision of the LW fuels estimation (rejecting null hypothesis H_{o4}). Using 2 nearest neighbors resulted in the smallest MSE (0.252).

Table 10.20. Characteristics (scaled values) of the models that correspond to the variograms and cross-variogram functions, in the relation between Live Woody [LW] (primary variable) and elevation [ELE] (auxiliary variable), for Cd. Madera, Chihuahua.

VARIABLE	FUNCTION	MODEL	NUGGET	SILL	RANGE
LW	Variogram	Spherical	0.0152	0.018862	999.99
ELE	Variogram	Exponential	0	0.000541	700
LW-ELE	Cross-variogram	Exponential	0.0003	0.000511	300

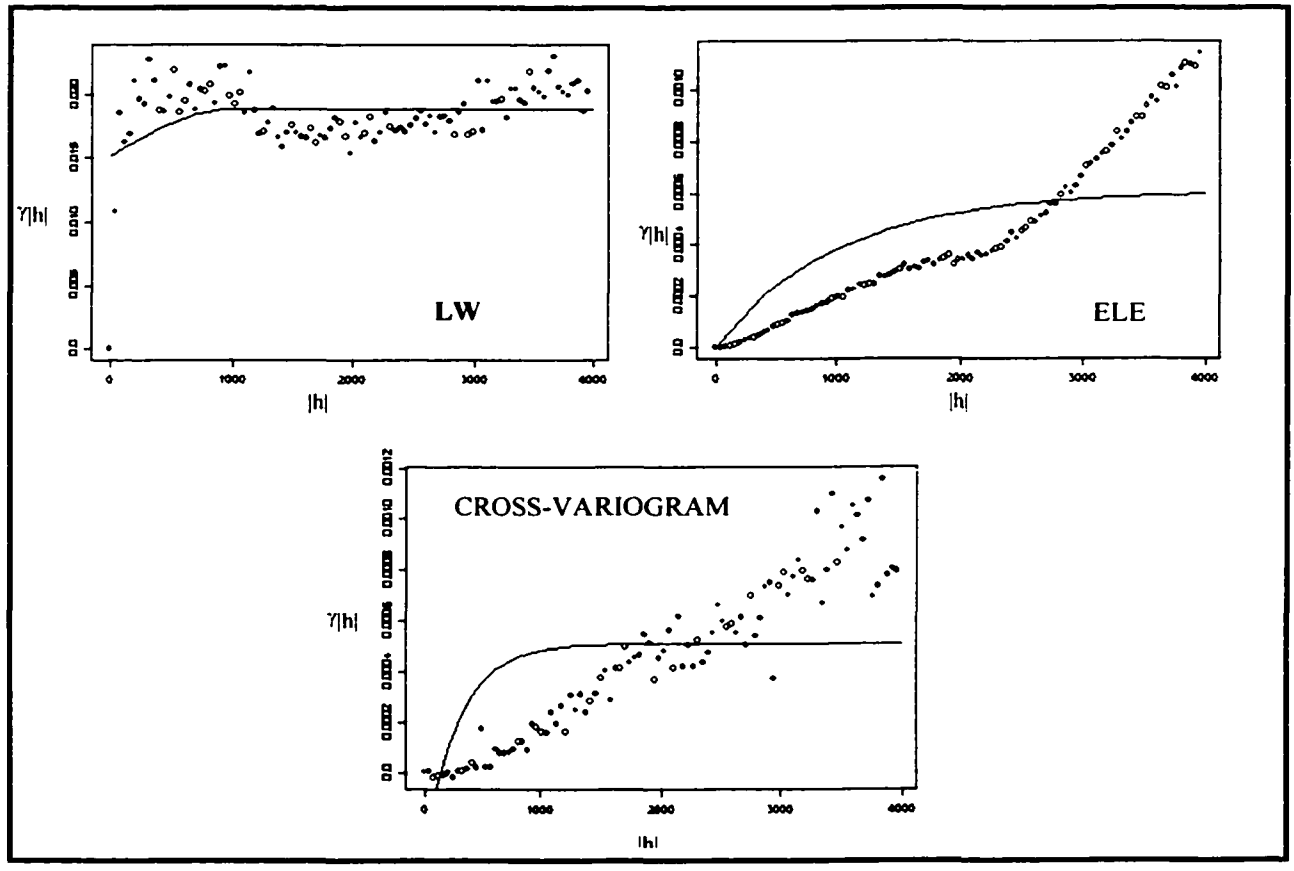

Figure 10.9. Experimental variograms (scaled values) and the corresponding models for Live Woody (LW) fuels [spherical] and elevation (ELE) [exponential] as secondary variable, and the corresponding cross-variogram [exponential]. The variogram values ($\gamma|h|$) are half the average squared difference between the paired data values. Cd. Madera, Chihuahua.

Residuals

The histogram depicted in Figure 10.10a shows that the distribution of residuals tends to be normal, with a mean close to zero. However, data tend to concentrate close to the mean, separating from the quantiles of the theoretical normal distribution at both sides (Figure 10.10b). The scatter plot of the residuals verses the estimated values (Figure 10.10d) indicates certain deviations from the underlying assumptions of the linear model in the higher estimated values, which affect the constancy of variance. There were some significant outliers. The plot of the true values verses the estimated values (10.10c) shows a positive linear relationship (r = 0.804). The ratio of variability (R^2) (Reich and Davis, 1998) between estimated values and observed values was 0.36.

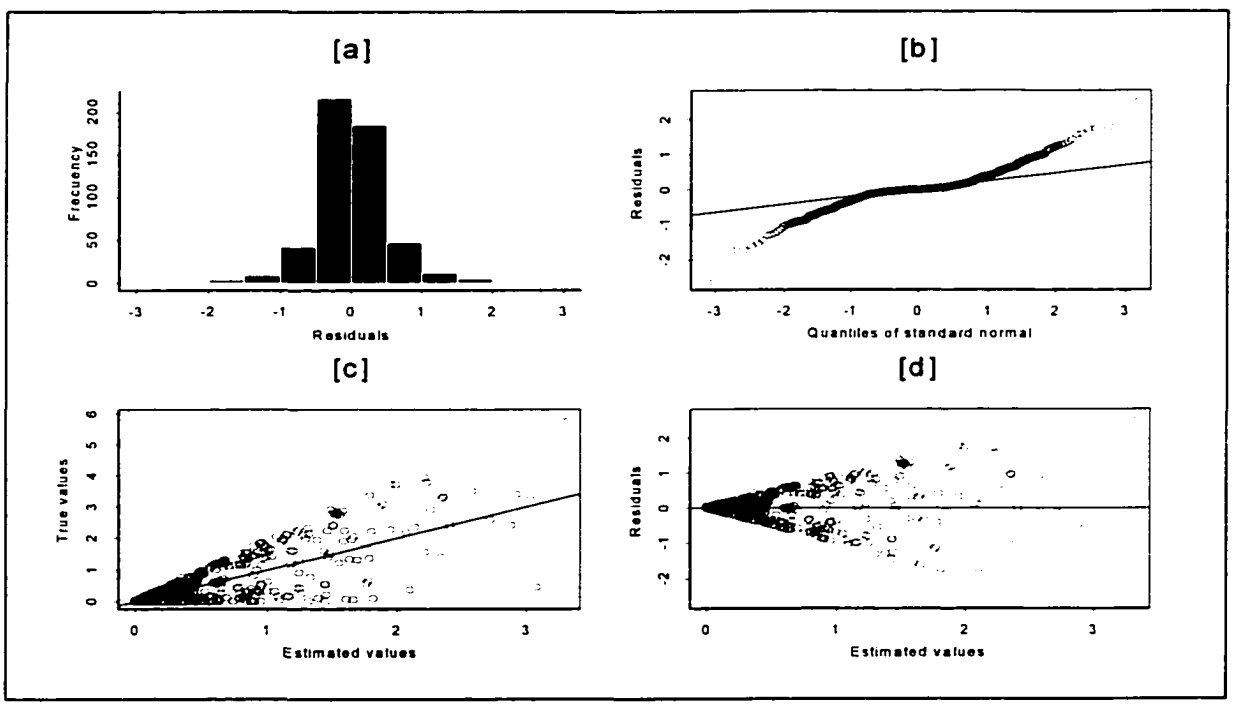

Figure 10.10. Graphical evaluation of cokriging estimations of Live Woody (LW) fuels based on elevation: (a) histogram of residuals; (b quantiles of residuals vs. quantiles of a normal distribution; (c) scatterplots of estimated values vs. true values; (d) scatterplots of estimated values vs. residuals. Cd. Madera, Chihuahua.

10.4.5 LW Fuel Map

The resulting contour map of the cokriging estimations of LW fuels, based on ELE, is displayed in Figure 10.11. Most of the area tends to have more than 1 ton/ha of LW fuels. The higher LW fuel loading occurred in the western portion of the study area. The spatial distribution of LW fuels is very heterogeneous in the areas with more than 2 ton/ha. The minimum value of the estimates was zero, while the maximum value was 3.2 ton/ha.

Figure 10.11 also shows a contour map and a surface map of the standard errors resulted in the estimation of LW fuels. The standard deviation was spatially distributed quite homogeneously. Most of the standard error values were lower than 0.925. The minimum value was 0.895, and the maximum standard error was 0.985.

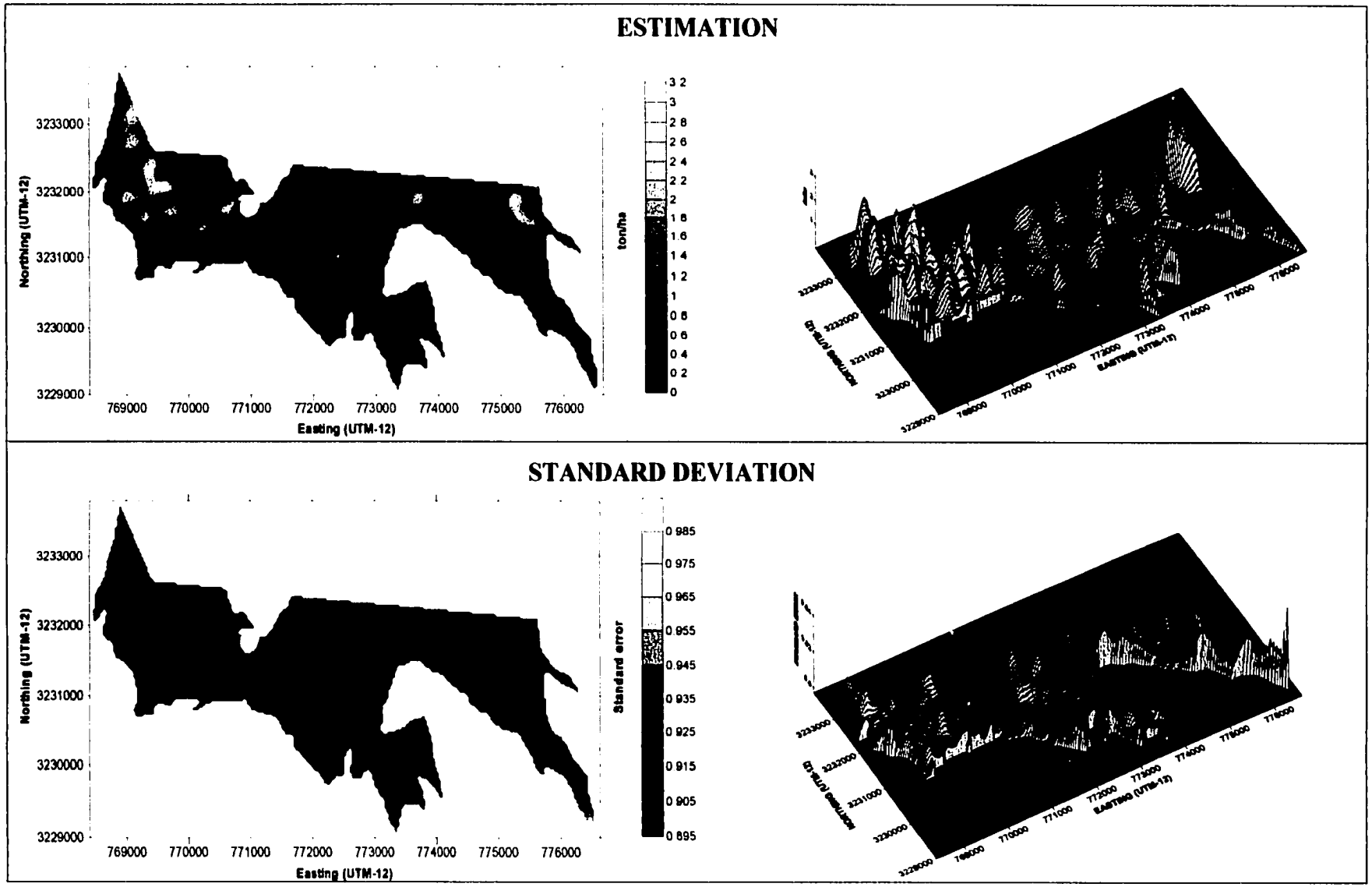

Figure 10.11. Spatial distribution of LW estimations based on Cokriging (with ELE as auxiliary data) for the study area (Cd. Madera Chihuahua): contour map (top-left) and surface map (top-right). Spatial distribution of the corresponding standard deviations: contour map (bottom-left) and surface map (bottom-right).

11 SPATIAL FIRE BEHAVIOR SIMULATION

The four fuel maps generated in this study reflect more accurately the spatial variation of fuel distribution. Therefore, one would expect that the performance of a simulation based on fuel maps would be different than a simulation based on fuel models. Although there are several spatial models for simulating fire behavior based on fuel models, before this project, no model existed that allowed simulation of the spatial behavior of fire, based on changes in fuels' loading. Thus, this section describes such a spatial model. Hypothesis H_{o5} (NOT DIFFERENT FIRE BEHAVIOR PERFORMANCE) is tested through an analytical comparison between such a model and a spatial model based on the fuel model concept.

11.1 Fire Behavior

The prediction of fire behavior is very complex and it involves many elements and their interactions. Therefore, in order to allow a better understanding of the goodness and limitations of this study, this section describes the fire behavior approach for which the spatial fire behavior simulation model was generated.

11.1.1 Effect of Fuels Loading

Fire behavior predictions are based on the fuel model concept, which is used to characterize certain fuel properties, such as fuel depth, surface-area-to-volume ratio, and fuels' loading (Andrews, 1986). However, the usefulness of this concept requires that the following fuel properties be constant for a given area (qualified into a given fuel-model):

- Loading for each fuel particle diameter size class (FL).
- Surface-area-to-volume ratio for each size class (S/V).

- Fuel bed depth (FD).
- Heat content of fuel (HC)
- Moisture of extinction (ME).

These properties could be divided into two groups: (1) those based directly on **fuels' quality** (physical and chemical characteristics), such as S/V, HC and ME; and (2) those based on **fuels' quantity**, such as FL and FD. It is difficult fuels' quality show a high spatial variability within a homogeneous forest (same species). On the other hand, fuels quantity can be affected by many factors, such as fire regime, prescribed fires, fuelwood consumption, or other natural perturbations (e.g. hurricanes). Nevertheless, the fuel-model concept considers fuel quantity spatially as static or constant for each fuel model (Table 11.1).

Table 11.1. Characteristic fuel loading (ton/ha) for fuel-model as documented by the International Fire Service Training Association (1998).

F.MODEL	TYPICAL FUEL COMPLEX	1-hr	10-hr	100-hr	LIVE
	Grass and grass-dominated				
1	Short grass (0.3048 m)	1.65	0.00	0.00	0.00
2	Timber (grass and understory	4.48	2.24	1.12	1.12
3	Tall grass (0.762 m)	6.75	0.00	0.00	0.00
	Chaparral and shrub fields				
4	Chaparral (1.829 m)	11.23	8.99	4.48	11.23
5	Brush (0.6096 m)	2.24	1.12	0.00	4.48
6	Dormant brush, hardwood slash	3.36	5.60	4.48	0.00
7	Southern rough	2.53	4.19	3.36	0.83
	Timber litter				
8	Closed timber litter	3.36	2.24	5.60	0.00
9	Hardwood litter	6.55	0.92	0.34	0.00
10	Timber (litter and understory)	6.75	4.88	11.23	4.48
	Slash				
11	Light logging slash	3.36	10.11	12.35	0.00
12	Medium logging slash	8.99	31.45	37.06	0.00
13	Heavy logging slash	15.71	51.65	62.88	0.00

11.1.2 Surface Fire Behavior System

An accurate definition of the spatial variations of fuel properties would allow a more accurate prediction of spatial fire behavior. Thus, the spatial model developed in this study considers changes of fuels' loading as a source of spatial variation of fire behavior, considering other fuel properties constant (as in the fuel-model concept). Since there was not a software package that predicts fire behavior punctually based solely on fuels' loading, a specific surface fire behavior system (SFBS) was developed in *Excel* (Appendix 11.1). To use this system, the user has to select a fuel model (to define the corresponding fuel properties) and then input the desired fuels' loading.

Considering that fuel quantities are not spatially constant, one could expect to have spatial variations of fire behavior within the same fuel model. To test this using the SFBS, an example was developed. Figure 11.1 displays the potential variations of rate of spread based on different 1-hour fuel-class loads, considering FMs 8, 9 and 10. The characteristic 1-HR fuels loads are 3.36, 6.55 and 6.75 ton/ha, respectively (Table 11.2). To project fire behavior for each FM, the characteristic fuels' loading (CFL) of the other FMs were held constant, with 5% moisture content (except for live woody, 50%). Wind velocity was 30 km/hr, with a wind correction factor of 0.2, and a slope percentage of 10. Increasing the 1-HR fuels' loading over its CFL incremented the rate of spread up to 36.7, 0.48 and 23.23% more, for FMs 8, 9 and 10, respectively, than the rate of spread based on the characteristic 1-HR fuel load. This is more marked in the case of FM 10. On the other hand, decreases of rate of spread are also possible if 1-HR fuels' loading

decrease. This is especially notable in the case of FM 9, which shows a pronounced decrease of rate of spread when 1-HR fuels loadings are lower than CFL.

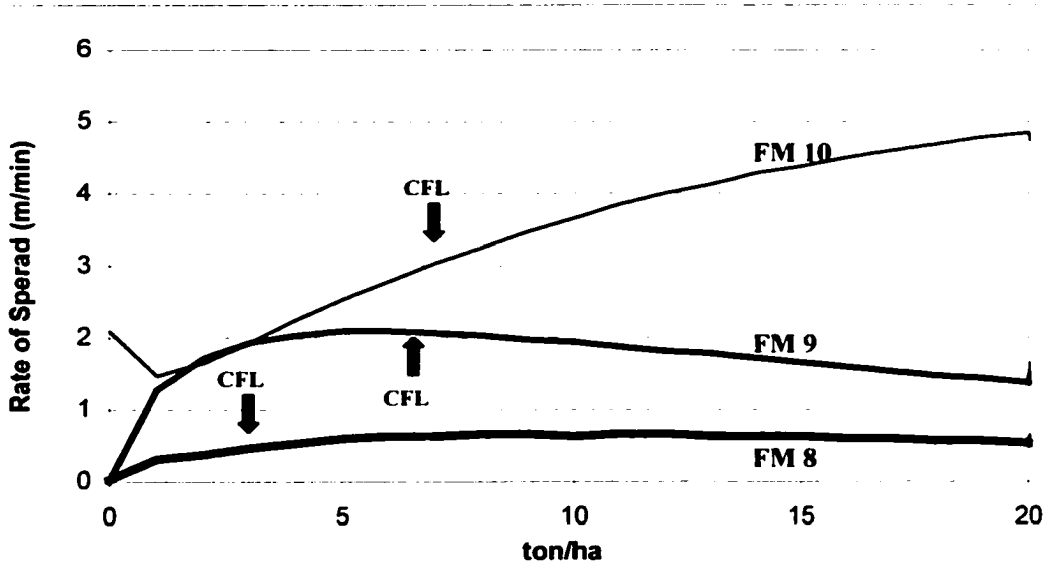

Figure 11.1. Variations of rate of spread in FM 8, 9 and 10, based on changes of 1-HR fuel loading. FM's characteristic 1-HR fuel load (CFL) are 3.36, 6.55 and 7.75 ton/ha respectively (International Fire Service Training Association, 1998).

11.2 Fire Behavior Spatial Model

The predictions resulting from SFBS reflect the fire behavior at a given point in space. Forest fires require an information system that can support spatial and temporal query, analysis, and modeling. A fundamental problem is to store spatio-temporal data in an efficient form in terms of data storage and operation (Yuan, 1994a). Therefore, a spatial simulation model (SSM) was developed, to determine the size, shape, and geographical location of fire behavior, based on spatial variations of fuel loads. Based on

the SFBS the algorithm of this model calculates fire behavior in each pixel deterministically (under a raster approach).

Table 11.2. Maximum increment of rate of spread (ROS) when incrementing 1-HR fuels loading for FM 8, 9 and 10. Moisture content: dead fuels 5%; live woody 50%. Wind velocity 30 km/hr (correction factor 0.2). Slope 10%.

FUEL MODEL	CHARACTERISTIC FUEL LOAD (ton/ha)	RATE OF SPREAD (m/min)	MAX. RATE OF SPREAD (m/min)	FUEL LOAD MAX. ROS (ton/ha)	INCREMENT (%)
8	3.36	0.49	0.67	9	36.7
9	6.55	2.07	2.08	5	0.48
10	6.75	2.97	3.66	10 (*)	23.23

(*) Since ROS continues increasing, this fuel load is used for comparison purposes.

11.2.1. Model Inputs

Many factors are needed to develop a model to estimate the behavior of a forest fire. There are four primary behavior inputs (Omi, 1997; Campbell *et al.* 1996): (1) Fuel classes determine how different terrain affects fire spread; (2) Fuel moisture has a tremendous impact on the intensity of a fire and the rate of spread; (3) Wind (direction and velocity) provides the most variable influence on fire behavior; and (4) Slope spreads a fire much more quickly than a level terrain. Based on this classification, Table 11.3 shows the inputs used in the SSM.

11.2.2 Model Outputs

The outputs resulting from the Spatial Simulation Model are some of the most important required in a decision making process regarding fire management (Omi, 1997; Veach *et al.* 1994; Albini, 1976). These include: **1) Rate of spread,** the rate of advance of the head of a fire (m/min); **2) Heat per unit area,** the amount of heat released per

square meter during the time that area in within the flaming front (kJ/m^2); **3) Fireline intensity,** the amount of heat released per meter of fire front per second (kW/m); **4) Flame length,** average length of flame (m) at a projection point; **5) Reaction intensity,** rate of heat released per square meter per minute (kJ/m^2/min); **6) Flame depth,** front-to-back distance of flame (m); and **7) Area,** estimation of area of fire (ha).

Table 11.3. Inputs used to run the Spatial Simulation Model developed for this project to predict fire behavior based on the Surface Fire Behavior System.

GROUP	INPUT	UNITS	INPUT FORMAT
Fuel model	FM 8	---	Grid map
	FM- 9	---	Grid map
	FM-10	---	Grid map
Fuel class loading	1-hr	ton/ha	Grid map
	10hr	ton/ha	Grid map
	100hr	ton/ha	Grid map
	LW	ton/ha	Grid map
Fuel moisture	1-hr moisture	%	Value
	10-hr moisture	%	Value
	100-hr moisture	%	Value
	LW moisture	%	Value
Wind	Direction	degrees	Value
	Velocity	km/hr	Value
	Wind adjust. factor	---	Value
Topography	Slope	%	Value
	Aspect	degrees	Value
Starting point	UTM coordinates	Northing	Value
		Easting	Value
Duration	Elapsed time	hours	Value
Correction factor	Adjustment	---	Value

Grid map: Raster matrix
Value: Numerical amount.

11.2.3 Spatial Simulation Model Architecture

Fire behavior computation is performed on a locational basis, where individual spatial units (cell based) of known spatial location describe reality (Yuan,1994b; Zack

and Minnich, 1991). The spatial model simulates fire behavior, such as fire spread area, deterministically based on the spatial variation of fuels' loading and environmental parameters (slope, aspect, and wind). It is assumed that fuels' moisture is constant. The model describes the changes in the spatial pattern of fire behavior from an initial time (t) to a given period (t+1).

This model was developed under the raster perspective (cell based), because this allowed working with point specified changes in fuels' loading. The ArcInfo databases are linked to the computer program through an Arc Macro Language (AML) program. The architecture of the algorithm used to develop this model is displayed in Figure 11.2.

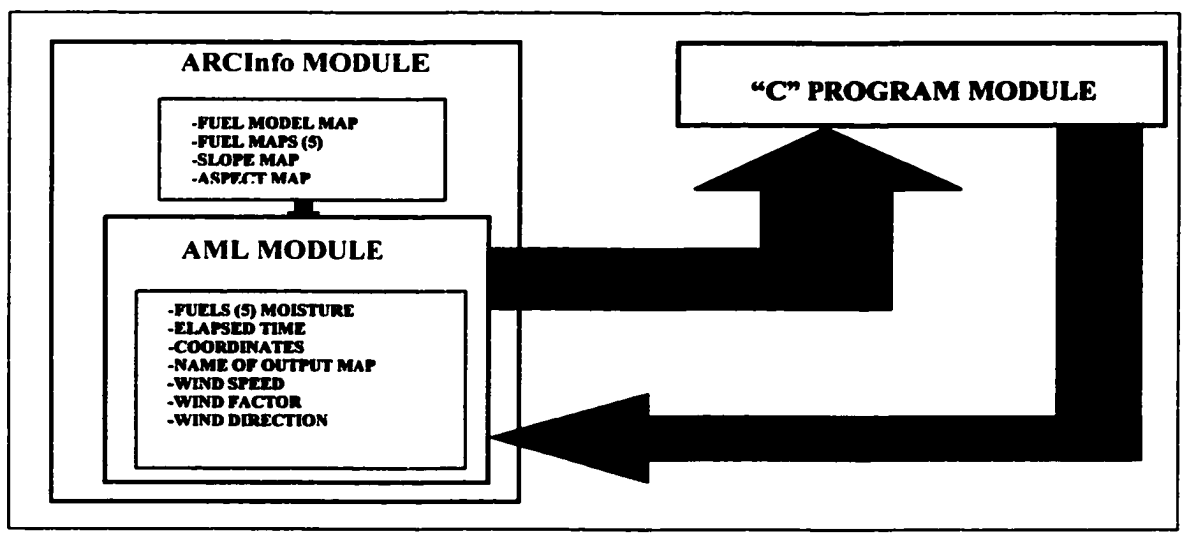

Figure 11.2. Basic structure of the algorithm to develop the Spatial Simulation Model to predict fire behavior used in this study. AML: Arc Macro Language.

ArcInfo Module. The spatial information for running the C program must be in an export grid format (asciigrid file) from ARC/Info. The structure of an asciigrid file is

composed of: a) a header with information about geographic location of the data set, number of rows and columns, and cell size; and b) a matrix with the values for each cell.

"C" Program Module. In this module most of the algorithm is developed (Figure 11.3). The "C" program works with 25 arguments (those shown in Table 11.3, plus 7 output maps). Based on the Surface Fire Behavior System, all the cells of the raster matrix of the study area are processed. As a result of this, a rate of spread matrix is generated. The values of this matrix are divided by the cell size, resulting in a matrix that represents the fractions of cells that are burned in one hour. To know how many hours (or cycles) are needed to burn each cell, the number 1 is divided by these cell values. The algorithm considers that values lower than 1 are equal to 1.

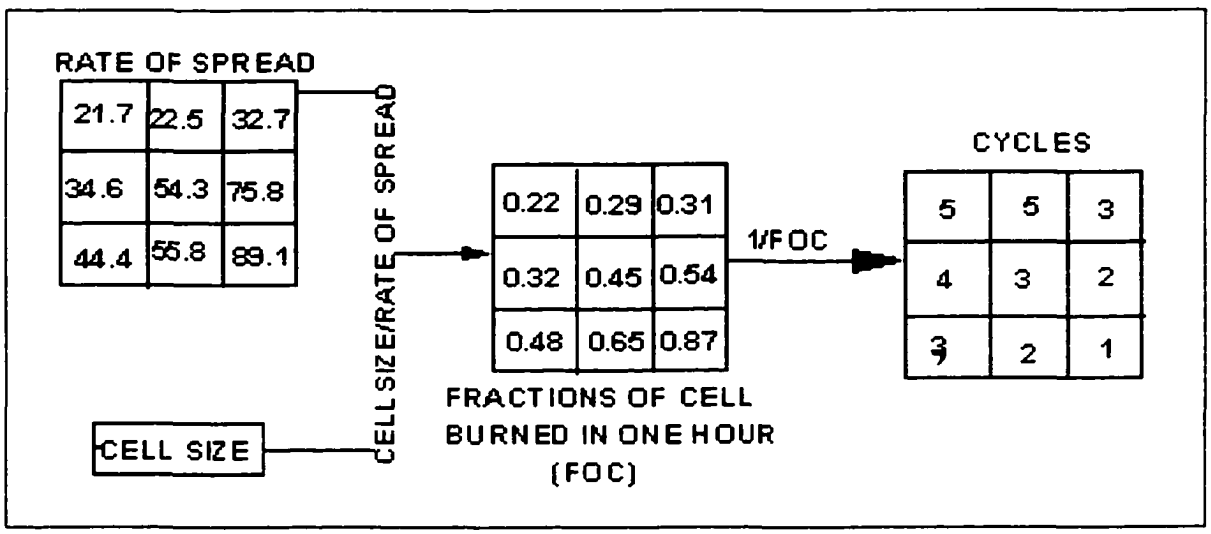

Figure 11.3. Definition of number of cycles per cell in the structure of the Spatial Simulation Model developed for this project.

Using a crosshair effect on the computer screen a starting point is defined, and its corresponding UTM coordinates are identified. Then in the first cycle, the algorithm checks that each cell surrounding the starting cell (8 possible) matches the following

conditions: 1) a cell exists in a given direction; 2) its value is different than the NODATA value and to zero, and is not negative (Figure 11.4). If any of these cells has the value of 1, the algorithm marks them as burnt, and as new "sparking" cells for the next cycle. Cells with values higher than 1 are not "burnt" yet, but their values are decreased by one unit until they are "burnt" (when their value is equal to 1). A cell is considered as "spark" until it has, at least, a non-burn adjacent cell. In the next cycle, the new "sparking" cells follows the same process, generating new starting cells, which, in the next cycle, will define new "sparking" cell, and so on until the established simulation time is completed. The number of cycles is defined with the given elapsed time. In the output asciigrid, the corresponding "burnt" cells are given the value of 1. Finally, the program calculates the number of hectares burned, and the percentage of total area that they represent.

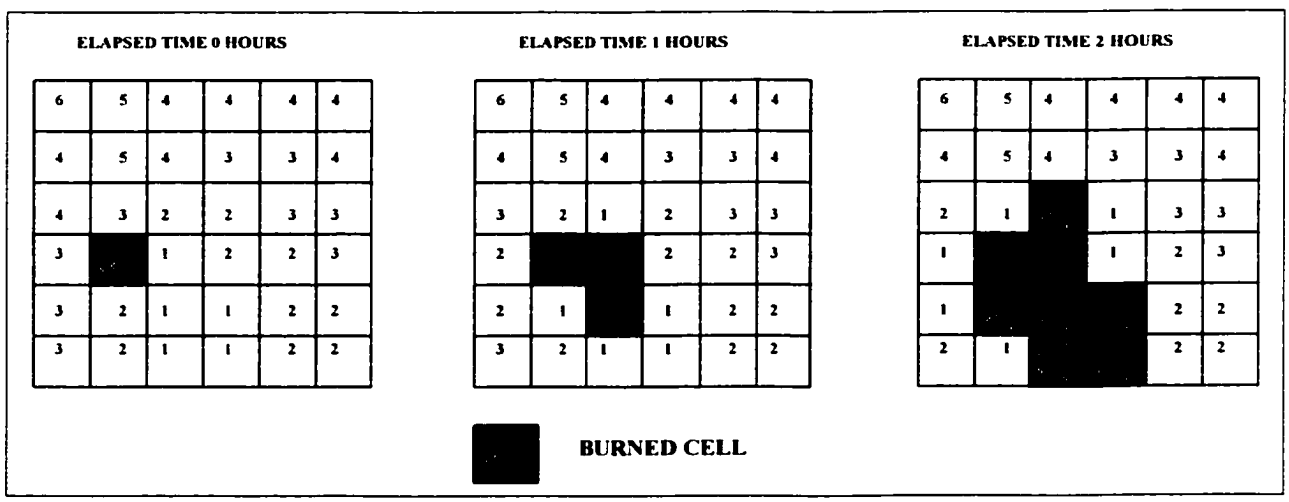

Figure 11.4. Graphical sequence of the Spatial Simulation Model algorithm to simulate fire spread area developed for this project.

AML Module: The AML works as an interface between ArcInfo and the "C" program. Its function is to prepare all the arguments needed for the "C" program. Firstly, it asks the

user to select the cover of the desired study area (which is displayed on the screen), then it asks for all the arguments shown in Table 13.2. Using a "cross hair", the user points to the cell for starting a fire spread simulation. As a result, the UTM coordinates of such point are defined. Then the program asks for the desired time to run the simulation, and for a name for the output asciigrid file. With all the needed arguments, the AML call the "C" program, which produces the output asciigrid files.

11.3 Spatial Fire Behavior Simulation

With the purpose of appreciating how fuel loading influences fire behavior, a simulation was run using the SSM. The validation of the SMM is beyond the scope of this project. Nevertheless, the performance of SSM was compared with FARSITE (Finney, 1998) under the same conditions.

11.3.1 Simulation Conditions

The moisture for 1-HR, 10-HR, 100-HR and LW fuels were 5, 7, 8 and 70 %, respectively. Wind speed was 30 km/hr, with a wind adjustment factor of 0.2, which corresponds to a fully-sheltered-fuels condition (closed canopy) (National Wildfire Coordinating Group, 1994). Wind direction (where the wind comes from) was 180^0. The stating point was selected randomly, corresponding approximately to the following coordinates (UTM-12): 3230731 [Northing], and 772279 [Easting].

11.3.2 Rate of Spread

Fire growth. Figure 13.5 displays the fire growth sequence of a fire behavior simulation run with the Spatial Simulation Model (SSM). A 1-HR fuels map is used as background in order to appreciate fire spread response to changes in fuel loading. Elevation contour lines are shown in order to appreciate slope effect. The total elapsed time was 7 hours. In general, fire spread is highly influenced by wind direction (from South to North).

In the first hour the fire went slowly to the northwest. Fire direction is clearer when 2 hours have passed. The fire tends to grow toward the NW because in such direction higher 1-HR fuels' loading occurs and the fire is passing from FM 8 to FM 9. At the very North of the starting point, fuel loads are lower. Thus, the fire spread is considerably slower in this direction. After 4 hours, it is clear that fire spread is mostly influenced by the fuels' distribution. The northern face of the fire spreads out over an FM 10 surface after 5 hours. As a result of this, after 6 hour both wind and FM 10 drive mostly fire toward N. At the same time, fuels' loading and slope define a faster spread toward NW. The NE face of the fire spread slower as a result of a lower amount of fuels' loading and a lower slope. In the 7-hours frame, both fuel loading and slope influence fire spread.

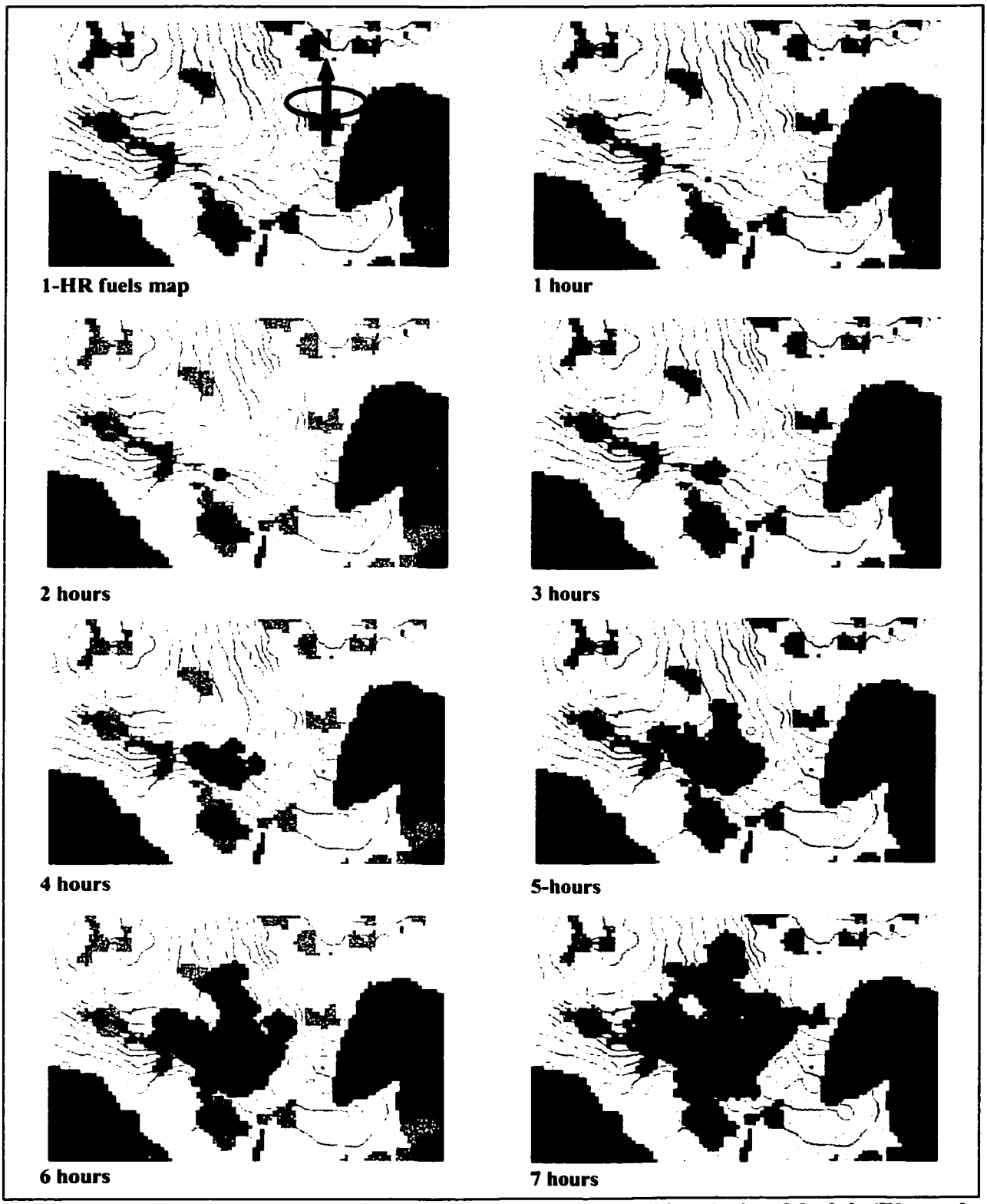

Figure 11.5. Fire growth sequence based on the Spatial Simulation Model. (Elapsed time: 7 hours). Background corresponds to the 1-HR fuels' spatial distribution. Darker tones represent higher fuel loads.

Fire spread, resulting from FARSITE, is also highly influenced by wind direction (Figure 11.6). In this case, fire responds to the fuel-models distribution only. In the first hour the fire runs to the North mostly into FM 8, resulting in a slow spread. Once the fire reaches an FM 9 area (frames 2-hr), it runs faster. After 3 hours the fire reaches an FM 10 area, which (together with wind) define mostly the fire spread direction. A similar fire growth pattern results in approximately the same area when SSM was used. Fire spread is slower at W and E direction. It was expected that slope could define a faster fire spread at the W direction, however this is clearer after 6 hours. After 5 hours fire runs downhill at the NE direction, thus fire spreads slower because the influence of slope.

Rate of spread spatial variation.

Figures 11.7 and 11.8 display the rate of spread spatial variation resulted from SSM and FARSITE, respectively. Since SSM develops a fuel model for each cell, such variation is more detailed. In general, areas with low fuels' loading define a low rate of spread. In the case of FARSITE, ROS shows certain patterns. The influence of fuel-models distribution is clear. FM-10 produced the higher rate of spread, while areas of FM-8 define a very slow ROS. SSM defined higher ROS classes (1.0-25.54 m/min) than FARSITE (0.07-2.83 m/min), which could be the result of high fuel loads.

11.3.3 Fireline Intensity

The amount of heat released per meter of fire front per second follows a similar pattern as ROS in both SSM (Figure 11.7) and FARSITE (Figure 11.8) simulations. SSM simulation defines a lower range of fireline intensity values (0.28-483.29 kW/m) than FARSITE (2.23-714.3 kW/m).

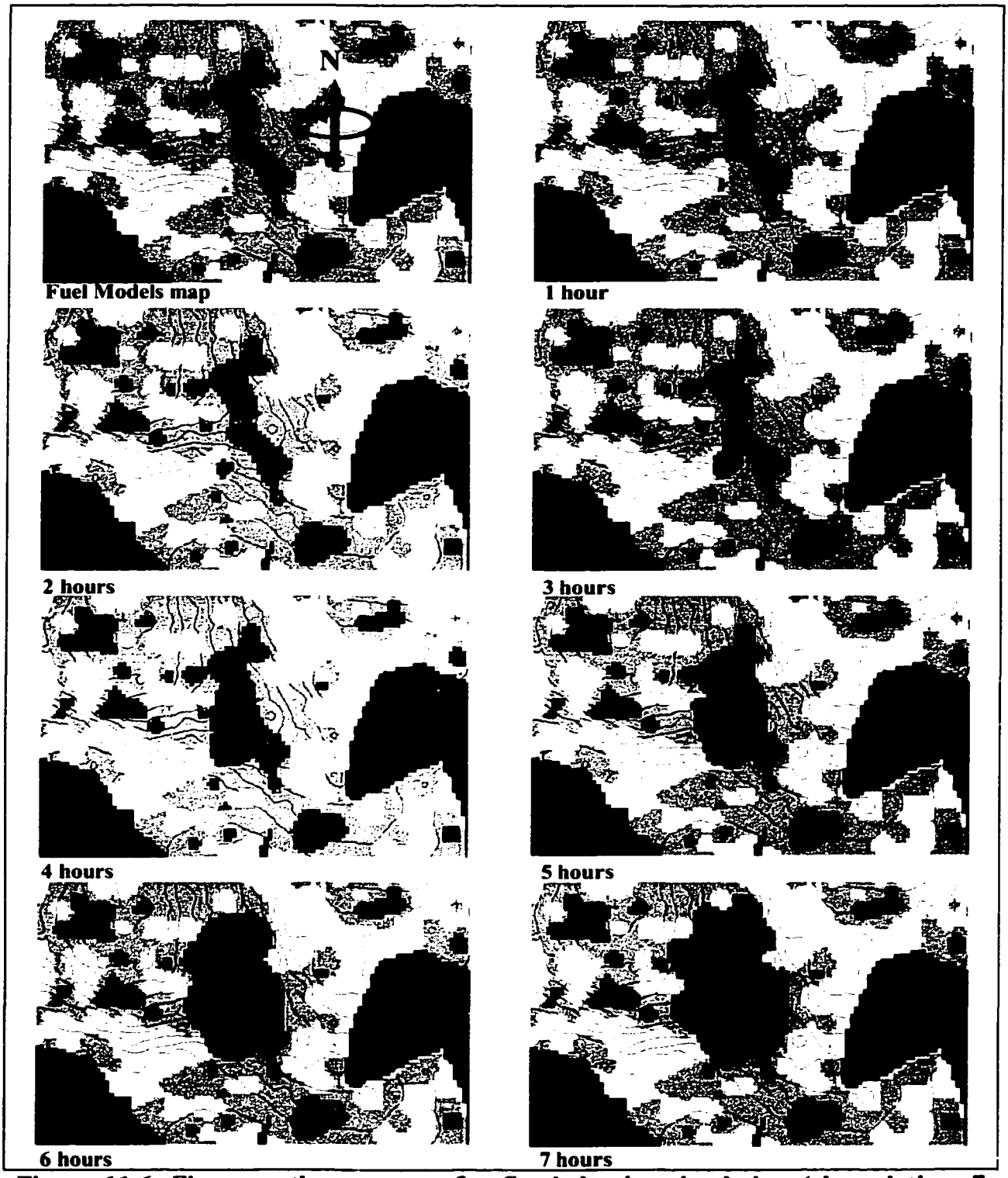

Figure 11.6. Fire growth sequence of a fire behavior simulation (elapsed time 7 hours), based on FARSITE. Background: FM 8 (yellow), FM 9 (green), FM 10 (dark green).

Both SSM and FARSITE defined higher fireline intensity in the area where FM 10 occurs. However, SSM defines some small areas at the W and S, with moderate fireline intensity. FARSITE output indicates, in general, low fire line intensity values out of the area under influence of FM 10. These differences obey the spatial variation of 1-HR fuels that is considered by SSM. Reaction intensity output is shown in Appendix 11.2 only for SSM simulation.

11.3.4 Heat per Unit Area

Spatial variations of heat per unit area are less heterogeneous in SSM (Figure 11.7), than rate of spread. Nevertheless, the influence of FM 10 is clear. In the case of FARSITE (Figure 11.8), the spatial distribution of this parameter responds basically to two groups: (a) high heat per unit area (HUA) values, which correspond to FM 10 distribution; and (b) low HUA values, grouping both FM 8 and FM 9 areas. In this case, the range of HUA values, between SSM and FARSITE are similar. However, SMM resulted in lower values of HUA.

11.3.5 Flame Length

Flame length (FL) spatial distribution for SSM (Figure 11.7) was very similar to fire line intensity. Same results were given by FARSITE (Figure 11.8). The resultant flame length values were higher using SSM than using FARSITE. As was expected, SMM resulted in high flame length values in those areas with higher fuels loading. However, FM 10 area defined the highest flame length. FM 10 occurrence influenced in the same way the distribution of flame length in FARSITE. The range of values of FL for

SSM goes from 0.305 to 2.627 m, while for FARSITE this range goes from 0.11 to 1.261 m. Flame depth map is shown in Appendix 11.3 only for the SSM simulation.

In general, wind direction had a strong influence on the fire shape in both SMM and FARSITE simulations. However, the different geometry of the fire growth resulting from SSM and FARSITE, suggest rejecting the null hypothesis H_{o5} (NO DIFFERENCE IN FIRE BEHAVIOR PERFORMANCE). The differences in fireline intensity, heat per unit area, and flame length between SSM and FARSITE reinforce rejecting the null hypothesis H_{o5}. However, further work is required to validate the performance of SSM.

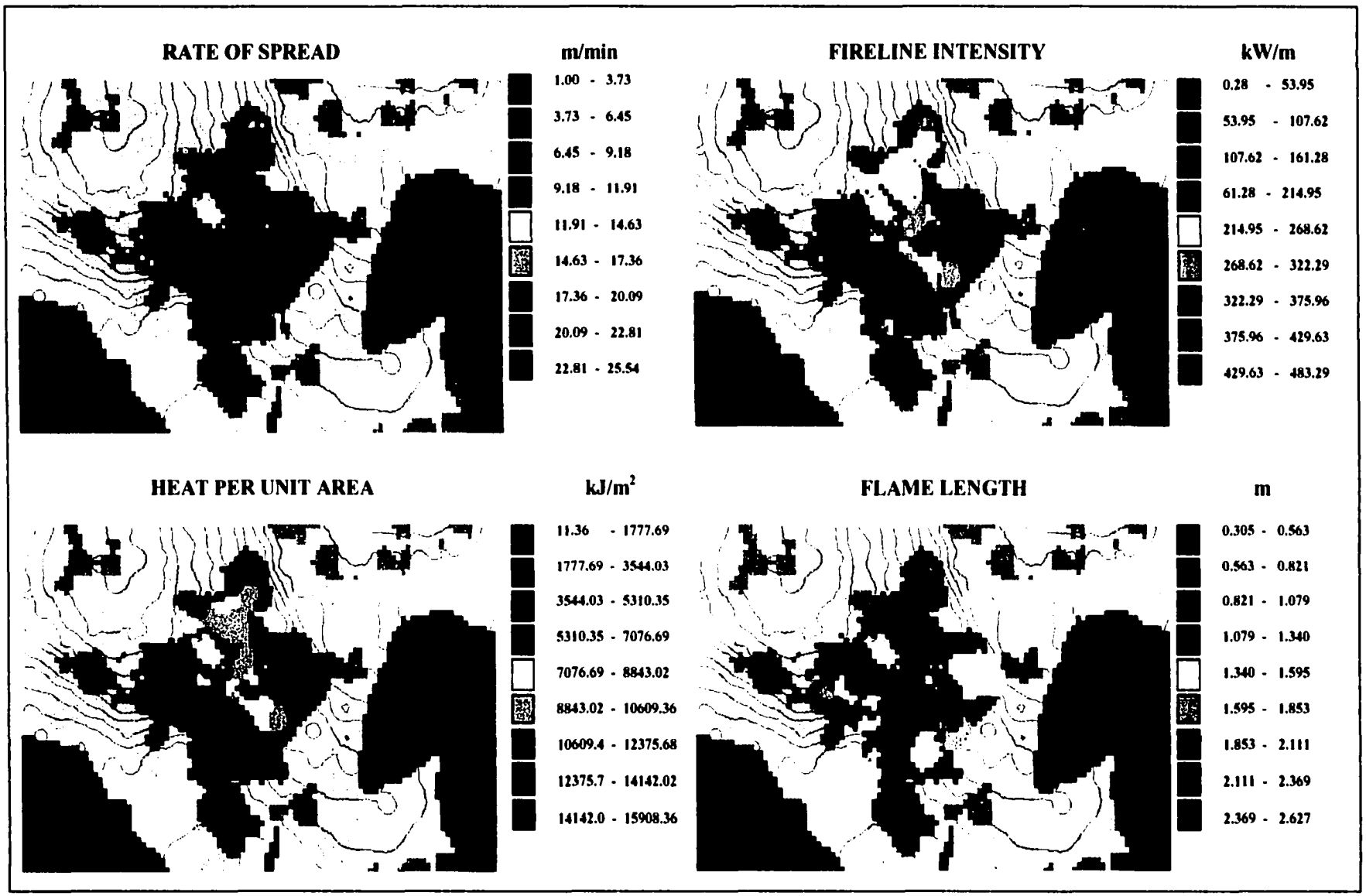

Figure 11.7. Output maps resulting from a fire behavior simulation based on the Spatial Simulation Model. Background corresponds to the 1-HR fuels' spatial distribution. Darker tones represent higher fuel loads.

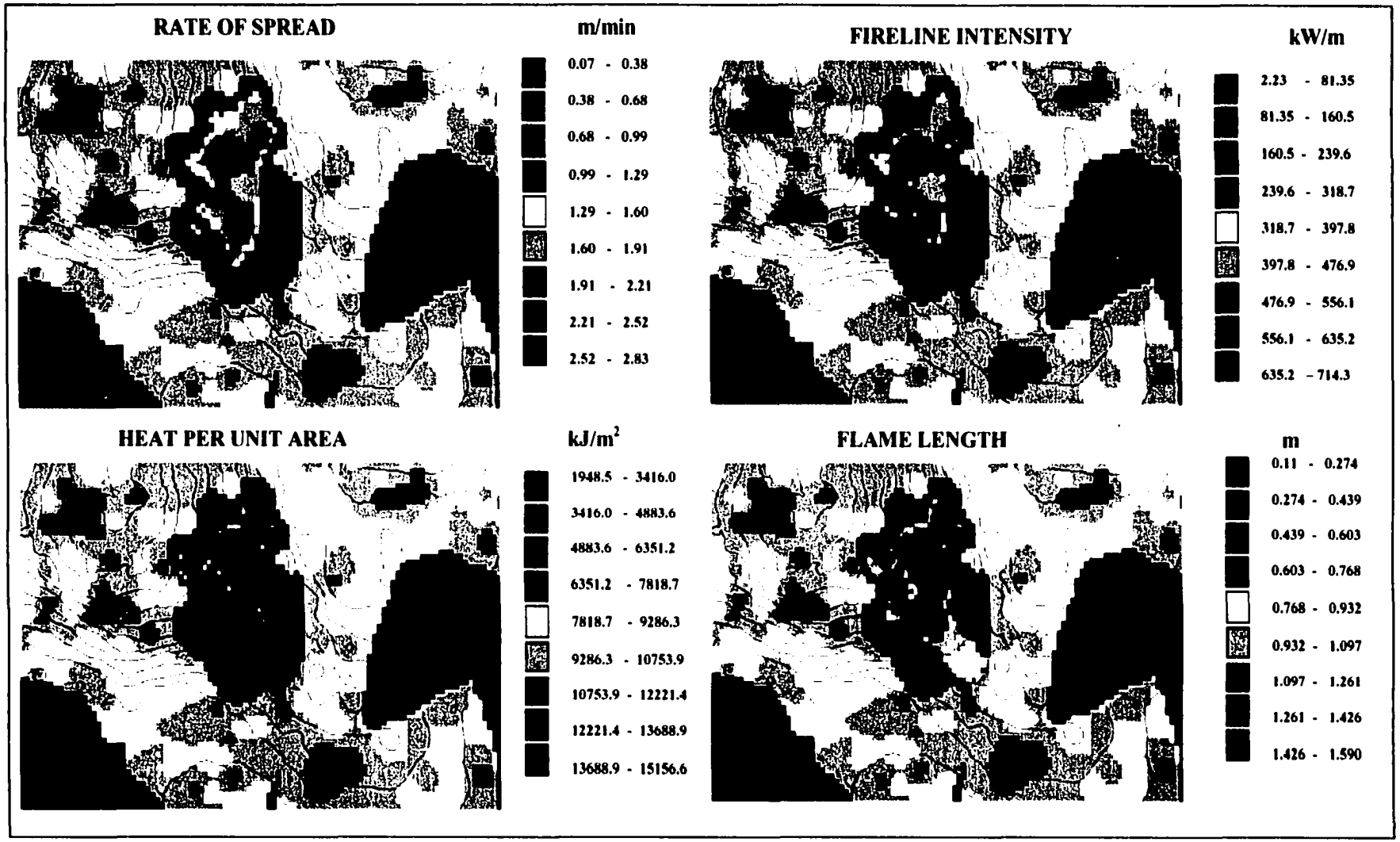

Figure 11.8. Output maps resulting from a fire behavior simulation based on FARSITE. Background corresponds to the 1-HR fuels' spatial distribution. FM 8 (yellow), FM 9 (green), FM 10 (dark green).

CHAPTER VI

12 DISCUSSION

The section starts with the discussion of the geostatistical approach used in this study. This discussion is focused in the analyses of the hypotheses stated, and the performance of geostatistical interpolation techniques compared with traditional alternatives. After that, the perspective to integrate the fuel loading maps into the fuel models concept is analyzed. Then the potential of a practical use of the fuel loading maps in the prediction of spatial fire behavior is discussed. After that, the advantages of the Conditional Fuels Loading Concept is analyzed. Finally some considerations on the fuel inventory methodology are discussed.

Spatial Interpolation

As was expected, the sample values of the four fuel classes (1-HR, 10-HR, 100HR and LW fuels), behave as a regionalized variable (see 4.3.1). Therefore, it was possible to model their spatial distribution. In all the cases, the spatial autocorrelation was enough to suggest rejecting the null hypothesis of no spatial autocorrelation (H_{o1}). Although this kind of preliminary spatial analysis could help to avoid unnecessary subsequent work, it was found that very few studies report its use. Moreover, the testing of cross-correlation, through bivariate Moran's *I*, is a relatively new concept (Bonham *et al.* 1995). Thus its use has been very limited. In this study, the results suggest that there was not enough evidence (P-value < 0.00) to support the null hypothesis of no spatial cross-correlation (H_{o2}). Therefore, some secondary variables (principally elevation) could be used to

predict the loading of the four fuel classes in areas not sampled using cokriging techniques.

Regardless the significant spatial correlation found in the preliminary analysis (both autocorrelation and cross-correlation), the spatial continuity was poor in all the four cases (principally for 100-HR and LW fuels). Nevertheless, in general, geostatistical interpolation techniques showed a better performance that the traditional interpolation techniques tested (Table 12.1). The results suggested that there was not enough evidence to support the null hypothesis H_{o3} (NO INCREASE IN PRECISION MODELING SPATIAL CONTINUITY) for 1-HR, 10-HR and LW fuels. However, the spatial continuity for 100-HR fuels was not enough to reject this hypothesis. Thus, in these cases at least, one traditional technique was better than the simple kriging ones.

Table 12.1. Table of the best interpolation techniques for each fuel class. Cd. Madera, Chihuahua

	RANKING		
FUEL CLASS	1st	2nd	3rd
1-HR	CK (ELE)	MP	BK:PK
10-HR	IDW (P1)	IDW (P2)	UK (1D)
100-HR	CK (ELE)	OK	IDW (P1)
LW	CK (ELE)	IDW (P1)	UK (1D)

On the other hand, the joint spatial continuity was enough to improve the estimation in three of the fuel classes (1-HR, 100-HR and LW fuels), which was reflected in the lowest mean square errors obtained. This suggests rejecting H_{o4} (NO INCREASE IN PRECISION MODELING JOINT SPATIAL CONTINUITY) in these three cases. In

other words, the MSE could be minimized fitting the resulted experimental variograms to some of the existing conditionally positive definite models, through cokriging techniques. Nevertheless in the case of 10-HR fuels, a traditional technique (IDW-power 1) resulted in the lowest mean square error, which suggests that there was not evidence to reject H_{o4}.

The process of searching for the "best" interpolation technique was iterative. The level of complexity is higher in the geostatistical techniques, because many parameters have to be not only defined, but also combined in order to produce the lowest MSE possible. Some of such parameters are: sill, lag, number of neighbors, and variogram model. Another aspect to consider was the practicability of each technique. In the case of the traditional techniques, the analysis processes were more straightforward and less complex. It was not possible to define a unique technique to use in all situations. However, in general, geostatistical techniques performed better that the traditional alternatives. Nevertheless, ranking all the 12 alternatives used in this study (based on MSE), and considering the four fuel classes, IDW (power 1) was ranked as the best general alternative. The other best techniques were cokriging, universal kriging (1^{st} degree), ordinary kriging, and block kriging. On other hand, the worst techniques were spline and Thiessen. Nevertheless, it is important to point out that such ranking is only for this study. Spline has been widely used in atmospheric interpolations with good results (Lennon and Turner, 1995; Wotling *et al.* 2000; Custer *et al.* 1996). Dowdall and Dea (1999) found a good agreement between a polygonal classification and the actual distribution of forest stands. Therefore, one cannot exclude any available interpolation technique. Furthermore, very few studies have compared different interpolation techniques (Hunner, 2000; Regniere and Sharov, 1999; Nalder and Wein, 1998; Phillips

et al. 1997). This situation is more critical in the forest fire scenario where no previous study was found similar to the present project. Only two studies related to the application of kriging and forest fire were found: (a) an analytical scheme to predetermine the minimal sampling intensity, in order to generate continuous fuel surface of desired reliability (Kalabokidis and Omi, 1995); and (b) a study to define the spatial pattern of the high severity burn areas (Robichaud, 1996). The lack of other studies similar to the present work limits the possibility of comparative analysis. However, the results showed in this study agree with other works (unrelated to forest fires) that each database requires a new search for the best interpolation technique (Hunner, 2000)

The fact that IDW obtained better results (e.g. for 10-HR fuels) than some geostatistic techniques could be due to three general conditions. First, when data are abundant, most interpolation techniques give similar results (Burrough and McDonnell, 1998). An assumption of kriging is that data are sparse. In this project, sample points were rather abundant (554 in an area of 1,400 ha). Second, kriging techniques take into account how clustered the nearby samples are. Thus, if the nearby samples are not strongly clustered in the estimations of a given point, all of the nearby samples could be used. Though the estimates could be improved by incorporating more nearby samples, they also could be adversely affected (Isaaks and Srivastava, 1989). Thus, one should use a technique that takes into account that samples clustering, such as kriging alternatives. Though some parts of the study area showed some cluster, the spatial distribution of the sample plots tended to be random. Third, kriging techniques assume that the variable under analysis has a normal distribution (Hunner, 2000). In this project, none of the fuel

classes showed a normal distribution, which is the usual condition in this kind of study (Weber and Englund, 1994). Nevertheless, after IDW (power 1), most of the kriging techniques performed better than the traditional interpolators.

Since the tested cross-correlations (bivariate Moran's *I*) were significant (P-value <0.05), this analysis suggested rejecting the null hypothesis of no spatial cross-correlation among all fuel classes. This was corroborated due to the fact that the use of ancillary data, through cokriging, improved the quality of the estimations. Many studies concur that the inclusion of ancillary variables has improved the estimations (Hunner, 2000; Asli and Marcotte, 1995; Phillips *et al.* 1992). In three of the four fuel classes examined, cokriging was ranked as the best interpolation technique. In contrast, in the case of 10-HR fuels cokriging was ranked 12 (worst). In these two situations the cokriging values were obtained through S-Plus software. GS+ was the other software package used to calculate cokriging, which was better than S-Plus only in the 10-HR fuels interpolation (ranked as 6^{th}). Therefore, it was found that two different software package could result in different estimations. This depends basically on the iterative capabilities of each software package. S-Plus allows more flexibility in specifying certain parameters than in GS+. Although, in this study, both packages showed exactly the same experimental variograms, their different estimations could be attributed to two major conditions: (1) The variogram models fitted to the spatial variation were different; and (2) As a result of the difference in the variogram models, the sill values were affected. In the case of GS+, such models tended to model certain global trends in the experimental variogram. Using universal kriging it is possible to take into account such a trend when minimizing the estimation

error (Hunner, 2000). This was corroborated, since the UK (power 2) was ranked 3. Using S-Plus it was possible to fit bounded variogram models (Armstrong, 1998) to the spatial distribution of the experimental variograms. This resulted in a better support for the kriging interpolations. The model resulted from GS+ defined a larger sill, which implies larger estimation variances (Isaaks and Srivastava, 1989). Nevertheless, GS+ software was friendlier to use when estimating ordinary kriging (point and block) and IDW.

The selection of ancillary data required an exhaustive analysis of the potential spatial correlation between each of the four fuel classes and the secondary data. Parameters such as the correlation coefficient, bivariate Moran's *I* (Bonham *et al.* 1995), and the stepwise process were useful to define the correlation between fuel classes and secondary variables. However, the visualization of the spatial distribution of such ancillary data was a key factor for their selection. Elevation (ELE) was the secondary variable that showed the best results when cokriging the three fuel classes. In all these cases the exponential model defined the lower MSE, which implies that there was a clear nugget and sill, but only a gradual approach to the range (Burrough and McDonnell, 1998). Principal Component 3 (PC3) performed similar to ELE, principally in the case of 1-HR fuels (the difference of MSE between ELE and PC3 was too low [0.162 and 0.163 respectively]). In this case, the Gaussian model resulted in the lower MSE, which means that the variation was very smooth and the nugget variance was very small compared to the spatially dependent random variation (Burrough and McDonnell, 1998). On the other

hand, total basal area (TBA) performed well as an auxiliary variable when cokriging both 1-HR fuels and LW fuels.

The fact that some variograms and cross-variograms do not fitted well to the corresponding experimental variograms does not implies that those functions are not useful. Indeed, according to Stein (1999), plotting the empirical variogram and then selecting a model that, to the eye, appears to fit its general shape can lead to severe model misspecification. The reason of this is that an experimental variogram is a poor tool for distinguishing exactly how smooth a differentiable process is. Moreover, although the empirical semivariogram can be a useful tool for random fields that are not differentiable, it is much less useful and can even be seriously misleading for differentiable random fields (Stein, 1999).

Fuel-Models Concept and Fuel Loading Maps

The spatial implementation of the fuel-model concept has caused many technical problems, such as the difficulty of mapping fuel-models in a given area. Furthermore, fuel models do not reflect the actual spatial variability of fuels' characteristics. Fuel-model maps tend to categorize large areas with the same fuel model, which define a homogeneous fire behavior (for a given projection period). This approach would be useful in areas where vegetation and fuels are spatially homogeneous, however, in practice this condition is very rare. Nevertheless, the current tendency of fuel mapping is based on the fuel-model perspective. In contrast, the present study allows taking into account potential spatial variation of fire behavior even within the same fuel-model. Since its algorithm is based on the spatial variation of fuel loading (represented in each

pixel [raster cell]), it is possible to appreciate the spatial variations of fire behavior at a level that depends on the raster resolution. In this project, fire behavior variation was estimated at a resolution of 30 x 30 m. This resolution is good enough to support prescribed burn planning at small scales, and to locating areas of high fire intensity (information valuable in a fire-fighting situation) at small scale. The scale level of spatial fire behavior predictions, based on the fuel-models approach, is limited to (1) the source of information (aerial photos, remote sensing, maps, etc) which supported the fuel model classification; and (2) how homogeneous (basically in vegetation), or heterogeneous the classified area is. The first condition also limits the approach illustrated in this project, however the second conditions do not affect it, because the used interpolation techniques allowed defining continuous surfaces that take into account the spatial variation of fuels loading.

Since 1972 the perspective in the use of the Rothermel model (Rothermel, 1972) has been the development of fuel models. Under this approach most of the effort has been focused on defining alternative ways to compute the Rothermel model. In this sense the system BEHAVE was developed, and lately NEXUS, which allows to make fire behavior prediction according to certain conditions (fuel moisture, wind speed, slope, etc.). However, the spatial component was still missing until the creation of FARSITE (Finney, 1998). As BEHAVE, FARSITE is also based on the fuel model concept, which implies that the conditions within each fuel model are homogeneous. Therefore, the spatial dynamic of fire behavior predictions [within a fuel model] has been limited only in the consideration of spatial changes in wind and slope. The methodology developed in this

study allows the estimation of the spatial distribution of fuels loading, as a support in spatial fire behavior predictions. A perfect spatial implementation of the Rothermel model should achieve two conditions: (a) to account with information (basically maps) of the spatial variation of not only wind and slope, but also of fuels' loading, surface-area-to-volume ratio for each fuel class, heat content of fuel, fuel bed depth, and moisture of extinction; and (b) to be able to define all those parameter at low scales.

The fuel model concept is useful in many cases (Keane *et al.* 1999b, Finney, 1998). However its use should be limited to general predictions of fire behavior to support fire management strategies at large scale. Then, the next step should be to define fire behavior at a smaller scale, basically to locate risky areas. The fuel model concept should be not eliminated, but complemented. In fact, the algorithm used in this study for the spatial predictions of fire behavior requires a previous classification of the study area into fuel models, because fuel characteristics (such as surface-area-volume ratio, and heat content) were considered constant (except fuels loading). Ottmar *et al.* (2000) proposed a more sophisticated alternative (Fuel Characteristic Classification [FCC]) that integrates the complexity of fuelbeds' structure, their physical attributes and the biological origin of their component. The fuelbeds biological origin is referred to the physiognomic variables of the fuelbeds [morphological, chemical and physical features]. Under this approach, an undefined number of FCC's could be generated, which will allow a better classification of a forest area. Nevertheless, both the FCC's and the fuel model concept have the same limitation that both are an indirect estimation of the expected fire behavior. This implies that the fire behavior within an area with similar characteristics (same FCC) will be spatially homogeneous. Although this approach will allow having more accurate fire

behavior estimations (or at least more alternatives of classification), the spatial implementation of FCC's will depend on the spatial distribution of the biophysical characteristics associated with such fire behavior. Nevertheless, the spatial distribution of fuels loading could change even within the same FCC (as in the fuel-model approach). Thus, the advantage of the perspective of the present study is that it can be used to complement both fuel model and FCC approaches. In fact, this integral conceptualization has been applied in other situations, such as the double sampling approach, where the level of classification accuracy of satellite imagery, and the information from sample plots is integrated in order to reduce costs and increase accuracy (Kalkhan *et al.* 1996).

Spatial Fire behavior

The spatial simulation of fire behavior in this study was implemented at a "point level", in which fire behavior is estimated at any point in the area of interest (based on the Surface Fire Behavior Simulation system). This approach only can be implemented under the raster GIS perspective. The only limitation would be the raster resolution (in this case 30 x 30 m). However, raster models could result in a geometric distortion to the fire shapes (produced by the fixed number of regular pathways where fire can travel), and they have difficulty in responding appropriately to temporal changes (e.g. direction and intensity of wind) (Finney, 1998). Nevertheless, increasing the raster resolution can minimize such geometric distortion. Furthermore, the spatial variation of fire behavior at small scales (heterogeneous conditions) requires levels of resolution that only can be managed under the cell automata (raster) approach (Liu and Chou, 1997). Using the vector approach (such as in FARSITE [Finney, 1998]), fire behavior is assumed

homogeneous within the entire fuel model area. Thus, this approach would be useful: (a) at large-scale levels, but with homogeneous landscapes; or (b) at small-scale levels with a fine differentiation and classification of fuel models. The latter has been the major problem of the fuel mapping process (Keane, 1999b).

It was possible to appreciate a considerable difference in the geometry of fire spread when comparing the simulation model of this study (SSM) versus FARSITE. However, since the fuels models map generated in this study was based on fuel loading (Conditional Fuels Loading Concept), it was possible to define a fine spatial distribution of fuel models. This level of definition would not be possible using traditional fuel model classifications. This did not allow appreciating a higher difference between SSM and FARSITE simulations. Nevertheless, many other factors are not considered in SSM nor in FARSITE, or any other wildfire growth simulation model. Thus objective comparisons are difficult. Factors such as the "chimney effect", wind activity generated within a burning area, heat transfer (by convection and radiation) to unburned areas, and detection of changes in the surface-area-volume ratio are only some examples that need to be considered to generate more accurate (or I should say, less erroneous) models. Its is clear that such level of detail will require consider the capabilities of other approaches, such as the 3D modeling that has been applied in the study of the atmospheric phenomena (Dean, 1998). For instance, the 3D approach will allow studying the spatial dynamic of wind not only at a horizontal perspective, but also at a vertical perspective. Therefore, phenomena such as vortex winds or "chimney effect" could be considered in spatial fire behavior predictions.

Conditional Fuels Loading Concept

Fuel model mapping in general has followed two trends: (1) indirect inferences, where some factors, presumably associated with fuel production, are related to a given fuel model such as vegetation, species and density (Keane *et al.* 1999a; Krauter, 1999; Chuvieco and Salas, 1996); and (2) expert consulting, which is a subjective alternative used for fuel model classification. Although a given forest can be classified into the fuel models that correspond, the limits between one fuel-model and another are difficult to delineate. Moreover, there is not any guarantee that the same area will receive the same classification by two or more experts. To avoid these two limitations, the Conditional Fuels Loading Concept (CFLC) was suggested in this study, based on the fuels' loading combination characteristic for each fuel-model. Since fuel is a basic element in a fire behavior prediction, a direct estimation of this factor will avoid the use of inference methodologies (which have resulted in highly variable accuracies [from 30 to 70% (Keane *et al.* 1999b)]). On the other hand, the application of the FPC does not require previous experience in fuel-models classification. Moreover, working within the same area the implementation of the CFLC will result in the same classification of the sample plots. The next step will be to interpolate such a classification, which can be through the use of some of the interpolation techniques illustrated in this study.

Many studies base their fuel-model mapping on the spatial distribution of tree species (Chuvieco and Salas, 1995). Comparing the species distribution with the fuel models map (based on the FPC), there is a strong spatial correspondence among them. *P. durangensis* and *Quercus spp* are spatially associated with the FM 9, while *P. arizonica*

occurs mostly in the zone of FM 8. The spatial pattern of FM 10 corresponds mostly to the areas with *P. ayacahuite*, while *P. engelmannii* can be located within both FM-9 and FM-8. Although *P. leiophylla* tends to occur mostly in FM-8, there was not a well defined correspondence for this species with a specific fuel model. These correspondences are very important when mapping fuel models, because the information gathered in the traditional forest inventories can be used to make a good approximation of the fuel models distribution.

Fuels Inventory

The first aspect that should be modified in the fuels sampling process (described in this study) is the way in which the stands and sub-stands are defined. Instead of basing such classification visually (photointerpretation), the information of previous inventories can be interpolated to define a better stratification of the spatial variation of specific factors (e.g. species, density, and age). A second modification is regarding the number of samples per sub-stand. Instead of defining samples based on the sub-stand size, the stratification approach will allows determining the number of samples based on the variance of each stratum. Moreover, the maps of error of estimation resulting from the kriging process can help to define areas where error is higher. With this information one can redesign the sampling strategy (Reich and Davis, 1998).

Fuel evaluation has to be as consistent as possible. However, though most of the studies reporting fuels evaluation are based on Brown's methodology (Brown *et al.* 1982), there is a wide variation in the sampling plot layouts. Therefore, evaluation of fuels in this study was based on: a) sampling plot layout that allow a more practical

measure of fuels; and b) field formats that allow recording some characteristics of the forest stand. These considerations were very useful in both the crews' training and in the inventory process. In average, between 10 and 12 minutes were required by crews to gather fuels data, which did not alter considerably the schedule of the tree inventory in which this study was based.

Although the use of depth of the fuel bed to estimate fuel loads has been reported in several studies (Brown *et al.* 1991; Flores and Benavides, 1994; Flores, 1997), none of them give a detailed description of the methodology used. Therefore, the following two aspects should be considered: (1) the simple measure of depth was not enough to make a good estimation of the litter loads. Thus, it was necessary to include other parameters that influence fuel loading measures, such as surface percentage covered by fuels. In this present study, this percentage was used as a correction factor. Although visually we can get good cover estimation (within the 0.0929 m^2 frame), Appendix 12.1 shows a proposed frame in order to estimate the percentage of fuel coverage more objectively, through the counting of covered internal squares; and (2) though measures of litter were consistent, the use of a normal ruler increases the risk of errors. Therefore, a more practical and objective device is suggested, which is illustrated in Appendix 12.2.

According to the results, there was a low amount of woody fuels (diameter >2.5 cm) in the study area. One explanation for this is that the study area is a source of fuelwood for the Cd. Madera people. Therefore, most of such material is removed from the forest. Though this situation could not alter fire rate of spread considerably, some

other fire characteristics could be affected, such as heat per unit area. In general, the fuel loads were highest in the east portion of the study area, principally for the live fuels. On the other hand, the western portion showed low loads. Live woody fuels loading were lowest in the central part of the study area. This fuels distribution could be influenced by the spatial distribution of tree species, density, height, and diameter. The Relative Spatial Continuity graphs (Figure 7.4) allow appreciating a very similar spatial continuity among 1-HR, 10-HR, and 100-HR fuels. However the variability among neighbors is more marked in the 100-HR fuels, while the 1-HR fuels showed a more stable continuity. Although some extreme values were removed to avoid their effect in the modeling of spatial continuity, only a maximum of 6.3% (corresponding to 10-HR fuels) of the total data was removed.

There is a lack of information regarding shrub and tree weights of the species in the study area. In this study the average of "medium shrubs" weights (Brown *et al.* 1982) was used. In the case of trees, the averages of all the species for each height category were used. This kind of basic information should be developed in future studies in México, considering also other factors, such as fuel production under the tree species of the study area. Moreover, an adequate characterization of forest fuels must include the determination of the surface area to volume ratio that corresponds to each class of fuel. This is very important, because the fuel model classifications developed for USA do not represent the particular conditions of the Mexican forest ecosystems. The different tree species association could define different conditions of fuel production.

13 CONCLUSIONS AND RECOMMENDATIONS

Conclusions

This project focused on the need for a comprehensive approach for forest fuels' mapping based on spatial interpolation techniques. The generation of four different fuel maps (1-hour [1-HR], 10-hours [10-HR], 100-hours [100-HR]; and live woody [LW]) allowed a more punctual definition of spatial fire behavior. This study compares five deterministic interpolation methods (spline, polygonal mapping, inverse distance weighting [power 1 and 2]) and seven geostatistical options (ordinary kriging, universal kriging [1st and 2nd degree], cokriging [S-Plus and GS+], point kriging and block kriging). Selection of these techniques was based on the following: (a) to compare the goodness of geostatistical alternatives in relation to traditional interpolation techniques; (b) to evaluate the more commonly used interpolation techniques; and (c) the availability of software packages. These twelve methods were used to define the continuous surfaces that more accurately represent the spatial distribution of each one of the four fuel classes. In general, it is important to emphasize that the conclusions of this study should be interpreted with caution due to the statistical limitations of the sampling strategy used by the forest inventory of the Ejido El Largo y Anexos. Accordingly, the major conclusions of this study were:

A) The spatial variations of fuels distribution within an area classified into a given fuel model could affect potential fire behavior. Thus, these internal fuel variations can be estimated and considered when predicting fire behavior.

B) There was spatial autocorrelation among the sample values of each of the four fuel classes (1-hour fuels, 10-hours fuels, 100-hours fuels, and live woody fuels). Since in all the cases the spatial autocorrelation was significant, the results suggest rejecting the null hypothesis H_{o1} (NO SPATIAL AUTOCORRELATION).

C) There was spatial cross-correlation between the sample values of each fuel class and ancillary data. The estimates derived using a combination of primary and ancillary data produced the best results (lower MSE). 1-HR, 100-HR, and LW fuels were best estimated by the correlation with ELE. The 10-HR fuels were better spatially cross-correlated with PC3. These results suggested rejecting of the null hypothesis H_{o2} (NO SPATIAL CROSS-CORRELATION).

D) It was possible to model the spatial continuity of each of the four fuel classes. The average spatial dissimilarity between data points allowed a good structural distribution (variogram), with sill, range and nugget effect were well defined. Traditional "conditionally positive definite" models were good enough to characterize the pattern of spatial continuity and to define weighting factors in kriging. Nevertheless, the null hypothesis was rejected H_{o3} (NO INCREASE IN PRECISION MODELING SPATIAL CONTINUITY) only in the case of 100-HR fuels. In the other three cases a traditional interpolation technique was better than the no-cokriging alternatives.

E) It was possible to model the joint spatial continuity of the regionalized variables, represented by each of the four fuel classes and ancillary data. However, it was suggested to reject the null hypothesis H_{o4} (NO INCREASE IN PRECISION MODELING SPATIAL CONTINUITY) only in the cases of 1-HR, 100-HR and LW fuels. In the case of 10-HR fuels, IDW (power 1) was better than all the geostatistical alternatives.

F) In general, geostatistical techniques performed better that the traditional alternatives. As a result of this, three out of the four fuel classes (1-HR, 100-HR, LW) were better modeled through kriging techniques. Inverse distance weighting (IDW, power 1) was the best alternative to define the spatial distribution of 10-HR.

G) Considering all the fuel classes, IDW showed a more constant performance, ranked as the best individual alternative. Reasons included abundant data, lack of clustering in samples, and assumption that the kriging techniques variables had a normal distribution (which was not true in this study).

H) It was not possible to establish a unique "best" spatial interpolation method. This coincides with the results reported in other studies that compare interpolation techniques (specially regarding geostatistical techniques). The reason for this is that each database requires its own search for the best estimation technique (Hunner, 2000), and that the best method depends on the "yardstick" (Isaaks and Srivastava, 1989) or purpose we choose. In this study, the lower MSE did not always correspond to the higher correlation coefficient.

I) The ancillary variables that showed the best performance when cokriged with fuel classes were elevation (ELE), principal component 3 (PC3), total number of species (TNS), total basal area (TBA), average height (AVEH), principal components (PC2), average coverage (AVEC), slope (SLP), and aspect (ASP).

J) The spatial modeling of a regionalized variable is a complex process that sometimes does not have to be based only in the fit of a model to a given experimental variogram.

K) There were notable differences of the fire behavior simulation resulting from the Spatial Simulation Model (SSM) and FARSITE. These differences suggest to reject the null hypothesis Ho5 (NO DIFFERENCE IN FIRE BEHAVIOR PERFORMANCE)

L) It was possible to develop a spatial model to predict spatial surface fire behavior based on the spatial distribution of the four fuel classes. The capability of this model to use fuels' information based on small cell sizes (raster resolution), allows evaluation of changes of spatial fire behavior at small scales. In fact, a pixel is the smallest unit where this model can simulate spatial fire behavior.

M) The Spatial Simulation Model (SSM) improves fire behavior prediction and description, because it considers the spatial variations of fuels' loading that occur within a fuel model. Current alternative spatial explicit models consider

that the variations of fire behavior, within the same fuel-model, are only caused by variations of wind and slope. The SSM approach takes into account variations not only in wind and slope, but also variations in fuels' loading. This allow a more precise determination of the potential spatial fire behavior

N) The proposed methodology can define a system that allows the systematic integration of information on forest fuels and ancillary data, not only at the stand level, but also at regional and landscape levels.

O) The fact that the Landsat TM5 image was taken approximately one month after completing the field survey could result in changes of the original reflectance properties of the sample plots. The fuels inventory started in August (before the rainy season), while the Landsat image was taken in the 23rd of August (during the rainy season).

Recommendations

During the process of this study, many question regarding its objectives were answered. However, many more questions arrived. Since their answer is beyond the scope of this study, the following recommendations have been defined based on such new questions, and under the perspective that they will lead to subsequent research of modeling spatial distribution of forest fuels:

A) In practice it is very difficult to characterize a regionalized variable completely (distribution, clustering, spatial continuity, etc). Therefore the criteria to select the

best interpolation alternative should be flexible (allowing assumptions). In this study all the kriging techniques tested belong to the field of linear geostatistics, which assumes a normality of the analyzed data. Under this perspective, another linear alternatives can be tested in the definition of the spatial distribution of fuels such as stratified kriging, factorial kriging, autocokriging, transitive kriging, and dual kriging (Goovaerts, 1997; Armstrong, 1998; Olea, 1991; Isaaks and Srivastava, 1989). Each of these alternatives considers different criteria to weighting the nearby variables in the interpolation process, which could characterize better the spatial distribution of the fuels evaluated in this study.

B) Linear geostatistical interpolation techniques may only be optimal when the variable under study has a normal distribution (Hunner, 2000). Since the fuel loadings evaluated in this study did not show a well defined normality, nonlinear methods should be tested in future research, such as disjunctive kriging, disjunctive cokriging, indicator kriging, indicator cokriging, logarithmic kriging, and lognormal kriging (Hunner, 2000; Armstrong, 1998; Goovaerts, 1997; Olea, 1991).

C) There is no guarantee that the spatial continuity of fuels' loading remains constant in any direction. When the spatial continuity is modeled at different directions, sometimes the tendency of the defined variograms is not the same, resulting in an anisotropic pattern (Armstrong, 1998). Therefore, future projects should study directional anisotropies in the variograms. Well behaved omnidirectional

variograms support to continue an exploration of the pattern of anisotropy with various directional variograms (Isaaks and Srivastava, 1989).

D) Since the spatial variability observed in a landscape is both large-scale and small-scale, interpolation of spatial fuels distribution must balance these two perspectives. Methodologies such as trend surface analysis, spectral analysis, wavelets, or regression models can be used to model the large-scale variability. Small-scale variability can be modeled trough different techniques such as kriging, and classification and regression trees (Reich, 2000).

E) The fuels' database of this study was gathered under a very peculiar sampling strategy (traditional Mexican forest inventory). However, some survey analyses have shown that such inventory methodology is not the most effective (Reich, 1999). Since the reliability of continuous surfaces is highly affected by the location and the intensity of the observations (Kalabokidis and Omi, 1995), further research is needed to defining the more adequate sample design when interpolating fuels spatial distribution. Maps of the standard deviation of estimation resulting from the kriging processes can help to redesign the sampling strategy (Reich, 1998).

F) Interpolation of the fuels' spatial distribution, based on direct measures, can result in very accurate estimations. However, this alternative is both costly and time consuming. On the other hand, indirect measures, mostly implemented with remote sensing techniques, are relatively cheaper and faster to implement. Nevertheless, these options have resulted in variable accuracy (e.g. 30-70%)

(Keane *et al.* 1999b). Therefore, future research on fuel spatial variability should take the advantages of both approaches. This can be possible through the implementation of double sampling methodologies, which allow integrating the definition of sample size and the number of classifications within the remotely sensed imagery. This could increase the accuracy and precision of the estimates (Kalkhan *et al.* 1996; Fule and Covington, 1994).

G) Forest fire phenomena are complex, thus a more accurate prediction of fire behavior should consider not only the evaluation of more variables, but also determine their spatial inter-dependencies (Reich and Bravo, 1999). Analyzing such variables independently of one another may lead to incorrect conclusions because of their spatial correlation (Reich, 1999). The multi-resource approach and geostatistical techniques can be used to generate and analyze new ancillary data for the estimation of spatial fuels distribution.

H) It is very rare to find projects of fuel models mapping that report, at the same time, an evaluation of the corresponding fuels loading. This information would allow further testing of the Conditional Fuels Loading Concept (CFLC) developed in this study. The CFLC was tested with information reported by Fischer (1981), and the result showed that the classification (into fuel-model) based on the calculated CFLC was the same as the classification defined by Fischer. The CFLC approach is objective (it does not depend on experience), and could be more accurate due to direct measures.

I) The polynomials defined in the trend surface analysis when using universal kriging, should not be restricted to the use of only the spatial coordinates. Other class of information that could help to define a potential trend in the data should be included. Thus, the information generated through the analysis of satellite imagery, Geographical Information System, and field inventory should be incorporated in that polynomial in order to evaluate their contribution to explain the potential spatial trend of the data.

J) The resultant fuel classes maps can be used for other purposes, such as: (a) evaluation of carbon budgets; (b) definition of fire risk areas; (c) to support evaluations of potential fire effects; (d) to define areas with potential for mushrooms growing; and to define habitat for certain wildlife species.

K) Geostatistical techniques can be used also to monitoring and predict changes in the spatial distribution of forest fuels. The temporal variation of fuels' loadings can be analyzed through kriging techniques, such as three-dimensional simple kriging. The temporal modeling of fuel distribution can be used to predict future fuel distribution maps (Hohn *et al.* 1993). Temporal and spatial autocorrelation of a natural phenomenon in a forest may be improved by including geostatistical components to summarize ecological dependence (Biondi *et al.* 1994; Liebhold *et al.* 1992). For instance, the temporal autocorrelation approach would allow predicting fuels' spatial distribution using information of fire regimes history and/or rate of fuel recovery as ancillary data.

L) Information regarding shrub and tree weights should be developed in future studies in México, considering also other factors, such as fuel production under different species. Moreover, an adequate characterization of forest fuels must include the determination of the surface area to volume ratio that corresponds to the different class of fuels that occur in a given area.

14 LITERATURE CITED

Aguirre B., C. and Reich, R.M. 1997. Integrated inventory and monitoring system for the Madrean-Apachian forest ecosystem complex. Proposal. USDA For. Serv. RMRS. Fort Collins, CO.

Aguirre B., C. and Reich, R.M. Unpublished. Assessment of forest inventory and monitoring networks in Northern Mexico: The Ejido "El Largo" case study. USDA For. Serv. RMRS. Fort Collins, CO.

Albini, F.A 1976. Estimating wildfire behavior and effects. USDA For. Serv. Gen. Tech. Rep. INT-30.

Allen, L.S. 1996. Ecological role of fire in the Madrean province. In: Proceedings: Effects of fire on Madrean province ecosystems. December. Fort Collins, Colorado. USDA, For. Serv. Gen. Tech. Rep. RM-GTR-289. pp 5-10.

Anderson, H.E. 1982. Aids to determining fuel models for estimating fire behavior. USDA, For. Serv. General Technical Report INT-122. 22p.

Anderson, H.E. 1989. Moisture diffusivity and response time in fine forest fuels. Canadian Journal of Forest Research 20: 315-325.

Andrews, P.L. 1986. BEHAVE: Fire Behavior Prediction and Fuel Modeling System-BURN Subsystem. Part I. USDA, Forest Service. Gen Tech. Rep. INT-194. 130 p.

Andronikov, S.V.; Davidson, D.A.; Spiers, R.B. 2000. Variability in contamination by heavy metals: sampling implications. Water, Air, and Soil Pollution 120: 29-45.

Armstrong, M. 1998. Basic linear geostatistics. Springer, New York. 153 pp.

Arnold, J.G.; Muttiah R.S.; Srinivasan, R; Allen, P.M. 2000. Regional estimation of base flow and groundwater recharge in the Upper Mississippi River basin. Journal of Hydrology Amsterdam 227: 21-40.

Asli, M. and Marcotee, D. 1995. Comparison of approaches to spatial estimation in a Bivariate context. Mathematical Geology 27(5): 641-658.

Atkinson, Peter M. and Lloyd, Chris D. 1997. Mapping precipitation in Switzerland with ordinary and indicator kriging. Journal of Geographic Information and Decision Analysis 2(2):72-86.

Berke, O. 1999. Estimation and prediction in the spatial linear model. Water, Air, and Soil Pollution 110: 215-237.

Beyerhelm, C. D. and Sando, R.W. 1982. Regression estimation of litter and one hour timelag fuel loading in aspen-northern hardwood stands. Forest Science 28: 177-180.

Biondi, Franco; Myers, Donald E., and Avery, Charles C. 1994. Geostatistically modeling stem size and increment in an old-growth forest. Canadian Journal of Forest Research 24(7):1354-1368.

Bishop, T.F.A.; McBratney, A.B.; Laslett, G.M. 1999. Modelling soil attribute depth functions with equal-area quadratic smoothing splines. Geoderma 91: 27-45.

Bonham, Ch. D.; Reich, R. M., and Leader, K. K. 1995. Spatial cross-correlation of Bouteloua gracilis with site factors. Grassland Science 41:196-201. GST-8

Borga, M.; Fattorelli, S.; Valentini, P.; Tsakiris, G.; Santos, M.A. 1994. Precipitation estimation for flood forecasting in a mountainous basin. In: Proceedings of the Second European conference of advances in water resources technology and management. Lisbon, Portugal, June. pp 403-410.

Bosiak, A. 1986. Detection and assessment of damage to forests, including that caused by air pollution and fires. Practical application of remote sensing in forestry. Edited by Sohlberg, S. and Sokolov, V.E. Martinus Nijhoff (ed.). The Netherlands. p. 187.

Bourennande, H.; King, D.; Chery, P.; Bruand, A. 1996. Improving the kriging of a soil variable using slope gradient as external drift. European Journal of Soil Science 47: 473-483.

Bovio, G.; Manca, R. and Perona, G.E. 1990. Locating forest fires by remote sensing. Monti e Boschi **41**: 5-10.

Bracq, P.; Delay, F. 1997. Transmisivity and morphological features in a chalk aquifer: a geostatistical approach of their relationship. Journal of Hydrology Amsterdam 191: 139-160.

Bringmark, E. and Bringmark,L. 1998. Improved soil monitoring by use of spatial patterns. Ambio 27(1): 45-52.

Brown, J.K. and Bevins, C.D. 1986. Surface fuel loadings and predicted fire behavior for vegetation types in the northern Rocky Mountains. USDA Forest Service, Intermountain Research Station. Res. Note INT-358.

Brown, D.E.; Reichenbacher, F.; Franson, S.E. 1994. A classification system and map of the biotic communities of North America. In Proccedings: Biodiversity and management of the Madrean Archipielago: The sky islands of southernwestern United States and northwestern Mexico. September 19-23. Tucson, Arizona. USDA For. Serv. Gen. Tech. Rep. RM-GTR-264. pp 109-125.

Brown, J.K.; Oberheu, R.D. and Johnston, C.M. 1982. Handbook for inventorying surface fuels and biomass in the Interior West. USDA Forest Service. Intermountain Forest and Range Experiment Station. General Technical Report INT-129.

Buckley, D. 2001. Minimizing wildfire damage. Imaging Notes, 16(1): 22-23.

Burgan, R.E. and Hartford, R.A. 1993. Monitoring vegetation greenness with satellite data.

USDA, Forest Service. Gen. Tech. Rep. INT-297. 13 p.

Burgan, R.E. and Rothermel, R.C. 1984. BEHAVE: fire behavior prediction and fuel modeling system-FUEL subsystem. USDA For. Serv. GTR. INT-167. 126 p.

Burgan, R.E. and Shasby, M.B. 1984. Mapping broad-area fire potential from digital fuel, terrain, and weather data. Journal of Forestry 82: 228-231.

Burgan, R.E.; Hartford, R.A.; Eideshink, J.C. 1996. Using NDVI to assess departure from average greenness and its relation to fire business. USDA For. Serv. Intermountain Research Station. General Technical Report INT-GTR-333. 8 p.

Burgan, Robert E.; Klaver, Robert W., and Klaver, Jacqueline M. 1998. Fuel models and fire potential from satellite and surface observations. International Journal of Wildland Fire 8(3):159-170.

Burgess, T.M., and Webster, R. 1980. Optimal interpolation and isarithmic mapping of soil properties II: block kriging. Journal of Soil Sciences 31: 333-341.

Burrough, P. A, and McDonnell. 1998. Principles of geographical information systems. Claredon Press Oxford; p. 333 p.

Burrough, P. A. 1986. Principles of geographical information systems for land resources assessment. Claredon Press Oxford; p. 193 p.

Burrough, P.A.; Maguire, D.J.; Goodchild, M.F.; Rhind, D.W. 1991. Soil information systems. Geographical information systems: Principles and applications. Vol. 2, Applications. Longman Group, UK. pp 153-169.

Burrows, D.M. and Burrows, W.H. 1992. Seed production and litter fall in some eucalypt communities in Central Queensland. Australian Journal of Botany, 40: 389-403.

Byers, M; McGrath, S.P.; Webster, R. 1987. A survey of the sulphur content of wheat grown in Britain. Journal of the Science and Food and Agriculture 38: 151-166.

Campbell, J.; Green, K.; Weinstein, D., and Finney, M. 1996. A. Fire growth modeling in an integrated GIS environment. In: SOFOR GIS "96. Southern Forestry Geopgraphic Information Systems Conference. pp 133-142.

Cappellini, V.; Mattii, L. and Mecocci, A. 1990. An intelligent system for automatic fire detection in forests. User contributions to satellite remote sensing programmes. Proceedings of the 9th EARSeL Symposium, 261-266.. Commission of the European Communities, Luxembourg.

Chou, Y.H. 1990. An efficient data structure for surface analysis in vector-based GIS. In:GIS '90 Symposium, an International Symposium on Geographic Information Systems. Forestry Canada. March. Vancouver, British Columbia. pp 417-421.

Chou, Yue Hong. 1989. Analyzing the spatial autocorrelation of polygonal data in GISGayk, William F. Urban and Regional Information Systems Association, Boston, Massachusetts.

Chou, Yue Hong. 1991. Map resolution and spatial autocorrelation. Geographical Analysis, 23(3): 228-246.

Chou, Yue Hong. 1992. Spatial autocorrelation and weighting functions in the distribution of wildfires. International Journal of Wildland Fire 2(4):169-176.

Chou, Yue Hong; Minnich, Richard A., and Salazar, Lucy A. 1990. Spatial autocorrelation of wildfire distribution in the Idyllwild quadrangle, San Jacinto Mountain, California. Photogrammetric Engineering & Remote Sensing 56(11):1507-1513

Chuvieco, E. and Congalton, R.G. 1989. Applications of remote sensing and geographic information systems to forest fire hazard mapping. Remote Sensing of Environment 29: 147-159.

Chuvieco, E. and Salas, J.. Mapping the spatial distribution of forest fire danger using GIS. International Journal of Geographical Information Systems 10(3):333-345.

Cliff, A. D. and Ord, J. Keith. Spatial autocorrelation. Pion Limited; 1973.

Collins, F.C. and Bolstad, P.V. 1995. A Comparison of Spatial Interpolation Techniques in Temperature Estimation. http://www.ncgia.ucsb.edu/conf/SANTA_FE_CD-ROM/sf_papers/collins_fred/collins.html

Coquet, Y. 1998. In situ measurement of the vertical linear shrinkage curve of soils. Soil and Tillage Research 46: 289-299.

Craig, C.; Cheney, P.; Thomas, P; Trabaud, L.; Williams, D. 1983. Fire in forestry. Volume I. Forest Fire behavior and effects. John Wiley & Sons. 450 p.

Crawford, C.A.G.; Hergert, G.W. 1997 Incorporating spatial trends and anisotropy in geostatistical mapping of soil properties. Soil Science Society of America Journal 61: 298-309.

Custer, S.G.; Farnes, P.; Wilson, J.P.; Snyder, R.D. 1996. A comparison of hand- and spline-drawn precipitation maps for mountainous Montana. Water Resources Bulletin 32(2): 393-405.

Czaplewski, R.L.; Reich, R.M., and Bechtold, W.A. 1994. Spatial autocorrelation in growth of undisturbed natural pine stand across Georgia. Forest Science 40(2): 314-328.

Daigle, J. 1999. FIRESTORM 2000 V 2.0. The wildland fire simulator. http://geocities.com/jjcricket_2000/.

Dean, D.J. 1998. Design of geographic information systems. Course Notes NR621. Department of Forest Sciences, Colorado State University.

Deeming, J.E.; Burgan, R.E.; Cohen, J.D. 1977. The National Fire Danger Rating System-

1978. USDA, Forest Service. Gen. Tech. Rep. INT-39. 66p.

Degenhardt, A and Hempel, G A. 1996.Comparison of site-quality methods involving spline functions: Biotechnical Faculty, University of Ljubljana; Ljubljana, Slovenia Deutscher Verband forstlicher Forschungsanstalten, Sektion Forstliche Biometrie und Informatik: 8. Tagung, Tharandt-Grillenburg, 25-28. September. 43-53.

DeMers, M.N. 1997. Fundamentals of Geographic Information Systems. J. Wiley & Sons, New York. 486 p.

Dessard, H. 1999. Comparison of design-based and model-based estimates for tropical forest resources with post-stratification. Annals of Forest Science 56: 651-665.

Dowdall, M.; O'Dea, J. 1999. Comparison of point estimation techniques in the spatial analysis of radium-226, radium-228 and potassium-40 in soil. Environmental Monitoring and Assessment 59: 191-209.

Durrans, S.R.; Burian, S.J.; Nix, S.J.; Hajji, A.; Pitt, R.E.; Fan, ChiYuan; Field, R.; Fan, C.Y. 1999. Polynomial-based disaggregation of hourly rainfall for continuous hydrologic simulation. Journal of the American Water Resources Association 35: 1213-1221.

Eidenshink, J.C. 1992. The 1990 conterminous U.S. AVHRR data set. Photogrammetric Engineering and Remote Sensing 58(6): 809-813.

ERDAS, Inc. 1997. ERDAS IMAGINE. Atlanta, Georgia.

ESRI. 1996. ARC/INFO. Redlands, California.

ESRI. 1998. ArcView. Redlands, California.

Estrada, P.A. 1999. Geostatistics as predictive tools to estimate Ixodes ricinus (Acari: Ixodidae) habitat suitability in the western Palearctic from AVHRR satellite imagery. Experimental and Applied Acarology 23: 337-349.

Everett, R.L.; Schellhaas, R.; Keenum, D.; Spurbeck, D.; Ohlson, P. 2000. Fire history in the ponderosa pine/Douglas-fir forests on the east slope of the Washington Cascades. Forest Ecology and Management 129: 207-225.

Fazakas, Z.; Nilsson, M.; Olsson, H.; Halldin, S.; Gryning, S.E.; Gottschalk, L.; Jochum, A.; Griend, A. 1999. Regional forest biomass and wood volume estimation using satellite data and ancillary data. Agricultural and Forest Meteorology 98-99: 417-425.

Finney, M.A. 1998. FARSITE: Fire Area Simulator—Model development and evaluation. USDA For. Serv., Gen. Tech. Rep. RMRS-GTR-4. 47 p.

Flannigan, M.D. and Wotton, B.M. 1989. A study of interpolation methods for forest fire danger rating in Canada. Canadian-Journal-of-Forest-Research 19(8): 1059-1066.

Flores G., J.G. 1997. Evaluacion del impacto ambiental de los incendios forestales en el Bosque de la Primavera. Temporada 1996. SAGAR. INIFAP. CIRPAC. Campo Experimental Colomos. Guadalajara, Jalisco. Mexico.

Flores G., J.G. and Benavides S., J.D. 1994. Influencia de dos tipos de quemas controladas en un bosque de pino en Jalisco. Folleto Tecnico No. 5. SAGAR. INIFAP. Campo Experimental Colomos. Guadalajara, Jal. Mexico. 12 pp.

Frandsen, W.H. and Andrews, P.L. 1979. Fire behavior in nonuniform fuels. USDA, Forest Service. Intermountain Forest and Range Experimental Station. Res. Paper INT-232.

Friedl, M. A.; Michaelsen, J; Davis, F. W.; Walker, H., and Schimel, D. S. 1994. Estimating grassland biomass and leaf area index using ground and satellite data. International Journal of Remote Sensing 15(7):1401-1420.

Fulé, P.Z. and Covington, W.W. 1994. Double sampling increases the efficiency of forest floor inventories for Arizona ponderosa pine forests. International Journal of Wildland Fire 4: 3-10.

Garzon, V.E. 1997. Computational Fluid Dynamics (CFD) simulation of forest fire spread. Mechanical Engineering Department. Univ. of Kentucky. Post-doctoral project.

Gold, C.M. 1989. Voronoi diagrams and spatial adjacency. In: Proceedings, G.I.S.-challenge for the 1990s. Ottawa, ON. pp. 1309-1316.

Golden Software Inc. 1999, SURFER 7, Golden, Colorado.

Gonzalez, O.J. and Zak, D.R. 1994. Geostatistical analysis of soil properties in a secondary tropical dry forest, St. Lucia, West Indies. Plant and Soil 163(1): 45-54.

Goovaerts, P. 1997. Geostatistics for natural resources evaluation. Applied geostatistics series. Oxford University Press. 483 pp.

Goovaerts, P. 2000. Geostatistical approaches for incorporating elevation into the spatial interpolation of rainfall. Journal of Hydrology Amsterdam 228: 113-129.

Goovaerts, P.; Journel, A.G. 1995. Integrating soil map information in modelling the spatial variation of continuous soil properties. European Journal of Soil Science, 46: 397-414.

Gorres, J.H.; Dichiaro, M.J.; Lyons, J.B.; Amador, J.A. 1998. Spatial and temporal patterns of soil biological activity in a forest and an old field. Soil Biology and Biochemistry, 30: 219-230.

Gray, A. 2001. Personal communication. Department of Biostatistics. PPD Development.

Green, D.G. 1983. Shapes of simulated fires in discrete fuels. Ecological modeling 20: 21-32.

Grewal, M.S.; Anil, K.; Kuhad, M.S. 1996. Spatial variation of fluorine in an indo-gangetic alluvial plain of India. Fluoride 29: 166-174.

Grimes, D.I.F.; Pardo, I.E.; Bonifacio, R. 1999. Optimal areal rainfall estimation using raingauges and satellite data. Journal of Hydrology Amsterdam 222: 93-108.

Guardado, J.L.; Sommers, W.T. 1977. Interpolation of unevenly spaced data using a parabolic leapfrog correction and cubic splines. USDA-Forest-Service-Research-Note,-Pacific-Southwest-Forest-and-Range-Experiment-Station.No. PSW-324. 5 p.

Hardwick, P.E.; Lachowski, H. Forbes, J.; Olson, J. Roby, K.; Fites, J. 1996. Fuel loading risk assessment Lassen National Forest. In: J.D. Greer, editor, Proceedings of the 7th Forest Service remote sensing application conference. Nassau Bay, Texas, April 6-April 10, 1998. American Society for Photogrammetry and Remote Sensing, Bethesda, Marylnd. pp 301-316

Hawkes, Brad; Goodenough, David; Lawson, Bruce; Alan, Thomson; Sahle, Wendmagegn; Niemann, Olaf; Fuglem, Peter; Beck, Judi; Bell, Bryan, and Symington, Phil. 1996. Forest fire fuel type mapping using GIS and remote sensing in British Columbia. GIS applications in natural resources. Fort Collins, CO.

Hill, M.J.; Hutchinson, M.F.; Kirby, A.C. 1989. Mapping herbage accumulation for the Hunter Region of Australia using climatic analysis, growth indices and field experiments. In: Proceedings of the XVI International Grassland Congress. Association Francaise pour la Production Fourragere. 4-11 October, Nice, France. 1369-1370.

Hobbs, R. J. and Atkins, L. 1988. Spatial variability of experimental fires in south-west Western Australia. Australian Journal of Ecology 13: 295-299.

Höck, B.K.; Payn, T.W. and Shirley, J.W. 1993. Using a geographic information system and geostatistics to estimate side index of *Pinus radiata* for Kaingaroa Forest, New Zealand. New Zealand Journal of Forestry Science 23: 264-277.

Hohn, Michael E.; Liebhold, Andrew M., and Gribko, Linda S. 1993. Geostatistical model for forecasting spatial dynamics of defoliation caused by the gipsy moth (Lepidoptera: Lymantriidae). Environmental Entomology 22(5):1066-1075.

Hudson, G.; Wackernagel, H. 1994. Mapping temperature using kriging with external drift: theory and an example from Scotland. International Journal of Climatology 14: 77-91.

Huhn, M.; Langner, W. 1999. Investigations on the correlation pattern in even-aged stands of larch. VI. Relationships between single tree height and diameter measurements and individual Thiessen polygon areas. Silvae Genetica 48: 87-91.

Hunner, G. 2000. Modeling forest stand structure using geostatistics, geographic information systems, and remote sensing. Ph.D. Dissertation. Forest Sciences Department. Colorado State University. 217 p.

Hunner, Gerhard; Mowrer, H. Todd, and Reich, Robin M. 2000. An accuracy comparison of six spatial interpolation methods for modelling forest stand structure on the Fraser Experimental Forest, Colorado. In: Proceedings of the 4th International Symposium on

Spatial Accuracy Assessment in Natural resources and Environmental Sciences. July, 2000. Amsterdan. pp 305-312.

Impara, P.C. 1997. Spatial and temporal patterns of fire in the forests of the Central Oregon Coast Range. Ph.D. Dissertation. Oregon State University. 354 p.

International Fire Service Training Association. 1998. Fundamentals of wildland fire fighting. Third Ed. Fire Protection Publications. Oklahoma State University. 472 p.

Isaaks, E.H. and Srivastava, R.M. 1989. An introduction to applied geostatistics. Oxford University Press. New York. 561 p.

Jensen, J.R. 1996. Introductory digital image processing. A remote sensing perspective. 2nd Edit.. Prentice-Hall Series in Geographic Information Science. Prentice-Hall, Inc. New Jersey. 310 p.

Johansen, R.W.; Lavdas, L.G. and Loomis, R.M. 1981. Estimating fuel weights before prescription burning shortleaf pine stands. Southern Journal of Applied Forestry 5: 128-131.

Juang, K.W.; Lee D.Y.; Juang, K.W.; Lee, D.Y. 2000. Comparison of three nonparametric kriging methods for delineating heavy-metal contaminated soils. Journal of Environmental Quality 29: 197-205.

Kalabokidis, K.D. and Omi, P.N. 1994. Isarithmic analysis of forest fire fuelbed arrays. Ecological modeling 80: 47-55.

Kalkhan, M. A.; Reich, R. M., and Czaplewski, R. L. 1996. Statistical properties of measures of association and the Kappa statistic for assessing the accuracy of remotely sensed data using double sampling. In: Spatial accuracy assessment in natural resources and environmental sciences. 2nd International Symposium.USDA, FS. GTR-277: 467-476.

Kallas, M. 1997. Armillaria root disease in the Black Hills of South Dakota. M.S. Thesis. Department of Forest Sciences, Colorado State University. Fort Collins, CO 80523.

Keane, R.E.; Burgan, R.; van Wagtendok. 1999b. Mapping wildland fuels for fire management across multiple scales: Integrating remote sensing, GIS, and biophysical modeling. USDA For. Ser. RMRS. Fire Sciences Laboratory, Fire Modeling Institute.

Keane, R.E.; Garner, J.L.; Schmidt, K.M; Long, D.G.; Menakis, J.P.; Finney, A.M. 1998b. Development of input data layers for the FARSITE Fire Growth Model for the Selway-Bitterroot Wilderness Complex, USA. USDA, Forest Service. Gen. Tech. Rep. RMRS-GTR-3. 66p.

Keane, R.E.; Long, D.G.; Schmidt, K.M.; Mincemoyer, S.; Garner, J.L. 1998. Mapping fuels for spatial fire simulations using remote sensing and biophysical modeling. In: Proceedings of the 7th Forest Service remote sensing application conference. J.D. Greer, (ed.) Nassau Bay, Texas, April 6-10, 1998. American Society for Photogrammetry and Remote Sensing. pp. 301-316.

Keane, R.E.; McNicoll, C.H.; Schmidt, K.M.; Garner, J.L. 1996. Spatially explicit ecological inventories for ecosystem management planning using gradient modeling and remote sensing. In: Proceedings of the Sixth Forest Service Remote Sensing Applications Conference. April 29-May3. Editor Greer, J.D. Denver Colorado. pp 135-145.

Keane, R.E.; Mincemoyer, S.A.; Schmidt, K.M.; Long, D. G.; Garner, J.L. 1999a. Mapping vegetation and fuels for fire management on the Gila National Forest Complex, New Mexico. USDA For. Serv. General Technical Report RMRS-GTR-CD-000. Ogden, UT: U.S. 90 pp.

Kenkel, N.C.; Hoskins, J.A.; Hoskins, W.D. 1989. Local competition in a naturally established jack pine stand. Canadian Journal of Botany 67: 2630-2635.

Kessell, S.R. 1976. Gradient modeling: A new approach to fire modeling and wilderness resource management. Environmental Management 1(1): 39-48.

Kessell, S.R. 1979. Gradient modeling, resource and fire management. Springer-Verlag. New York. 433 p.

Kourtz, P.H. 1978. An application of Landsat digital technology to forest fire fuel type mapping. Commonwealth Forestry Review 57: 144-148.

Krauter, Karl. 1999. Remote sensing of fuel models on East side Sierra ecosystems. In: California Association for Fire Ecology (CAFE) 1999 Symposium. Fire Management: Emerging Policies and New Paradigms. Nov 16-19; San Diego, California.

Kravchenko, A.N. and Bullock, D. G. 1999. A comparative study of interpolation methods for mapping soil properties. Agronomy-Journal 91: 393-400.

Kravchenko, A.N.; Bullock, D.G.; Robert, P.C.; Rust, R.H.; Larson, W.E. 1999. Comparison of interpolation methods for mapping soil P and K contents. In: Proceedings of the Fourth International Conference on Precision Agriculture. American Society of Agronomy. Minnesota, USA. 19-22 July, 1998. pp 267-279.

Ladewig, E; Marlander, B. 1997. Determination of optimum N-supply in sugar beet by different mathematical methods. Zeitschrift-fur-Pflanzenernahrung-und-Bodenkunde 160: 85-88.

Lark, R.M. 2000. A comparison of some robust estimators of the variogram for use in soil survey. European Journal of Soil Science 51: 137-157.

Laslett, G. M.; McBratney, A. B.; Pahl, P. J., and Hutchinson, M. F. 1987. Comparison of several spatial prediction methods for soil pH. Journal of Soil Science 38:325-341.

Lee, Sunyoung; Cho, Sungzoon, and Wong, Patrick M. 1997. Rainfall prediction using artificial neural networks. Journal of Geographic Information and Decision Analysis 2(2):253-264.

Lee, Y.J. and Kvarv, E. 1983. Assessment of log debris using Landsat MSS data at Williston Lake, British Columbia. Canadian Journal of Remote Sensing 9: 111-124.

Lennon, J.J. and Turner, J.R.G. 1995.Predicting the spatial distribution of climate: Temperature in Great Britain. Journal of Animal Ecology 64(3): 370-392.

Levin, S.A. and Pacala, S.W. 1997. Theories of simplification and scaling of spatially distributed process. In: Spatial ecology. Tilman, D and Kareiva, P. Princenton (ed.) University Press. Princenton, New Jersey. pp 271-295.

Levine, Megan and McKinley, Sky. Cubic Spline Interpolation [Web Page]. 1999. Available at:http://online.redwoods.cc.ca.us/instruct/darnold/laproj/Fall98/SkyMeg/splinepres/index.htm.

Li, B.L.; Yeh, T.C.J.; Li, B.L. 1999. Cokriging estimation of the conductivity field under variably saturated flow conditions. Water Resources Research 35: 3663-3674.

Liebhold, A.; Hohn, M.E.; Gribko, L.R.; Liebhold, A.M. and Barret, H.R. 1993. Forecasting the spatial dynamics of gypsy moth defoliation using 3-dimensional kriging. In: Proceedings: Spatial analysis and forest pest management. USDA Forest Service. Northeastern Forest Experiment Station, No. NE-175. pp 150-159.

Liebhold, A.M.; Zhang, X.; Hohn, M.E.; Elkinton, J.S.; Ticehurst, M.; Benzon, G.L.; Campbell, R.W. 1991. Geostatistical analysis of gypsy moth (Lepidoptera: Lymantriidae) egg mass populations. Environmental Entomology 20: 1407-1417.

Liu, P.S. and Chou, Y.H. 1997. A grid automation of wildfire growth simulation. In: Proceedings of the 1997 ESRI User Conference. San Diego, California. http://www.esri.com/library/userconf/proc97/proc97/to200/pap158/p158.htm.

Lopes, V.L. 1996. On the effect of uncertainty in spatial distribution of rainfall on catchment modelling. Catena 28: 107-119.

Lopez, C.; Samper, J.; Soares, A.; Gomez, H.J.; Froidevaux, R. 1996. Numerical aspects of the universal kriging method for hydrological applications. In: Proceedings of GeoENV I geostatistics for environmental applications. Lisbon, Portugal, 18-19 Nov. pp 65-76.

Lowell, K. 1996. Discrete polygons or a continuous surface: which is the appropriate way to model forest cartographically? In: Spatial Accuracy Assessment in Natural Resources and Environmental Sciences. USDA Forest Service Gral. Tech. Rep. RM-GTR-277. Fort Collins, Colorado. pp 235-242.

Mackey, B.G.; McKenney, D.W.; Yang,YinQian; McMahon, J.P.; Hutchinson, M.F.; Yang, Y.Q. 1996. Site regions revisited: a climatic analysis of Hills' site regions for the province of Ontario using a parametric method. Canadian-Journal-of-Forest-Research 26(3): 333-354.

Magnussen, S. 1996. A coordinate-free area variance estimator for forest stands with a fuzzy outline. Forest Science 42: 76-85.

Mandallaz, D. 1993. Geostatistical methods for double sampling schemes: application to combined forest inventories. Swiss Federal Institute of Technology. Zurich. 133 p.

Markus, L.; Berke, O.; Kovacs, J.; Urfer, W. 1999. Spatial prediction of the intensity of latent effects governing hydrogeological phenomena. Environmetrics 10: 633-654.

Martinez, C.A. 1996. Multivariate geostatistical analysis of evapotranspiration and precipitation in mountainous terrain. Journal of Hydrology Amsterdam 174: 19-35.

MathSoft, Inc. 1999. S-PLUS 2000. Seattle, Washington.

Matson, M. and Holben, B. 1987. Satellite detection of tropical burning in Brazil. International Journal of Remote Sensing 8: 509-516.

McCaw, W.L.; Neal, J.E. and Smith, R.H. 1997. Fuel accumulation following prescribed burning in young even-aged stands of karri (*Eucalyptus diversicolor*). Australian Forestry 59; 171-177.

Meeuwig, R.O.; Miller, E.L.; Budy, J.D. 1979. Estimating pinyon and juniper fuel and biomass from aerial photographs. U.S. Forest Service, Intermountain Forest and Range Experiment Station. Research Note, INT-274. 9 pp.

Meshalkina, J.L.; Stein, A.; Dmitriyev, Ye A. 1995. Spatial variability of penetration data on Russian plots in different land use. Soil Technology 8: 43-59.

Metzger, K.L. 1997. Modeling forest stand structure to a ten meter resolution using Landsat TM data. M.S. Thesis. Department of Forest Sciences, Colorado State University. Fort Collins, CO 80523. 123 p.

Meuli, R.; Schulin, R.; Webster, R. 1998. Experience with the replication of regional survey of soil pollution. Environmental Pollution 101: 311-320.

Microsoft. 1997. Excel 97. Redmond, Washington.

Mimikou, M.A.; Baltas, E.A. 1996. Flood forecasting based on radar rainfall measurements. Journal of Water Resources Planning and Management 122: 151-156.

Montas, H.J.; Haghighi, K.; Engel, B. A. 1998. Numerical solution of integro-partial differential contaminant transport equations. In: ASAE Annual International Meeting. American Society of Agricultural Engineers. Orlando, Florida, USA, 12-16 July. ASAE Paper no. 983179. 12 pp.

Nalder I.A.; Wein, R.W. 1998. Spatial interpolation of climatic normals: test of a new method in the Canadian boreal forest. Agricultural and Forest Meteorology 92: 211-225.

Nash,M.S.; Toorman, A.; Wierenga, P.J.; Gutjahr, A.; Cunningham, G.L. 1992. Estimation of vegetative cover in an arid rangeland based on soil-moisture using cokriging. Soil Science 154: 25-36.

National Wildfire Coordinating Group. 1994. Intermediate wildland fire behavior. S-290. National Interagency Fire Center. Boise, Idaho. 360 p.

Nemes, A; Wosten, J.H.M.; Lilly, A; Voshaar, J.H.O.1999. Evaluation of different procedures to interpolate particle-size distributions to achieve compatibility within soil databases. Geoderma 90: 187-202.

Oberthur, T.; Goovaerts, P.; Dobermann, A. 1999. Mapping soil texture classes using field texturing, particle size distribution and local knowledge by both conventional and geostatistical methods. European Journal of Soil Science 50: 457-479.

Olea, R.A. 1991. Geostatistical Glossary and Multilingual Dictionary. Oxford University Press, New York.

Omi, P.N. 1997. Forest fire management. F424 course. University Text. Colorado State University. 117 pp.

Ottmar, R.; Sandberg, D.V.; Cushon, G.; Key, J.L. 2000. Fuel characteristic classification. Characterizing wildland fuelbeds in the United States. Fire and Environmental Research Applications. 12 p.

Panagoulia, D. 1992. Hydrological modelling of a medium-size mountainous catchment from incomplete meteorological data. Journal of Hydrology Amsterdam 137: 279-310.

Parresol, B.R.; McCollum, J.; Bouman, O.T.; Brand, D.G. 1997. Characterizing and comparing landscape diversity using GIS and a contagion index. Journal of Sustainable Forestry 5: 249-261.

Pereira G., P. and Diogo, P. 1994. FireGIS. A cellular automata forest fire simulator using GIS. NOVASOFT-GASA. Universidade Nova de Lisboa. Portugal.

Pereira, M.C. and Setzer, A.W. 1993. Spectral characteristics of fire scars in Landsat-5TM images of Amazonia. International Journal of Remote Sensing 14: 2061-2078.

Phillips, D.L.; Dolph, J.; Marks, D. 1992. A comparison of geostatistical procedures for spatial analysis of precipitation in mountainous terrain. Agricultural and Forest Meteorology 58: 119-141.

Phillips, D.L.; Lee, E.H.; Herstrom, A.A.; Hogsett, W.E.; Tingey, D.T. 1997. Use of auxiliary data for spatial interpolation of ozone exposure in southeastern forests. Environmetrics 8: 43-61.

Potter, B. and Eenigenburg, J. 1999. Interpolation Techniques for Late-Spring Freeze Data. Atmospheric Disturbance Climatology. North Central Research Station Forestry Sci. Laboratory. http://climate.usfs.msu.edu/climatology/Freezemaps.html#idsw.

Pozdnyakova, L.; Zhang, R.D.; Zhang, R.D. 1999. Geostatistical analyses of soil salinity in a large field. Precision Agriculture 1: 153-165.

Price, D.T.; McKenney, D.W.; Nalder, I.A.; Hutchinson, M.F.; Kesteven, J.L. 2000. A comparison of two statistical methods for spatial interpolation of Canadian monthly mean climate data. Agricultural and Forest Meteorology 101: 81-94.

Prudhomme, C. and Reed, D.W. 1999. Mapping extreme rainfall in a mountainous region using geostatistical techniques: a case study in Scotland. International Journal of Climatology 19: 1337-1356.

Punyawardena, B.V.R.; Kulasiri, D. 1998. Spatial interpolation of rainfall in the dry zone of Sri Lanka. Journal of the National Science Council of Sri Lanka 26: 247-262.

Pyne, S.J. 1984. Introduction to wildland fire. Fire management in the United States. John Wiley & Sons, Inc. 455 p.

Ramírez M., H. 1980. On the relevance of geostatistical theory and methods to forest inventory problems. Ph.D. Dissertation. University of Georgia. 163 p.

Raspe, S.; Feger, K.H.; Zottl, H.W. 1989. Inventory of element pools in the root biomass of a 100-year-old Norway spruce (*Picea abies*) stand in the Black Forest. Angewandte-Botanik 63: 145-163.

Regniere, J. and Sharov, A. 1997. Forecasting gypsy moth flight in the northeastern US with BioSIM. In: Integrating spatial information technologies for tomorrow. pp 99-103.

Regniere, J. and Sharov, A. 1999. Simulating temperature-dependent ecological processes at the sub-continental scale: male gypsy moth flight phenology as an example. International Journal of Biometeorology 42: 146-152.

Reich, R. M. 2000. Application of classification and regression trees (CART). Rangeland Ecosystem Science Seminar, January 25. Colorado State University

Reich, R. M. and Geils, B. W. 1992. Review of spatial analysis techniques. Spatial analysis and forest pest management. USDA, FS. Gen. Tech. Rep. NE-175; 142-149.

Reich, R. M.; Mielke Jr., P. W. and Hawksworth, F. G. 1991. Spatial analysis of ponderosa pine tree infected with dwarf mistletoe. Canadian Journal of Forest Research 21:1808-1815.

Reich, R.M. 1999. Integrating spatial statistics with GIS and remote sensing in designing multi-resource inventories. Rangeland Ecosystem Science Seminar, January 26. Colorado State University

Reich, R.M. and Bravo, V.A. 1999. Integrating spatial statistics with GIS and remote sensing in designing multiresource inventories. In: Proceedings of the North American Science Symposium: Toward a unified framework for inventoring and monitoring forest ecosystem resources. Aguirre B., A. and Rodriguez F., C. (ed.). USDA For. Serv. Proceedings RMRS-P-12. pp 202-207.

Reich, R.M. and Davis, R. 1998. Quantitative spatial analysis. Course notes for NR/ST 523. Colorado State University, Fort Collins. 420 p.

Rizzo, D.M. and Dougherty, D.E. 1994. Characterization of aquifer properties using artificial neural networks: neural kriging. Water Resources Research 30: 483-497.

Roberts, D.W.; Li, B.L. 1996. Landscape vegetation modelling with vital attributes and fuzzy systems theory. Ecological Modelling 90: 175-184.

Robertson, G.P. 2000. GS+. Geostatistics for the environmental sciences. Gamma Design Software. 200 p.

Robichaud, P.R. 1996. Spatially-varied erosion potential from harvested hillslopes after prescribed fire in the interior northwest. Ph.D. Dissertation. Major in Agricultural Engineering. University of Idaho. 219 p.

Rothermel, R C. 1972. A mathematical model for predicting fire spread in wildland fuels. USDA For. Serv. Research Paper INT-115.

Rothermel, R.C.; Hartford, R.A.; Chase, C. H. 1994. Fire growth maps for the 1988 Greater Yellowstone Area fires. USDA, Forest Service. Intermountain Research Station. General Technical Report INT-304.

Sackett, S.S.; Haase, S.M.; Harrington, M.G. 1996. Prescribed burning in Southwestern ponderosa pine. In Proceedings: Effects of fire on Madrean province ecosystems. December. Fort Collins, Colorado. USDA, For. Serv. Gen. Tech. Rep. RM-GTR-289. pp 178-186.

Salazar, L.A. 1982. Remote sensing techniques aid in preattack planning for fire management. 1982. USDA, For. Serv. Pacific Southwest Forest and Range Experiment Station. PSW-RP-162. 19 pp.

Samra, J.S.; Gill, H.S. and Bhatia, V.K. 1989. Spatial stochastic modeling of growth and forest resource evaluation. Forest Science 35: 663-676.

Scott, J. and Reinhardt, E. 1999. NEXUS. Fire behavior assessment system. Systems for Environmental Management. Missoula, MT.

Singh, T. 1987. Estimating downed-dead roundwood fuel volume in central Alberta. Information Report, Northern Forestry Centre, Canadian Forestry Service. NOR X 289. 23 pp.

Soderstrom, M.; Magnusson, B. 1995. Assessment of local agroclimatological conditions-a methodology. Agricultural and Forest Meteorology 72: 243-260.

Stein, Michael L. 1999. Interpolation of spatial data. Some theory for kriging. Springer. 247 p.

Stow, D.; Hope, A.; McKinsey, D.; Pray, H. 1993. Deriving dynamic information on fire fuel distributions in southern California chaparral from remotely sensed data. Landscape and Urban Planning 24: 113-127.

Trangmar, B.B.; Yost, R.S.; Uehara, G. 1986. Spatial dependence and interpolation of soil properties in West Sumatra, Indonesia: I Anisotropic variation. Soil Sci. Soc. Am. J. 50: 1391-1395.

UCODEFO 2, 1997. Aplicacion del invenstario forestal continuo (I.F.C.) en los bosques del "Ejido El Largo", Chihuahua, Mexico. Unidad de Conservacion y desarrollo Forestal No. 2. Cd. Madera, Chihuahua. Mexico. 34 pp.

vanLeeuwen, E.P.; Draaijers, G.P.J.; Erisman, J.W.; VanLeeuwen, E.P. 1996. Mapping wet deposition of acidifying components and base cations over Europe using measurements. Atmospheric-Environment 30: 2495-2511.

Wackernagel, H.; Webster, R.; Oliver, M.A. and Bock, H.H. 1988. A geostatistical method for segmenting multivariate sequences of soil data. Classification and related methods of data analysis. 641-650.

Weber, D.D. and Engud, E.J. 1994. Evaluacion and comparison of spatial interpolators II. Mathematical Geology 26((: 589-604.

Webster, R. and Oliver, M.A. 1989. Optimal interpolation and isarithmic mapping of soil properties. VI Disjunctive kriging and mapping the conditional probability. Journal of Soil Science 40: 497-512.

Weise, D.R. and Biging, G.S. 1997. A qualitative comparison of fire spread models incorporating wind and slope effects. Forest Science 43(2): 170-180.

Wilson, B.A.; Ow, C.F.Y.; Heathcott, M.; Milne, D.; McCaffrey, T.M.; Ghitter, G. and Franklin, S.E. 1994. Landsat MSS classifications on fire fuel types in Wood Buffalo National Park, Northern Canada. Global Ecology and Biogeography Letters 4. 33-39.

Wotling, G; Bouvier, C; Danloux, J; Fritsch, J.M. 2000. Regionalization of extreme precipitation distribution using the principal components of the topographical environment. Journal of Hydrology Amsterdam 233: 86-101.

Xia, Y.L.; Fabian, P.; Stohl, A.; Winterhalter, M.; Xia, Y.L. 1999. Forest climatology: estimation of missing values for Bavaria, Germany. Agricultural and Forest Meteorology 96: 131-144.

Yuan, M. 1994a. Acquiring experts' knowledge to build wildfire representation in GISs. In: Proceedings of ESRI User Conference'94.

Yuan, M. 1994b. Representation of wildfire in Geographical Information Systems. Ph.D. thesis, State University of New York at Buffalo.

Zack, J.A. and Minnich, R.A. 1991. Integration of geographic information systems with a diagnostic wind field model for fire management. Forest Science 37(2): 560-573.

Zanetti, P.; Delfine, S.; Alvino, A. 1999. A mathematical approach for estimating light absorption by a crop from continuous radiation measurements and restricted absorption data. Computers and Electronics in Agriculture 22: 71-81.

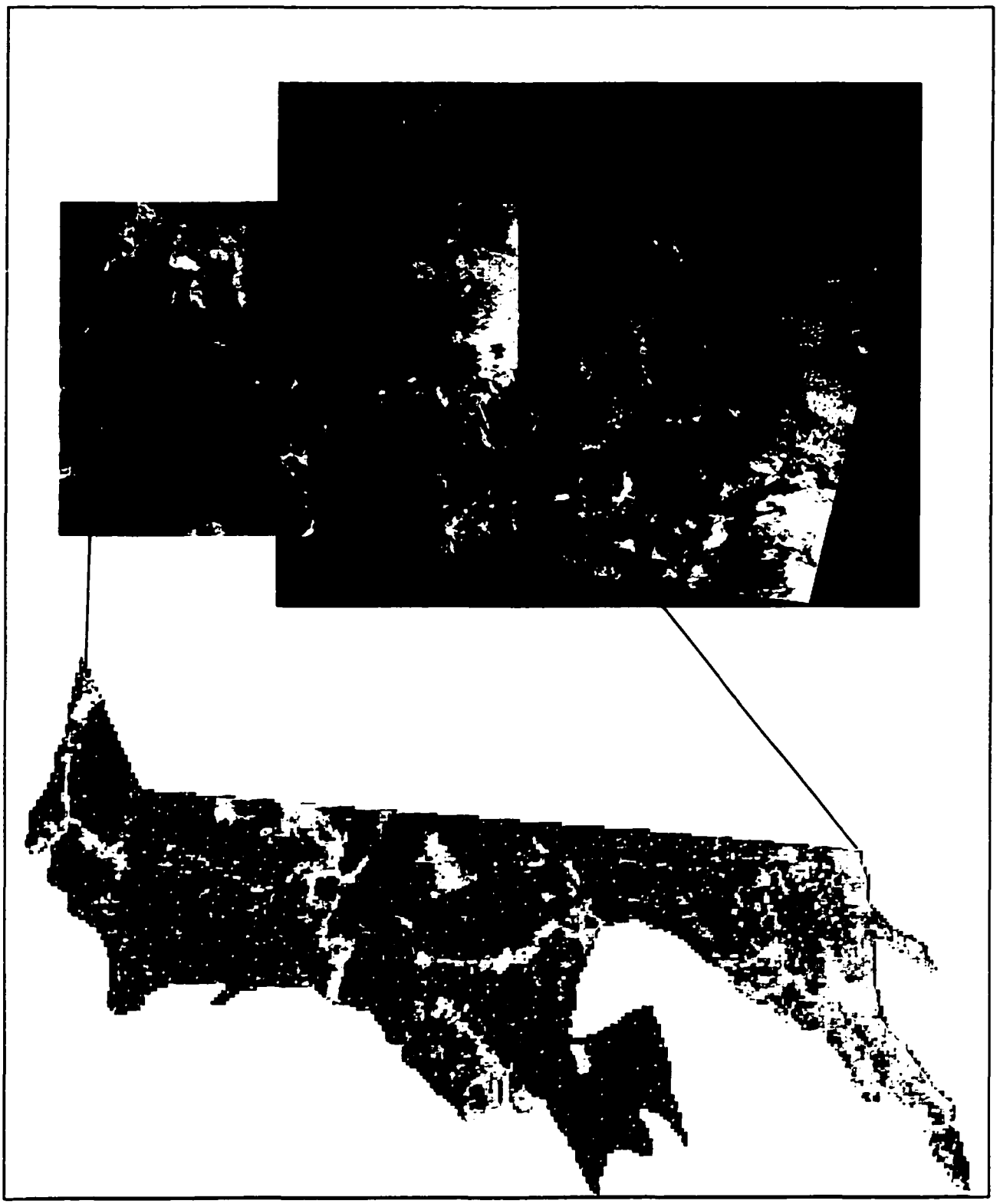

Appendix 6.1. Landsat TM5 image corresponding to the Path 34, and Row 40, where the study area was located (at NE of Chihuahua, México).

Appendix 7.1. Sampling errors associated with the sampling of forest fuels. Fuels survey was carried out based on the temporary forest inventory design of Ejido El Largo y Anexos, Chihuahua (Mexico).

STAND	1-HR			10-HR			100-HR			LW		
CODE	MEAN	VARIANCE	S.ERROR	MEAN	VARIANCE	S.ERROR	MEAN	VARIANCE	S.ERROR	MEAN	VARIANCE	S.ERROR
289	1.261	0.564	24.311	0.800	0.469	35.714	1.806	19.289	99.273	0.956	1.595	53.946
291	1.710	1.013	39.253	0.739	1.163	103.211	3.612	44.737	130.931	0.851	0.720	70.552
396	1.561	0.474	22.760	1.138	1.200	49.682	3.161	20.660	71.903	0.061	0.016	104.714
365	1.289	0.544	29.559	2.241	5.395	50.282	2.890	43.246	117.514	0.245	0.075	54.282
324	1.457	0.579	27.921	2.064	3.375	47.573	5.676	57.642	71.493	0.203	0.137	100.862
364	1.869	0.479	13.747	1.178	1.460	38.103	4.428	40.632	51.711	0.687	0.727	45.291
285	1.860	0.351	15.932	1.111	1.394	58.916	7.706	78.041	59.199	0.479	0.333	58.413
321	2.050	0.291	6.634	1.314	0.817	18.074	9.238	118.533	30.180	0.350	0.259	37.903
389	2.612	0.382	10.092	1.084	0.966	40.561	5.583	64.281	61.239	0.668	0.572	49.417
387	1.612	0.490	15.600	1.525	1.938	32.781	5.232	111.457	74.947	0.184	0.154	74.251
391	0.860	0.350	68.858	1.149	1.258	97.590	14.449	173.978	91.287	0.314	0.077	88.145
357	2.279	0.309	28.153	2.791	1.258	40.184	3.612	17.398	115.470	0.048	0.009	204.257
353	1.687	0.097	26.159	1.314	0.863	100.000	7.224	104.387	200.000	0.286	0.001	17.622
356	2.207	0.547	38.701	3.941	0.863	33.333	19.265	278.364	100.000	0.162	0.021	102.858
344	1.046	0.064	27.867	1.532	0.575	57.143	7.224	52.193	115.470	0.059	0.003	113.972
355	1.144	0.010	9.917	4.926	0.216	13.333	14.449	156.580	100.000	0.737	0.310	87.266
358	1.949	0.531	19.987	1.220	0.720	37.198	8.538	165.121	90.756	0.349	0.303	84.329
384	2.353	0.472	13.339	1.883	1.964	38.435	10.837	118.202	47.294	0.280	0.177	70.746
383	1.572	0.255	17.821	1.213	2.649	74.458	2.779	30.781	110.755	0.164	0.035	63.041
363	1.645	0.466	25.027	1.861	1.280	49.635	11.740	222.754	89.895	0.229	0.117	105.689
393	2.012	0.158	22.798	2.189	4.026	105.830	7.224	52.193	115.470	0.691	0.342	84.646
312	2.169	0.477	12.030	1.830	4.900	45.730	6.391	72.348	52.203	1.021	1.350	49.661
250	1.864	0.820	26.941	1.920	9.092	87.121	9.031	85.746	72.506	0.218	0.157	121.410
385	1.824	0.543	36.112	1.182	0.302	41.574	2.890	15.658	122.474	0.129	0.031	122.689
386	2.717	0.045	9.035	1.806	0.971	54.545	5.418	47.844	127.657	0.069	0.019	200.000
287	1.708	0.071	17.993	1.095	0.575	80.000	9.633	278.364	200.100	0.379	0.047	66.102
286	2.294	0.262	18.212	1.095	0.633	59.330	5.160	116.814	158.325	0.497	0.147	58.286
323	1.569	0.375	45.069	0.657	0.000	0.000	14.449	52.193	57.735	0.028	0.000	71.106
395	1.804	0.112	18.593	0.985	0.144	38.490	3.612	52.193	200.000	0.334	0.107	97.985
350	2.522	0.401	28.976	3.284	3.451	80.000	19.265	278.364	100.000	0.619	0.220	87.416
349	1.978	0.093	13.784	1.839	0.302	26.726	8.669	88.729	97.183	0.115	0.015	108.179
319	1.896	0.182	31.836	0.657	0.863	198.485	0.000	0.000	0.000	1.280	2.140	161.220
317	1.329	0.062	26.579	3.284	0.000	0.000	18.061	26.097	40.000	0.213	0.006	51.944
316	2.903	0.074	10.838	0.657	0.863	198.485	9.633	69.591	100.000	0.173	0.017	86.687
315	2.184	0.556	21.586	1.970	2.013	45.542	5.780	20.877	50.000	0.160	0.143	157.594
352	1.998	0.058	9.832	3.503	7.879	65.431	15.894	219.212	83.320	0.182	0.042	85.084
351	2.034	0.193	16.331	1.032	1.417	87.197	10.837	99.167	75.031	0.256	0.317	166.416
318	0.945	0.014	14.264	1.314	0.431	57.735	0.000	0.000	0.000	2.132	2.174	79.876
354	2.253	0.581	21.394	4.006	5.890	38.314	13.004	55.673	36.289	1.135	1.573	69.913
320	2.320	0.514	18.641	3.164	3.694	36.625	16.419	230.599	55.771	0.598	0.315	56.612
348	2.494	0.317	6.887	2.164	3.061	24.373	9.934	82.138	28.851	1.215	1.341	30.534
314	2.544	0.211	9.024	2.586	5.146	43.859	9.288	99.792	57.487	0.680	0.558	56.710
281	2.436	0.265	14.089	2.335	4.110	57.876	4.128	32.310	104.083	1.494	1.589	56.246
313	2.575	0.300	8.184	2.463	2.544	24.478	8.562	108.550	46.835	0.809	1.023	50.017
MAX	2.903	1.013	68.858	4.926	9.092	198.485	19.265	278.364	200.100	2.132	2.174	204.257
MIN	0.860	0.010	6.634	0.657	0.000	0.000	0.000	0.000	0.000	0.028	0.00004	17.622
OVERALL	2.010	0.560	3.220	1.740	2.790	8.400	7.450	92.850	11.360	0.663	0.814	13.076

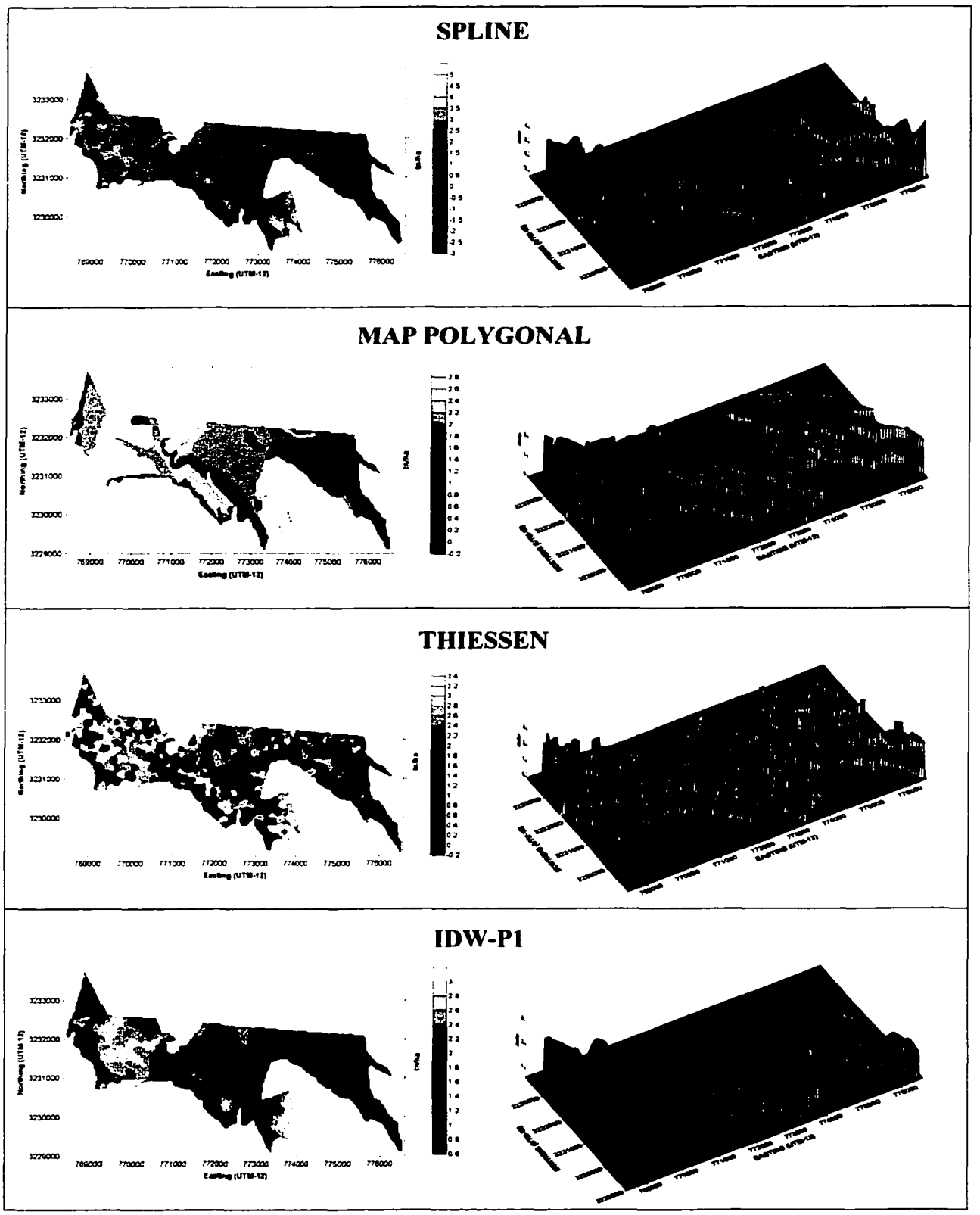

Appendix 10.1. Contour and surface maps corresponding to each of the twelve different spatial interpolation techniques applied to 1-HR.

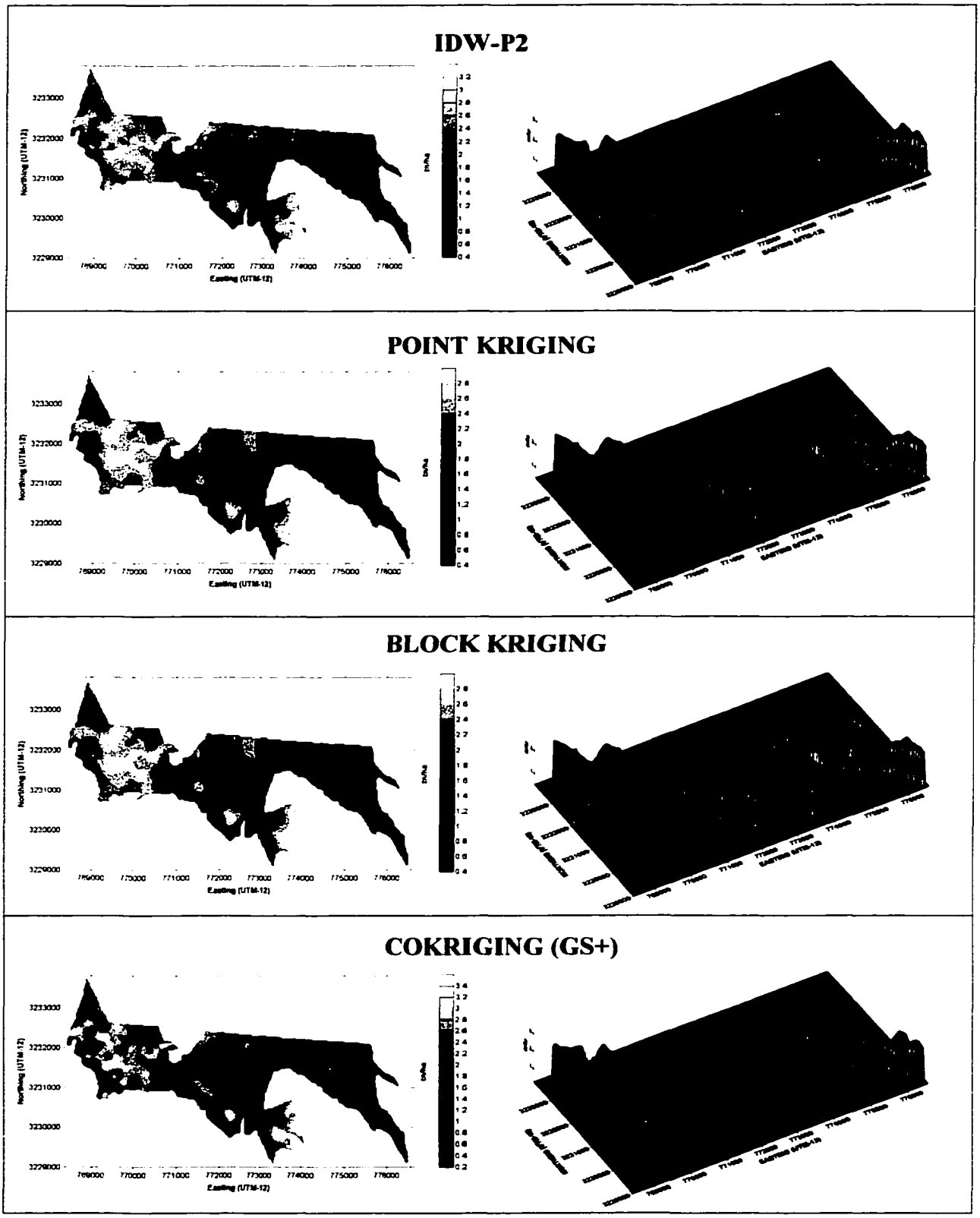

Appendix 10.1. Continued

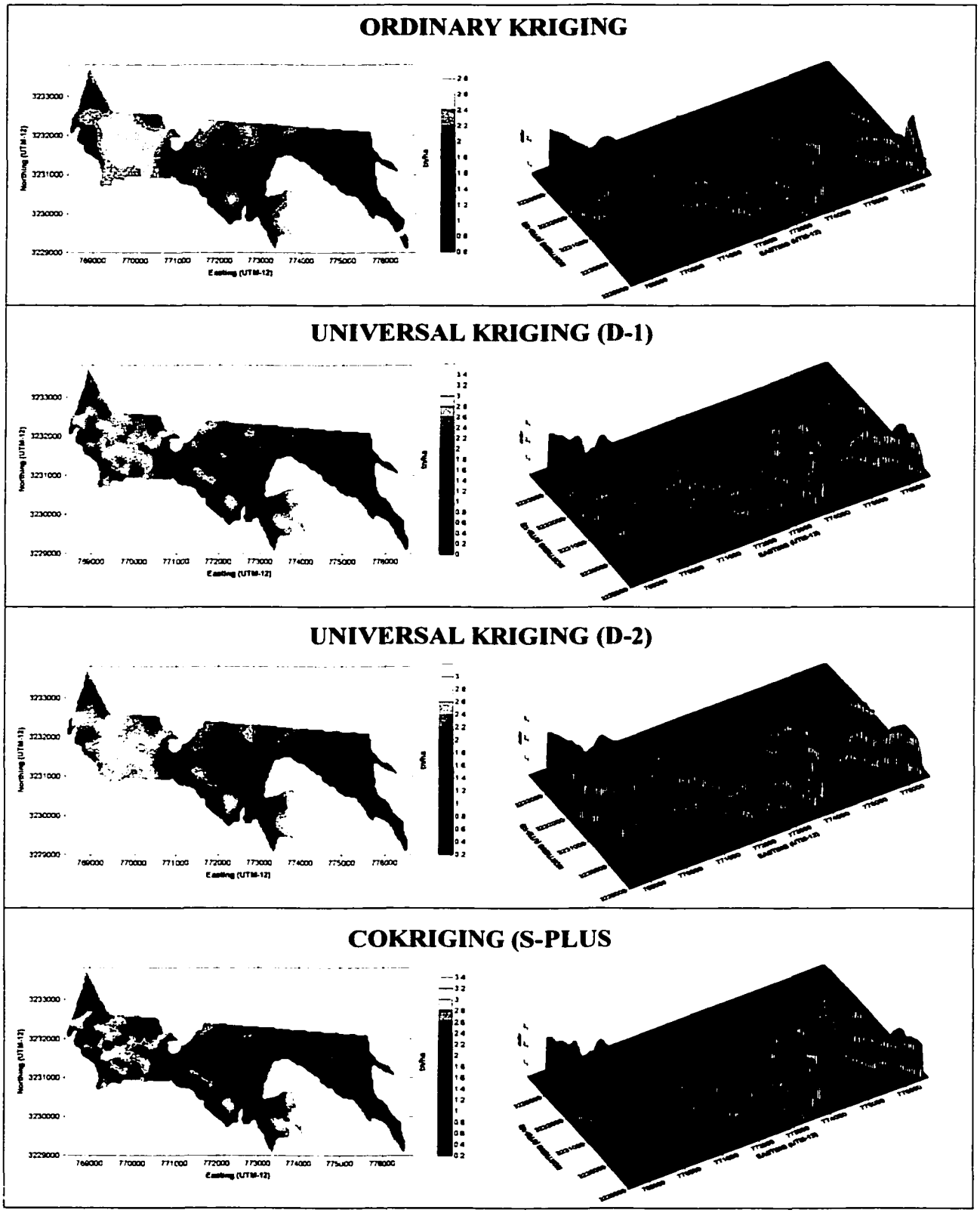

Appendix 10.1. Continued

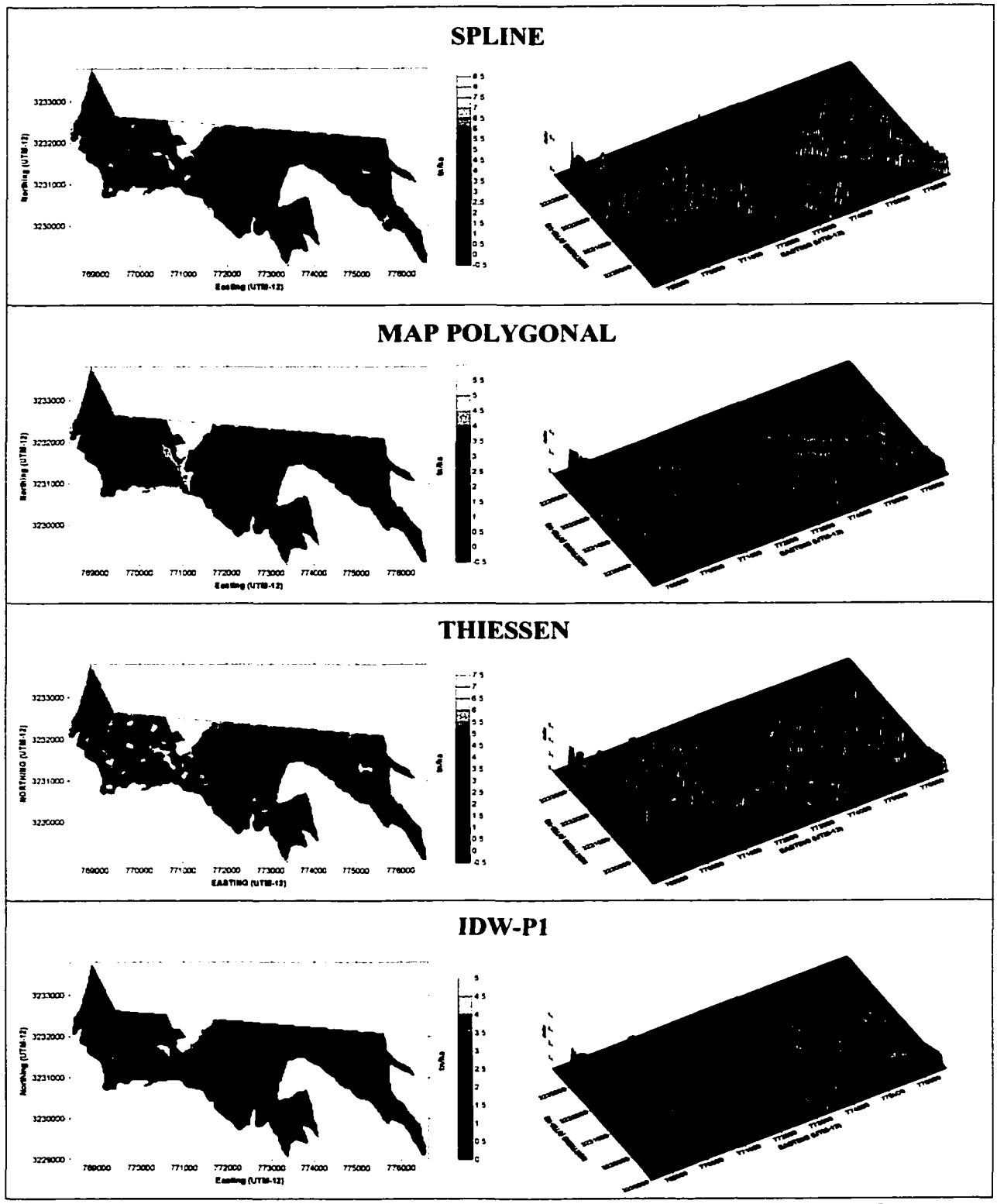

Appendix 10.2. Contour and surface maps corresponding to each of the twelve different spatial interpolation techniques applied to 10-HR.

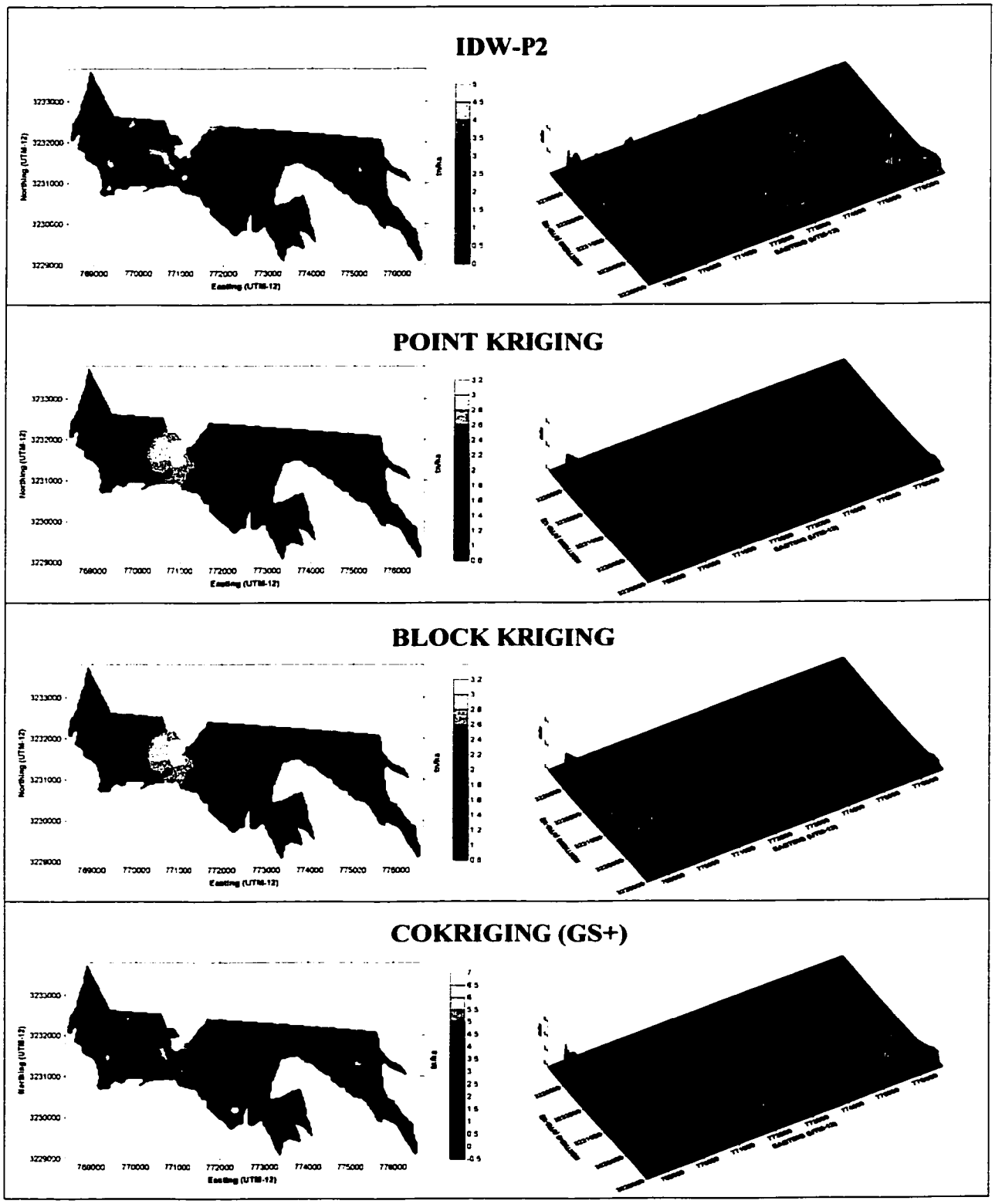

Appendix 10.2. Continued

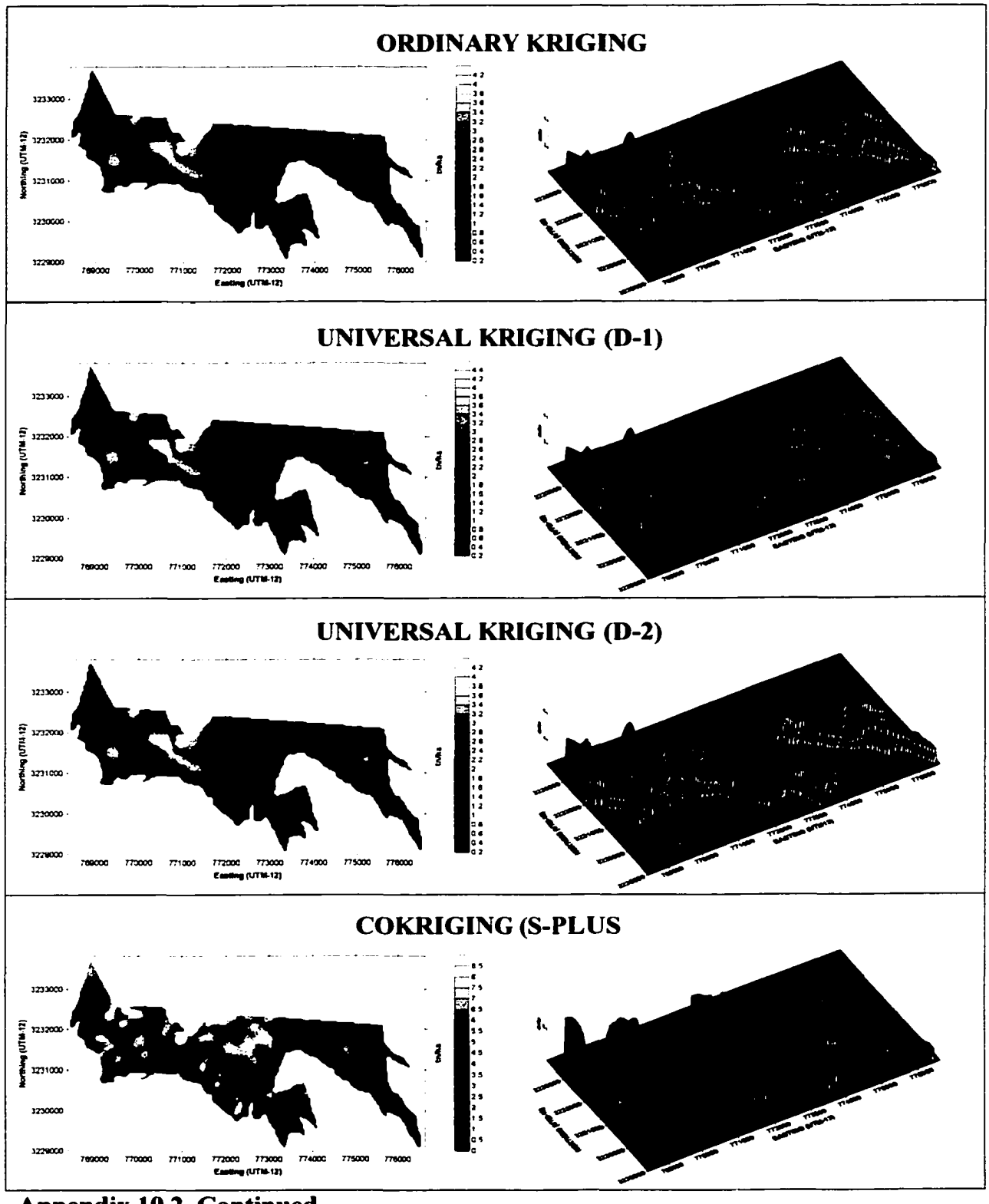

Appendix 10.2. Continued

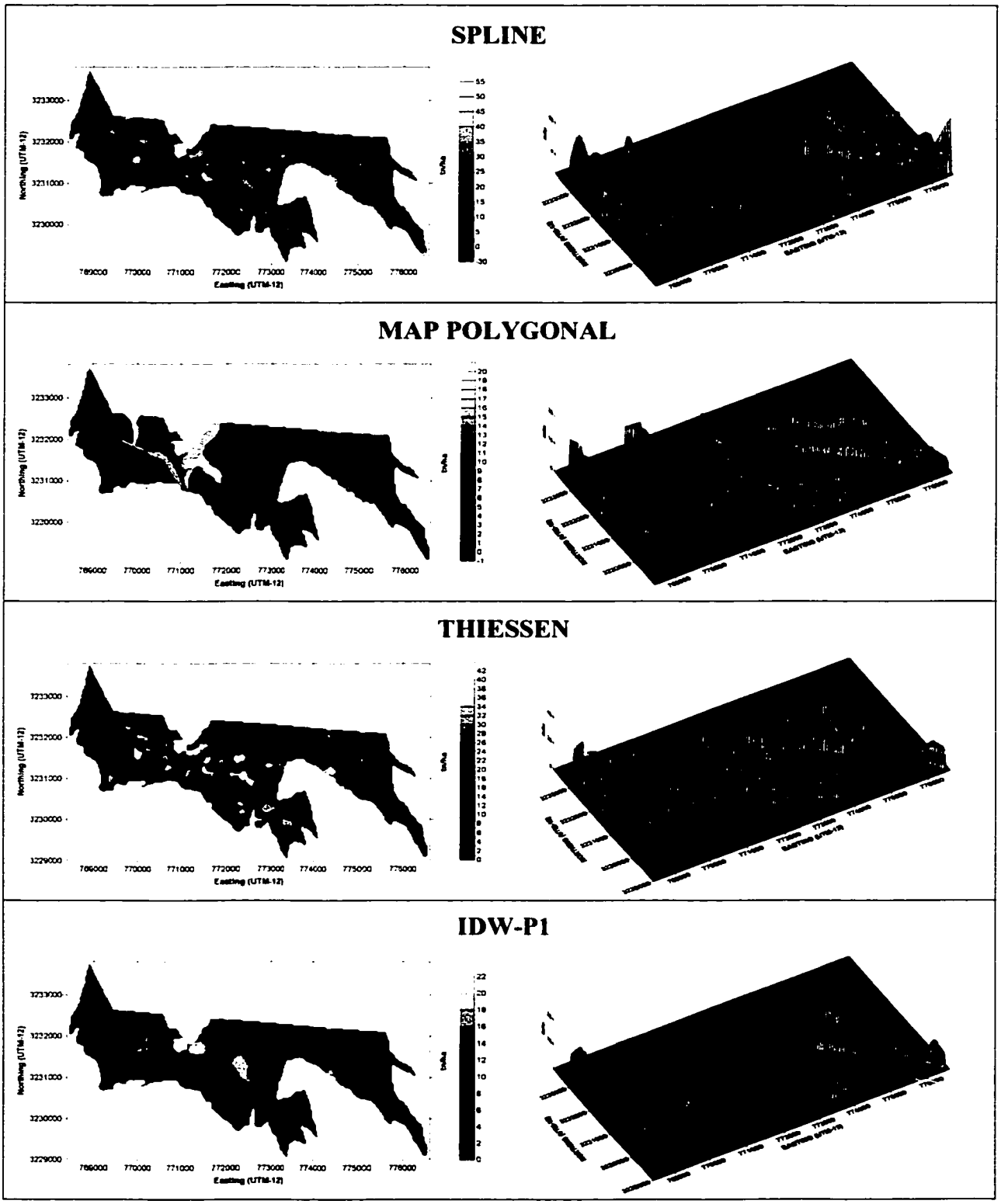

Appendix 10.3. Contour and surface maps corresponding to each of the twelve different spatial interpolation techniques applied to 100-HR.

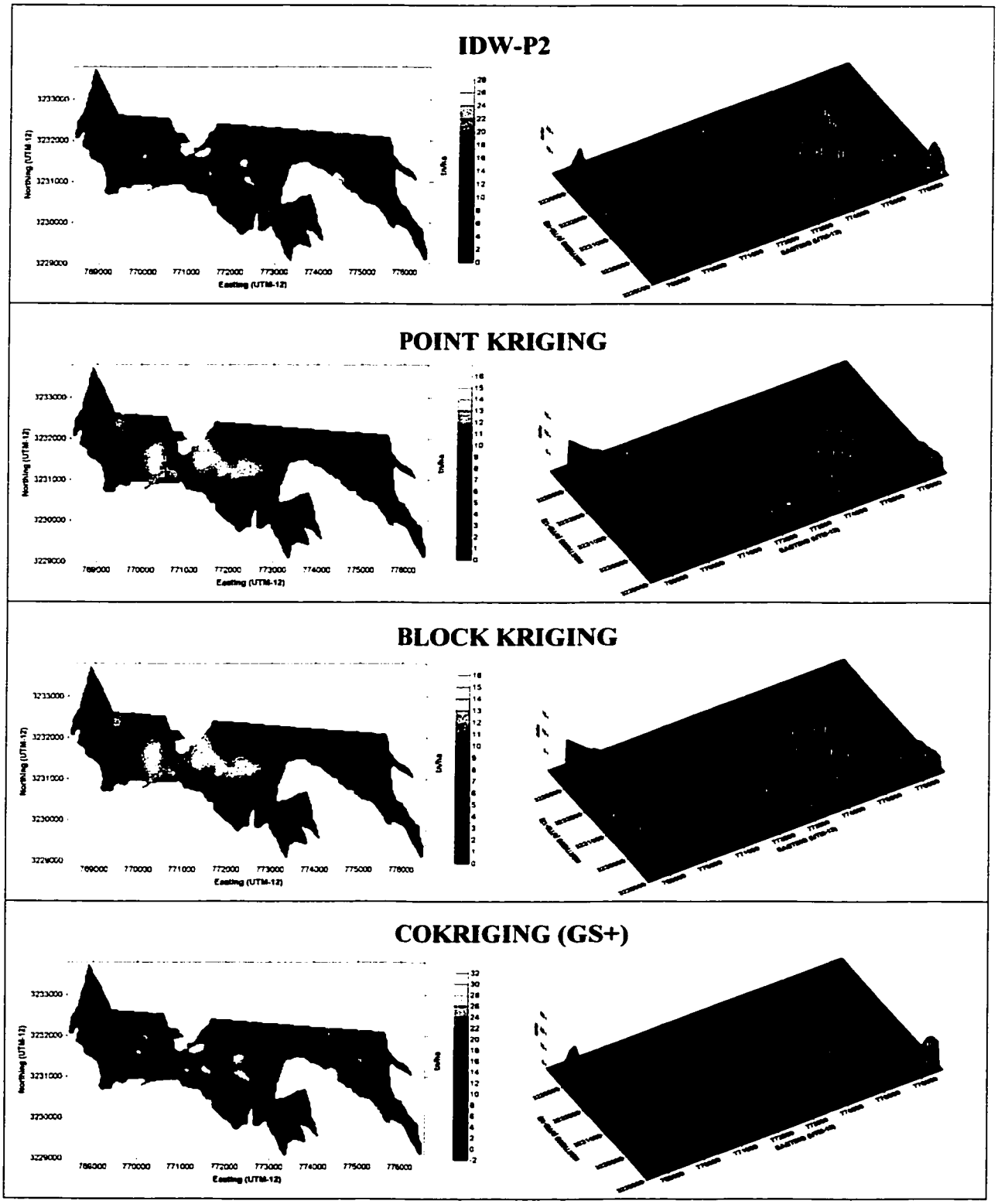

Appendix 10.3. Continued

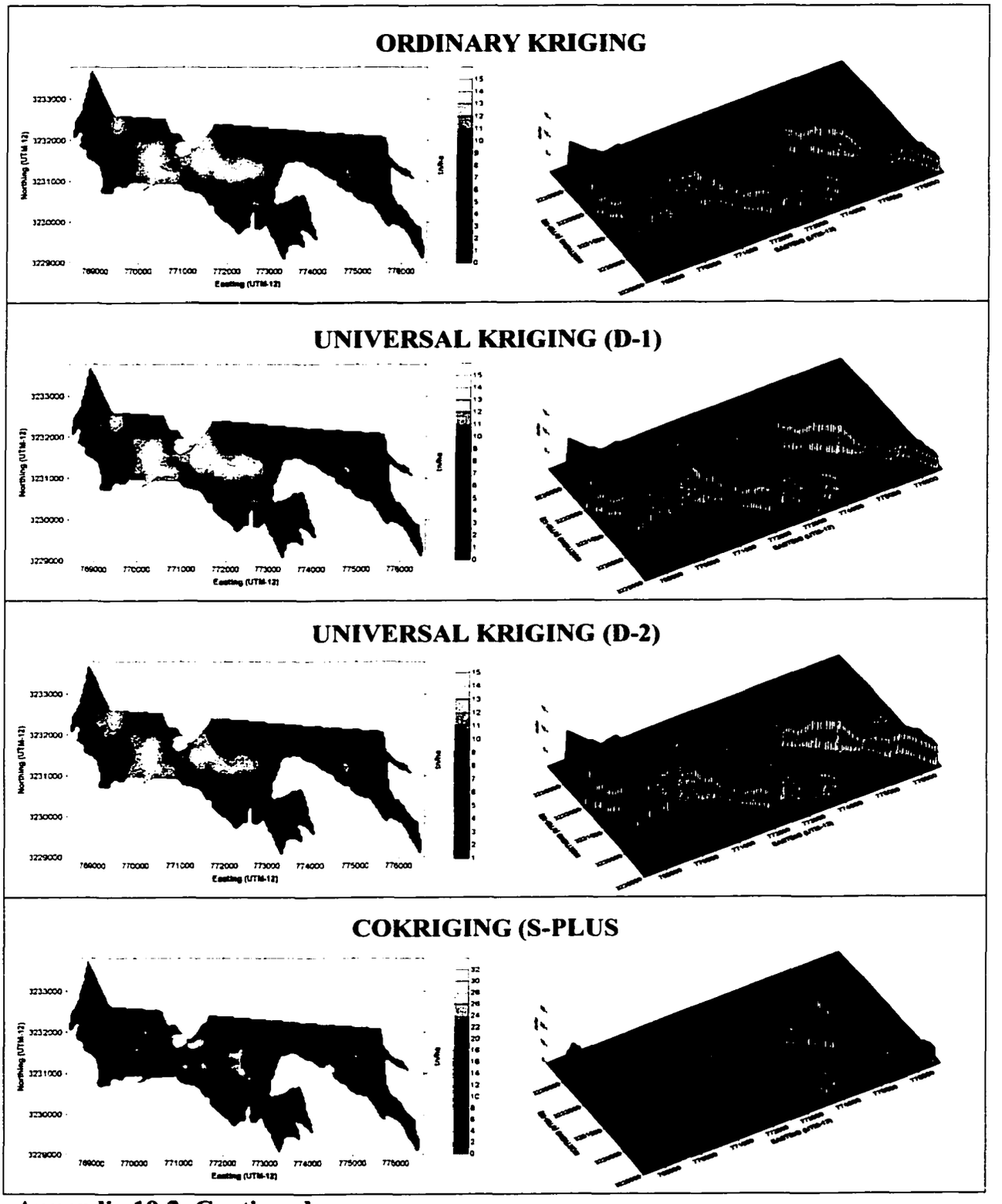

Appendix 10.3. Continued

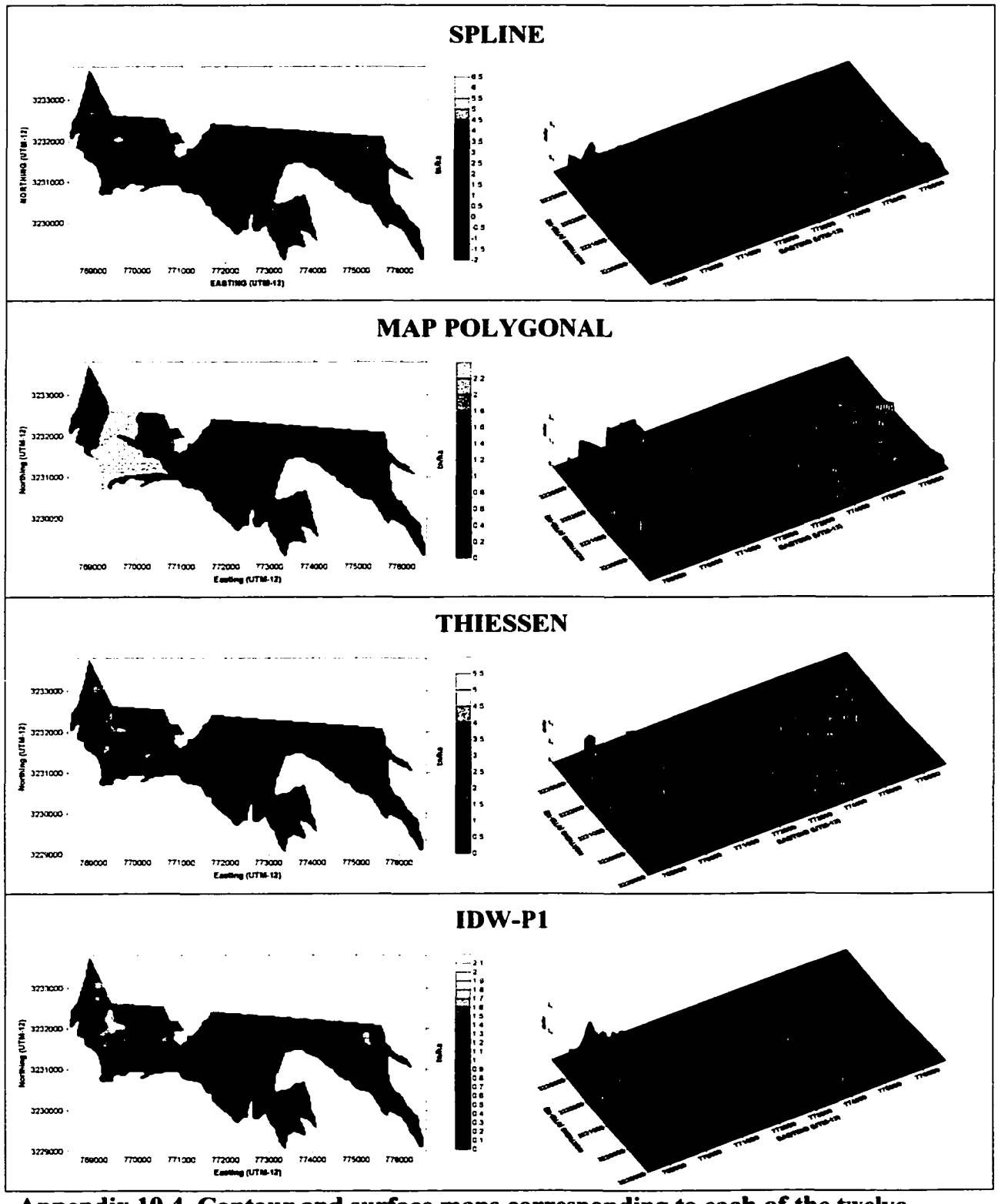

Appendix 10.4. *Contour and surface maps corresponding to each of the twelve different spatial interpolation techniques applied to LW.*

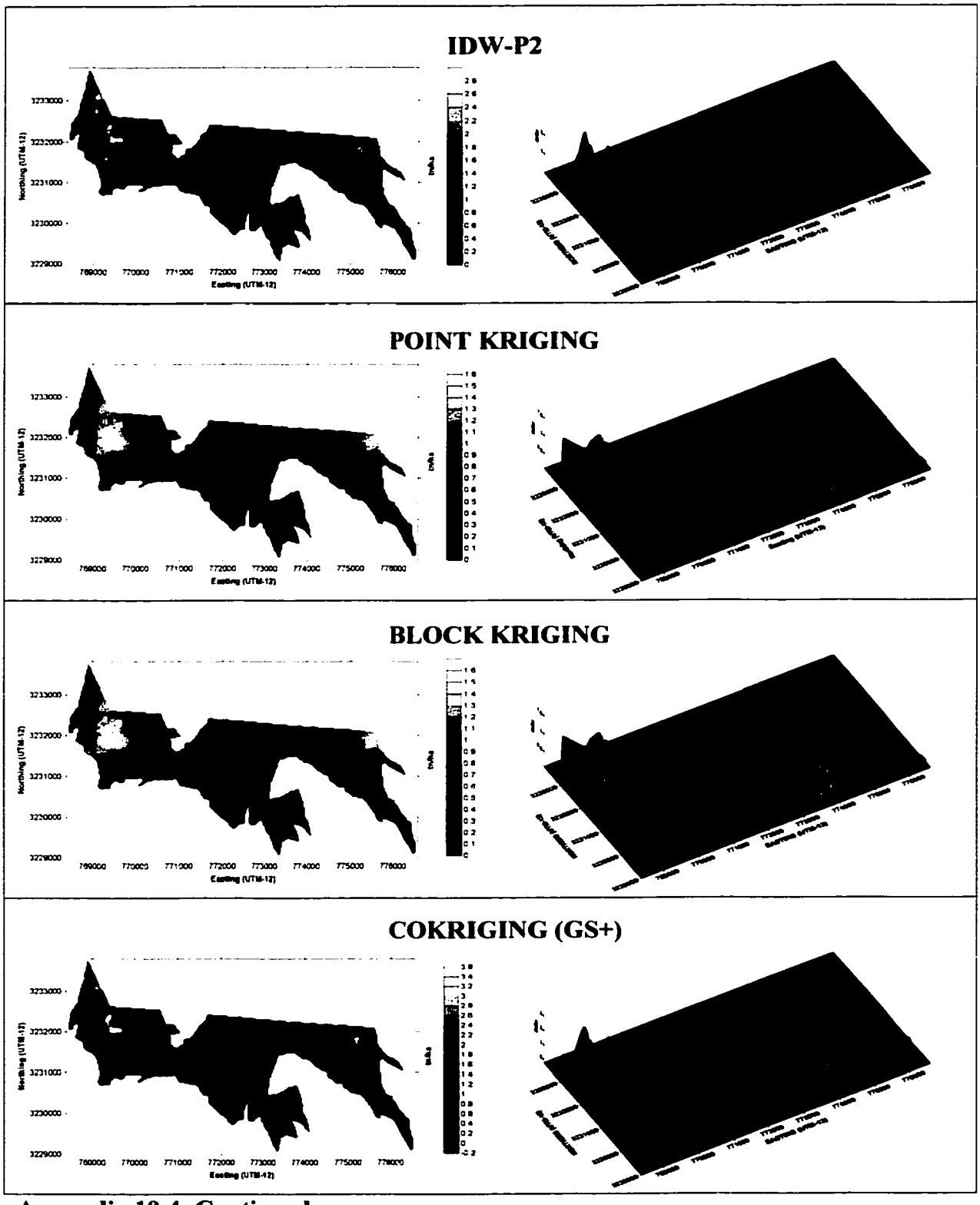

Appendix 10.4. Continued

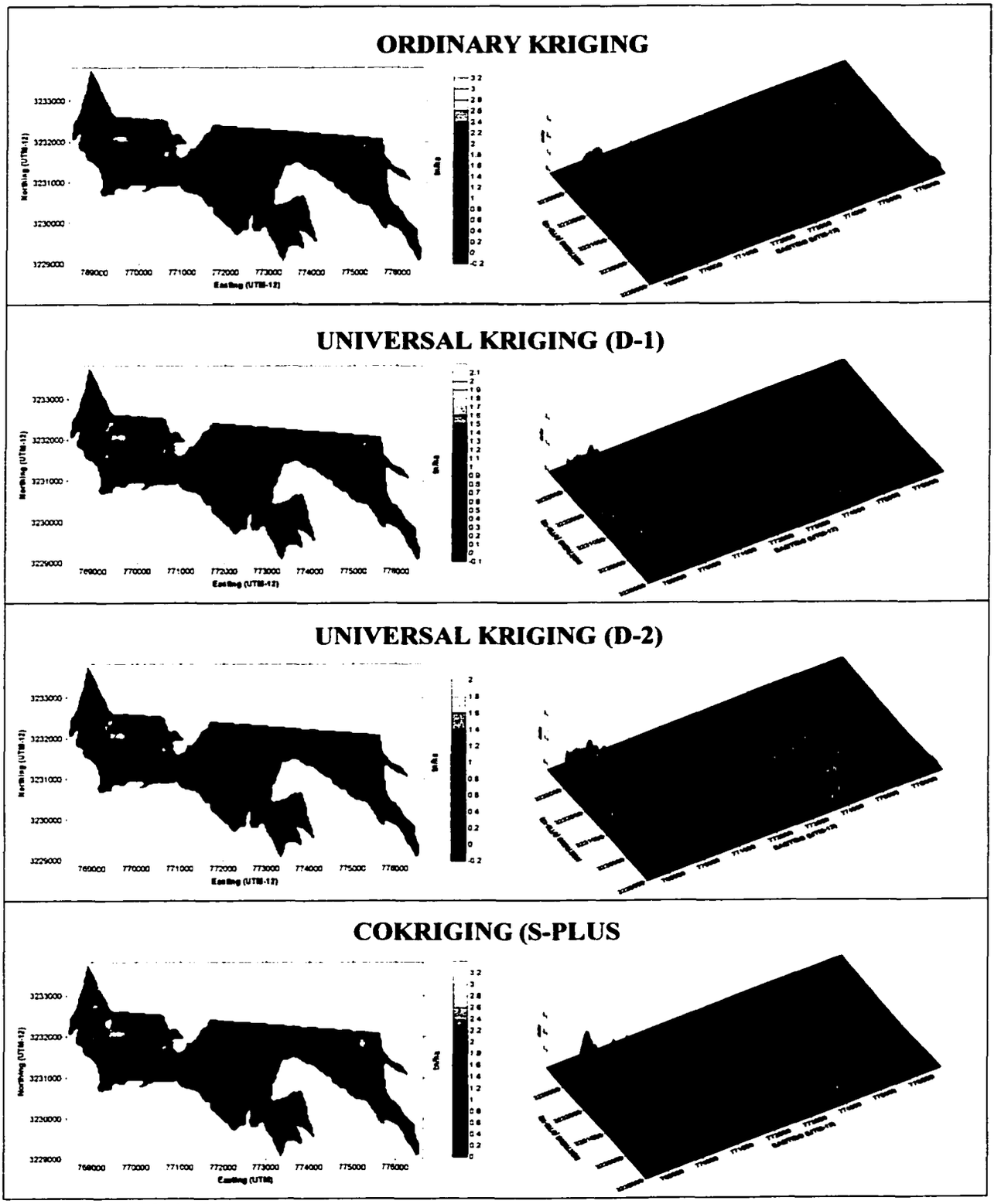

Appendix 10.4. Continued

Grass-Grass dominated

Short grass(1ft)	FUEL CLASS	Tn/ha	lb/sqft	% MOISTURE	WIND VELOCITY				CORRECTION		
1	1-hr	1.73	0.033	2	10.0 km/hr	DIRECTION	1		FACTOR		
	10-hr	0	0	0	6.2 MPH	clockwise from uphill					
	100-hr	0	0	0	0. WRF		EMW(km/hr)		1		
	L. HERB.	0	0	0	SLOPE	ASPECT	0				
	L. WOODY	0	0	0	% 10	degrees azimuth					
	RATE OF SPREAD		FIRELINE INTENSITY		HEAT U. AREA	FLAM LENGTH			REACTION INTENSITY		FLAME DEPTH
	16 chains/hr										
	17.85 feet/min		33	Btu/ft/s	11 Btu/sqft	2.2	ft		1009 Btu/sqft/min		1.96 ft
	5.43 m/min					0.6	m				0.60 m
	326.08 m/hr										
Timber+Grass	FUEL CLASS	Tn/ha	lb/sqft	% MOISTURE	WIND VELOCITY				CORRECTION		
2	1-hr	4.94	0.093	5	65.0 km/hr	DIRECTION	40		FACTOR		
	10-hr	2.47	0.047	5	40.3 MPH	clockwise from uphill					
	100-hr	1.24	0.023	5	0. WRF		1 EMW(km/hr)		1		
	L. HERB.	0	0	0	SLOPE	ASPECT	40				
	L. WOODY	1.24	0.023	50	% 40	degrees azimuth					
	RATE OF SPREAD		FIRELINE INTENSITY		HEAT U. AREA	FLAM LENGTH			REACTION INTENSITY		FLAME DEPTH
	112 chains/hr										
	123.16 feet/min		1050	Btu/ft/s	51 Btu/sqft	11.0	ft		3708 Btu/sqft/min		16.99 ft
	37.51 m/min					3.3	m				5.18 m
	2250.53 m/hr										

Appendix 11.1. Part of the INPUT/OUTPUT interface used in FUEGO, a surface fire behavior system that estimate fire behavior based on fuel loading within an area qualified with a given fuel model.

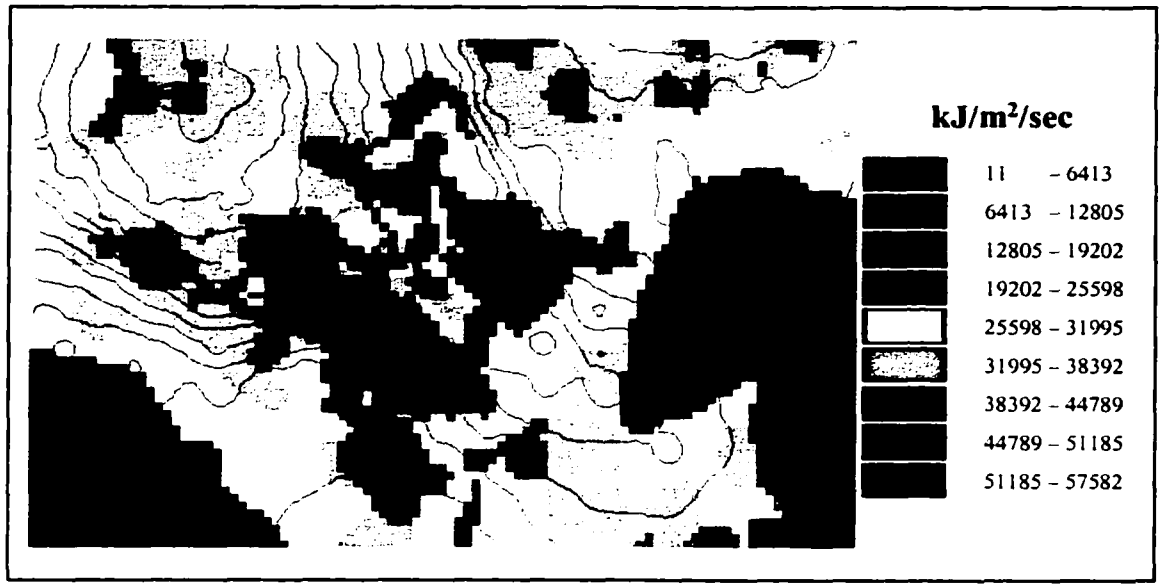

Appendix 11.2. Reaction intensity resulted from a fire behavior simulation, based on the Spatial Simulation model. Background correspond to the spatial variation of 1-HR fuels loading.

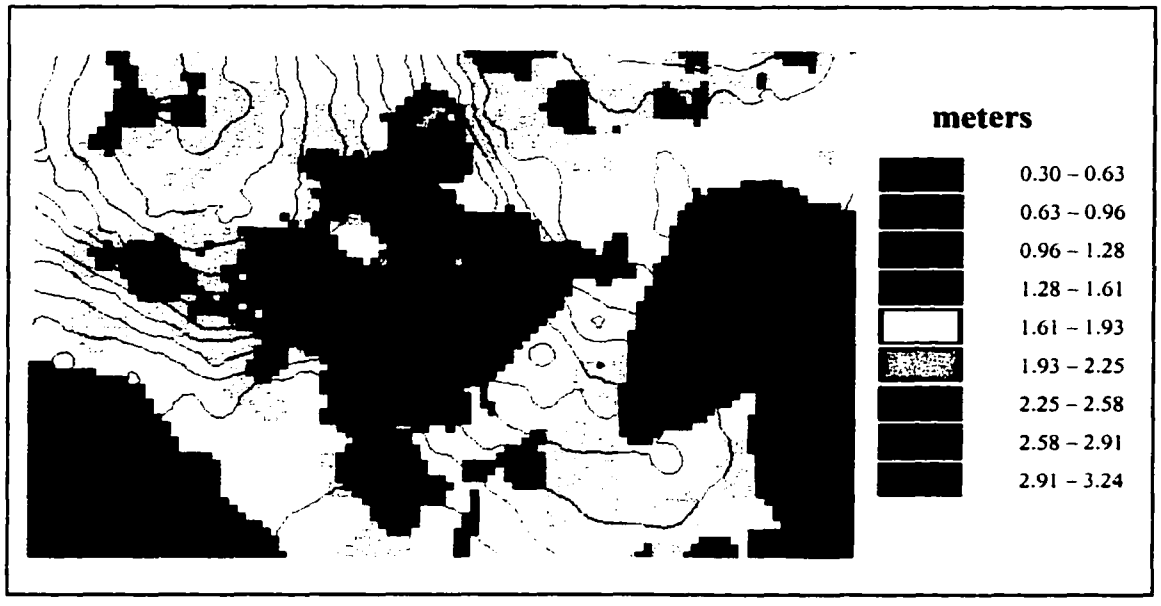

Appendix 11.3. Flame depth resulted from a fire behavior simulation, based on the Spatial Simulation model. Background correspond to the spatial variation of 1-HR fuels loading.

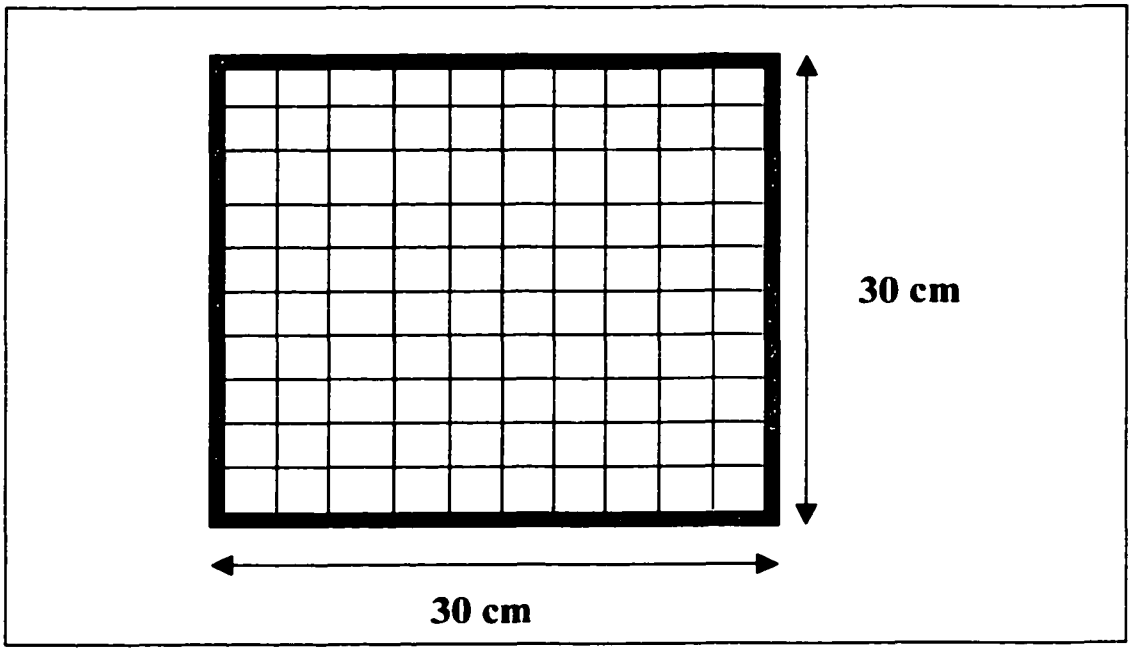

Appendix 12.1. Fuel sampling frame (approximately 1 ft^2). The internal division are used to evaluate the percentage of the frame area covered by duff or litter.

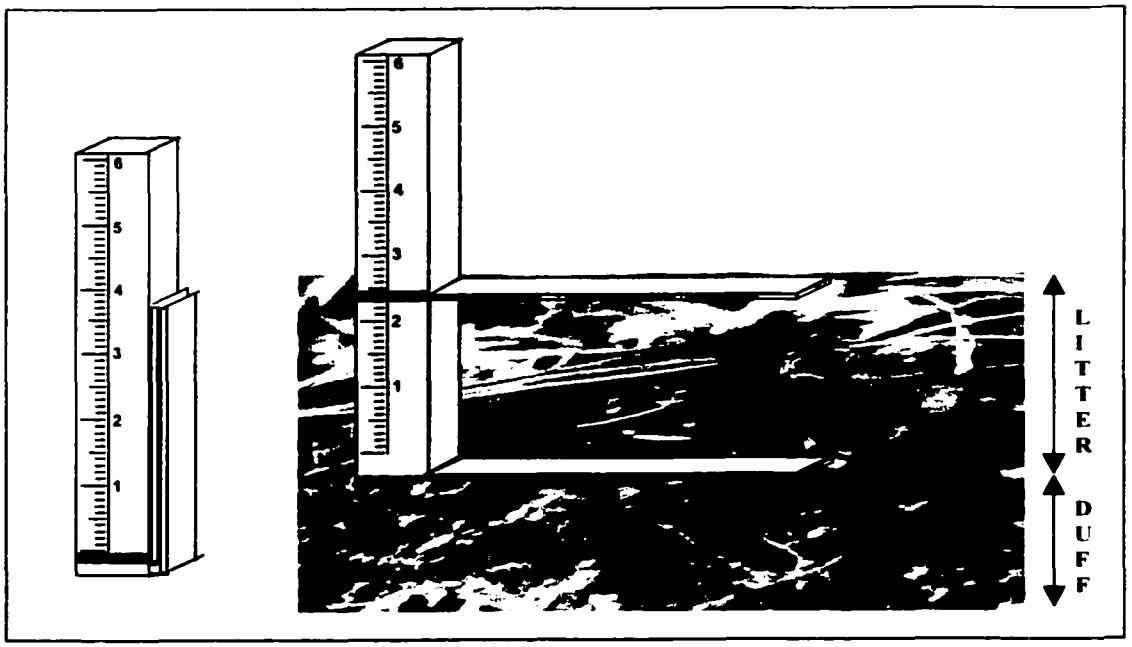

Appendix 12.2. Ruler adapted for duff and litter depth measuring. The lower horizontal level is fixed, while the upper level can be moved.